

RESEARCH & REVIEWS IN ENGINEERING

December 2022

Editor

Prof. Dr. Coşkun ÖZALP

gece
kitaplığı

İmtiyaz Sahibi / Publisher • Yaşar Hız
Genel Yayın Yönetmeni / Editor in Chief • Eda Altunel
Kapak & İç Tasarım / Cover & Interior Design • Gece Kitaplığı
Editörler / Editors • Prof. Dr. Coşkun ÖZALP
Birinci Basım / First Edition • © Aralık 2022
ISBN • 978-625-430-558-0

© copyright

Bu kitabın yayın hakkı Gece Kitaplığı'na aittir.

Kaynak gösterilmeden alıntı yapılamaz, izin
almadan hiçbir yolla çoğaltılamaz.

The right to publish this book belongs to Gece Kitaplığı.

Citation can not be shown without the source, reproduced in any way
without permission.

Gece Kitaplığı / Gece Publishing

Türkiye Adres / Turkey Address: Kızılay Mah. Fevzi Çakmak 1. Sokak

Ümit Apt. No: 22/A Çankaya / Ankara / TR

Telefon / Phone: +90 312 384 80 40

web: www.gecekitapligi.com

e-mail: gecekitapligi@gmail.com



Baskı & Cilt / Printing & Volume

Sertifika / Certificate No: 47083

Research & Reviews in Engineering

December 2022

Editor

Prof. Dr. Coşkun ÖZALP

CONTENTS

CHAPTER 1

ADJUNCT CULTURES IN YOGURT PRODUCTION

Çisem BULUT ALBAYRAK, Cem Aykut METİN 1

CHAPTER 2

THREE-PHASE POWER MEASUREMENT WITH DSPIC

Erdem ILTEN, Haris CALGAN, Metin DEMİRTAS..... 23

CHAPTER 3

RECTIFIER CIRCUIT DESIGN FOR GSM AND ISM BAND RF ENERGY HARVESTING SYSTEMS

AYSU BELEN 37

CHAPTER 4

DESIGN AND DEVELOPMENT OF AN ARDUINO-BASED LIQUID SOAP DISPENSER AND AN AUTOMATED HAND SANITIZER

Osman Emre YILDIRIM, Mecit ÖGE,

Tuba ÖZDEMİR ÖGE..... 47

CHAPTER 5

ENVIRONMENTAL RISK ASSESSMENT FOR MUNICIPAL SOLID WASTE COMPONENTS AND SITE SELECTION IN TURKEY

Onur DERSE , Murat OTURAKÇI..... 57

CHAPTER 6

DATA DRIVEN SURROGATE MODELLING ASSISTED OPTIMIZATION OF MICROSTRIP MONOPOLE ANTENNA

Peyman MAHOUTI, Mehmet Ali BELEN, Ozlem TARI..... 71

CHAPTER 7

**A STUDY ON REMOTE MONITORING OF AN AIR QUALITY
SENSOR**

Tuba ÖZDEMİR ÖGE, Mecit ÖGE..... 81

CHAPTER 8

**GEOLOGICAL SOURCES, CLASSIFICATION AND NEW
TECHNICAL APPLICATIONS OF GEMSTONES**

Yeşim ÖZEN..... 91

CHAPTER 9

**CONVERGENT-DIVERGENT NOZZLE CFD ANALYSIS
WITH DIFFERENT DIVERGENT ANGLE AND NPR**

N.Filiz TUMEN OZDIL, Mehmet Emin TASKİN..... 115

CHAPTER 10

**PREDICTION STUDY FOR LONG-TERM WIND SPEED
USING MACHINE LEARNING METHODS**

Serap AKCAN, Metin ÖZŞAHİN..... 133

CHAPTER 11

**CLASSIFICATION AND REGULATIONS OF UNMANNED
AERIAL VEHICLES**

Faruk GÜNER, Hilmi ZENK..... 145

CHAPTER 12

**EVALUATION OF THE EFFECT OF TRAIN-TEST
SPLIT RATIO FOR THE PREDICTION OF DAILY PAN
EVAPORATION OF ÇORUM PROVINCE**

Okan Mert KATİPOĞLU..... 167

CHAPTER 13

**AN OVERVIEW ON CHARACTERISTICS OF CERAMIC
MATERIALS USED IN SEVERAL APPLICATIONS AND
RECENT TRENDS**

Fatma İrem ŞAHİN, Nil ACARALI..... 179

CHAPTER 14

**PROCEDURES FOR DETERMINING THE VALUE OF
TREASURY IMMOVABLES, QUESTIONS AND POSSIBLE
SOLUTION SUGGESTIONS**

Nuri ERDEM 193

CHAPTER 15

**DATA DRIVEN SURROGATE MODELLING APPROACH
FOR ACCURATE MODELLING OF REFLECTARRAY UNIT
ELEMENTS**

Peyman MAHOUTİ 215

CHAPTER 16

**GEOGRAPHICAL INFORMATION SYSTEMS (GIS) WITH
INTELLIGENCE TRANSPORTATION SYSTEM (ITS) IN
SOMALIA**

Hatice Canan GÜNGÖR, Abdinasir Osman MOHAMED 227

CHAPTER 17

**SUSTAINABLE TECHNIQUES IN COASTAL MANAGEMENT
AND PLANNING**

Oylum GÖKKURT BAKİ 237

CHAPTER 18

HEAT-MASS TRANSFER ANALOGY OF IMPINGING JETS

Abdullah BINGOL, Nevin CELİK, Ihsan DAGTEKİN 257



CHAPTER 1

ADJUNCT CULTURES IN YOGURT PRODUCTION

Çisem BULUT ALBAYRAK¹, Cem Aykut METİN²

1 Corresponding author: Asst. Prof. Dr. Aydın Adnan Menderes University, Engineering Faculty, Food Engineering, Aydın,TURKIYE, <https://orcid.org/0000-0002-7993-5372>, cisembulut@gmail.com

2 . Food Engineer, Aydın Adnan Menderes University, Engineering Faculty, Food Engineering, Aydın,TURKIYE, <https://orcid.org/0000-0002-7551-9355>, 171801026@stu.adu.edu.tr

INTRODUCTION

Fermented dairy products have been traditionally manufactured and consumed since ancient times. Yogurt is known as one of the oldest fermented dairy products and The word “yogurt” is believed to have originated from the Turkish word “yogurmak,” and it means to thicken, coagulate, or curdle (Fisberg and Machado, 2015). First yogurt production is thought to come from Middle East Region. Yogurt production was initially relied on traditional practices, experiences and empirical processes. Although traditional yogurt production is based on using previous product in the yogurt fermentation, defined starter cultures have been used for years in commercial productions (Yıldız, F, 2016). In the last century, there has been great interest for consumption and industrial production around the world due to valuable nutritional and health properties. It is a good source for many nutritionally important substances such as proteins, various minerals (calcium, phosphorus, magnesium, and zinc.) and vitamins (riboflavin, thiamin, vitamin B12, folate, niacin). Additionally, it can be preferred by lactose intolerant people because lactose in milk is converted into lactic acid. In particular, research results associated the health benefits affected its popularity. Also, product innovations and availability of different kinds of yogurt enhanced the yogurt consumption (Das et al.,2019).

In the market, three main types of yogurt styles can be found as set yogurts, stirred yogurts and drinking yogurts. Set yogurts are generally fermented ‘in pack’, and have a firm gel structure and ‘natural’ flavor. Stirred yogurts are sheared after fermentation and they have semi-solid consistency. Stabilizers, fruit pieces and flavours are included in most of the stirred yogurt production. Moreover, drinking yoghurt is manufactured by diluting fermented yogurt with water and/or fruit concentrate. They are more similar to acidified milk drinks (Das et al.,2019).

Common yogurt production is based on fermenting cow’s milk using mainly two lactic acid bacteria (LAB) species with 1:1 ratio of *Lactobacillus delbrueckii* ssp. *bulgaricus* and *Streptococcus salivarius* ssp. *thermophilus* (Yıldız, F, 2016) and its manufacturing steps are presented in Figure 1. First, milk is filtrated to remove debris. Then presence of antibiotics is checked because antibiotic residue can inhibit yogurt starter bacteria. In the next step, fat t and solid content of milk is standardized to make good quality yogurt. Then, milk is homogenized and during homogenization fat globules size is reduced to 1-2 µm. This process prevents the separation of fat and incorporation is enhanced. After, homogenization, heat treatment is performed (90-95°C for 5-10 min or 80-85°C for 30 min). During thermal treatment, pathogenic microorganisms are destroyed and enzymes are inactivated. Also, it causes changes in protein structures which is important in gel structure. Then, the milk is cooled to suitable temperature (43

°C) for starter cultures and yogurt starters were added. After incubation at 42-43 °C for 3-4 h (until suitable acid development pH 4.5), it is cooled and stored at refrigerator conditions. During refrigeration, viscosity increases, much firmer gels are obtained and casein micelles are stabilized.

Currently, there has been also existed increasing interest for yogurt non-starter adjunct cultures. In particular, probiotics cultures have been widely used. Although most of the commercial probiotics have been included in *Bifidobacteria* and *Lactobacillus* genera, potential of new species and strains have been taken attention due to the technological and specific health benefit advantages. Moreover, various cultures have been developed for different purposes such as texture improvement, aroma and flavor supporting and biopreservation. In this chapter, recent literature sources were examined and evaluated to discuss current researches and trends.

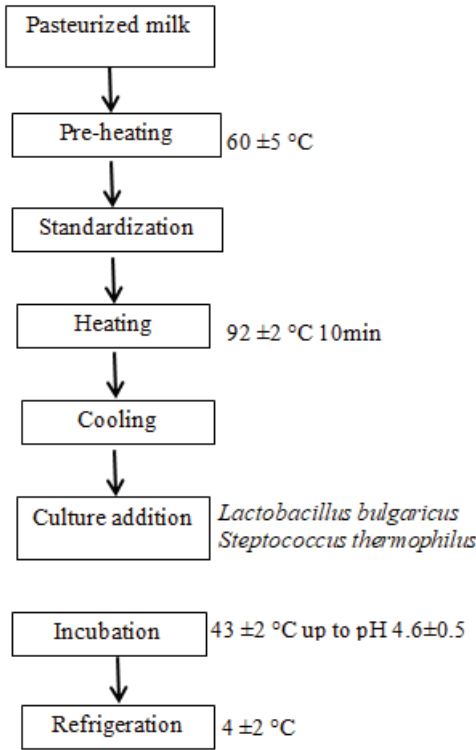


Figure 1: Flowchart of yogurt production

YOGURT ADJUNCT CULTURES

Selection of suitable yogurt cultures plays important role in overall quality properties of the final product. Main yogurt manufacturing is based on starter culture activities (*L. bulgaricus* and *S. thermophilus*). These bac-

teria are inoculated 1:1 ratio in the same time because they have symbiotic relationship. First, *S. thermophilus* growth is observed and pH and redox potential is decreased. This change presents preferable conditions for *L. bulgaricus*. Another symbiotic relationship can be observed for proteolytic activity. *S. thermophilus* is weakly proteolytic and it can not hydrolyze the milk protein but *L. bulgaricus* has protease enzymes and convert casein to smaller amino acids. They increase acidity by secreting lactic acid in milk and they also coagulate proteins while producing specific yogurt flavor substances. These LAB combinations are used in the form of starter cultures and provide controlled fermentation, prevention of contamination and the growth of undesirable microorganisms and maintain standard quality and production. Starter cultures are preparations of one or more strains of one or more microbiological species mostly they are responsible for initiation of fermentation and provide desirable and predictable taste and structure for the fermented products. In different commercial forms, they can be inoculated directly or subcultured prior to production (Erkuş 2007).

Secondary cultures, or adjunct cultures can be defined as any cultures that are intentionally added during manufacturing of fermented foods and they are not responsible for primary acid production and initiating fermentation. Adjunct culture term has been widely used in cheese productions (Irlinger et al., 2017). Non-starter cultures and also known as adjunct cultures can also be included in yogurt production for different purposes. Probiotic cultures have been widely used in yogurt production to improve health properties. In addition, different specific cultures can be developed for flavor and texture improvement, enhancing the shelf life and safety.

Probiotic Adjunct Cultures for Yogurt Production

Probiotics are defined as live microorganisms that when administered adequate amounts, confer a health benefit on the host (Nyanzi et al., 2021). They can show beneficial health effects through several mechanisms such as prevention of gastrointestinal diseases, and enhancing intestinal microbiota, immune modulation properties, cholesterol reducing, blood pressure lowering, anticancer, pathogen inhibition and antioxidant activities (Roo-bab et al., 2020). To exert beneficial health effects, they must keep viability during storage and gastrointestinal passage and enough viable cells (10^6 CFU/g) must be provided (Das et al., 2019). Another important criteria for the selection of probiotic candidates are antimicrobial activity and safety considerations associated with their antibiotic susceptibility and virulence potential (Motahari et al., 2017). Therefore, tolerance the acid and bile salt environment, bile salt hydrolysis, viability during digestion, auto aggregation and coaggregation abilities, adhesion properties on intestinal cells, antimicrobial properties, antibiotic sensitivity tests are common methods used to select and develop probiotic strains (Gao et al., 2021).

Yogurt has been one of the most preferred vehicles for carrying of probiotic microorganisms for years. Beside its own nutritious and health promoting properties, it can be suitable for matrix to delivery probiotics (Gao et al., 2021). Selected strains should have good adaptation in yogurt environment and positive effects on yogurt quality can be also another desirable property. Although the most common probiotic microbial species belong to *Lactobacillus* and *Bifidobacteria* genera, various species and strains are available in the current days (Table 1). Initially, limited number of probiotic strains was used in yogurt productions and most of them were isolated from human. During years, new strains have been obtained from fermented food environments and their probiotic potentials were investigated. Common health benefits of probiotics are presented in Table 2. Recently, new health benefits have been investigated for specific species and strains isolated from various environments (Gao et al., 2021). Probiotic fermented dairy products, which are a healthy functional food present high number of beneficial bacteria that ferment food-borne indigestible carbohydrates in the human intestine.

Lactic Acid Bacteria (LAB)

LAB contribute in various food fermentations and can be found in different environments in high number (Cheese, yogurt, table olive, sourdough, etc). They are group of heterologous bacteria that ferment carbohydrates and produce lactic acid. Main food associated LAB genera are *Lactobacillus*, *Streptococcus*, *Lactococcus*, *Pediococcus* and *Leuconostoc*. They are non-sporulating, facultative anaerobic, Gram positive, oxidase and catalase negative bacteria. In probiotic bacteria *lactobacillus* genus is one of the most crowded group. Recently advanced DNA sequencing studies revealed new categories for this genus (Nyanzi et al., 2021). These are: *L. delbrueckii* group; *Paralactobacillus*; as well as 23 novel genera: *Acetilactobacillus*, *Agrilactobacillus*, *Amylolactobacillus*, *Apilactobacillus*, *Bombilactobacillus*, *Companilactobacillus*, *Dellaglioia*, *Fructilactobacillus*, *Furfurilactobacillus*, *Holzapfelia*, *Lacticaseibacillus*, *Lactiplantibacillus*, *Lapidilactobacillus*, *Latilactobacillus*, *Lentilactobacillus*, *Levilactobacillus*, *Ligilactobacillus*, *Limosilactobacillus*, *Liquorilactobacillus*, *Loigolactobacillus*, *Paucilactobacillus*, *Schleiferilactobacillus*, and *Secundilactobacillus*.

Although probiotic researches were more focused to *lactobacillus* genus, limited species of other genera have also probiotic potential and used probiotic yogurt formulations (Linares et al., 2016; Akpınar et al., 2020).

Bifidobacteria

Bifidobacteria are one of the common group of probiotic organisms and they can be found naturally in the colon environment (Shori, 2021).

In the past, they were classified under the genus *Lactobacillus*, however after further phylogenetic studies, they are classified under phylum Actinobacteria (Shori,2021). *B. bifidum*, *B. infants*, and *B. lactis* are the widely applied probiotic species. They are anaerobic, Gram positive, non-spore forming, non-pathogenic bacteria. They have been used in industrial production of various probiotic formulations, foods and yogurts.

Others

Yeast species such as *S. boulardi* have also probiotic potential and can be used in various formulations (Kalkan et al., 2018). Moreover, some sporulating probiotic bacteria such as *Bacillus coagulans* and *Bacillus classuii* have attracted the attention due to their stability during storage and they presented good adaptation food processing and storage conditions (Cao et al.,2022). Moreover, *Propionibacterium freudenreichii* was also used as adjunct cultures in yogurt production to improve the health status by conjugated linoleic acid and propionic acid (Zahed et al.,2021).

Table 1: Common probiotic microorganisms (adopted by Nyanzi et al., 2021)

<i>Lactobacillus</i> species (previous genus)	Current taxonomic nomenclature	<i>Bifidobacterium</i> species	Other species
<i>Lactobacillus acidophilus</i>	Not changed	<i>B. adolescentis</i>	<i>Bacillus cereus</i>
<i>Lactobacillus amylovorus</i>	Not changed	<i>B. animalis</i>	<i>Clostridium butyricum</i>
<i>Lactobacillus brevis</i>	<i>Levilactobacillus brevis</i>	<i>B. breve</i>	<i>Enterococcus faecalis</i>
<i>Lactobacillus casei</i>	<i>Lactocaseibacillus casei</i>	<i>B. bifidum</i>	<i>Enterococcus faecium</i>
<i>Lactobacillus crispatus</i>	Not changed	<i>B. infantis</i>	<i>Escherichia coli</i>
<i>Lactobacillus delbrueckii ssp. bulgaricus</i>	Not changed	<i>B. lactis</i>	<i>Lactococcus lactis ssp. cremoris</i>
<i>Lactobacillus fermentum</i>	<i>Limosilactobacillus fermentum</i>	<i>B. longum</i>	<i>Lactococcus lactis ssp. lactis</i>
<i>Lactobacillus gasseri</i>	Not changed		<i>Leuconostoc mesenteroides ssp. dextranicum</i>
<i>Lactobacillus helveticus</i>	Not changed		<i>Pediococcus acidilactici</i>
<i>Lactobacillus johnsonii</i>	Not changed		<i>Propionibacterium freudenreichii</i>
<i>Lactobacillus lactis</i>	<i>Lactobacillus delbrueckii ssp. lactis</i>		<i>Saccharomyces boulardii</i>
<i>Lactobacillus reuteri</i>	<i>Limosilactobacillus reuteri</i>		
<i>Lactobacillus rhamnosus</i>	<i>Lactocaseibacillus rhamnosus</i>		

Table 2: Common health benefits of specific probiotics strains (adopted from Nyanzi et al., 2021)

Health benefits	Probiotic strains	Outcomes
Treatment of lactose tolerance and enhanced digestion	<i>Lactobacillus johnsonii</i> La1, <i>Lactobacillus salivarius</i> ,	Inhibition of the pathogens and decreased urease activity
Improved intestinal microflora	<i>Lactobacillus acidophilus</i> LB	
Control of <i>Helicobacter pylori</i> infection obial balance		
Enhancement of intestinal function	<i>L. rhamnosus</i> GG, <i>Lactobacillus casei</i> ,	Controlling of acute diarrhea due to the bacterial infections
Cholesterol lowering	<i>Bifidobacterium lactis</i> BB12,	
Synthesis of vitamins	<i>Bifidobacterium bifidum</i> ,	
Treatment and prevention of diarrhea caused by pathogenic bacteria and viruses	<i>Streptococcus thermophilus</i>	
Stimulation of the mucosal immune system	<i>L. casei</i> Shirota <i>L. rhamnosus</i> HN001 <i>L. acidophilus</i> HN017 <i>B. lactis</i> HN019	Enhancement of immune parameters
Colon cancer prevention	<i>L. rhamnosus</i> GG <i>L. rhamnosus</i> LC-705 <i>L. casei</i> Shirota <i>L. acidophilus</i> LA-2 <i>Bifidobacterium</i> sp. <i>Propionibacterium</i> sp.	Preventing or delaying onset of cancer in the gastrointestinal system
Bacterial and yeast vaginitis	<i>L. acidophilus</i> <i>L. rhamnosus</i> GG	Vaginitis is treated by through regulation of microflora by supporting health ones
Prevention of genitourinary infections	<i>L. rhamnosus</i> GR-1 <i>Lactobacillus reuteri</i> RC-14	Reducing the risk of infections by regulation of microflora
Allergic symptoms	<i>L.rhamnosus</i> GG <i>Bifidobacterium animalis</i> BB12	Prevention the onset of allergic diseases
Inflammatory bowel syndrome	<i>L. rhamnosus</i> GG	Therapy in inflammatory

Although yogurt as itself has many health benefits and contain high number of viable fermenting bacteria, developing probiotic yogurt products has also growing scientific and public interest during years (Table 3). In yogurt production, in addition to starter cultures, probiotic microorganisms with specific health claims have wide range of application for years (Gao et al., 2021). Initially, one of the important problem was to maintain the required viability during storage. To overcome viability loss during storage and gastrointestinal passage, several techniques such as removal of oxygen, microencapsulation have been proposed (Gao et al., 2021). Moreover, selection of more resistant strains and application of spore former probiotic strains were also suggested (Cao et al., 2022). Different probiotic combinations and effects on rheological and organoleptic properties were examined (Soni et al., 2020). Moreover, developing new probiotics strains with new specific health benefits has also taken attention in recent years. New finding in clinical evidences supports that some microorganism can produce neurotransmitters and it can effect mental health by different ways. For example, some LAB strains can produce GABA and they can have antidepressant effect. Those specific traits can be evaluated in psychobiotics a special class of probiotics. Therefore, specific probiotics can be designed and used in probiotic yogurts. In one of the study, probiotic yogurt was produced by using *L. acidophilus* LA5 and *B. lactis* BB12 (1×10^7 CFU) and its consumption on mental health and HPA axis was evaluated. Their presence showed positive effect on mental status in this work (Mohammadi et al., 2016).

In one of the another recent study, probiotic bacteria (*B. animalis* BB-12 and *L. acidophilus* LA-5) and some additional ingredients were added into yogurt and their effects on some characteristics of cow and goat dessert yogurts were investigated (Papaioannou et al., 2022). Dessert yogurt samples were analyzed in terms of physiochemical parameters, rheological properties, and sensory qualities. For cow dessert yogurts, Probiotic free dessert yogurts were more acceptable than probiotic ones in contrary for goat dessert yogurt probiotic ones were more preferred.

Although, LAB and *Bifidobacteria* have been widely used in probiotic yogurt formulations, other species such as *Bacillus coagulans* were also used recently (Cao et al., 2022). Inclusion of *B. coagulans* GBI-30 in yogurt formulation was examined by microbiological, chemical analysis for 14 days of at 4 °C. A high bacterial stability was maintained during the storage. Also similar sensory scores were obtained to the control group. Improved milk acidification and proteolysis were provided by *B. coagulans* supplementation. Furthermore, 12 discriminatory volatiles were analyzed. During shelf life, post-acidification can lead the loss of viability of probiotic cells and it seems an important problem. At this point, spore forming probiotic strains can be promising solution strategy.

Table 3: Main findings for probiotic adjunct cultures in yogurt production.

Probiotic bacteria	Sources and main characteristics of probiotic bacteria	Main result	References
<i>Enterococcus faecium</i> and <i>Enterococcus durans</i> strains	Isolated from cheese. They tolerated low pH and bile salt. The candidates have high antimicrobial property and they are sensitive to vancomycin.	Significant changes in the acidity, textural and microbiological properties of adjunct culture containing yogurt, however the sensory properties were not significantly different. It provided additional functional properties required bacterial count.	(Akpınar et al.,2020)
<i>Lactobacillus casei</i> Zhang	Isolated from naturally fermented koumiss. It has high tolerance to acid environment and bile salt. High <i>in vitro</i> cell capacity.	High viability was observed >10 ⁸ CFU/g Probiotic yogurt had a higher elasticity index and lower solid–liquid balance. Cohesiveness and viscosity index were higher than the control. More EPS was determined.	(Bai et al., 2020)
<i>Lactobacillus helveticus</i> R0052	<i>Lb. helveticus</i> R0052 was provided in freeze dried form. It has potential health benefits.	They performed two different process for greek-style yogurt production and tested yogurt manufacturing provided higher probiotic count than probiotic yogurt.	(Moineau-Jean et al., 2019)
<i>Lactobacillus helveticus</i> H9	Isolated from Tibetan kurut with high angiotensin-converting enzyme-inhibitory (ACEI) and antihypertensive activities.	Improved milk acidification and proteolysis is observed. 15 key volatile compounds were detected. Increased ACEI activity is observed.	(Zhou et al.,2019)
<i>Lactobacillus casei</i> ATCC393	Isolation source is dairy products.	Probiotic cell immobilization provided higher viability during storage and improved protection during gastrointestinal passage. Sea buckthorn berries were successfully carrier for cell immobilization.	(Terpou et al.,2019)

<i>Streptococcus thermophilus</i> APC151	Isolation source is the digestive tract of fish. It can produce high level GABA.	Both yogurts indicated comparable pH profiles, viscosity, water holding capacity, and chemical composition. GABA was not determined in the control.	(Linares et al., 2016)
<i>Lactobacillus paracasei</i> , <i>Lactobacillus casei</i> and <i>Lactobacillus plantarum</i>	Isolated from Kimchi Bile salt and acid tolerance. They have beta galactosidase activity.	The probiotic counts were 1.0×10^9 CFU/mL during storage.	(Cho et al., 2013)
<i>Lactobacillus paracasei</i> ssp. <i>paracasei</i> and <i>Lactobacillus acidophilus</i>	Isolated from newborn infant faeces. They have ability to grow metabolize and goat milk to show resistance to ,gastrointestinal conditions, cholesterol removal , diacetyl production	The mixed culture provided growth enhancement, improved acidification and increased acetaldehyde. Potential probiotic bacteria amount was 10 times the minimal limit.	(Xanthopoulos et al.,2012)
<i>Lactobacillus casei</i> Zhang	Obtained from Koumis and it has high tolerance to digestion solutions and the results were similar to other commercial strains.	High acid production and proteolytic activity was reported. High viable count (1.0×10^9 CFU/mL) was observed during storage.	(Guo et al., 2009)

Aroma Cultures for Yogurt Production

Flavor is obtained by presence of variety of volatile compounds. Yogurt flavor can be result various parameters such as type of milk, processing conditions, type of starter bacteria and presence of other additives. Starter culture type affects acidification rate, kind and amount of aroma volatiles and nonvolatile metabolites of yogurt. During fermentation, several biochemical reactions achieve by enzymatic degradation and oxidation of fats, proteins, and carbohydrates in milk environment. All these reactions result in production of key volatile flavors in yogurt. In yogurt fermentation, LAB can produce over 400 volatiles compounds. In particular, volatile organic compounds have great impact on yogurt flavor, and many factors can affect the generation of this volatiles.Yogurt flavor compounds can be categorized into several classes (Farag et al., 2021) as followings:

- Non-volatile carboxylic acids (Examples; lactic, pyruvic acids)
- Volatile carboxylic acids (Examples; butyric and acetic acids)
- Carbonyl compounds (Examples; acetaldehyde)

- Diketones (Examples; diacetyl [2,3-butanedione] and 2,3-pentanedione)
- Other organic compounds (Examples; amino acids and byproducts formed by thermal degradation)

Mostly, carbonyl compounds such as acetaldehyde, acetone, 2-butanone, diacetyl, and ethyl acetate provide main contributions to typical yogurt flavor (Figure 2).

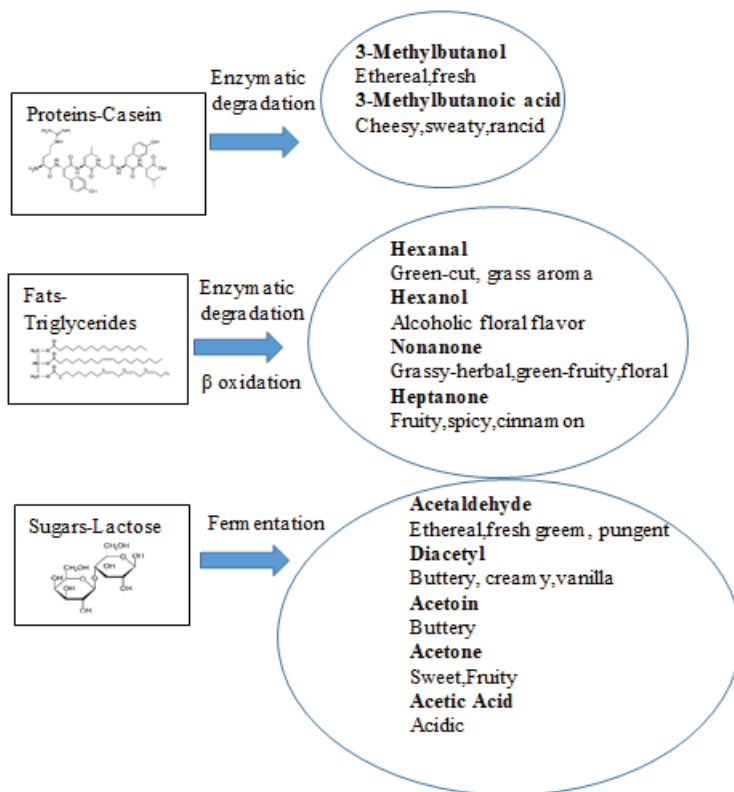


Figure 2: Main chemical reactions of milk components for key volatile flavor production in yogurt (Adapted by Farag et al., 2021)

The main flavor components of yogurt can also be grouped as volatile or non-volatile compounds. They can be already found in milk and also produced during fermentation process. Diverse volatile compounds were detected in yogurts and among them, acetaldehyde and diacetyl are known as characteristic compounds, and they are also considered indicators of yogurt quality (Tian et al., 2019). For yogurt aroma profiling several methods can be conducted. Headspace solid-phase microextraction (SPME) cou-

pled to gas chromatography and mass spectrometry (GC-MS) was widely used in yogurt volatile compounds. SPME has a fast sample preparation procedure and combines several steps into simplified form. Again, gas chromatography flame ionization detector was also proposed (GC-FID) for the analysis aromatic compounds (Farag et al., 2021).

Although common yogurt starter LAB cultures produce most of the important flavor compounds, specific carefully selected LAB strains can be developed and proposed as aroma adjunct cultures (Tian et al., 2019; Dan et al., 2020). Specific LAB strains that improve yogurt flavor can be used as aroma adjunct cultures. For example, some LAB strains can promote citrate metabolisms and produce acetoin, diacetyl, and 2, 3-butanediol (Tian et al., 2019).

In recent years, Tian et al. (2019) published a study on determining and selecting aroma producer lactic acid bacteria to improve aroma and flavor properties of yogurt. In this work, aroma producer strains were obtained from Tibetan kefir grains. Two *L. plantarum* strains were isolated and selected on their acetaldehyde and diacetyl production properties. Those bacteria were used as adjunct culture and positive effects on the aromatic profile of yogurt were observed. The isolated strains did not affect the acid development in the yogurt. The isolated strains increased the volatile metabolites such as acetaldehyde, diacetyl, and acetoin. Those aroma producer LAB strains provided higher acetaldehyde, diacetyl, and acetoin amounts than control production. At the end of the study, these two strains of *L. plantarum* were found to be suitable aroma cultures as adjuncts in yogurt production due to their contribution for the flavor characteristics of the end product. Carbonyl substances such as acetaldehyde, acetoin, and diacetyl were predominant in the aromatic profile. Acetaldehyde presents a green apple or nutty flavor. Acetaldehyde concentration of yogurt produced by adjunct cultures (*Lactobacillus plantarum* 1-33, 4.66 mg/L) was two times higher than control yogurt (2.40 mg/L). Moreover, diacetyl and acetoin also contribute butter and cream aroma of yogurt. These compounds can be generated by carbohydrate fermentation or citrate metabolism. Diacetyl concentration of yogurt produced by flavor cultures (*L. plantarum* 1-33, 9.03 mg/L, *L. plantarum* 1-34, 12.21 mg/L) were higher than control (3.36 mg/L). In addition, acetoin is another flavor compound it reduces the harshness of diacetyl and support a mild creamy flavor. Among acid compounds, acetic acid also plays important role in yogurt flavor. If the acetic acid concentration is too high a vinegar flavor can become a problem. Moreover, acetic acid concentration of yogurt produced by adjuncts, culture were lower than control yogurt. Another finding is the presence of lower dimethyl sulfate (1-34 (0.67 mg/L) concentration in yogurt produced by adjunct cultures than in control yogurt. The addition

of flavor adjunct culture can also improve the flavor properties of yogurt by inhibiting the generation of undesirable flavor compounds.

In the another study, the effect of probiotic cultures on aroma property was investigated (Papaioannou et al., 2021). *Bifidobacterium* BB-12-free cow's milk dessert yogurts contained acetaldehyde, 2,3-butanedione, 2,3-pentandione, 3-OH-2-butanone, 2-propanone, hexanoic acid and limonene as the main volatiles, while probiotic containing cow's milk yogurts contained acetaldehyde, pentanal, hexanal, the same ketones, acetic acid and limonene.

Texture Adjunct Cultures for Yogurt Production

Structural, rheological, and sensational properties are important for good quality yogurt. Numerous styles have been practiced to enhance the texture quality such as adding the solids in milk and adding stabilizers similar to pectin starch and gelatin. Still, these approaches have not met consumers' needs for products containing as many food additives as possible. As an alternative to these methods, exopolysaccharide (EPS) produced by LAB is an another natural alternative source. In the past years, EPS produced by LAB has been used as viscosifiers, texturizers, and emulsifying ingredients and is of special interest in the fermented milk industry. Polysaccharides, which are a polymeric molecule, consist of monosaccharides linked together in a long chain structure via glycosidic bonds. It is widely found in plants, animals and microorganisms. EPSs are a polysaccharide derivative produced by microorganisms that connect to the cell wall or are secreted into the surrounding. EPS, known as an aid in the communication process between cells, Also, plays an important role in protecting microorganisms against harsh conditions such as low water activity, low or high pH, osmotic stress, presence of antimicrobial or toxic compounds and phages (Tiwari et al., 2021).

In general, EPS is used as a stabilizer, emulsifier, viscosity increaser, gelling agent and water-binding agent to contribute to the consistency of many food products such as jam, jelly, yogurt, bread, and beverages. In similar way, EPS has also potential in yogurt and dairy products to develop its functional, technological and rheological properties. EPS can also improve the sensory properties (mouthful, shininess, clean-cut, ropiness, and creaminess) of yogurt (Tiwari et al., 2021). Moreover, syneresis, which is seen as a major problem in yogurt, can be reduced by EPS producing LAB strains (Han et al. 2016). In yogurt fermentation, the pH drops due the conversion of the lactose to lactic acid and casein micelles become unstable. During acid development (below pH 5.3), they irreversibly coagulate to form a gel. EPS have role in managing the shear of whey to stabilize the gel structure for thickness of the dairy product. EPS provides

contribution for improving rheological and textural properties in the end product. Several commercially available EPS producing LAB strains or the combinations for yogurt production are listed in Table 4. In addition to these technological benefits, EPS has also beneficial health properties such as antioxidant, antitumor and immunomodulatory effects, cholesterol reduction, and prebiotic role in the intestinal area (Zhu et al., 2018).

Table 4: Commercial EPS producing starter cultures for yogurt production (Tiwari et al., 2021)

Starter Code	Bacteria species	Company
HARMONY 1.0	<i>S. thermophilus</i> , <i>L. delbrueckii</i> ssp. <i>bulgaricus</i> , <i>L. fermentum</i>	Chr. Hansen, Denmark
TWIST 1.0	<i>S. thermophilus</i> , <i>L. jonhsonii</i> , <i>L. delbrueckii</i> ssp. <i>bulgaricus</i>	Chr. Hansen, Denmark
YF-L902	<i>S. thermophilus</i> , <i>L. delbrueckii</i> ssp. <i>bulgaricus</i>	Chr. Hansen, Denmark
YF-L901	ND	Chr. Hansen, Denmark
YO-FLEX PREMIUM 1	ND	Chr. Hansen, Denmark
YO-MIX 601, YO MIX 621	<i>S. thermophilus</i> , <i>L. delbrueckii</i> ssp. <i>bulgaricus</i>	Visby (Danisco cultor, Turkey)
ASCC-1275	<i>S.thermophilus</i>	Australian Starter Cultures Research Centre (Werribee, Australia)
CHCC-2389, CHCC-4239	<i>S. thermophilus</i> ,	Chr. Hansen Culture
CHCC-3984, CHCC-769	<i>L. delbrueckii</i> ssp. <i>bulgaricus</i>	Collection (CHCC)
NCDC-402, NCDC-399-K2 and NCDC-401 IG16 strain	<i>L. lactis</i> ssp. <i>lactis</i> , <i>S. thermophilus</i>	Natioanal collection of dairy cultures (NDRI, India)

Recently, Wang et al. (2022) investigated the fermentation properties of a new strain of *Leuconostoc mesenteroides* (XR1) and investigated the effect of EPS on the microstructure, texture, and rheological features of yogurt. This new strain was obtained from wild kefir grain environment. It has high EPS production property and favorable fermentation characteristics. Added EPS enhanced the water holding capacity (WHC) and modified microstructure. Moreover, the steric barrier created between EPS and protein molecules increased viscoelastic properties and fermented milk containing EPS had more complex viscosity. As a result, it has been proven that XR1 EPS as more natural organic additive can reduce the using of

chemical additives in dairy products.

Amatayakul et al. (2006) compared the whey separation patterns in set yogurts and they examined the effect of solid content and adding of EPS producing cultures on whey separations. In this study, four strains were tested as; non-EPS-producing *Streptococcus thermophilus* ASCC 1342, *Lactobacillus delbrueckii* ssp. *bulgaricus* ASCC 1466, capsular EPS-producing *S. thermophilus* ASCC 285, and ropy EPS-producing *S. thermophilus* ASCC 1275. Whey separation levels were determined. Yogurt made with EPS producing strain exhibited a greater reduction in whey separation in both solid components than yogurt made with non-EPS starter by the siphon method. There was no difference in the whey separation measured by the drainage method between yogurts with the same solid amount (9% and 14%). Higher whey separation at 9% solids, as determined by centrifugation, was observed in yogurts made with EPS starter cultures compared to non-EPS producing strains.

In another study, Han et al. (2016) tested the EPS and viscosity of milk fermented by 19 *S. thermophilus* isolates. Isolates were obtained from Chinese dairy products they had high exopolysaccharide production. The EPS content of fermented milk using *S. thermophilus* zlw TM11 strains was 380 mg/L. This fermented milk had viscosity of 7716 mpa/s. *S. thermophilus* zlw TM11 strains was selected because of this high exopolysaccharide content and high viscosity properties. Later, this strain was used in combination with *L. bulgaricus* and this combination was designated SH-1. The quality of yogurt fermented with SH-1 and two commercial starter cultures was compared. The exopolysaccharide content of SH-1 fermented yogurt was shown to be similar to that of YF-L711 fermented yogurt and significantly higher than YO-MIX 465. Moreover, yogurt fermented with SH-1 had the lowest syneresis (8.5%) and better texture and feel than yogurts fermented with YO-MIX 465 and YF-L711. It revealed that the proposed EPS producer starter SH-1 could be used in the industrial productions and reduces the amount of stabilizer addition.

In recent years, Morais et al (2021) analyzed the potential of *Limosilactobacillus mucosa* CNPC007 as an autochthonous culture in the production of goat's milk Greek yogurt. In this study, techno-functional, physicochemical and sensory properties of control yogurt containing only starter culture and probiotic yogurt were evaluated. According to the results, yogurt added to the probiotic strain had a lower proteolysis index. Yogurt with added probiotic strain has almost 1.5 times higher viscosity than control yogurt. This result was achieved due to the higher production of exopolysaccharides.

Biopresevative Adjunct Cultures in Yogurt Production

In yogurt production, particularly fungal spoilage can cause some problems. Spoilage microorganism with their metabolites and enzymes cause undesirable changes and deterioration in dairy products. Although some chemical preservatives can be used in different countries in yogurt production, they are not permitted by regulations in Turkey. Defined cultures or their metabolites, or the combination of both, can be designed as biopreservative for extending shelf-life of yogurt and preventing microbial spoilage.

In recent years, there is an increasing consumer and commercial trends for reducing chemical preservatives. The evolution of European legislation has directed industries to reduce the chemical preservatives in fermented milk products. At this point, the use of microbial cultures that control spoilage microorganisms has valuable potential (Delavenne et al., 2013).

Common biopreservative microorganisms include LAB. Also, various metabolites, bacteriocins and natural enzymes systems can be used as biopreservatives. Biopreservative cultures can be used in different food industries such as baking, fruit and vegetables and dairy (Buehler et al., 2018). Although there have been many studies for biopreservative cultures in different food production areas, limited research has existed in yogurt production.

In recent years, Fayyaz et al. (2020) evaluated the protective properties of *Lactobacillus* binary/ ternary culture combinations in yogurt production. They used 3 lactic acid bacteria (*L. reuteri*, *L. helveticus*, *L. acidophilus*) in combinations against 5 spoilage yeast (*Debaryomyces hansenii*, *Rhodotorula mucilaginosa*, *Kluyveromyces marxianus*, *Kluyveromyces lactis*, *Yarrowia lipolytica*). They characterized yogurt samples during fermentation and storage by determining acidity, WHC (water holding capacity), apparent viscosity, texture profile analysis, enumeration of LAB and sensory analysis. Significant reduction in pH during cold storage was found. Including of protective cultures resulted increase in WHC during fermentation and storage. Increase in WHC due to the decrease in pH seems in parallel to LAB growth and it leads enhancing in yogurt curd stability. Also, increase in hardness and adhesiveness was observed. In the result of antifungal analysis, *Lactobacillus reuteri* was the most active LAB against yeast species and it was followed by *Lactobacillus acidophilus*. Moreover, *Kluyveromyces marxianus* was the most resistant yeast and it was followed by *Rhodotorula mucilaginosa*. Finally, they suggest that inoculation of LAB strains at 5% (v/v) can enhance both biochemical and sensorial properties and provide efficient preservation. Those cultures can be used to replace the chemical preservatives or reduce their amounts and can be used as biocontrol agents in other commercial applications.

Buehler et al. (2018) evaluated the potential of two commercially

available protective cultures against fungi spoilage in Greek yogurt production. They produced yogurt with and without biopreservative cultures by inoculating a cocktail of 5 yeast and one mold with two inoculum levels (10^1 and 10^3 CFU/g). After storing at 7 °C and fungal numbers were determined. At day 23 of storage, fungal concentrations reached the spoilage stage ($\geq 10^5$ CFU/g) in all productions at both cell concentrations. Surface mold over 76 days was not observed in any of the formulations with preservative cultures. At the end of the study, all of the control yogurts without biopreservative cultures showed surface mold up to day 23.

CONCLUSIONS

Overall marketability of yogurt can be improved by different technologies and by developing new adjunct cultures. Among those studies, probiotic yogurts have been more focused and studied in comprehensively. Yogurt is one of the most preferred environments to deliver probiotics to consumers. For the development of probiotic yogurt, it is necessary to select strains with strong probiotic features with acceptable safety, technological, sensory and functional properties. The sensory properties of probiotic yogurt may negatively affect consumer acceptability; therefore, carefully selected probiotic strains should keep or improve organoleptic features. Within in the advance in developing new strains with different health claims, wide range of probiotic yogurt products in the market can be expected in the future works.

Another research area for adjunct culture development is on flavor cultures. One of the most important features in consumer perception is the aroma of yogurt. However, the aroma preferences differ according to geography around the world. The reactions that occur during the making of yogurt affect the taste of yogurt, such as enzymatic degradation, oxidation and fermentation. Adjunct cultures that improve flavor properties of yogurt can attract the marketability of different kinds of yogurts.

Also, specific cultures that improve texture profiles of yogurt can be designed. In particular EPS producing strains have important potential and can be used in different combinations. Moreover, biopreservative cultures can provide the extension the shelf life by inhibiting the undesirable mold and yeast growth. The results of these researches can provide valuable contributions to meet consumer demands for clean-label products.

Adjunct cultures designed for specific aims should meet consumer preferences for yogurt quality. Understanding consumer preferences is one the important feature for product development and it presents significant variations around the world in different geography and publics. Those cultures should not generate undesirable chemical and physical properties and should be compatible with yogurt starter cultures.

REFERENCES

- Akpınar, A., Saygili, D., & Yerlikaya, O. (2020). Production of set-type yoghurt using *Enterococcus faecium* and *Enterococcus durans* strains with probiotic potential as starter adjuncts. *International Journal of Dairy Technology*, 73(4), 726-736.
- Amatayakul, T., Sherkat, F., & Shah, N. P. (2006). Syneresis in set yogurt as affected by EPS starter cultures and levels of solids. *International Journal of Dairy Technology*, 59(3), 216-221.
- Bai, M., Huang, T., Guo, S., Wang, Y., Wang, J., Kwok, L. Y., ... & Bilige, M. (2020). Probiotic *Lactobacillus casei* Zhang improved the properties of stirred yogurt. *Food Bioscience*, 37, 100718.
- Buehler, A. J., Martin, N. H., Boor, K. J., & Wiedmann, M. (2018). Evaluation of biopreservatives in Greek yogurt to inhibit yeast and mold spoilage and development of a yogurt spoilage predictive model. *Journal of dairy science*, 101(12), 10759-10774.
- Cao, J., Yu, L., Zhao, J., Zhang, H., Chen, W., & Zhai, Q. (2022). Genomic analysis of *B. coagulans* ATCC 7050T reveals its adaption to fermented milk as an adjunct starter culture for yogurt. *LWT*, 154, 112721.
- Cho, Y. H., Hong, S. M., & Kim, C. H. (2013). Isolation and characterization of lactic acid bacteria from kimchi, Korean traditional fermented food to apply into fermented dairy products. *Food Science of Animal Resources*, 33(1), 75-82.
- Das, K., Choudhary, R., & Thompson-Witrick, K. A. (2019). Effects of new technology on the current manufacturing process of yogurt-to increase the Das, K., Choudhary, R., & Thompson-Witrick, K. A. of yogurt. *Lwt*, 108, 69-80.
- Delavenne, E., Ismail, R., Pawtowski, A., Mounier, J., Barbier, G., & Le Blay, G. (2013). Assessment of lactobacilli strains as yogurt bioprotective cultures. *Food Control*, 30(1), 206-213.
- Erkuş, O. (2007). *Isolation, phenotypic and genotypic charecterization of yoghurt starter bacteria*. Izmir Institute of Technology (Turkey).
- Farag, M. A., Saleh, H. A., El Ahmady, S., & Elmassry, M. M. (2021). Dissecting yogurt: The impact of milk types, probiotics, and selected additives on yogurt quality. *Food Reviews International*, 1-17.
- Fayyaz, N., Shahidi, F., & Roshanak, S. (2020). Evaluation of the bioprotectivity of *Lactobacillus* binary/ternary cultures in yogurt. *Food Science & Nutrition*, 8(9), 5036-5047.
- Fisberg, M., & Machado, R. (2015). History of yogurt and current patterns of consumption. *Nutrition reviews*, 73(suppl_1), 4-7.
- Gao, J., Li, X., Zhang, G., Sadiq, F. A., Simal-Gandara, J., Xiao, J., & Sang, Y. (2021). Probiotics in the dairy industry—Advances and opportuni-

- ties. *Comprehensive Reviews in Food Science and Food Safety*, 20(4), 3937-3982.
- Gu, Y., Li, X., Xiao, R., Dudu, O. E., Yang, L., & Ma, Y. (2020). Impact of *Lactobacillus paracasei* IMC502 in coculture with traditional starters on volatile and non-volatile metabolite profiles in yogurt. *Process Biochemistry*, 99, 61-69.
- Guo, Z., Wang, J., Yan, L., Chen, W., Liu, X. M., & Zhang, H. P. (2009). In vitro comparison of probiotic properties of *Lactobacillus casei* Zhang, a potential new probiotic, with selected probiotic strains. *LWT-Food Science and Technology*, 42(10), 1640-1646.
- Han, X., Yang, Z., Jing, X., Yu, P., Zhang, Y., Yi, H., & Zhang, L. (2016). Improvement of the texture of yogurt by use of exopolysaccharide producing lactic acid bacteria. *BioMed research international*, 2016.
- Holzapfel, W. H., R. Geisen, and U. Schillinger. 1995. Biological preservation of foods with reference to protective cultures, bacteriocins and food-grade enzymes. *Int. J. Food Microbiol.* 24:343–362.
- Irlinger, F., Hélinck, S., & Jany, J. L. (2017). Secondary and adjunct cultures. In *Cheese* (pp. 273-300). Academic Press.
- Kalkan, S., Öztürk, D., & Selimoğlu, B. S. (2018). Determining some of the quality characteristics of probiotic yogurts manufactured by using microencapsulated *Saccharomyces cerevisiae* var. *boulardii*. *Turkish Journal of Veterinary & Animal Sciences*, 42(6), 617-623.
- Linares, D. M., O'Callaghan, T. F., O'Connor, P. M., Ross, R. P., & Stanton, C. (2016). *Streptococcus thermophilus* APC151 strain is suitable for the manufacture of naturally GABA-enriched bioactive yogurt. *Frontiers in Microbiology*, 7, 1876.
- Moineau-Jean, A., Champagne, C. P., Roy, D., Raymond, Y., & LaPointe, G. (2019). Effect of Greek-style yoghurt manufacturing processes on starter and probiotic bacteria populations during storage. *International Dairy Journal*, 93, 35-44.
- Motahari, P., Mirdamadi, S., & Kianirad, M. (2017). Safety evaluation and antimicrobial properties of *Lactobacillus pentosus* 22C isolated from traditional yogurt. *Journal of Food Measurement and Characterization*, 11(3), 972-978.
- Mohammadi, A. A., Jazayeri, S., Khosravi-Darani, K., Solati, Z., Mohammadpour, N., Asemi, Z., ... & Eghtesadi, S. (2016). The effects of probiotics on mental health and hypothalamic–pituitary–adrenal axis: a randomized, double-blind, placebo-controlled trial in petrochemical workers. *Nutritional neuroscience*, 19(9), 387-395.
- Morais, J. L., Garcia, E. F., Viera, V. B., Pontes, E. D. S., de Araújo, M. G. G., de Figueirêdo, R. M. F., ... & de Oliveira, M. E. G. (2022). Autochthonous adjunct culture of *Limosilactobacillus mucosae* CNPC007 improved the

techno-functional, physicochemical, and sensory properties of goat milk Greek-style yogurt. *Journal of Dairy Science*.

Nyanzi, R., Jooste, P. J., & Buys, E. M. (2021). Invited review: Probiotic yogurt quality criteria, regulatory framework, clinical evidence, and analytical aspects. *Journal of Dairy Science*, 104(1), 1-19.

Papaioannou, G. M., Kosma, I. S., Dimitreli, G., Badeka, A. V., & Kontominas, M. G. (2022). Effect of starter culture, probiotics, and flavor additives on physico-chemical, rheological, and sensory properties of cow and goat dessert yogurts. *European Food Research and Technology*, 1-12.

Papaioannou, G., Kosma, I., Badeka, A. V., & Kontominas, M. G. (2021). Profile of Volatile Compounds in Dessert Yogurts Prepared from Cow and Goat Milk, Using Different Starter Cultures and Probiotics. *Foods*, 10(12), 3153.

Roobab, U., Batool, Z., Manzoor, M. F., Shabbir, M. A., Khan, M. R., & Aadil, R. M. (2020). Sources, formulations, advanced delivery and health benefits of probiotics. *Current Opinion in Food Science*, 32, 17-28.

Shori, A. B. (2021). Application of *Bifidobacterium* spp in beverages and dairy food products: an overview of survival during refrigerated storage. *Food Science and Technology*.

Soni, R., Jain, N. K., Shah, V., Soni, J., Suthar, D., & Gohel, P. (2020). Development of probiotic yogurt: Effect of strain combination on nutritional, rheological, organoleptic and probiotic properties. *Journal of Food Science and Technology*, 57(6), 2038-2050.

Terpou, A., Papadaki, A., Bosnea, L., Kanellaki, M., & Kopsahelis, N. (2019). Novel frozen yogurt production fortified with sea buckthorn berries and probiotics. *LWT*, 105, 242-249.

Tian, H., Shi, Y., Zhang, Y., Yu, H., Mu, H., & Chen, C. (2019). Screening of aroma-producing lactic acid bacteria and their application in improving the aromatic profile of yogurt. *Journal of Food Biochemistry*, 43(10), e12837.

Tiwari, S., Kavitate, D., Devi, P. B., & Shetty, P. H. (2021). Bacterial exopolysaccharides for improvement of technological, functional and rheological properties of yoghurt. *International Journal of Biological Macromolecules*, 183, 1585-1595.

Wang, L., Gu, Y., & Lv, Z. Processing properties of yogurt as affected by the EPS produced by *Leuconostoc mesenteroides* XR1. *International Journal of Food Science & Technology*. (2022)

Xanthopoulos, V., Ipsilandis, C. G., & Tzanetakis, N. (2012). Use of a selected multi-strain potential probiotic culture for the manufacture of set-type yogurt from caprine milk. *Small ruminant research*, 106(2-3), 145-153.

Yildiz, F. (2016). *Development and manufacture of yogurt and other functional dairy products*. CRC press.

Zahed, O., Khosravi-Darani, K., Mortazavian, A. M., & Mohammadi, A. (2021).

Bacterial conjugated linoleic acid bio-fortification of synbiotic yogurts using *Propionibacterium freudenreichii* as adjunct culture. *Italian Journal of Food Science*, 33(SP1), 1-11.

- Zhou, T., Huo, R., Kwok, L. Y., Li, C., Ma, Y., Mi, Z., & Chen, Y. (2019). Effects of applying *Lactobacillus helveticus* H9 as adjunct starter culture in yogurt fermentation and storage. *Journal of dairy science*, 102(1), 223-235.
- Zhu, Y., Wang, X., Pan, W., Shen, X., He, Y., Yin, H., ... & Liu, S. (2019). Exopolysaccharides produced by yogurt-texture improving *Lactobacillus plantarum* RS20D and the immunoregulatory activity. *International journal of biological macromolecules*, 121, 342-349.



CHAPTER 2

THREE-PHASE POWER MEASUREMENT WITH dsPIC

Erdem ILTEN¹, Haris CALGAN², Metin DEMİRTAS³

1 Dr. Öğr. Üyesi, Balıkesir Üniversitesi, Mühendislik Fakültesi, Elektrik-Elektronik Mühendisliği Bölümü, Kontrol ve Kumanda Sistemleri ABD E-mail: erdemilten@balikesir.edu.tr

2 Dr., Balıkesir Üniversitesi, Mühendislik Fakültesi, Elektrik-Elektronik Mühendisliği Bölümü, Elektrik Makinaları ABD E-mail: haris.calgan@balikesir.edu.tr

3 Prof. Dr., Balıkesir Üniversitesi, Mühendislik Fakültesi, Elektrik-Elektronik Mühendisliği Bölümü, Elektrik Makinaları ABD E-mail: mdtas@balikesir.edu.tr

1. INTRODUCTION

Power measurement modules are used in the various industrial systems such as electrical vehicles, electronic components, circuits etc. They are employed to measure output powers that translate electrical quantities into digital signals. Thanks to technological advances, these kinds of data acquisition systems become cheaper, light weighted and easier programmable. With the more powerful microprocessors as well as signal processing techniques, the simultaneous power measurement can be done accurately.

Generally, three-phase power measurement systems have high price with restricted operation range. They require three phase voltage and currents, and calculate the active, reactive powers and power factor. However, they need a powerful microcontroller with adequate memory to calculate the frequency and phase angles. Moreover, digital filters and detecting algorithms may cause performance losses. To deal with these challenges, more powerful microcontroller can be employed. But this time, there will be a price increase and complexity in algorithm.

Technological developments have increased the performance of data acquisition systems, allowing measurements made with special equipment, and the application of cheaper methods with the same accuracy. Devices that are constantly being developed with increases in analog-to-digital conversion performance allow more powerful signal processing techniques to be applied in industrial applications. Especially microcontroller devices are used in industrial applications with other electronic components to measure data such as voltage, current, power and to control the system. In electrical networks, dsPICs (Digital Signal Peripheral Interface Controller) are widely utilized to design electronic meters to measure current, voltage, power, power factor, electrical energy, etc. These meters display the active power, reactive power, power factor on LCD or LED display. Some of them have capable of sending energy consumption information to remote places via the internet or global system for mobile communications.

Santos and Ramos used a dsPIC microcontroller as processor and a DDS (Direct Digital Synthesizer) to simulate the proposed measurement circuit. Their test circuit is composed by reference impedance and unknown impedance components. dsPIC is communicated with a PC by RS-232 to USB converter to store data. Then the results are analyzed. LCD is used to display the measurement results (Santos & Ramos, 2011).

Arote et al. presented an electronic three-phase four-wire energy meter. All data are received in the digital domain to evaluate the results. The proposed meter shows the voltage, current, active and reactive Power, and power factor on the display (Arote et al., 2016).

Villani et al. studied low-cost power meter for three-phase systems. The proposed power meter can be measure current and voltage signals, simultaneously. It provided precise measurements which are power factor, apparent, active and reactive powers (Villani et al., 2016).

Altomonte et al. developed a cloud-connected smart energy meter for single and polyphase measurement. The evaluation process is executed by STPM3x chips consisting of an analog and a digital section (Altomonte et al., 2021). The study was implemented in three stages.

Grigoras and Neagu designed a smart meter data-based three-stage algorithm to calculate the power/energy losses in three-phase networks (Grigoras & Neagu, 2019).

Mukaila et al. designed a single-phase power factor meter. They used the zero crossing detection method to calculation of power factor. Arduino and LCD are used to evaluate the data taken from the system and to show the information on the screen. Input voltage and current signals are sent to op-amp by means of transformers to determine the power factor. A potentiometer is used to adjust the LCD contrast (Mukaila et al., 2020).

P. D. More et al. presented a study about the microcontroller-based smart calibration meter, which includes AC voltmeter and ammeter, watt-meter, and energy meter calibration. This study consists of three parts: control, metering and display. The atmega328p microcontroller was used to control and program the system (More, et al., 2018).

Guia et al. developed Root Mean Square (RMS) measurement system based on fast discrete Wavelet by using dsPIC33FJ32GP202 microcontroller. The method can be used as real-time in sinusoidal and non-sinusoidal electrical power systems. MATLAB and Proteus ISIS were used for simulations (Guia et al., 2020).

The instrument developed in this work strives to obtain more precise power measurement module that controlled by a dsPIC. The utilized microcontroller controls the entire hardware by taking all of the signals and by progressing as analog digital converters and by calculating the necessary outputs. The most important signal processing in this hardware is the digital filters and phase locked loop algorithms. These features allow the estimation of the powers and power factor regardless of being effected by sensor noises.

As aforementioned before, this type of hardware design requires advance programming skills. However, Matlab/Simulink program is employed here to develop the required algorithms. Afterwards, by means of MPLAB Device Blocks for Simulink, the created algorithm is compiled and deployed to the dsPIC (Ilten, 2022). The most valuable advantage of

this method lies on graphical programming of dsPIC (Ilten et al., 2022).

This chapter is organized as follows: three phase measurements are given in the second section. In the third section, microcontroller-based experimental realization of the designed method is explained and simulated. The fourth section provides a brief discussion with results. Finally, the conclusion is the last section.

2. THREE-PHASE MEASUREMENT

Three-phase voltages and currents are measured by 10-bit analog to digital converter (ADC) unit of dsPIC via 6 channels sequentially. The ranges of ADC inputs are between 0-3.3 V_{dc}. Therefore, all values to be read are scaled to the 0-3.3 V_{dc} range. Scaling operations are performed on the electrical circuit. Obtained digital values are used to calculate the root mean square (RMS) voltages (V) and currents (A). Also, frequency (Hz), power factor, active (W) and reactive power (VAR) are calculated via this data. These calculations are explained in the following sub-sections. dsPIC pins (dsPIC33FJ32MC204) are presented in Figure 2.1 (Microchip, 2012).

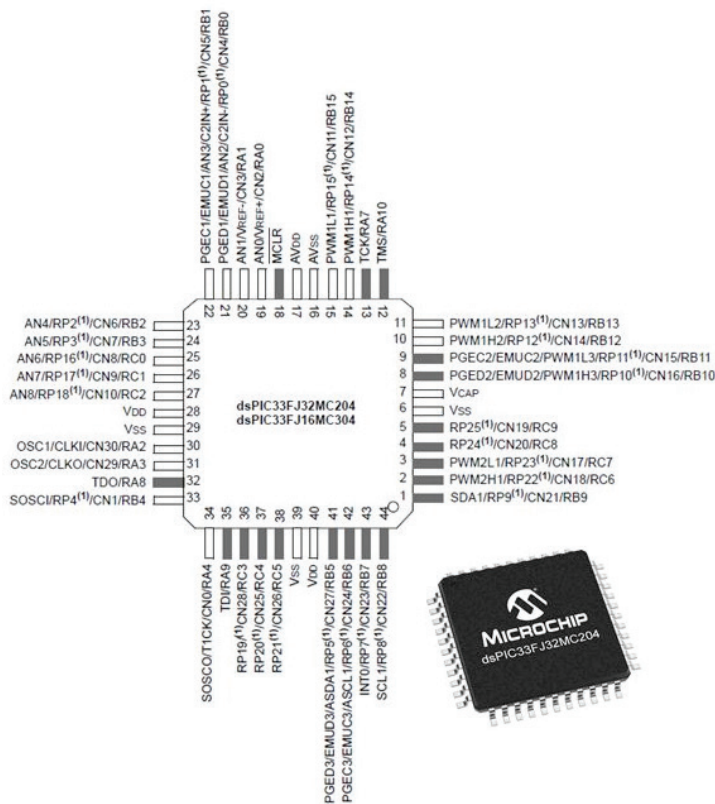


Figure 2.1: *dsPIC* pins

2.1 Voltage measurement

Each phase voltage is measured via ADC and calculated as RMS value in dsPIC algorithm. RMS voltage calculation block diagram for single phase is presented in Figure 2.2.



Figure 2.2: *RMS voltage calculation*

In Figure 2.2, measured digital value (ADC output) is converted to

voltage with multiplied by $\frac{3.3}{2^{10}}$. Then, by subtracting 1 at this value, the offset in the measuring circuit is removed. Sliding window method is used in the RMS calculation part. Sliding window method is given in Figure 2.3.

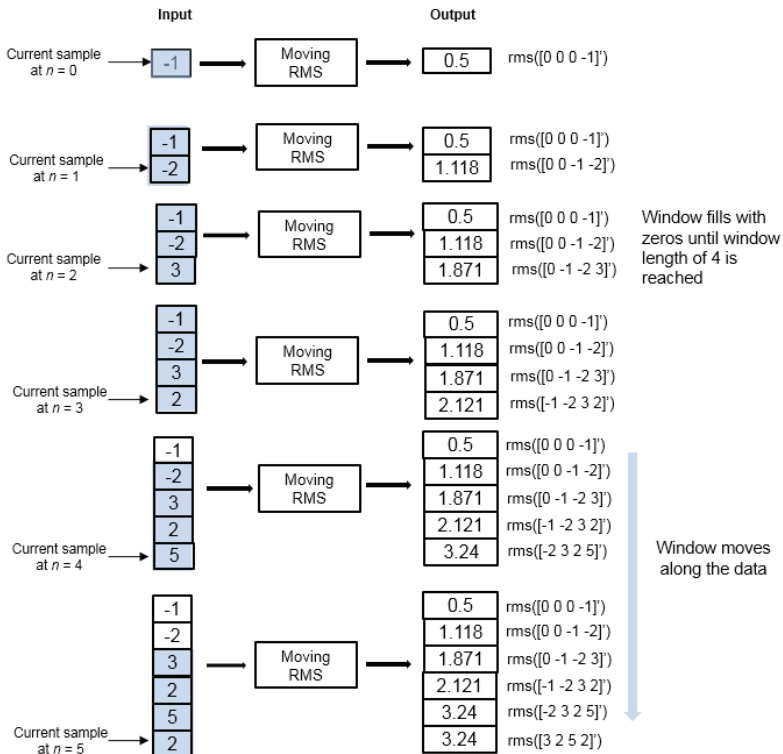


Figure 2.3: *Sliding window method of RMS calculation*

When calculating RMS in the sliding window method, the current sample and the previous $L_{en}-1$ sample are included in the calculation. L_{en} is the length of the sliding window. When calculating the initial $L_{en}-1$ values, the algorithm fills the sliding window with zeros because the window does not yet have enough data (MathWorks, 2021). Finally, the calculated RMS value was multiplied by $220\sqrt{2}$ because the amplitude of power supply is set to 1 V.

2.2 Current measurement

Each phase current is measured via ADC and calculated as RMS value in dsPIC algorithm. RMS current calculation block diagram for single phase is presented in Figure 2.4.



Figure 2.4: RMS current calculation

In Figure 2.4, measured digital value (ADC output) is converted to

current with multiplied by $\frac{3.3}{2^{10}}$. Then, by subtracting 1 at this value, the offset in the measuring circuit is removed. Sliding window method is used in the RMS calculation part same as voltage calculation. Lastly, the calcu-

lated RMS value was multiplied by 50 ($\frac{1}{50}$ is the gain value for currents in electric circuit) and was brought to true current scale.

2.3 Frequency measurement

Frequency is measured on single phase. Phase-locked loop method is used for frequency and phase angel calculation as shown in Figure 2.5.

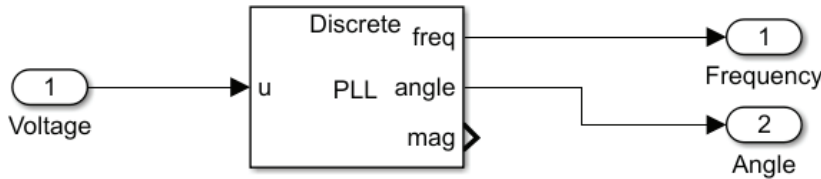


Figure 2.5: Frequency and phase angel calculation

PLL block generates a sinus signal that approximates to $u(t)$ as below (MathWorks, 2021):

$$y(t) = A(t) \sin\left(\phi_0 + \int 2\pi f(t) dt\right)$$

Here $y(t)$ and A are the estimate of $u(t)$ and estimate of amplitude of $u(t)$, respectively. ϕ_0 is the initial phase angle of $u(t)$. The estimated phase angle ϕ can be defined as follows (MathWorks, 2021):

$$\phi(t) = \phi_0 + \int 2\pi f(t) dt$$

In the above equation, f is the frequency. Figure 2.6 shows the overall structure of the PLL (MathWorks, 2021).

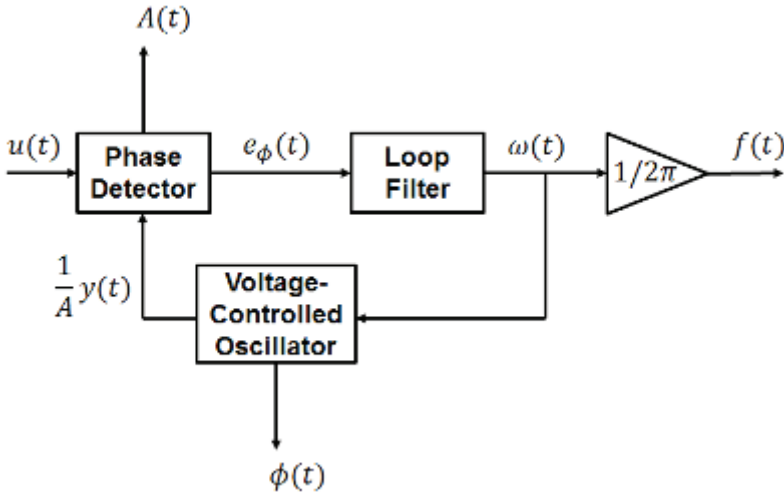


Figure 2.6: PLL structure

In Figure 2.6, the phase detector generates an error signal according to e_ϕ (phase difference). The phase detector also generates an estimate output of the amplitude A . Loop filter block provides an estimation of ω by filtering out the high-frequency components of e_ϕ . The voltage-controlled oscillator produces the angular speed to calculate ϕ (estimated phase angle).

This block also produces $\frac{1}{A}y$ (normalized-synthesized sinusoid). Simulink block diagram of PLL is given in Figure 2.7.

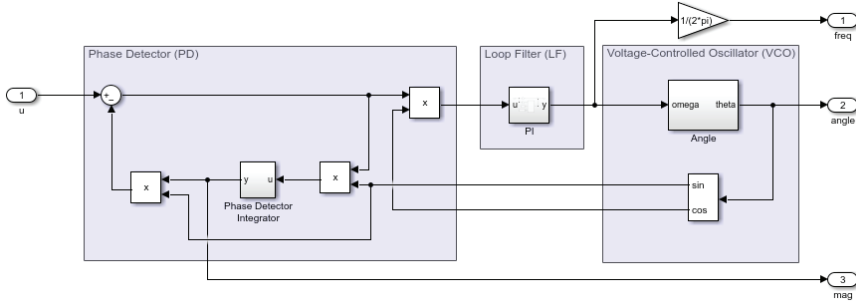


Figure 2.7: PLL Simulink block diagram

2.4 Power factor measurement

Power factor is cosine of phase angle difference of voltage and current signals. Phase angles are calculated via PLL blocks for single phase. Phase angle difference and power factor are calculated as illustrated in Figure 2.8.

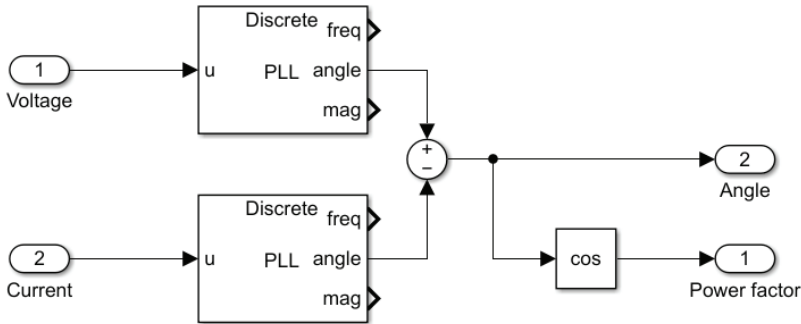


Figure 2.8: Phase angle difference and power factor calculation

2.5 Active and reactive power measurement

Active and reactive powers are calculated for single phase as follows:

$$P = U * I * \cos \varphi$$

$$Q = U * I * \sin \varphi$$

Where P is the active power as Watt (W), Q is the reactive power as Volt-Ampere reactive (VAr), φ is the phase angle difference as radian. Three phase active and reactive powers for balanced system are calculat-

ed by multiplying the power equations of the single phase by 3 as shown below:

$$P_{3\phi} = 3 * U * I * \cos \varphi$$

$$Q_{3\phi} = 3 * U * I * \sin \varphi$$

Where $P_{3\phi}$ is the three phase active power and $Q_{3\phi}$ is the three phase reactive power. Balanced three phase active and reactive powers are calculated in Simulink as shown in Figure 2.9.

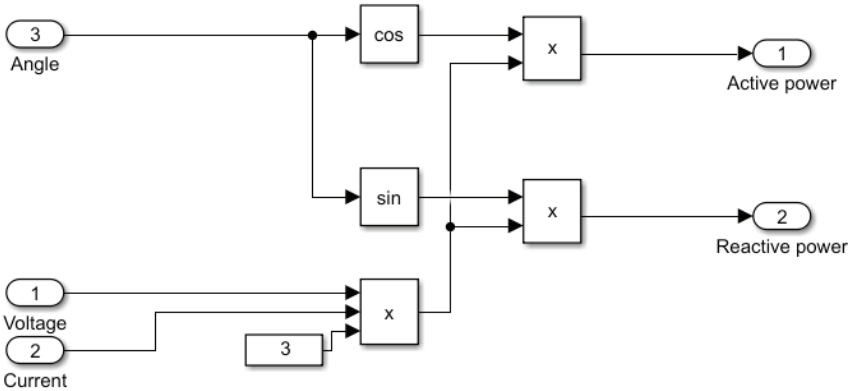


Figure 2.9: Active and reactive power calculation

3. SIMULATIONS

Three-phase voltages and currents, frequency, power factor, active and reactive powers are calculated via dsPIC and monitored on 20x4 LCD. dsPIC algorithm is designed on Simulink as shown in Figure 3.1.

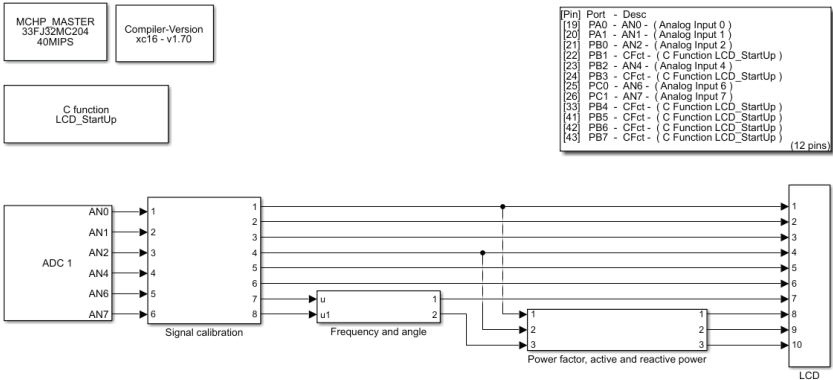


Figure 3.1: Simulink scheme of the measurement system

Firstly, the three-phase current and voltage values read with the ADC block in Figure 2.9 are calibrated. Then, current and phase angle are calculated over a phase. Then power factor, active power and reactive power are calculated. Finally, all the calculated values are printed on the LCD. The simulation of the designed system has been made in Proteus program. The prepared circuit diagram is given in Figure 3.2.

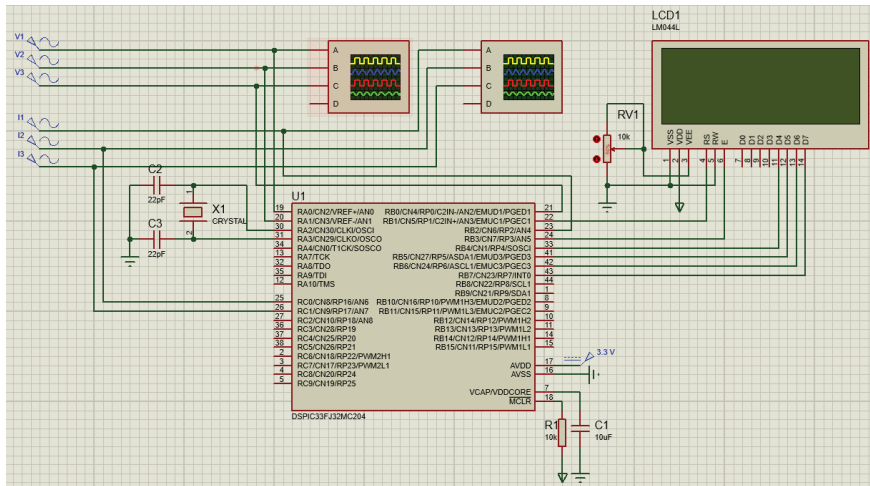


Figure 3.2: *Proteus simulation scheme for the measurement system*

In Figure 3.2, transducer connections are made to the microcontroller ADC input for three-phase current and voltage measurement. LCD connection is provided via D port. The simulation test result is presented in Figure 3.3.

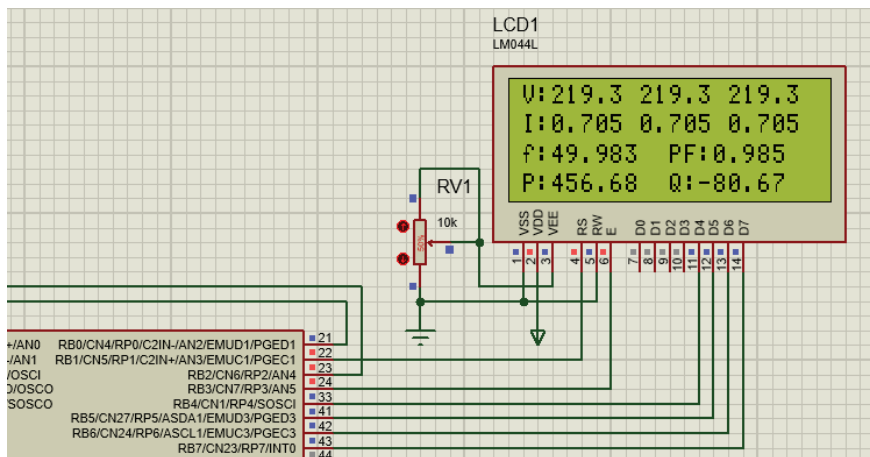


Figure 3.3: *Simulation test for the measurement system*

Figure 3.3 gives the display of values on the LCD. Phase voltages are displayed in the first line, phase currents in the second line, frequency and power factor in the third line, active and reactive power in the last line. Scope view of transducer outputs for three-phase voltages and currents are illustrated in Figure 3.4 and Figure 3.5.

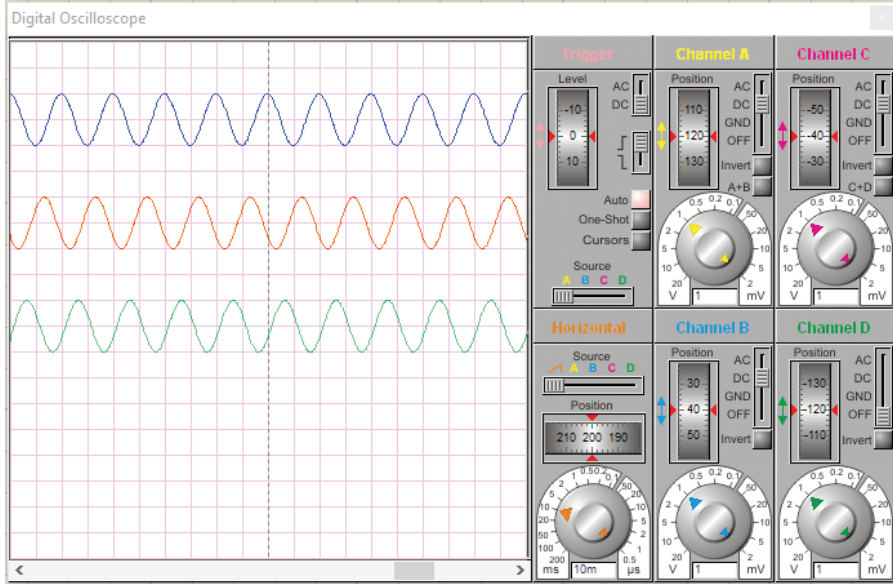


Figure 3.4: The outputs of voltage transducers (U_a , U_b , U_c)

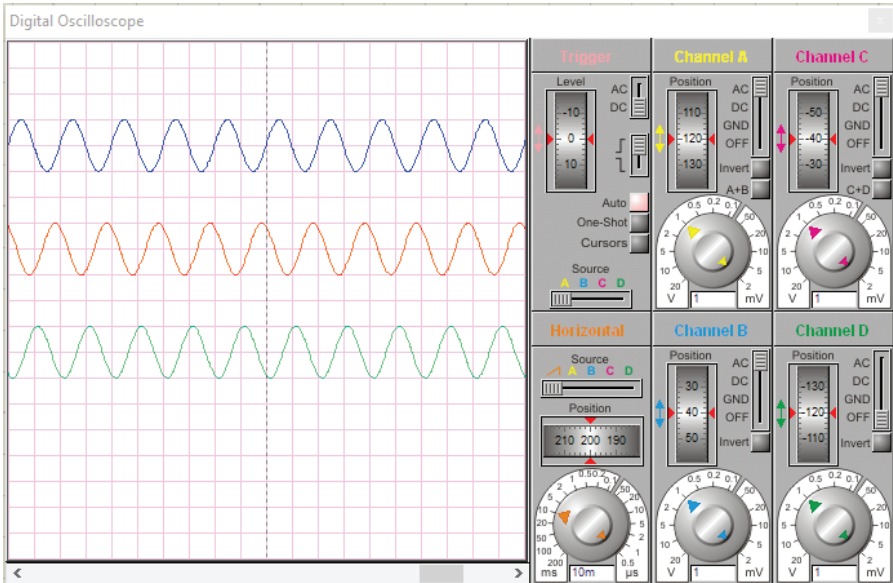


Figure 3.5: The outputs of current transducers (I_a , I_b , I_c)

CONCLUSION

This paper presents a digital platform that has low-cost and simple programming methods to calculate active power, reactive power, frequency, and power factor by using MATLAB/Simulink tools. The obtained results are shown on the screen of LCD. The control software is developed in the MATLAB/Simulink environment, which provides simple and intuitive programming tools. Thus, implementation of the software application becomes very simple and easy for power measurement. The algorithm used for the calculation is compiled and loaded to the dsPIC by MPLAB device blocks. This method is very easy compared to PIC programming code written and provides great convenience to programmers. The developed digital instrument is capable of measuring power in the amplitude range from 0 Watt to 15 kWatt at frequencies ranging from 18 Hz up to 81 Hz. USB and RS-232 connections provide ease of communication with the PC for the users. The results verified that a low-cost device and simple programming algorithm provide a digital meter capable of producing accurate results on measurement of power, frequency and power factor and etc.

REFERENCES

- Altomonte, A., Arena, F., Riccio, M., & Irace, A. (2021). A New Three-Phase Smart Meter for Cloud Connection: Network Architecture and Performances. *Engineering Proceedings*, 10(1), 46.
- Arote, S., Mulay, G. N., & Khaparde, A. (2016). Design and implementation of smart three phase energy meter. *2016 International Conference on Smart Grid and Clean Energy Technologies (ICSGCE)*, 44–49.
- Grigoras, G., & Neagu, B.-C. (2019). Smart Meter Data-based three-stage algorithm to calculate power and energy losses in low voltage distribution networks. *Energies*, 12(15), 3008.
- Guia, H. E., Soukkou, A., Meneceur, R., & Mohrem, A. (2020). Design and Implementation of Real Time RMS Measurement System based on Wavelet Transform Using dsPIC-type Microcontroller. *International Journal of Image, Graphics and Signal Processing (IJIGSP)*, 12(6), 43–56.
- Ilten, E. (2022). Conformable fractional order controller design and optimization for sensorless control of induction motor. *COMPEL-The International Journal for Computation and Mathematics in Electrical and Electronic Engineering*.
- Ilten, E., Calgan, H., & Demirtas, M. (2022). Design of induction motor speed observer based on long short-term memory. *Neural Computing and Applications*, 34(21), 18703–18723.
- MathWorks. (2021). *MATLAB documentation*. The MathWorks.
- Microchip. (2012). *dsPIC33FJ32MC204 datasheet*. <https://www.microchip.com/en-us/product/dsPIC33FJ32MC204>
- Mukaila, A. A., Olugbemi, I., & Sule, E. E. (2020). Design and Construction of A Single-Phase Power Factor Meter. *Electrical Science & Engineering*, 2(2).
- P. D. More, Vaibhav Chougule, Shubham Powar, Vikas Jadhav, Suhas Redekar, A. P. (2018). Microcontroller Based Smart Calibration Meter. *International Journal of Engineering Research in Electrical and Electronic Engineering*, 4(2), 2395–2717.
- Santos, J., & Ramos, P. (2011). DSPIC-based impedance measuring instrument. *Metrology and Measurement Systems*, 2.
- Villani, C., Benatti, S., Brunelli, D., & Benini, L. (2016). A contactless three-phase autonomous power meter. *2016 IEEE SENSORS*, 1–3.



CHAPTER 3

RECTIFIER CIRCUIT DESIGN FOR GSM AND ISM BAND RF ENERGY HARVESTING SYSTEMS

AYSU BELEN¹

¹ Asist. Prof. Dr., İskenderun Technical University, Iskenderun Vocational School of Higher Education, aysu.belen@iste.edu.tr, ORCID ID: 0000-0001-5038-424X

1. Introduction

RF energy harvester for low power systems gives a tremendous support for growth acceleration of Internet of Things (IoT) applications. RF harvester designs had improved battery life performance of many systems such as biomedical sensors, logistic support systems, smart home, and machine to machine communications systems. The main concern in design process of high performance RF harvester systems is that the design can achieve a high level of power conversion efficiency to have a specified output voltage (V_{OUT}) level from RF rectifier with respect to the aimed applications operational requirement. However such task is not trivial due to the pareto like relations of design performance criteria's and trade-offs between circuit complexity, power conversion efficiency performance, output voltage, cost, and size of the overall system [1].

In our daily life, there are wireless sensor networks in many areas such as factories smart buildings even human body or biomedical devices. RF signals are broadcast from millions and even billions of different devices, including mobile base stations, TV broadcasts, handheld radios and mobile phones, and this number is increasing by daily basis due to the increasing number of users and their increased demands [2], [3]. It can be said that one of the most interesting findings presented by [4] is that the number of broadband mobile devices has reached more than one billion. In a typical urban area location, a device may receive signals from multiple WiFi transmitters, or detection of signals at 100mW power level from public access points in enclosed areas is expected [4]. Considering these data, it is stated that RF energy harvesting circuits can be used to extend the battery life of low-power devices or to eliminate battery usage [5], [6]. In [7] it had been shown that a broadband RF power harvesting in the 2 to 18 GHz band range can be achieved via use of antenna array structures. One of the interesting studies that should be given as an example of far-field RF energy harvesting studies is the performance examination of a TV broadcasting station with 960KW output energy and an RF harvester system at a distance of 4 Km by Intel Research Seattle [8]. Another similar far-field RF energy harvesting study was a performance review of an AM radio transmitter station with an output power of 5 kW and an RF harvester system 2.4 Km away [9]. As a result of the widespread demand for use of low power designs, manufacturers are focused on developing products that can satisfy this request of "very low power consumption" and "extremely low power consumption" criteria's. For example, the 16-bit "very low power consumption" MSP430FR597 microprocessor produced by Texas Instruments draws approximately 400 μ A in active mode and only 0.4 μ A in standby mode [10]. No matter how low power consumption these products have, it is necessary to monitor the power level of their batteries. At this stage, energy harvesting cycles have emerged. There are also studies on

the use of energy harvesting circuits, increasing the battery life of mobile phones, laptops and tablets [11], [12]. Within the scope of this study, a single-layer rectifier circuit is proposed to be used in GSM and ISM bands.

The rectifier circuit input impedance is designed as 50ohm matching stage. In this layer, -10dB bandwidth between 1.8GHz and 2.5GHz is obtained by using microstrip stub structure and interdigital capacitor. With the low power levels obtained, the battery life of the sensors and devices used in wireless communication applications will be extended.

2. RF Energy Harvester Design

The block diagram of the RF energy harvester system is shown in Figure 1. The first component of the system, the antenna; It acts as a collection of electromagnetic signals in the environment. The impedance matching circuit eliminates the impedance mismatch between the rectifier circuit and the antenna input, preventing losses in the system. The DC output power of the rectified signal is filtered by the DC filter circuit before being transferred to the load. In the design phase, the RF rectifier circuit is designed with an input impedance of 50ohm.

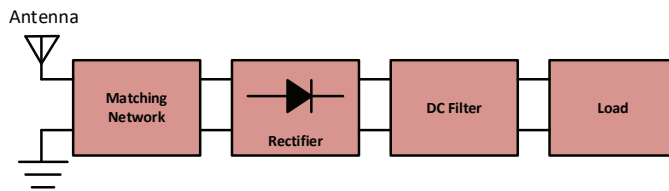


Figure 1. *RF Energy Harvesting Block Diagram*

2.1 Matching Network Design

The difference between RF energy harvesters and wireless power transmission systems is that the harvesters operate at very low power. For this reason, harvesters need to work as efficiently as possible. The task of efficiently transferring the power received from the environment to the rectifier by means of the antenna is performed by the harmonizing layer. Due to the non-linear operating characteristics of the diode, which is a rectifier circuit element, there may be impedance mismatches. We can minimize these inconsistencies by using the alignment layer. By eliminating the energy reflections that may occur at the RF signal input at the matching stage, the decrease of the output voltage will be prevented. Within the scope of this study, matching is achieved by using microstrip interdigital capacitor and microstrip stub structures in the matching layer of the RF rectifier circuit.

2.2 Schottky Diode Selection

One of the most important design parameters to be considered in RF energy harvesting is diode selection. Due to the low power values of the

energy in the environment in such studies, the diodes to be selected should have a high switching speed as well as a low turn-on voltage value as possible [13]. Within the scope of the proposed study, lumped elements and SMS-7630 schottky diode element were used to design the broadband rectifier circuit that will operate at the targeted 1.8 and 2.4 GHz frequencies.

Table 1 Schottky diodes and their parameters

Diode	Vt (V)	Vb (V)	Rs (ohm)	Jc (pF)
HSMS-2860	0.65	7	6	0.18
HSMS-8202	0.35	4	14	0.26
SMS-7630	0.34	2	20	0.14
SMS7621	0.55	3	12	0.1
MA-40417	0.65	11	4.9	0.04

To select the best diode element for the determined operating frequency (1.8-5 GHz), some commercial products available in the market have been examined and listed with their parameters in Table 1. As can be seen from the table, the lowest Vt value is obtained with the SMS-7630 element. This shows that the diode can be activated with a lower input power compared to other elements, and therefore it will be the best choice. Another important parameter, Jc, the high value of this value in other diode structures shows that the performance of the elements will deteriorate at high frequencies. Although MA-40417 and SMS-7621 elements have better values, a higher input power will be needed due to the threshold values of these elements, SMS7630 has a low forward bias voltage (60–120 mV @ 0.1 mA). Therefore, the most suitable diode structure that can be used within the scope of the study was chosen as the SMS-7630 element.

2.3 Load Impedance Selection

Electronic components used in wireless communication systems have a certain load impedance, operating performance decreases when operating outside these ranges. For this reason, choosing the load impedance range is an important criterion in RF rectifier circuits.

2.4 Rectifier Design

With the widespread use of wireless communication systems, there are signals in many frequencies in the environments. The representation of the single-stage rectifier circuit, which aims to convert the existing signals in the environment as an energy source, is given in figure 2. In Figure 2, low-power RF signals are collected with high output voltage by using D1 and D2 zero-bias low barrier schottky diodes. At the input of the circuit, a matching stage has been added according to the 50ohm input impedance. The matching stage is important for maximum power transfer to the rectifier stage of the antenna.

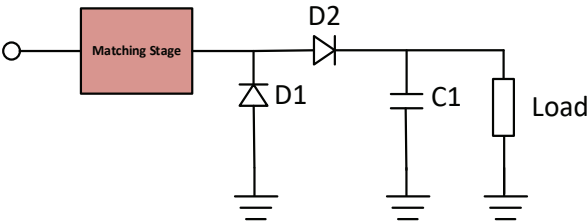
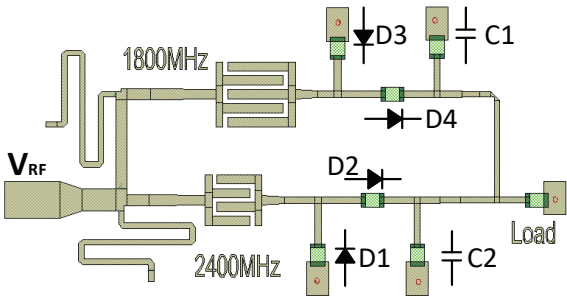
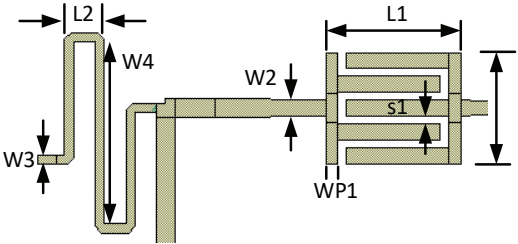


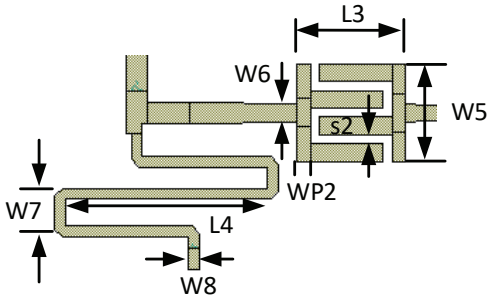
Figure 2. Single Stage Full Wave Rectifier



(a)



(b)



(c)

Figure 3. (a) Single stage Full Wave Rectifier Printed Circuit Illustration, (b) Matching Stage @1.8 GHz, (c) Matching Stage @2.4 GHz.

A broadband single-stage rectifier circuit design covering 1.8 GHz (GSM) and 2.4 GHz(ISM) bands is proposed in this study. By applying an input power between +30dBm and -30dBm, the power level that can be obtained from the load is monitored. The schematic circuit representation of the harmonized circuit is given in Figure 3. SMS7630 is used as D1 diode model, C1 capacitance value is 100pF. Circuit dimensions are 45mmX30mm.

Table 2 Matching network design parameter list [mm]

L1	5.14	W1	4.58
L2	10.5	W2	0.88
L3	3	W3	2.25
L4	29	W4	0.5
WP1	0.65	W5	3
WP2	0.65	W6	1.3
S1	0.4	W7	1.6
S2	0.4	W8	0.5

The matching circuit is designed as it is shown in Figure 3. This matching circuit includes interdigital capacitor and microstrip stub elements. The matching solid variable parameters are given in Table 2. In Figure 4, the return loss (S11) of the circuit is given and as can be seen, it has a value less than -10dB in the targeted operating band range. A bandwidth of -10dB was obtained between 1.8GHz and 2.45GHz.

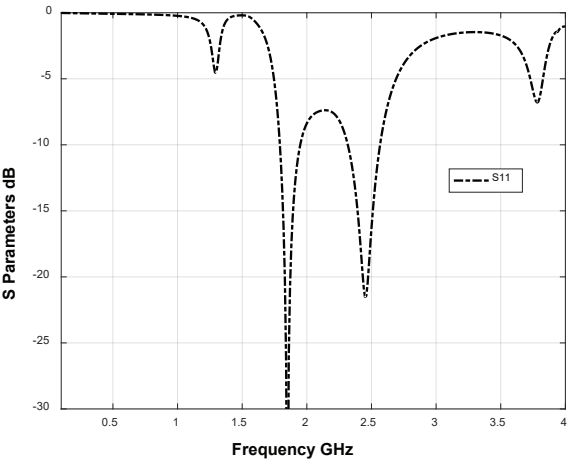


Figure 4. Return loss performance of the single stage matched design.

Although the efficiency is high in the low-load resistor in the rectifier circuit, the voltage value obtained at the output is low. Also in Fig. 5, the efficiency versus frequency of design for -10 dBm power level is presented. As it can be seen from Fig. 6, the design achieves 60% and 65% efficiency at 1.8 and 2.4 GHz respectively.

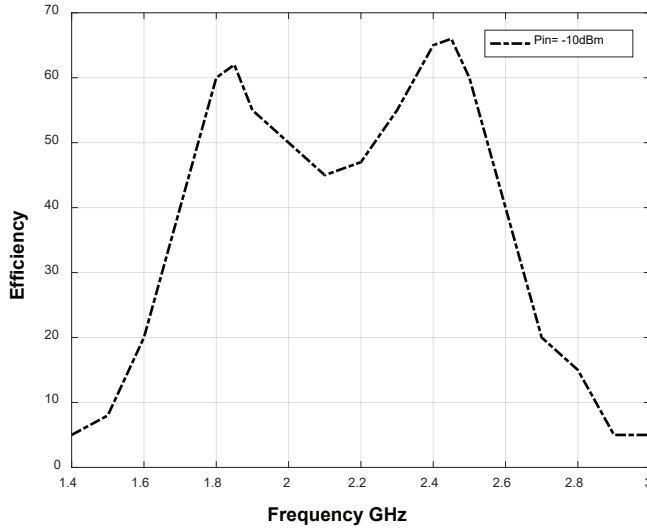


Fig. 5 The efficiency versus frequency

In order to clearly present the performance superiority of the proposed design, a performance comparison with counterpart designs in literature had been done. As it can be observed from Table 3, not only the proposed design has better performance measure in means of being dual band and efficiency rate but also in means of size and fabrication complexity it is superior to the counterpart designs. While the counterpart work that has similar dual band characteristic [Table 3 ref 14] can only achieve a similar efficiency at first operation (60.4% v.s. 60%) band its second band efficiency is extremely lower than the proposed work (17% v.s. 65%). in counterpart works only [Table 3 ref 15] has better efficiency performance than the proposed work however its drawbacks are (i) being single band (2.45 GHz), have a larger PCB surface (87x80 [mm]) compared to the proposed work (50x30 [mm]).

Table 3. Comparison to recently Reported Rectifiers

Works	Frequency GHz	Dimension [mm]	Fabrication Complexity	Efficiency %
[14]	0.98 / 1.8	100x90x0.8	Easy 2 layers PCB	60.4 / 17
[15]	2.45	87x80x0.6	Easy 2 layers PCB	80.3
[16]	2.45	110x100x4.7	Medium 3 layers PCB	63
[17]	1.8-2.5	70x70x13.2	Difficult 3D PCB	70
[18]	1.8 / 2.1	380x350x1.5	Easy 2 layers PCB	50
[19]	1.8	45x45x0.8	Easy 2 layers PCB	61
This work	1.8 / 2.4	50x30x1.5	Easy 1 layer PCB	60 / 65

4. Result and Discussion

Within the scope of this study, a single-layer rectifier circuit is proposed to be used in GSM and ISM bands. The rectifier circuit input impedance is designed as 50ohm matching stage. a -10dB bandwidth between 1.8GHz and 2.5GHz is obtained by using microstrip stub structure and interdigital capacitor. In the simulation studies, the rectifier efficiency and output voltage change were investigated by changing the value of the load resistance value. It has been observed that the efficiency of the single-stage rectifier circuit is high at low load resistance, and the output voltage is high at high load resistance. Here, the importance of choosing the load resistor according to the application in which the RF rectifier circuit will be used is understood. At 0dBm input power, 38mV at 100ohm load resistance at 1.8GHz, 141mV at 100Kohm load resistance, and 125.6mV at 100ohm load resistance at 2.4GHz, 199mV output voltage at 100Kohm load resistance was obtained. With the low power levels obtained, the battery life of the sensors and devices used in wireless communication applications can be extended. Furthermore, a performance comparison of the proposed work with counterpart works in literature had been done in means of size, efficiency operation band and complexity of fabrication. As a results not only the proposed design achieves better efficiency performance at the aimed operation frequencies of 60% at 1.8 and 65% 2.4 GHz, but it is also has smaller PCB size and simpler manufacturing complexity compared to the counterpart designs in literature.

Kaynaklar (References)

- [1] Xu, L. D., He, W. and Li, S., "Internet of Things in Industries: A Survey," *IEEE Transactions on Industrial Informatics*, vol. 10, no. 4, pp. 2233-2243, Nov. 2014.
- [2] Paradiso, J.A., Starner, T., "Energy scavenging for mobile and wireless electronics." *IEEE Pervasive Comput.*, vol.4, no.1, pp.18-27, 2005.
- [3] Rebello, J., 2010, Global wireless subscriptions reach 5 billion. Available: <http://www.isuppli.com/Mobile-and-Wireless-communications/News/Pages/Global-Wireless-Subscriptions-Reach-5-Billion.aspx>
- [4] Cheng, Y.-C., Chawathe, Y., LaMarca, A., Krumm, J., "Accuracy characterization for metropolitan-scale Wi-Fi localization," *Proc. Third Int. Conf. on Mobile Systems*, pp. 233-245, 2005.
- [5] Gilbert, J. M., Balouchi, F., "Comparison of energy harvesting systems for wireless sensor networks," *Int. J. Autom. Comput.*, vol. 5, no.4, pp. 334-347, 2008.
- [6] Curty, J.-P., Joehl, N., Krummenacher, F., Dehollain, C., Declercq, M., "A model for m-power rectifier analysis and design," *IEEE Trans. Circuits Syst. I*, vol.52, no.12, pp. 2771-2779, 2000.
- [7] Hagerty, J.A., Helmbrecht, F.B., McCalpin, W.H., Zane, R., Popovic, Z.B., "Recycling ambient microwave energy with broadband rectenna arrays," *IEEE Trans. Microw. Theory Tech.*, vol.52, no.3, pp. 1014-1024, 2004.
- [8] Sample, A., Smith, J., "Experimental results with two wireless power transfer systems," *Proc. IEEE RWS*, 16-18, 2009.
- [9] Ostafte, H., "Power out of thin air: ambient RF energy harvesting for wireless sensors," 2010. Available: <http://powercastco.com/PDF/Power-Out-of-Thin-Air.pdf>
- [10] MSP430FR597x(1), Mixed-Signal Microcontrollers, Available: <http://www.ti.com/lit/ds/slase66b/slase66b.pdf>, (Accessed on 05/04/2021).
- [11] Liang, X., Zhao, T., Jiang, W., Yu, X., Hu, Y., Zhu, P., Zheng, H., Sun, R., Wong, C.-P., "Highly transparent triboelectric nanogenerator utilizing in-situ chemically welded silver nanowire network as electrode for mechanical energy harvesting and body motion monitoring," *Nano Energy*, vol.59, pp.508-516, 2019.
- [12] Song, G. J., Kim, K.-B., Cho, J. Y., Woo, M. S., Ahn, J. H., Eom, J. H., Ko, S. M., Yang, C. H., Do Hong, S., Jeong, S. Y., "Performance of a speed bump piezoelectric energy harvester for an automatic cellphone charging system," *Applied Energy*, 247, 221-227, 2019.
- [13] Yan, H., Montero, J. G. M., Akhnoukh, A., de Vreede, L. C. N., Burghart, J. N., "An integration scheme for RF power harvesting. 8th Annu. Workshop Semiconductor Advances Future Electron. Sensors," Veldhoven, the

Netherlands, 2005.

- [14] Arrawatia, M., Baghini, M. S. and Kumar, G. "Broadband bent triangular omnidirectional antenna for RF energy harvesting," *IEEE Antennas Wireless Propag. Lett.*, vol. 15, pp. 36–39, 2016.
- [15] Sun, H., Guo, Y. X., He, M. and Zhong, Z. "Design of a high-efficiency 2.45-GHz rectenna for low-input-power energy harvesting," *IEEE Antennas Wireless Propag. Lett.*, vol. 11, pp. 929–932, 2012.
- [16] Harouni, Z., Cirio, L., Osman, L., Gharsallah, A., and Picon, O., "A dual circularly polarized 2.45-GHz rectenna for wireless power transmission," *IEEE Antennas Wireless Propag. Lett.*, vol. 10, pp. 306–309, 2011.
- [17] Song, C., Huang, Y., Zhou, J., Zhang, J., Yuan, S., and Carter, P., "A high efficiency broadband rectenna for ambient wireless energy harvesting," *IEEE Trans. Antennas Propag.*, vol. 63, no. 8, pp. 3486–3495, Aug. 2015.
- [18] Sun, H., Guo, Y. X., He, M., and Zhong, Z., "A dual-band rectenna using broadband Yagi antenna array for ambient RF power harvesting," *IEEE Antennas Wireless Propag. Lett.*, vol. 12, pp. 918–921, 2013.
- [19] Miaowang Zeng, Andrey S. Andrenko, , Xianluo Liu, Zihong Li, and Hong-Zhou Tan, "A Compact Fractal Loop Rectenna for RF Energy Harvesting" *IEEE Antennas And Wireless Propagation Letters*, vol. 16, 2017



CHAPTER 4

DESIGN AND DEVELOPMENT OF AN ARDUINO-BASED LIQUID SOAP DISPENSER AND AN AUTOMATED HAND SANITIZER

*Osman Emre YILDIRIM¹, Mecit ÖGE²,
Tuba ÖZDEMİR ÖGE³*

1 Optician, Tekirdağ, o.emre2001@gmail.com

2 Asst. Prof. Dr. Bartın University, Faculty of Engineering, Architecture and Design, Department of Mechanical Engineering, Kutlubey-Yazıcılar Campus, 74100 Bartın, Turkey; E-mail: mecitoge@bartin.edu.tr, ORCID ID, <https://orcid.org/0000-0001-5243-0828>.

3 Asst. Prof. Dr. Bartın University, Vocational School of Health Services, Bartın, Turkey, 74100, E-mail: tozdemir@bartin.edu.tr, ORCID ID, <https://orcid.org/0000-0001-6690-7199>

1. Introduction

The current work involves the design and manufacturing of two different devices, a mechanically activated liquid soap dispenser and an automated hand sanitizer. The reason for manufacturing separate devices for the dispensing disinfectant and liquid soap is the different viscosities of these materials. The lower viscosity of liquid disinfectant as compared to liquid soap allows the use of a mini submersible pump, thus allowing the design of a simpler and cost-effective system to dispense hand disinfectant. For dispensing liquid soap, which cannot be dispensed by use of a submersible pump due to higher viscosity, a system mechanically activated by a mini servo motor that has enough power to mechanically activate soap dispensers commercially available in the market was designed and manufactured. On the other hand, the mechanically activated system can also be used for hand sanitizing purpose. The design of two different systems addressing diverse needs was thus aimed. It was found after a literature survey (Sumbawati et al. 2020; Lesmana et al. 2020; Janayanda et al. 2021; Hang & Dung, 2021; Ramadan & Marlinda, 2021; Jagne & Biranware, 2022; Vishal Raj, 2022; Lee et al. 2020) that, the systems designed so far for liquid soap dispensing with height adjustment to fit all soap dispensers in the market, or those specifically designed for soap dispensing and hand sanitizing purposes either occupy much space with higher cost, or they do not appeal to the end user in terms of appearance, usage or marketing.

In the current study, the electronic and mechanical components of the mechanically activated system were covered by a compact polymer container with a sliding cap designed with a computer aided design (CAD) software to allow easy replacement of the battery and easy access to the electronic components for repair and maintenance. Another polymer part, fastened to the plain surface of the dispenser allows easy attachment of the designed device onto hand dispensers available in the market. The system designed for hand sanitizing purpose on the other hand involves the use of a mini submersible water pump and is designed to contain a standard sized disinfectant bottle widely available in the market. In the system, the electronic components are placed on the upper section of the polymer contained that can be accessed by a removable cap. The polymer components of the hand sanitizing system comprising three polymer components and those of the mechanically activated system comprising two polymer components were initially designed with a CAD software and then they were manufactured via 3D printing. The development stages involve the mechanical and electronic design of the proposed systems, the design of the containers with a CAD software followed by 3D printing; the coding for both systems on Arduino IDE interface, and the assembly of the mechanical and electronic components within the polymer containers, which were

afterwards applied on commercially available containers.

2. Design and Development of Automated Hand Sanitizer

The three-dimensional design drawings of the automated hand sanitizer are shown in Figure 1 and Figure 2. Figure 3 shows the electronic circuit diagram of the system. The electronic system and the container comprise the main parts of the designed system. The used electronic components involve IR sensor, TIP32C transistor, resistor, mini submersible water pump, battery holder, battery, plastic hose, electronic circuit container, time relay and jumper cables. A silicon gun and a soldering iron were also used for fastening purposes.

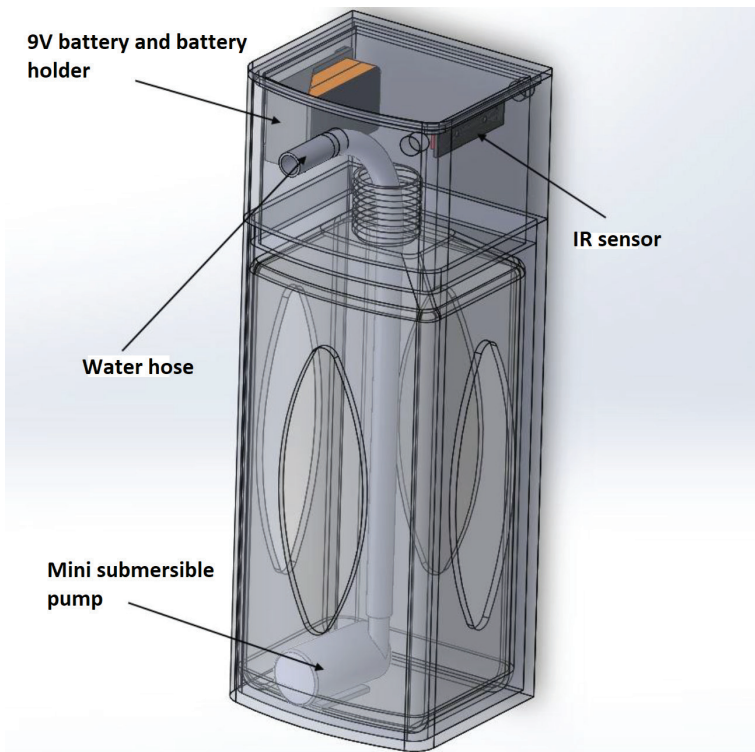


Figure 1. 3D drawing of automated hand sanitizer designed with CAD software

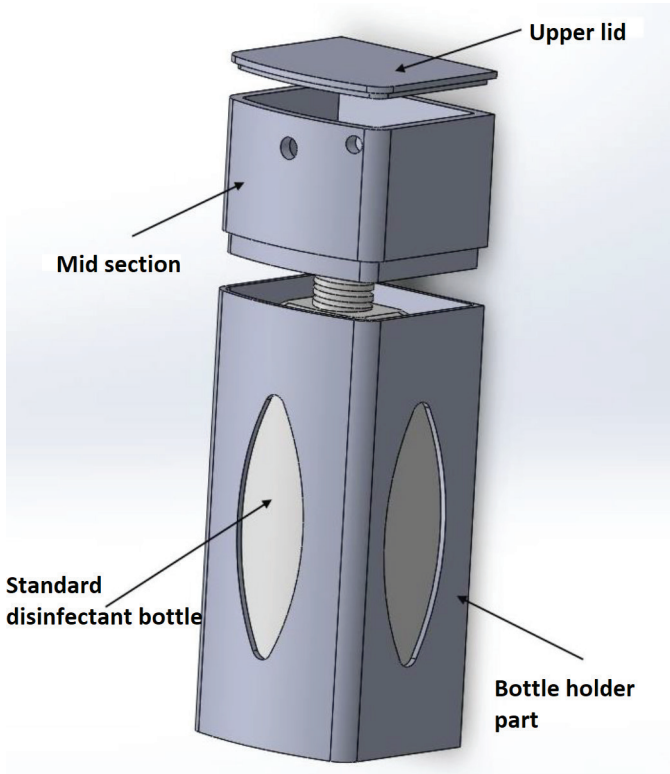


Figure 2. *Polymer container parts of the automated hand sanitizer designed with CAD software and fabricated via 3D printing.*

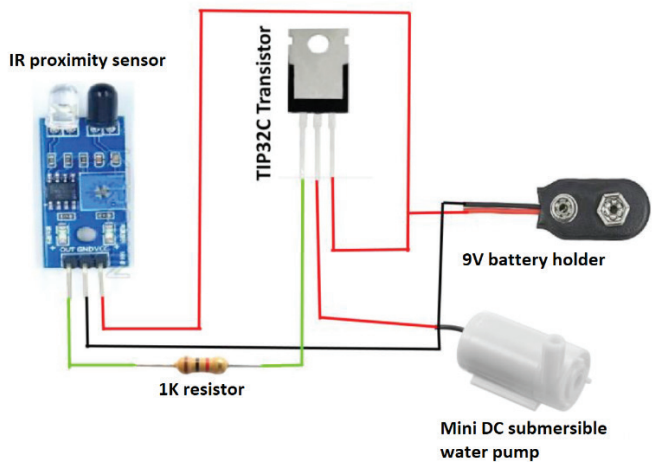


Figure 3. *The circuit diagram of the designed automated hand sanitizer.*

Brief information related to the components of the automated hand

sanitizer are listed below:

As shown in Figure 4a, IR sensor is equipped with a pair of infrared receiver and transmitter. It can be easily implemented in any environment. It transmits an infrared signal with a specific frequency when an obstacle is encountered in the transmitting direction. The effective distance range can be adjusted between 2-30 cm with a potentiometer. The operating voltage is between 3.3 V – 5 V. The IR sensor is easily applicable in a wide range of applications with its easy assembly.

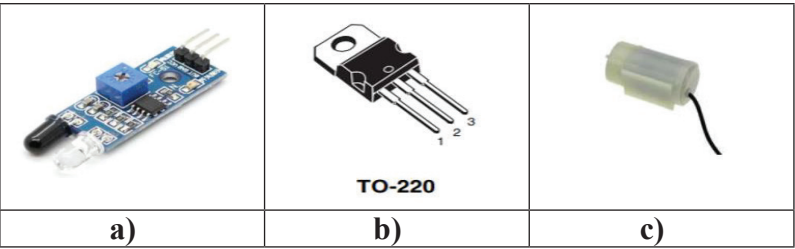


Figure 4. a) IR sensor b) Power transistor c) Mini submersible water pump

TIP32C is a TIP type transistor in TO-220 style (Figure 4b). TIP32C is also a BJT PNP type transistor. TIP32C has 3 A collector current and 100 V collector-emitter voltage. It is widely used in medium power linear and switching applications. The mini submersible water pump operates with very low power consumption between DC 3 V – 6 V (Figure 4c). The 3D printed polymer container components are shown in Figure 5 and Figure 6.



Figure 5. 3D printed polymer container parts of the automated hand sanitizer.

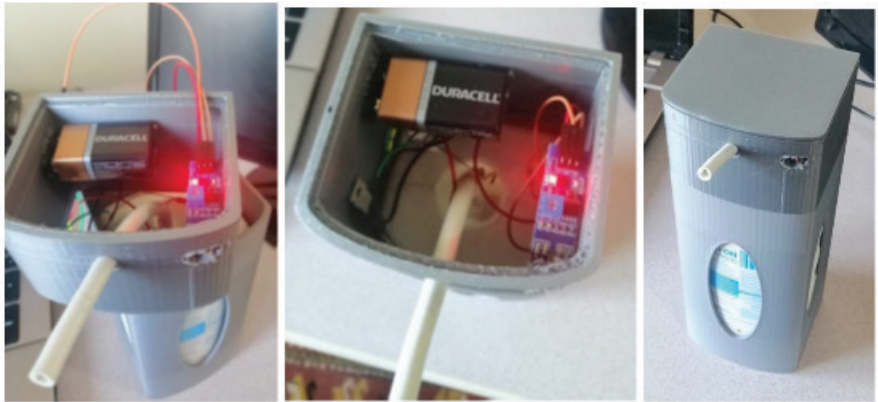


Figure 6. *The images of automated hand sanitizer after the assembly of the electronic components.*

3. Design and Development of Arduino Based Liquid Soap Dispenser

The three-dimensional design drawings of the device are shown in Figure 7 and Figure 8. The electronic system and polymer container parts comprise the main parts of the system. The electronic design involves IR sensor, mini servo motor, Arduino Nano microcontroller, 9 V battery holder, 9 V battery and jumper cables. A silicon gun and a soldering iron were used for fastening purposes.

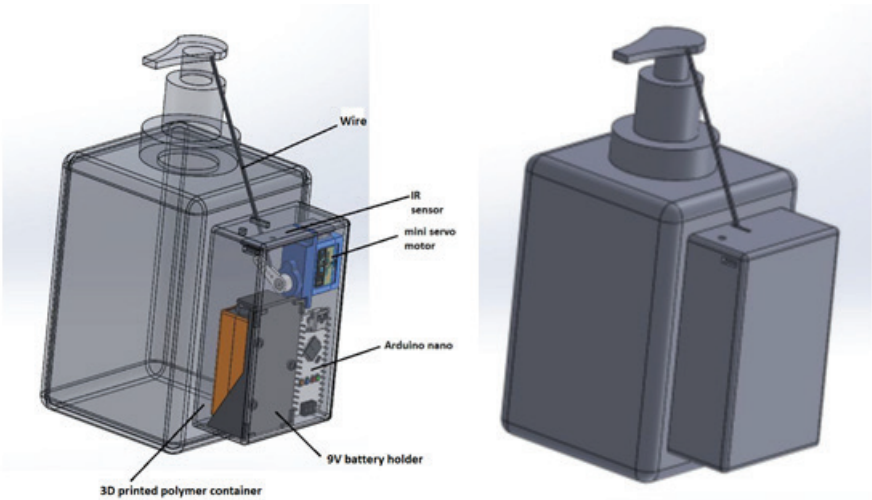


Figure 7. *3D CAD design of the mechanically activated liquid soap dispenser*

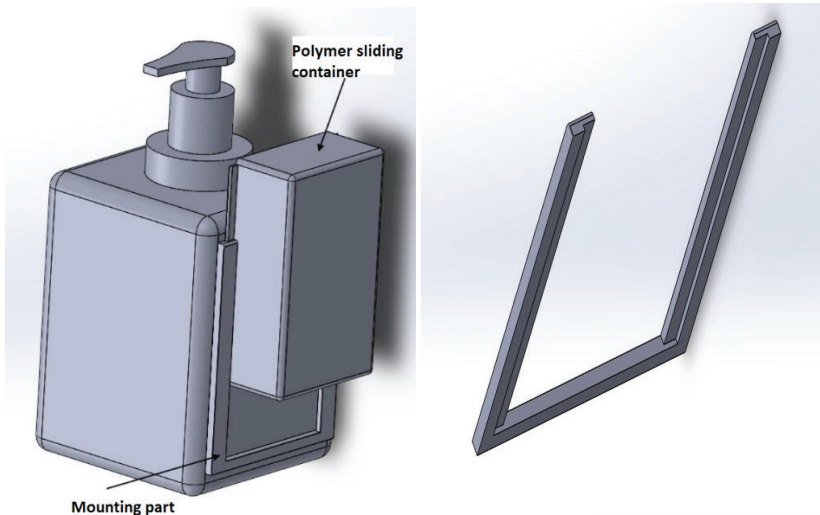


Figure 8. CAD design images of 3D printed polymer parts of the mechanically activated liquid soap dispenser

The circuit diagram of the mechanically activated arduino-controlled liquid soap dispenser is shown in Figure 9.

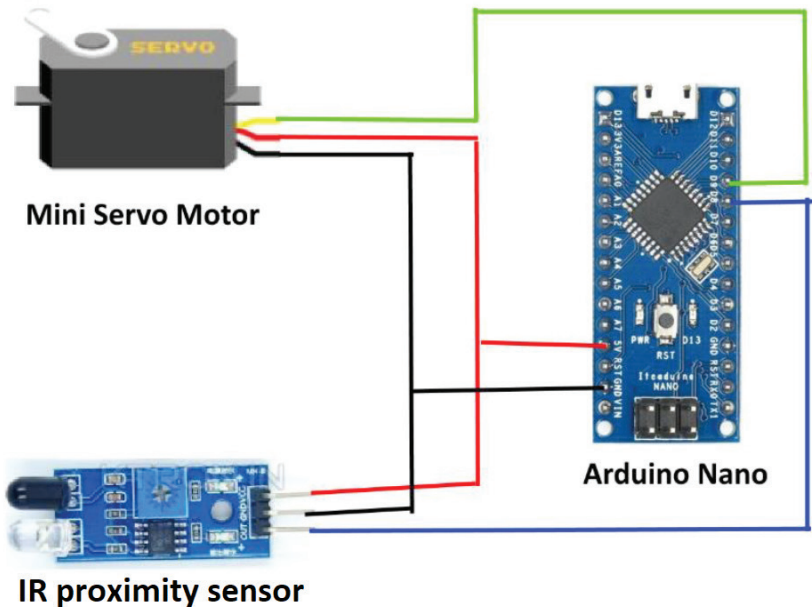


Figure 9. The circuit diagram of the automated liquid soap dispenser

The components of the liquid soap dispenser that are not available in the automated hand sanitizer are briefly explained below:

SG90 mini servo motor is in 23.1 X 12.2 X 29 mm dimensions with 9 gr weight. It has an operating voltage of 4.8 - 6.0 V (DC). Motion speed is 0.1 s/60° at 4.8 V. Stall torque is 1.8 kg/cm at 6 V. It operates within the angle range of 0-180° by means of a plastic gearbox. The operating PWM signal is 500-2400 μ s. A representative picture of the SG90 mini servo motor is given in Figure 10.



Figure 10. *SG90 Mini Servo Motor*

Arduino Nano is equipped with 14 digital output (6 of which has PWM support) and 8 analog inputs. DC pin current 40 mA. Input voltage range is 7-12 V (DC), operating voltage is 5 V. Arduino Nano has 32 kb flash memory supporting an integrated Atmel Atmega328 microprocessor. The image of Arduino Nano is shown in Figure 11.

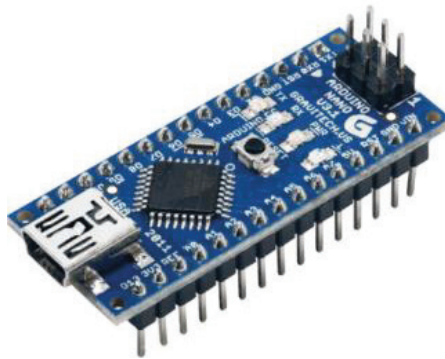


Figure 11. *Arduino Nano*

The final mounted image of the manufactured mechanically activated liquid soap dispenser is shown in Figure 12.

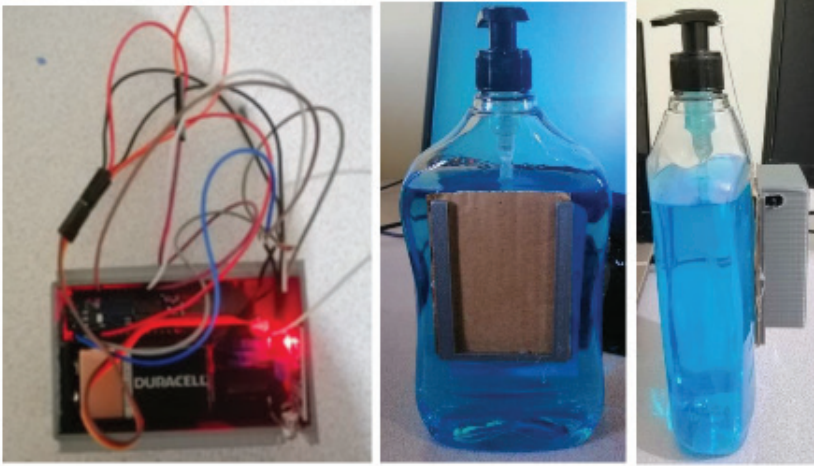


Figure 12. *The mounted final image of mechanically activated liquid soap dispenser*

4. Conclusion

In the present work, two different devices, an automated hand sanitizer, and a mechanically activated Arduino-based liquid soap dispenser were designed and developed. The dispensing of disinfectant with the automated hand sanitizer is achieved by use of a standard disinfectant bottle. Mechanically activated soap dispenser, on the other hand is designed and developed to fit any commercially available conventional soap dispenser having a plain surface, and its electronic components are hidden in a 3D printed polymer container. When compared to similar devices introduced in the literature, the devices designed and developed in this work are advantageous in terms of cost-effectiveness and usability. It is shown by this study that, the devices are applicable and adaptable to manual dispensers that are commercially available and widely used in the market. The following studies by the authors aim to improve the design and usability of the devices before they are presented to the end-user.

Acknowledgements

This work is supported by TUBITAK 2209 (2021-Fall Term) student project titled: “Design and Development of an Arduino-Based Liquid Soap Dispenser and an Automated Hand Sanitizer”. The authors also acknowledge the valuable helps and support of Technician Ender TOGAÇ.

References

- Hang, D.T., Dung, N.T. (2021). Research and Integrate the Body Thermal Measuring, Washing Hand Automatically without Touching, and Giving Free Face Mask for Epidemic Prevention. SSRG International Journal of Electrical and Electronics Engineering, 8(4): 8-14. DOI: 10.14445/23488379/IJEEE-V8I4P102.
- Jagne, S., Biranware, S. (2022). Automatic Hand Sanitizer Dispenser. International Research Journal of Modernization in Engineering Technology and Science. 4(8):292-297.
- Janayanda, N., Nikhil, M., Shreyas, P.B., Ananya, T.R., Channabasavanna, S.G., Dutt. P. S., Vekate Gowda, T. (2021). Low-Cost Automatic Hand Sanitizer Dispenser: Developed and Dispatched Against the Covid-19 Pandemic in India. JETIR, 8(8): 76-82.
- Lee, J., Lee, J.Y., Cho, S.M., Yoon, K.C., Kim, Y.J., Kwang, G.K. (2020). Design of Automatic Hand Sanitizer System Compatible with Various Containers. Healthc Inform Res. 26(3): 243–247. DOI: 10.4258/hir.2020.26.3.243.
- Lesmana, J., Halim, A., Irawan, P.A. (2020). Design of automatic hand sanitizer with ultrasonic sensor. IOP Conf. Series: Materials Science and Engineering, (1007-012164). DOI:10.1088/1757-899X/1007/1/012164
- Ramadan, A.P., Marlinda, L. (2021). Design of automatic hand sanitizer based on Arduino Uno Microcontroller. Sinkron : Jurnal dan Penelitian Teknik Informatika, 6(1): 157-167. DOI : <https://doi.org/10.33395/sinkron.v6i1.11174>
- Sumbawati, M.S., Chandra, A., Wrahatnolo, T., Endah, L. (2020). Design Automatic Hand Sanitizer Microcontroller Based using Arduino Nano and Ultrasonic Sensors as an Effort to Prevent the Spread of Covid-19. International Joint Conference on Science and Engineering (IJCSE 2020)At: Indonesia. DOI: 10.2991/aer.k.201124.025
- Vishal Raj, I.P., Prithiv Raj, A., Ragul, P., Balaji, V. (2022). Automatic Sanitizer Dispenser Machine Using Arduino, Student Journal of Electrical and Electronics Engineering, 1(1):1-6.



CHAPTER 5

ENVIRONMENTAL RISK ASSESSMENT FOR MUNICIPAL SOLID WASTE COMPONENTS AND SITE SELECTION IN TURKEY

Onur DERSE¹ , Murat OTURAKÇI²

1 Department of Industrial Engineering, Faculty of Engineering, Tarsus University, 33400, Tarsus, Mersin, Türkiye; onurderse@tarsus.edu.tr ; <https://orcid.org/0000-0002-4528-1999>

2 Department of Industrial Engineering, Faculty of Engineering, Bakırçay University, 33400, İzmir, Türkiye; murat.oturakci@bakircay.edu.tr ; <https://orcid.org/0000-0001-5946-3964>

INTRODUCTION

Uncontrolled population growth, urbanization, the development of industry, the change in consumption habits, and the development of technology cause an increase in the amount of solid waste. Uncontrolled disposal of waste causes problems in the water, soil, air, flora, and fauna systems, and is becoming a major concern, especially in developing countries due to various environmental problems such as greenhouse gas formation [1].

Waste management includes activities such as prevention of waste generation, reduction from source, collection, separation, reuse, recycling, disposal, and waste management is an environmentally, socially, and economically beneficial process [2]. Hence, studies on waste management have significantly increased in recent years [3, 4].

The increase in the rate of municipal solid waste generation in cities due to urbanization, industrialization, and rapid population growth [5] increases the trend toward landfills designed to increase environmental protection [6]. In a global context, solid waste management disposal of waste by landfill is the most frequent way preferred in developing countries [7]. A landfill for solid waste is a common solution used for the final disposal of municipal solid waste (MSW) in Turkey [6].

The site selection of landfills is one of the most important steps in MSW management, and the site selection process requires the evaluation and analysis of various criteria [8] and is a complex process [9]. The landfill selection process aims to identify areas that will minimize hazards to the environment and public health [10], so a systematic process should be developed and followed to ensure that an appropriate site is selected [6]. When the studies on MSW site selection are examined, Nas et al. [6] and Uyan [10] deal with the MSW site selection problem for Konya province in Turkey. Yesilnacar et al. [11] aim to apply MCDA integrated with GIS to select possible areas of MSW landfills for Turkey. Yildirim [8] evaluates two landfills for site selection in the province of Trabzon in Turkey. As a result of the study, the suitability values of the two landfills in the cost surface map showed that these sites are not suitable for solid waste landfills. Kharat et al. [9] deal with the MSW landfill selection problem with the integrated MCDM method. Chabok et al. [12] use a fuzzy multi-criteria decision-making method integrated with GIS to select the optimum location for municipal solid waste (MSW) landfills in accordance with standard storage guidelines and environmental and socio-economic criteria for Iran. Hereher et al. [7] aimed to identify suitable locations for landfills in the Muscat Governorate of Oman.

It is important landfill site selection for MSW operations be performed after risk assessment, as MSW formation creates environmental risks.

Since site selection is a critical decision, the site to be selected must be evaluated from many aspects. In the literature, risk assessments in waste management systems, in general, have been examined within the scope of hazardous waste.

Landfill site selection for MSW is a strategic decision for municipalities. There are many managerial, operational, environmental and physical factors that affect these decisions. In order to establish an MSW facility, the existing facilities and environmental risk factors must first be examined in detail. From this point of view, it is necessary to examine ISO14001 standards and integrate them into environmental risk assessments. Emissions to the air; released waste to water and soil; raw material, natural resources, and energy usage; global warming; radiation; vibration; products and by-products should all be considered when considering environmental factors, according to ISO 14001 [13]. Design and development, manufacturing processes, packaging and transportation, waste management, extraction and distribution of raw materials and natural resources, product usage and life, wildlife and biodiversity should all be taken into account when deciding on environmental factors [13]. In particular, the importance of evaluating environmental risk factors according to five significant impact categories has been emphasized in many studies [13-15].

A landfill for solid waste is a common solution used for the final disposal of MSW in Turkey [6]. There are studies on MSW site selection in Turkey [6, 10, 11, 16]. The aim of this study is to make a site selection decision for a city that does not have an MSW facility, based on the risk score to be obtained from an integrated risk analysis, based on the effects of solid waste types in Turkey on different impact categories.

In the study, first, environmental assessment reports of all cities in Turkey were examined and joint MSWs in Turkey were decided in these reports. Then, the effects of these MSWs on the five impact categories in the ISO 14000 standard (air, soil, water, flora and fauna) were evaluated with the L Type (5*5) Matrix method. In the next stage of the study, cities without facilities were determined according to the information obtained from the environmental assessment reports of all cities in the country; the amount of solid waste per capita in these cities and the risk scores of the cities were integrated to obtain individual risk scores for cities without facilities. Then, the location selection process was carried out for the city with the highest risk score, with the help of goal programming to make the decision to establish a facility. For the site selection, the optimum location was determined by considering the parameters and constraints of Hydrology, Air quality index, Soil & topography, Habitat, flora and fauna with four objectives of Cost, Environment Impact, and Social Acceptance and Risk.

MATERIALS AND METHODS

The main material of this study is the “City Environmental Assessment Report of 2020” obtained from the official website of “Republic of Turkey Ministry of Environment, Urbanization and Climate Change” [17]. According to the information obtained from the reports published in 2020, Paper, cardboard; plastic; Metal; glass; Wooden; Textile; battery (small); Battery (Medium, Big); Toner-Cartridge; Lighting Equipment; Electric-Electronic Equipment; Medicines; Vegetable waste oil; bulky waste; Vehicle maintenance/repair Equipment; Dangerous waste; Organic waste; Mixed (plastic, paper, glass, metal) were determined as the basic MSWs.

The steps of the study are presented in Figure 1.

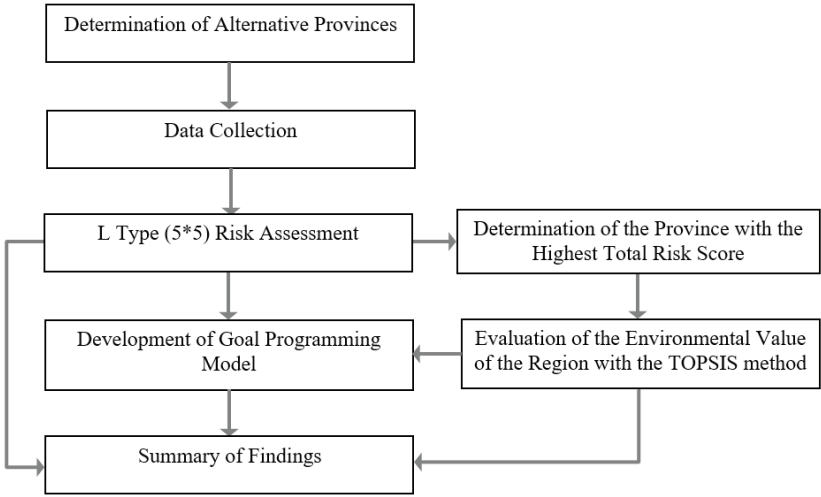


Figure 1. Flow of the study

L Type (5*5) Risk Assessment

L type (5x5) matrix method is used widely among risk assessment methods in occupational health and safety. In the classic L type (5x5) method the probability of occurrence of the risk and its severity are evaluated together. According to the evaluation scores, the risk priority number (RPN) is calculated by multiplying those two factors. RPN scores are divided into five groups as negligible, acceptable, mid-level, important and unacceptable risks.

TOPSIS Method

TOPSIS method, developed by Hwang and Yoon [18], is based on the fact that the best alternative chosen is the closest to the positive ideal solution and the farthest from the negative ideal solution [19]. TOPSIS is a method that is frequently used to rank the order of preference of alternatives and to give decision-makers more opportunities to set criteria prior-

ities [20]. The application steps of this method, whose steps are stated by Hwang and Yoon [18], can be defined as follows. First, a decision matrix is created and normalized by the decision-makers. Then the normalized matrix is transformed into a weighted normalization matrix. After the normalization matrix was created, ideal and negative ideal solution sets were created to calculate ideal and negative ideal distance values. The ideal solution relative proximity is calculated as the final step of the TOPSIS approach [21].

Developed Goal Programming Model

Goal Programming is a method applied to linear programming problems where there are many goals or objectives. Unlike linear programming, which directly optimizes goals, goal programming is used to manage conflicting goals by minimizing deviations between goal values and actual results. Within the scope of this study, an integrated goal programming model has been developed with the TOPSIS method and the L Type (5*5) Risk Assessment method.

The goal programming model of the study is presented below, and the indices and definitions used in the decision model are as follows: The i and j indices in the goal programming model used to decide where the facility to be established is in the province with the highest risk score (Bartın) represent the districts in Bartın. These indices consist of Merkez, Amasra, Kurucaşile, and Ulus districts. The g index represents goals and includes Cost, Environment Impact, Social Acceptance and Risk. c_i represents the cost on a district basis and is considered an assumption. env_i represents the environmental impact value on a district basis and the results obtained as a result of the TOPSIS method are used for this parameter. r represents the risk score on the basis of the city and is the parameter value obtained by the total amount of waste per capita on the city basis of the total score for the impact categories in Bartın. The values of waste amount per capita according to the district are taken from the 2020 Environmental Assessment Report of Bartın [22]. sa_i represents social acceptability by district; pi represents the amount of waste collected on a district basis. The w_i values represent the weight of the goals. ds_{ij} is the distance between districts and tr_{ij} is the transportation cost between districts. x_i is the binary decision variable that expresses whether there will be an installation in i^{th} district. cap is the decision variable that expresses the required capacity of the MSW facility to be established. $goal_g$ value represents the g^{th} goal value, dg^+ , dg^- values present the positive and negative deviation values from the g^{th} goal.

In the developed goal programming model; Equation 1 expresses the objective function. In the equation, cost minimization, minimization of environmental value impact, environmental risk minimization and social

acceptability maximization are expressed respectively. Equation 2 is the constraint equation that includes land cost and transportation cost. Equation 3, Equation 4, and Equation 5 were constraint equations including environmental impact value, risk, and social acceptability, respectively. Equation 6 is the equation that gives the required capacity for the area or areas where the installation decision is made. Equation 8 and Equation 9 define the decision variables.

$$d_1^+ * w_1 + d_2^+ * w_2 + d_3^+ * w_3 + d_4^- * w_4 \quad (1)$$

$$\sum_i \sum_j ds_{ij} * x_{ij} * tr_{ij} + \sum_j x_i * c_i - d_1^+ + d_1^- = goal_1 \quad (2)$$

$$\sum_i x_i * env_i * cap - d_2^+ + d_2^- = goal_2 \quad (3)$$

$$\sum_i x_i * r_i - d_3^+ + d_3^- = goal_3 \quad (4)$$

$$\sum_i x_i * sa_i * cap - d_4^+ + d_4^- = goal_4 \quad (5)$$

$$\sum_i x_i * cap \geq \sum_i p_i \quad (6)$$

$$x_i \in \{0,1\} \quad (7)$$

$$cap, d_{\varepsilon}^+, d_{\varepsilon}^- \geq 0 \quad (8)$$

RESULTS AND DISCUSSION

*Results of L Type (5*5) Risk Assessment*

The effects of the solid waste types specified in the Turkey 2020 Environmental City Assessment Report [22] on the ISO 14000 impact categories were evaluated according to the L Type (5*5) Matrix method and the results are presented in Table 1.

Table 1. *L Type (5*5) Evaluation of Solid Waste Types According to Impact Categories*

SOLID WASTE TYPES	IMPACT CATEGORIES														
	AIR			SOIL			WATER			FLORA			FAUNA		
	P	S	RPN	P	S	RPN	P	S	RPN	P	S	RPN	P	S	RPN
Paper, cardboard	3	3	9	3	3	9	3	3	9	3	3	9	3	3	9
Plastic	3	4	12	4	3	12	3	3	9	3	3	9	3	4	12
Metal	4	3	12	3	3	9	3	3	9	3	3	9	3	3	9
Glass	3	3	9	3	3	9	3	3	9	3	4	12	4	3	12
Wooden	2	3	6	3	3	9	3	3	9	3	3	9	3	3	9
Textile	3	3	9	3	4	12	4	4	16	4	3	12	3	3	9
Battery (small)	4	5	20	5	4	20	4	4	16	4	4	16	4	5	20
Battery (Medium, Big)	3	5	15	5	4	20	4	3	12	3	3	9	3	5	15
Toner-Cartridge	3	4	12	4	3	12	3	3	9	3	3	9	3	4	12
Lighting Equipment	2	3	6	3	3	9	3	3	9	3	3	9	3	3	9
Electric-Electronic Equipment	2	3	6	3	3	9	3	3	9	3	3	9	3	3	9
Medicines	4	5	20	5	5	25	5	5	25	5	5	25	5	5	25
Vegetable waste oil	4	5	20	5	5	25	5	5	25	5	5	25	5	5	25
Bulky waste	3	3	9	3	3	9	3	3	9	3	4	12	4	3	12
Vehicle maintenance/repair Equipment	3	3	9	3	3	9	3	3	9	3	3	9	3	3	9
Dangerous waste	5	5	25	5	5	25	5	5	25	5	5	25	5	5	25
Organic waste	5	5	25	5	5	25	5	5	25	5	5	25	5	5	25
Mixed (plastic, paper, glass, metal)	4	3	12	3	3	9	3	3	9	3	4	12	4	3	12
TOTAL IMPACT SCORES	236			257			243			245			258		

According to the results in Table 1, the effects of all solid waste types on impact categories were examined separately. Then, the total effects of these cultivars on the Air, Soil, Water, Flora, and Fauna impact categories were calculated. When the results were examined, soil and Fauna were determined as the categories most affected by solid wastes. However, it is striking that the other category's total scores are not low either. For the air category, dangerous waste and organic waste are the riskiest wastes. Medicines, Vegetable waste oil, Dangerous waste, and organic waste types emerge as the riskiest wastes for Soil, Water, Flora and Fauna categories. Studies based on Air, Soil, Water, Flora and Fauna impact categories were not found, but with organic wastes [23], dangerous wastes [21, 24], vegetable waste oil wastes [25], medicines and risk studies on waste [26] are available.

In Table 2, the impact category weights of the cities that do not have integrated solid waste facilities are presented. While determining these weights, city environmental reports were examined, air quality, soil structure and quality, water quality, flora and fauna structures were taken into account. The weights were determined as a result of the joint opinion of the experts who contributed to the preparation of the report. While determining the weights, it was considered that the air quality was close to the criteria of “clean air space”, the fertility of the soil structure, the cleanliness of the water, and the fact that the flora and fauna structures were not damaged; thus their weights are assigned to be higher.

Table 2. *Impact Category Weights by Province*

PROVINCES	IMPACT CATEGORIES				
	AIR	SOIL	WATER	FAUNA	FLORA
AĞRI	0.20	0.15	0.15	0.30	0.20
ARDAHAN	0.20	0.20	0.15	0.30	0.15
ADIYAMAN	0.15	0.20	0.20	0.30	0.15
ARTVİN	0.30	0.10	0.20	0.20	0.20
BATMAN	0.10	0.30	0.20	0.20	0.20
BARTIN	0.30	0.10	0.20	0.20	0.20
DİYARBAKIR	0.15	0.20	0.20	0.30	0.15
HAKKARİ	0.20	0.20	0.20	0.20	0.20
KARABÜK	0.25	0.10	0.20	0.20	0.20
KARS	0.25	0.15	0.20	0.30	0.10
MUŞ	0.15	0.20	0.15	0.30	0.20
ŞIRNAK	0.20	0.15	0.15	0.30	0.20
TUNCELİ	0.20	0.25	0.15	0.30	0.10

Since the weights of the impact categories in the will differ, the impact of solid waste types on these categories will change, the total risk scores calculated according to the assigned category weights are presented in Table 3.

Table 3. *Weighted Risk Scores of Cities*

CITIES	IMPACT CATEGORIES				
	AIR	SOIL	WATER	FAUNA	FLORA
AĞRI	47.2	38.55	36.45	51.6	49
ARDAHAN	47.2	51.4	36.45	38.7	36.75
ADIYAMAN	35.4	51.4	48.6	38.7	36.75
ARTVİN	70.8	25.7	48.6	51.6	49
BATMAN	23.6	77.1	48.6	51.6	49
BARTIN	70.8	25.7	48.6	51.6	49
DİYARBAKIR	35.4	51.4	48.6	38.7	36.75
HAKKARİ	47.2	51.4	48.6	51.6	49
KARABÜK	59	25.7	48.6	51.6	49
KARS	59	38.55	48.6	25.8	24.5
MUŞ	35.4	51.4	36.45	51.6	49
ŞIRNAK	47.2	38.55	36.45	51.6	49
TUNCELİ	47.2	64.25	36.45	25.8	24.5

After calculating the weighted risk scores, the amount of waste per capita in the determined provinces should also be included in the risk scores. Since the amount of waste per capita increases, it is predicted that the hazard to the environment will increase. Hence, the amount of waste per capita was obtained from the city environmental assessment reports [22], and the total risk score of each city was calculated by integrating it with the risk scores calculated in Table 3 and presented in Table 4.

Table 4. *Final Risk Score Calculation of Selected Cities*

PROVINCES	Amount of Waste Per Capita	IMPACT CATEGORIES					TOTAL RISK SCORE
		AIR	SOIL	WATER	FAUNA	FLORA	
AĞRI	1.51	47.2	38.55	36.45	51.6	49	336.43
ARDAHAN	1.78	47.2	51.4	36.45	38.7	36.75	374.69
ADIYAMAN	1.01	35.4	51.4	48.6	38.7	36.75	212.96
ARTVİN	1.49	70.8	25.7	48.6	51.6	49	366.09
BATMAN	0.87	23.6	77.1	48.6	51.6	49	217.41
BARTIN	2.06	70.8	25.7	48.6	51.6	49	506.14
DİYARBAKIR	1.11	35.4	51.4	48.6	38.7	36.75	234.04

HAKKARİ	0.81	47.2	51.4	48.6	51.6	49	200.72
KARABÜK	1.35	59	25.7	48.6	51.6	49	315.77
KARS	1.89	59	38.55	48.6	25.8	24.5	371.29
MUŞ	0.85	35.4	51.4	36.45	51.6	49	190.27
ŞIRNAK	1.49	47.2	38.55	36.45	51.6	49	331.97
TUNCELİ	1.23	47.2	64.25	36.45	25.8	24.5	243.79

According to Table 4, the city with the highest risk score is BARTIN with a total score of 500.14. This city is followed by ARDAHAN, KARS and ARTVİN.

Results for TOPSIS Method

In the study, various criteria are taken into account to be used in goal programming. The criteria in Table 5 were used in the goal programming model, in which 4 goals (Cost, Environment Impact, Social Acceptance, and Risk) were handled within the scope of Economic, Social, and Environmental.

Table 5. Evaluation Criteria

Hydrology	HY	Contamination of surface and groundwater resources by leachate is a primary concern, so the hydrology assets are important.	[9, 27]
Air quality index	AQ	Air quality represents the cleanliness of the region's airspace.	[28]
Soil & topography	ST	A suitable soil and topography structure and presence should be in order to provide installation.	[9]
Habitat, flora and fauna	HF	Areas with natural flora and fauna and habitat are not suitable as they can cause major disruption to landfills. Therefore, attention should be paid to high flora and fauna and habitat areas.	[9]

The criteria in Table 5 were evaluated on a district basis with the TOPSIS method. In the applied TOPSIS method, Soil&topography data is obtained from the agricultural land amounts of the districts from 2020 Environmental Assessment Report of Bartın [22]. Habitat, flora and fauna data are taken from Unused Agricultural Area and Grassland from the 2020 Environmental Assessment Report of Bartın as well [22]. Air quality and hydrology values were scored with expert opinion. Table 6 presents the evaluation matrix of the determining criteria.

Table 6. Decision matrix for TOPSIS

		Merkez	Amasra	Kurucaşile	Ulus
Hydrology	HY	0.53	0.8	0.73	0.13
Air quality	AQ	4	5	2	2
Soil & topography	ST	348691	38933	19906	260774
Habitat, flora and fauna	HF	81363	17137	539	181628

Table 7 represents their order of importance according to the TOPSIS application. While the environmental value is highest for the Ulus, it is followed by Merkez, Kurucaşile and Amasra.

Table 7. Order of Importance

Districts of Bartın	Importance Values
Merkez	0.573242
Amasra	0.067695
Kurucaşile	0.252953
Ulus	0.863445

Results of Goal Programming Model

In the weighted goal programming model, Cost, Environment Impact, Social Acceptance and Risk goals are taken into account. When the decision variables are examined, the establishment of the MSW facility in Amasra is the most appropriate decision according to the decision variable x_1 . According to the cap decision variable, a facility with a capacity of 5392.164 tons/month should be established. When the weights are removed in the goal programming model, it is seen that the results do not change and are parallel. In Table 8, the goal values and the values taken from the goal are available. Goal 1 includes the values of economic targets, Goal 2 environmental targets, Goal 3 social acceptability targets and Goal 4 risk targets. Since the first three target values are minimization, the value is entered as 0.

Table 8. Order of Importance

	Economic Value	Environment Impact Value	Risk Value	Social Value	Acceptance
Goal value	0	0	0	10	
d_g^+	39140	377.451	208.85	0	
d_g^-	0	0	0	3	

CONCLUSION

In this study, risk assessment of solid waste types according to different impact categories (Air, Soil, Water, Flora and Fauna) was performed and then weighted risk scores were calculated by considering the amount of waste per capita in 13 cities in Turkey that do not have facilities. It was decided to establish an MSW facility for the city with the highest risk score, and the weighted goal programming model was used for facility location selection. Evaluation of each solid waste type according to different impact categories in the study; The determination of total risk scores according to the amount of waste in different cities and the use of different parameters and goals for site selection show that the study is a unique study using an integrated combination of methods.

In this study, cities in Turkey that do not have MSW facility were taken into consideration. While making the evaluation, economic factors, environmental factors, social factors and risk factors are taken into consideration. As a result of the study, the province of Bartın was selected among the 13 cities that were considered, due to its high-risk value, and the districts within the city of Bartın are evaluated with the goal programming model with the objectives of economic factors, environmental factors, social factors and risk factors. As a result of the study, the Amasra district emerges as the optimum location. The fact that the Amasra district has a high social acceptability rate, low environmental vulnerability and low-risk score shows that choosing this district has appropriate results.

Since the application of a risk assessment method that includes more parameters may give sensitivity to the results of the study, it is planned to be considered in future studies. In addition, it is thought that increasing the constraints and parameters for the goal programming model will increase the objectivity of the study.

REFERENCES

- [1] Saxena, S., Srivastava, R. K., & Samaddar, A. B. (2010). Sustainable waste management issues in India. *IUP Journal of Soil & Water Sciences*, 3(1).
- [2] Sahar, I. A. (2019). Waste management analysis from economic-environment sustainability perspective. *People*, 109, 87-2.
- [3] Demirbas, A., Alamoudi, R. H., Ahmad, W., & Sheikh, M. H. (2016). Optimization of municipal solid waste (MSW) disposal in Saudi Arabia. *Energy Sources, Part A: Recovery, Utilization, and Environmental Effects*, 38(13), 1929-1937.
- [4] Perrot, J. F., & Subiantoro, A. (2018). Municipal waste management strategy review and waste-to-energy potentials in New Zealand. *Sustainability*, 10(9), 3114.
- [5] Gupta, N., Yadav, K. K., & Kumar, V. (2015). A review on current status of municipal solid waste management in India. *Journal of environmental sciences*, 37, 206-217.
- [6] Nas, B., Cay, T., Iscan, F., & Berkay, A. (2010). Selection of MSW landfill site for Konya, Turkey using GIS and multi-criteria evaluation. *Environmental monitoring and assessment*, 160(1), 491-500.
- [7] Hereher, M. E., Al-Awadhi, T., & Mansour, S. A. (2020). Assessment of the optimized sanitary landfill sites in Muscat, Oman. *The Egyptian Journal of Remote Sensing and Space Science*, 23(3), 355-362.
- [8] Yildirim, V. (2012). Application of raster-based GIS techniques in the siting of landfills in Trabzon Province, Turkey: a case study. *Waste Management & Research*, 30(9), 949-960.
- [9] Kharat, M. G., Kamble, S. J., Raut, R. D., Kamble, S. S., & Dhume, S. M. (2016). Modeling landfill site selection using an integrated fuzzy MCDM approach. *Modeling Earth Systems and Environment*, 2(2), 1-16.
- [10] Uyan, M. (2014). MSW landfill site selection by combining AHP with GIS for Konya, Turkey. *Environmental earth sciences*, 71(4), 1629-1639.
- [11] Yesilnacar, M. I., Süzen, M. L., Kaya, B. Ş., & Doyuran, V. (2012). Municipal solid waste landfill site selection for the city of Şanlıurfa-Turkey: an example using MCDA integrated with GIS. *International Journal of Digital Earth*, 5(2), 147-164.
- [12] Chabok, M., Asakereh, A., Bahrami, H., & Jaafarzadeh, N. O. (2020). Selection of MSW landfill site by fuzzy-AHP approach combined with GIS: case study in Ahvaz, Iran. *Environmental Monitoring and Assessment*, 192(7), 1-15.
- [13] Kokangül, A., Polat, U., & Dağsuyu, C. (2018). A new approach for environmental risk assessment. *Human and Ecological Risk Assessment: An International Journal*, 24(1), 90-104.

- [14] Gajdzik B. 2012. Comprehensive classification of environmental aspects in a manufacturing enterprise. *Metalurgija* 51(4):541–4.
- [15] Nguyen QA, and Hens L. 2015. Environmental performance of the cement industry in Vietnam: The influence of ISO 14001 certification. *J Clean Product* 96(1):362–78.
- [16] Tercan, E., Dereli, M. A., & Tapkın, S. (2020). A GIS-based multi-criteria evaluation for MSW landfill site selection in Antalya, Burdur, Isparta planning zone in Turkey. *Environmental Earth Sciences*, 79(10), 1-17.
- [17] “City Environmental Assessment Report of 2020”, “Republic of Turkey Ministry of Environment, Urbanization and Climate Change”, <https://ced.csb.gov.tr/il-cevre-durum-raporlari-i-82671>
- [18] Hwang, C. L., & Yoon, K. (1981). Multiple attribute decision making: a state of the art survey. *Lecture notes in economics and mathematical systems*, 186(1).
- [19] Shukla, A., Agarwal, P., Rana, R. S., & Purohit, R. (2017). Applications of TOPSIS algorithm on various manufacturing processes: a review. *Materials Today: Proceedings*, 4(4), 5320-5329.
- [20] Derse, O., & Yontar, E. (2020). SWARA-TOPSIS Yöntemi İle En Uygun Yenilenebilir Enerji Kaynağının Belirlenmesi [Determination Of The Most Appropriate Renewable Energy Source by SWARA-TOPSIS Method]. *Endüstri Mühendisliği [Journal of Industrial Engineering]*, 31(3), 389-419.
- [21] Derse, O., Oturakci, M., & Dagsuyu, C. (2022). Risk Analysis Application to Hazardous Material Transportation Modes. *Transportation Research Record*, 2676(3), 586-597.
- [22] <https://ced.csb.gov.tr/2020-yili-il-cevre-durum-raporlari-i-102101>
- [23] Sahlström, L. (2003). A review of survival of pathogenic bacteria in organic waste used in biogas plants. *Bioresource technology*, 87(2), 161-166.
- [24] Erkut, E., & Verter, V. (1995). A framework for hazardous materials transport risk assessment. *Risk Analysis*, 15(5), 589-601.
- [25] Niu, B., Zhang, H., Zhou, G., Zhang, S., Yang, Y., Deng, X., & Chen, Q. (2021). Safety risk assessment and early warning of chemical contamination in vegetable oil. *Food Control*, 125, 107970.
- [26] Bound, J. P., & Voulvoulis, N. (2006). Predicted and measured concentrations for selected pharmaceuticals in UK rivers: implications for risk assessment. *Water Research*, 40(15), 2885-2892.
- [27] Jamshidi-Zanjani, A., & Rezaei, M. (2017). Landfill site selection using combination of fuzzy logic and multi-attribute decision-making approach. *Environmental Earth Sciences*, 76(13), 1-14.
- [28] Sumathi, V. R., Natesan, U., & Sarkar, C. (2008). GIS-based approach for optimized siting of municipal solid waste landfill. *Waste management*, 28(11), 2146-2160.



CHAPTER 6

DATA DRIVEN SURROGATE MODELLING ASSISTED OPTIMIZATION OF MICROSTRIP MONOPOLE ANTENNA

*Peyman MAHOUTI¹, Mehmet Ali BELEN²,
Ozlem TARİ³*

1 Assoc. Prof. Yıldız Technical university, Department of Avionics Orcid ID: 0000-0002-3351-4433

2 Assoc. Prof., İskenderun Technical University, Department of Electric and Electronic Orcid ID: 0000-0001-5588-9407

3 Assoc. Prof. İstanbul Arel University, Department of Mathematics and Computer Science Orcid ID: 0000-0001-7127-5915

Introduction

An antenna is a device that is used to transmit or receive electromagnetic signals. They are designed to transmit or receive radio waves, which are a type of electromagnetic radiation. Antennas can be designed in a variety of shapes and sizes, depending on the specific frequency and type of signal that they are intended to transmit or receive. Some common types of antennas include dipole antennas, which are shaped like two straight rods or wires that are connected in the middle; loop antennas, which are shaped like a coil of wire; and Yagi antennas, which are made up of several parallel elements arranged in a specific configuration. Antenna is the key element in all wireless Radio Frequency (RF) and microwave system designs [1]. Antennas have a wide range of applications with respect to their operation frequency. For applications such as RADAR or satellite communications design with wide range and high frequency (X band) [2-3] are demanded while for other applications such as head imaging designs with lower frequencies, such as 1-4 GHz for an acceptable pareto for resolution of image and penetration level of signal into human head [4].

Microstrip antennas are one of the most commonly used models most especially for the wireless communication applications that requirements such as low profile, and specified performance criteria such as high gain, directed and or manipulated radiation pattern and wide operation band. A microstrip monopole antenna is a type of radio antenna that is made by printing a conductor pattern on a substrate, such as a printed circuit board (PCB). The substrate is typically made of a dielectric material, such as a plastic or ceramic, which has a lower electrical conductivity than metal. The conductor pattern is typically printed on one side of the substrate, and the other side is left open or is covered with a ground plane. The microstrip monopole antenna consists of a single conductor element that is suspended above the ground plane and is fed by a coaxial cable. The antenna is often used at frequencies in the range of several hundred megahertz to several gigahertz, and it has a relatively small size and low profile compared to other types of antennas [5]. From many different application examples for microstrip antennas (MA), following examples are the some of the extensively being seen in literature, such as aircraft, spacecraft, satellites, and missiles communication stages where size, weight, cost, performance, ease of installation are at most importance [6-8].

Optimizing an antenna can be challenging, depending on the specific type of antenna and the desired performance goals. Some factors that can make optimization difficult include: (I) Complexity of the antenna design: Some antenna designs, such as phased arrays or multi-element systems, can be more complex to optimize due to their multiple components and interactions. (II) Frequency range and bandwidth: The desired frequency

range and bandwidth of the antenna can affect the optimization process, as different frequencies and bandwidths may require different antenna designs or adjustments. (III) Physical constraints: The physical size and shape of the antenna, as well as the materials it is made from, can impact its performance and may need to be considered during optimization. (IV) Environmental factors: The location and surroundings of the antenna can affect its performance, such as nearby structures or interference from other sources. Overall, optimizing an antenna requires a thorough understanding of antenna design and principles, as well as the ability to analyse and adjust various factors to achieve the desired performance. It may require multiple iterations and testing to arrive at the optimal solution [9].

However, usage of direct EM solver for design optimization of microwave antenna designs is not a computationally efficient approach due to the highly expensive simulation cost of 3D EM simulators [10]. A computationally efficient method for design optimization of microwave stages is Surrogate modelling approach [11-14]. Surrogate modeling is a technique used in machine learning and optimization to approximate a complex, computationally expensive model or process with a simpler, more efficient model [11]. This allows for faster prediction or optimization without sacrificing accuracy. Surrogate models are often used when it is impractical or infeasible to use the original model directly, such as when the original model requires a large amount of data or resources to run. Surrogate models can be used in a variety of applications, including predicting the outcome of simulations, optimizing the design of engineering systems, and improving the performance of machine learning algorithms [12-14].

Herein optimization of a microstrip monopole antenna (MMA) via the use of surrogate modelling approach is taken under study. Firstly a 3D model of MMA is developed in a full wave EM simulation tool. Then a data set for creating the surrogate model is generated via the 3D EM model. Series of regression algorithms are then deployed for creating the data driven surrogate models. As the next step, the most accurate and optimal data driven solution will be deployed as surrogate model to assist the optimization search protocol for a computationally efficient design optimization process.

Trapezoidal Microstrip Monopole Antenna

In this work a trapezoidal monopole is design presented in Fig. 1 is taken as a study case example of proposed surrogate model assisted optimization process. Following specs can be considered as critical concern during the 3D EM modeling of the trapezoidal MMA. (i) Design must have a 50Ω input impedance. (ii) The length parameters determines the lowest operating frequency. (iii) The upper operating frequency is determined based on the width of radiating element and substrate material pa-

rameters (height, thickness, dielectric constant).

Here based on the design parameters given in Fig. 1 and their boundary conditions in Table 1 a data set for training the surrogate models are generated. For generating the data set Latin-Hyper-Cube Sampling method is used with 1000 samples. The ratio of training and test (holdout) data samples are arranged as 80-20 percent of the whole samples. Within the given range of design variables many different design geometry can be obtained each of which can be used for different application with respect to the operation frequency. Here the operation range is taken between 1-14 GHz with step size of 0.1 GHz.

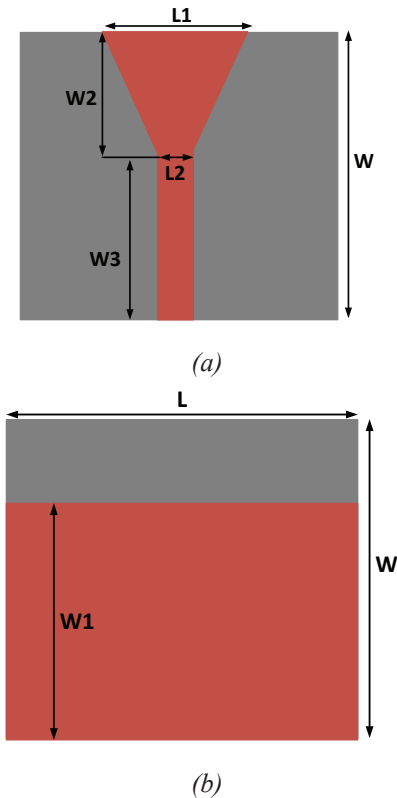


Fig. 1.Schematic of trapezoidal MMA (a) Top, (b) Ground, Layer.

Table 1. Lower & Upper boundary values of Trapezoidal MMA variables in [mm]. $W=50$, $L= 65$ [mm].

L1	1-35	W1	1-35
L2	1-15	W2	1-20
W3		1-35	

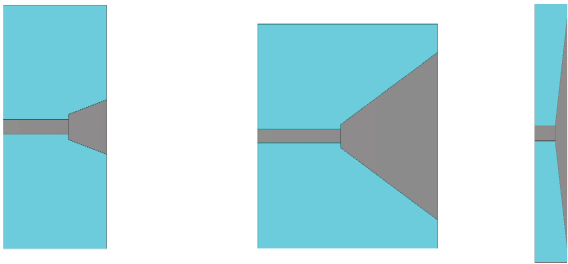


Fig. 2. Different design views for the Trapezoidal MMA for different design values.

Data Driven Surrogate Modeling of Trapezoidal MMA

In this section following artificial intelligence based regression methods had been deployed to create a surrogate model representation of the studied MMA design; (i) Multi-layer-perceptron (MLP), (ii) Support Vector Regression machine (SVRM), (iii) Gaussian Process Regression (GPR). Each of the models are trained with a k-fold cross validation with fold parameter equal to 4, and 20% of the whole data is left out to be used as test (holdout) data set to observe the models over fitting performance. With respect to the Relative Mean Error (RME) metric SVRM had shown best performance characteristic both in k-fold and hold-out data sets. The hyper parameters and obtained results given in Table 2 are obtained via a simple grid search optimization process of each model which are coded in MATLAB environment. In the next stage the obtained SVRM surrogate model will be used to assist a meta-heuristic optimization process to design series of antenna model for different operation bands.

Table 2. Regression performance of algorithms for the holdout and k-fold validation

Model	Hyper-Parameters	K-fold/Holdout RME [%]
MLP	[Hidden-Layer size; Neurons; Activation function]=[2; 15-25; tangent sigmoid]	8.7/9.8
SVRM	[Kernel-function; Kernel Type; Epsilon]=[Radial; Epsilon; 0.075]	3.9/4.6
GPR	[Kernel; Prediction-technique; block size]=[matern (5/2); Block-coordinate; 1000]	5.9/7.1

Data Driven Surrogate Model Assisted Optimization of Trapezoidal MMA

Since data driven surrogate modeling approach can significantly improve the computational time of antennas compared to 3D EM simulators usage of meta-heuristic optimization algorithms is a viable solution

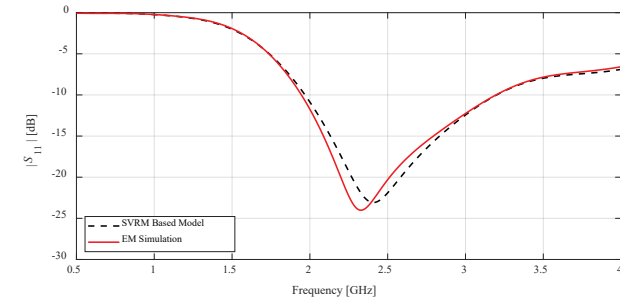
for this type of optimization problems. Although there are series of high performance optimization techniques based on different species and their hunting, mating or other behaviours, the effect of convergence speed of these algorithm can be neglected thanks to the significant acceleration of surrogate modelling. Here one of the traditional optimization algorithms Particle Swarm Optimization (PSO) [15] is used for conducting the optimal design parameter search based on the following cost function Eq (1),

$$x^* = \arg \min_x [\max \{ |S_{11}(x, f_r)| \}] \quad (1)$$

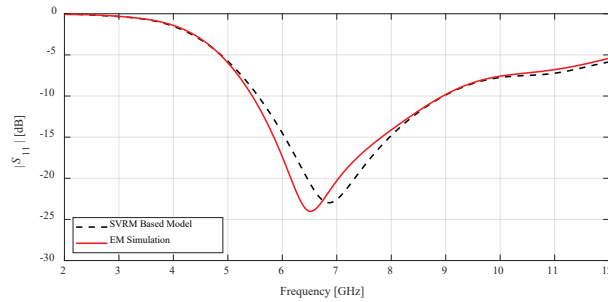
x is the input vector of variables of $[W_1, W_2, W_3, L_1, L_2], [f_r]$ targeted operating frequency. Here, it is aimed to obtained there different antenna model for three different operation band. The study cases and their optimally obtained geometrical design variables are as follows:

- Case I: Antenna operates 2.4 GHz. The optimally selected design variables are $W_1=31.90$ $W_2=15.85$, $W_3=33.65$, $L_1=33.45$, $L_2=6.65$, $L_3=$ all in [mm].
- Case II: Antenna operates 7 GHz. The optimally selected design variables are $W_1=11.45$, $W_2=5.70$, $W_3=12.25$, $L_1=11.95$, $L_2=2.45$ all in [mm].
- Case III: Antenna operates 10 GHz. The optimally selected design variables are $W_1=7.85$, $W_2=3.95$, $L_1=8.35$, $W_3=8.65$, $L_2=1.85$ all in [mm].

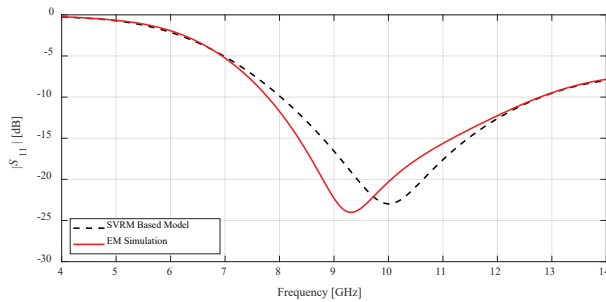
Furthermore the 3D EM simulated results and the surrogate model response of each study case are presented in Fig. 3. As it can be seen form the figure the proposed surrogate modelling approach not only achieves to find the requested geometrical design variables to bring the requested response form the design but also the obtained results are in high agreement with 3D EM simulation results.



(a)



(b)



(c)

Fig. 3. Simulated scattering parameter of SVRM and 3D EM simulator for (a) Case I, (b) Case II, (c) Case III.

Conclusion

In this work design optimization of a Trapezoidal Microstrip Monopole Antenna (MMA) had been solved with a computationally efficient approach based on data driven surrogate modelling techniques. The data samples obtained via 3D EM simulators had been used to create a surrogate representation of the handled antenna problem. Based on performance comparison of series of regression algorithms SVRM found to be the optimal solution for this problem. Then for validation of the propose approach three different study case is taken under study as an optimization

problem to be solved via the proposed approach and the obtained results are compared with results of 3D EM full wave simulator results. As it can be seen from the results the proposed surrogate modelling approach not only achieves to find the requested geometrical design variables to bring the requested response from the design but also the obtained results are in high agreement with 3D EM simulation results.

Acknowledgment

We would like to express our special thanks of gratitude to the Aktif Naser Elektronik and DataRobot, for providing researcher licenses for CST and DataRobot.

REFERENCES

- [1] Ahdi Rezaeieh, S., Zamani, A., Abbosh, A. M. (2015). 3-D Wideband Antenna for Head-Imaging System with Performance Verification in Brain Tumor Detection. *IEEE Antennas and Wireless Propagation Letters*, 14, pp. 910-914. <https://doi.org/10.1109/LAWP.2014.2386852>
- [2] Hornby, Gregory S., Jason D. Lohn, and Derek S. Linden. "Computer-automated evolution of an X-band antenna for NASA's space technology 5 mission." *Evolutionary computation* 19, no. 1 (2011): 1-23.
- [3] Kuo, Fang-Yao, and Ruey-Bing Hwang. "High-isolation X-band marine radar antenna design." *IEEE Transactions on Antennas and Propagation* 62, no. 5 (2014): 2331-2337.
- [4] Suganthi, S., and P. T. Selvan. "Trapezoidal Microstrip Patch Antenna Array for Low Frequency Medical Applications." *Wireless Personal Communications* 126, no. 2 (2022): 1721-1732.
- [5] Calik, N, Belen, MA, Mahouti, P. Deep learning base modified MLP model for precise scattering parameter prediction of capacitive feed antenna. *Int J Numer Model*. 2020; 33:e2682. <https://doi.org/10.1002/jnm.2682>
- [6] Rop K, Konditi D, Ouma H, Musyoki S. Parameter optimization in design of a rectangular microstrip patch antenna using adaptive neuro-fuzzy inference system technique. *IJTPE Journal*, ISSN 2012: 2077–3528.
- [7] Kasabegoudar VG, Upadhyay DS, Vinoy K. Design studies of ultra-wideband microstrip antennas with a small capacitive feed. *International Journal of Antennas and Propagation* 2007; 2007.
- [8] Singh I, Tripathi V. Micro strip patch antenna and its applications: a survey. *Int. J. Comp. Tech. Appl* 2011; 2(5): 1595–1599.
- [9] Belen, A., Günes, F., Palandoken, M. et al. 3D EM data driven surrogate based design optimization of traveling wave antennas for beam scanning in X-band: an application example. *Wireless Netw* 28, 1827–1834 (2022). <https://doi.org/10.1007/s11276-022-02937-7>
- [10] Koziel, S., Pietrenko-Dabrowska, A. Low-cost quasi-global optimization of expensive electromagnetic simulation models by inverse surrogates and response features. *Sci Rep* 12, 19894 (2022). <https://doi.org/10.1038/s41598-022-24250-1>
- [11] S. Koziel and A. Pietrenko-Dabrowska, "Tolerance Optimization of Antenna Structures by Means of Response Feature Surrogates," in *IEEE Transactions on Antennas and Propagation*, vol. 70, no. 11, pp. 10988-10997, Nov. 2022, doi: 10.1109/TAP.2022.3187665.
- [12] A. Pietrenko-Dabrowska, S. Koziel, J. W. Bandler and J. E. Rayas-Sanchez, "EM-Driven Tolerance Optimization of Compact Microwave Components Using Response Feature Surrogates," 2022 IEEE/MTT-S International Microwave Symposium - IMS 2022, 2022, pp. 107-110, doi: 10.1109/IMS37962.2022.9865578.

- [13] *Pietrenko-Dabrowska, A., Koziel, S. & Ullah, U. Reduced-cost two-level surrogate antenna modeling using domain confinement and response features. Sci Rep 12, 4667 (2022). <https://doi.org/10.1038/s41598-022-08710-2>*
- [14] *S. Koziel and A. Pietrenko-Dabrowska, "Tolerance-Aware Multi-Objective Optimization of Antennas by Means of Feature-Based Regression Surrogates," in IEEE Transactions on Antennas and Propagation, vol. 70, no. 7, pp. 5636-5646, July 2022, doi: 10.1109/TAP.2022.3145462.*
- [15] *Marini, Federico, and Beata Walczak. "Particle swarm optimization (PSO). A tutorial." Chemometrics and Intelligent Laboratory Systems 149 (2015): 153-165.*



CHAPTER 7

A STUDY ON REMOTE MONITORING OF AN AIR QUALITY SENSOR

Tuba ÖZDEMİR ÖGE¹, Mecit ÖGE²

1 Assoc. Prof. Dr. Bartın University, Vocational School of Health Services, Department of Medical Services and Techniques, Opticianry Program, Bartın, Turkey. E-mail: tozdemir@bartin.edu.tr, ORCID ID, <https://orcid.org/0000-0001-6690-7199>.

2 Asst. Prof. Dr. Bartın University, Faculty of Engineering, Architecture and Design, Department of Mechanical Engineering, Kutlubey-Yazıcılar Campus, 74100 Bartın, Turkey; ORCID ID, <https://orcid.org/0000-0001-5243-0828>.

Introduction

The preliminary steps of industrial progress involving the emergence of mass production with the first industrial revolution; and application of production lines with the second industrial revolution, were followed by digitization of industrial systems with the third industrial revolution. In the recent decades, the world has been undergoing a fast transformation of these digitized industrial systems into “smart” industrial systems through incredibly accelerated flow of data enabled by Internet of Things (IoT) compatible smart devices, data processing technologies such as Big Data Analytics and Artificial Intelligence (AI) technologies such as Machine Learning (ML).

The GSM Association (GSMA) forecasts that, the number of IoT devices will globally reach around 25 billion by year 2025, with a sharp increase from 10.3 billion in year 2018 (GSMA, 2019). All these hardware and data components of the fourth industrial revolution, also known as Industry 4.0, collectively contribute to the development of smart cyber-physical industrial systems that communicate with each other and autonomously react to their environment, thus paving the way towards a more human-less industry, which is also referred to as Industry 5.0. The real-life applications of IoT mainly consist of its use in complex automated domains such as Industrial Automation Systems (IAS), Building Automation Systems (BAS) and manufacturing systems, which is also referred to as Industrial Internet of Things (IIoT) (Thuluva, et al., 2020). The non-uniformity of vast amount of data received from diverse sources in these complex automation systems (Thuluva, et al., 2020) and the need for structuring and classifying them, in addition to the timely and costly process of making modifications on engineering tools employed to build automation systems (Bangemann, et al., 2014), render the design, development and deployment of new IoT applications on commissioned automation systems a challenging task. Such challenges have led to the development of user-friendly, Visual Programming Language (VPL) based IoT application development tools such as Node-Red. With the help of such VPL-based tools, end-users are liberated from the enormous burden of data structuring and may concentrate on developing and configuring their IIoT applications without having to possess extensive technical knowledge. Moreover, the developed IoT applications can be controlled via web services by use of service-oriented architectures (Jammes & Smit, 2005; Thuluva, et al., 2020). Among these VPL based solutions, Node-RED is one of the most-commonly used ones as an open-source application development tool by which several hardware (sensors, actuators, etc.), application programming interfaces (APIs) and other services (collectively referred to as “nodes”) are visually manipulat-

ed to simulate flows between these elements, as a means to determine the system's behavior (Torres, et al., 2020). Node-RED was developed as an open-sourced side-project by Nick O'Leary and Dave Conway-Jones from the Emerging Technology Services Group of IBM in 2013, and it has been an open-source tool since then (Nodered.org, 2022). Screenshots related to the installation and running of Node-RED on a Windows operating system are shown in Figure 1.

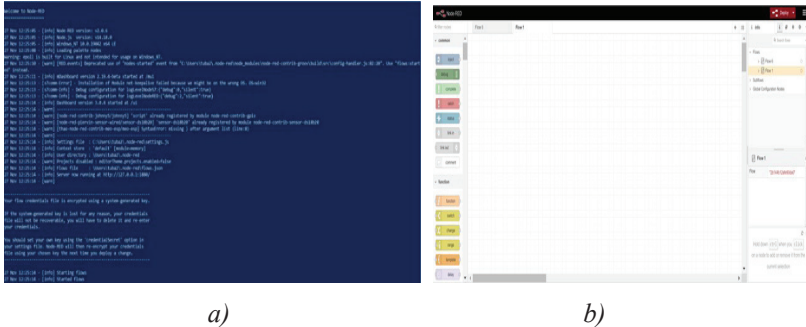


Figure 1. a) Node-RED installation screen, and b) Node-RED user interface.

The application range of Node-RED can be extended to virtually all fields where IoT technologies are applied ranging from domestic to industrial scale, hence the increasing number of studies on the subject. Lu, et al. (2020) used Node-RED application development software and an ESP8266 Wi-Fi based NodeMCU microcontroller board, the Message Queuing Telemetry Transport (MQTT) messaging protocol, and MySQL tools for database management to design a home monitoring system for monitoring environmental parameters and remotely controlling home appliances (Lu, et al., 2021). In another work, Sicari et al., (2018) proposed the use of Node-RED in testing the behavior of IoT-based smart transport and logistics environments and highlighted the tool's efficiency due to its user-friendly interface and usability of its components (Sicari et al., 2018). Ferencz and Domokos (2020) addressed the advantages of Node-RED in rapidly developing prototypes for IIoT applications. They also highlighted Node-RED's advantages in data visualization along with MQTT's effectiveness in building business logic (Ferencz & Domokos, 2020). Thuluva, et al. (2020) chose Node-RED to determine whether Semantic Web technologies and standardized W3C WoT (World Wide Web Consortium – Web of Things) technologies can be used to improve semantic interoperability for IoT applications (Thuluva, et al. 2020). Torres et al. (2020) proposed some improvements on Node-RED to enhance its observability and debugging mechanisms, and empirically tested these improvements. They concluded that, their attempts resulted in a reduction in development times and the

number of failed system deployments (Torres, et al. 2020). Degreef et al. (2019) proposed an open-source, low-cost automation system for educational purposes using Node-RED and Raspberry Pi (Degreef, et al. 2019). Rajalakshmi and Shahnasser (2017) proposed a way to bring Node-RED into the cloud using IBM's Bluemix platform to improve the communication between IoT devices and users (Rajalakshmi & Shahnasser, 2017). Simpkin, et al., (2020) proposed methods to bring Node-RED workflows into decentralized environments of execution using vector symbolic architectures (VSA) to enable them to operate on edge networks (Simpkin, et al. 2020).

In this study, air quality measurement values were obtained in ppm using Wemos D1 Esp8266 Wi-Fi Card and MQ135 air quality sensor. The remote control and monitoring of the data received from the sensor was achieved with Node-RED flow diagrams, ThingSpeak platform and OTA programming.

Method

Internet of Things (IoT) is a technology to enable all objects to access the Internet and communicate with other devices. IoT applications use communication technologies such as Bluetooth and Wi-Fi for connectivity.

The MQ-135 is an air quality measurement sensor. Its length is 32 mm, width is 22mm and height is 30 mm. It works with 5V voltage and has digital (TTL/Transistor-Transistor Logic) and analog outputs. Concentration range is between 10 to 1000 ppm (MQ-135 Datasheet, 2022). An image of MQ-135 sensor is shown in Figure 2.

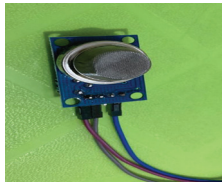


Figure 2. *MQ-135 sensor*

The Wemos D1 Board is controlled by the ESP8266 chip (32-bit processor). Wemos D1 Esp8266 Wi-Fi Board consists of 11 digital I/O pins and 1 analog (input) pin. The power input supports 9-24 V input voltages.

http://arduino.esp8266.com/stable/package_esp8266com_index.json in Additional circuit boards manager URLs' in File > Preferences was typed to program with Arduino IDE before OTA programming (Figure 3).

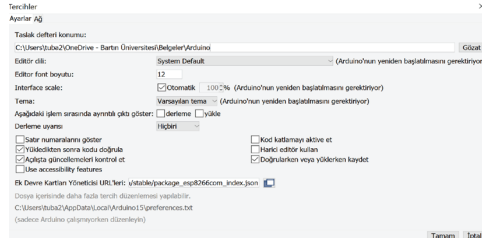


Figure 3. http://arduino.esp8266.com/stable/package_esp8266com_index.json



Figure 4. Over-The-Air (OTA) programming on *Wemos D1 Esp8266* Wi-Fi Card

In this study, we provide information on how to program the Esp8266 over Wi-Fi without connecting to the computer with a USB cable. Illustration of Wi-Fi enabled micro controller (Wemos D1 Esp8266 Wi-Fi Card) is shown in Figure 4.

BasicOTA code (Figure 5a) was written in Arduino IDE. After OTA programming (Figure 5b), the card was connected to a network with an IP address (Figure 5c). Port screen is shown in Figure 5d. After selecting Tools > Card > Wemos D1 R2, the settings were made as CPU Frequency: “80MHz”, Flash Size: “4M (3M SPIFFS)”, upload speed: “115200”. The card connected to the network appears under the Tools menu PORT in the Arduino IDE (Figure 5).

a) (Arduino OTA)-(BasicOTA code)

```

#include <ESP8266WiFi.h>
#include <ESP8266WebServer.h>
#include <ESP8266OTA.h>
#include <ArduinoOTA.h>

//Define PORTS
#define PORT "Digikey_8021_4020"
#define USER "17N0y0000"

void setup()
{
  ...
  ...
  ...
}

void loop()
{
  ...
  ...
  ...
}

```

b) OTA programming

COM4

Ready
IP address: 192.168.1.135

c) Card is connected to a network and has an IP address.

mq135-6 | Arduino 1.8.16

Doğruya Düzeltme Yasak Araçlar Yardım

mq135-6

```

#include <ESP8266.h>
#include "MQ135.h"

//Define pins
#define DOUT_PIN 4
#define DOUT_PIN2 5
#define DOUT_PIN3 6
#define DOUT_PIN4 7
#define DOUT_PIN5 8
#define DOUT_PIN6 9
#define DOUT_PIN7 10
#define DOUT_PIN8 11
#define DOUT_PIN9 12
#define DOUT_PIN10 13
#define DOUT_PIN11 14
#define DOUT_PIN12 15
#define DOUT_PIN13 16
#define DOUT_PIN14 17
#define DOUT_PIN15 18
#define DOUT_PIN16 19
#define DOUT_PIN17 20
#define DOUT_PIN18 21
#define DOUT_PIN19 22
#define DOUT_PIN20 23
#define DOUT_PIN21 24
#define DOUT_PIN22 25
#define DOUT_PIN23 26
#define DOUT_PIN24 27
#define DOUT_PIN25 28
#define DOUT_PIN26 29
#define DOUT_PIN27 30
#define DOUT_PIN28 31
#define DOUT_PIN29 32
#define DOUT_PIN30 33
#define DOUT_PIN31 34
#define DOUT_PIN32 35
#define DOUT_PIN33 36
#define DOUT_PIN34 37
#define DOUT_PIN35 38
#define DOUT_PIN36 39
#define DOUT_PIN37 40
#define DOUT_PIN38 41
#define DOUT_PIN39 42
#define DOUT_PIN40 43
#define DOUT_PIN41 44
#define DOUT_PIN42 45
#define DOUT_PIN43 46
#define DOUT_PIN44 47
#define DOUT_PIN45 48
#define DOUT_PIN46 49
#define DOUT_PIN47 50
#define DOUT_PIN48 51
#define DOUT_PIN49 52
#define DOUT_PIN50 53
#define DOUT_PIN51 54
#define DOUT_PIN52 55
#define DOUT_PIN53 56
#define DOUT_PIN54 57
#define DOUT_PIN55 58
#define DOUT_PIN56 59
#define DOUT_PIN57 60
#define DOUT_PIN58 61
#define DOUT_PIN59 62
#define DOUT_PIN60 63
#define DOUT_PIN61 64
#define DOUT_PIN62 65
#define DOUT_PIN63 66
#define DOUT_PIN64 67
#define DOUT_PIN65 68
#define DOUT_PIN66 69
#define DOUT_PIN67 70
#define DOUT_PIN68 71
#define DOUT_PIN69 72
#define DOUT_PIN70 73
#define DOUT_PIN71 74
#define DOUT_PIN72 75
#define DOUT_PIN73 76
#define DOUT_PIN74 77
#define DOUT_PIN75 78
#define DOUT_PIN76 79
#define DOUT_PIN77 80
#define DOUT_PIN78 81
#define DOUT_PIN79 82
#define DOUT_PIN80 83
#define DOUT_PIN81 84
#define DOUT_PIN82 85
#define DOUT_PIN83 86
#define DOUT_PIN84 87
#define DOUT_PIN85 88
#define DOUT_PIN86 89
#define DOUT_PIN87 90
#define DOUT_PIN88 91
#define DOUT_PIN89 92
#define DOUT_PIN90 93
#define DOUT_PIN91 94
#define DOUT_PIN92 95
#define DOUT_PIN93 96
#define DOUT_PIN94 97
#define DOUT_PIN95 98
#define DOUT_PIN96 99
#define DOUT_PIN97 100
#define DOUT_PIN98 101
#define DOUT_PIN99 102
#define DOUT_PIN100 103
#define DOUT_PIN101 104
#define DOUT_PIN102 105
#define DOUT_PIN103 106
#define DOUT_PIN104 107
#define DOUT_PIN105 108
#define DOUT_PIN106 109
#define DOUT_PIN107 110
#define DOUT_PIN108 111
#define DOUT_PIN109 112
#define DOUT_PIN110 113
#define DOUT_PIN111 114
#define DOUT_PIN112 115
#define DOUT_PIN113 116
#define DOUT_PIN114 117
#define DOUT_PIN115 118
#define DOUT_PIN116 119
#define DOUT_PIN117 120
#define DOUT_PIN118 121
#define DOUT_PIN119 122
#define DOUT_PIN120 123
#define DOUT_PIN121 124
#define DOUT_PIN122 125
#define DOUT_PIN123 126
#define DOUT_PIN124 127
#define DOUT_PIN125 128
#define DOUT_PIN126 129
#define DOUT_PIN127 130
#define DOUT_PIN128 131
#define DOUT_PIN129 132
#define DOUT_PIN130 133
#define DOUT_PIN131 134
#define DOUT_PIN132 135
#define DOUT_PIN133 136
#define DOUT_PIN134 137
#define DOUT_PIN135 138
#define DOUT_PIN136 139
#define DOUT_PIN137 140
#define DOUT_PIN138 141
#define DOUT_PIN139 142
#define DOUT_PIN140 143
#define DOUT_PIN141 144
#define DOUT_PIN142 145
#define DOUT_PIN143 146
#define DOUT_PIN144 147
#define DOUT_PIN145 148
#define DOUT_PIN146 149
#define DOUT_PIN147 150
#define DOUT_PIN148 151
#define DOUT_PIN149 152
#define DOUT_PIN150 153
#define DOUT_PIN151 154
#define DOUT_PIN152 155
#define DOUT_PIN153 156
#define DOUT_PIN154 157
#define DOUT_PIN155 158
#define DOUT_PIN156 159
#define DOUT_PIN157 160
#define DOUT_PIN158 161
#define DOUT_PIN159 162
#define DOUT_PIN160 163
#define DOUT_PIN161 164
#define DOUT_PIN162 165
#define DOUT_PIN163 166
#define DOUT_PIN164 167
#define DOUT_PIN165 168
#define DOUT_PIN166 169
#define DOUT_PIN167 170
#define DOUT_PIN168 171
#define DOUT_PIN169 172
#define DOUT_PIN170 173
#define DOUT_PIN171 174
#define DOUT_PIN172 175
#define DOUT_PIN173 176
#define DOUT_PIN174 177
#define DOUT_PIN175 178
#define DOUT_PIN176 179
#define DOUT_PIN177 180
#define DOUT_PIN178 181
#define DOUT_PIN179 182
#define DOUT_PIN180 183
#define DOUT_PIN181 184
#define DOUT_PIN182 185
#define DOUT_PIN183 186
#define DOUT_PIN184 187
#define DOUT_PIN185 188
#define DOUT_PIN186 189
#define DOUT_PIN187 190
#define DOUT_PIN188 191
#define DOUT_PIN189 192
#define DOUT_PIN190 193
#define DOUT_PIN191 194
#define DOUT_PIN192 195
#define DOUT_PIN193 196
#define DOUT_PIN194 197
#define DOUT_PIN195 198
#define DOUT_PIN196 199
#define DOUT_PIN197 200
#define DOUT_PIN198 201
#define DOUT_PIN199 202
#define DOUT_PIN200 203
#define DOUT_PIN201 204
#define DOUT_PIN202 205
#define DOUT_PIN203 206
#define DOUT_PIN204 207
#define DOUT_PIN205 208
#define DOUT_PIN206 209
#define DOUT_PIN207 210
#define DOUT_PIN208 211
#define DOUT_PIN209 212
#define DOUT_PIN210 213
#define DOUT_PIN211 214
#define DOUT_PIN212 215
#define DOUT_PIN213 216
#define DOUT_PIN214 217
#define DOUT_PIN215 218
#define DOUT_PIN216 219
#define DOUT_PIN217 220
#define DOUT_PIN218 221
#define DOUT_PIN219 222
#define DOUT_PIN220 223
#define DOUT_PIN221 224
#define DOUT_PIN222 225
#define DOUT_PIN223 226
#define DOUT_PIN224 227
#define DOUT_PIN225 228
#define DOUT_PIN226 229
#define DOUT_PIN227 230
#define DOUT_PIN228 231
#define DOUT_PIN229 232
#define DOUT_PIN230 233
#define DOUT_PIN231 234
#define DOUT_PIN232 235
#define DOUT_PIN233 236
#define DOUT_PIN234 237
#define DOUT_PIN235 238
#define DOUT_PIN236 239
#define DOUT_PIN237 240
#define DOUT_PIN238 241
#define DOUT_PIN239 242
#define DOUT_PIN240 243
#define DOUT_PIN241 244
#define DOUT_PIN242 245
#define DOUT_PIN243 246
#define DOUT_PIN244 247
#define DOUT_PIN245 248
#define DOUT_PIN246 249
#define DOUT_PIN247 250
#define DOUT_PIN248 251
#define DOUT_PIN249 252
#define DOUT_PIN250 253
#define DOUT_PIN251 254
#define DOUT_PIN252 255

```

Wifi101 / WIFIPINA Firmware Updater

Kart: "LOLIN(WiFiMod) D1 R1"

Upload Speed: "115200"

CPU Frequency: "80 MHz"

Flash Size: "4MB (FS-2MB OTA ~ 1019KB)"

Debug port: "Disabled"

Debug Level: "Hicbi"

WiFi Variant: "v2 Lower Memory"

VTables: "Flash"

C++ Exceptions: "Disabled (new aborts on oom)"

Stack Protection: "Disabled"

Erase Flash: "Only Sketch"

SSL Support: "All SSL ciphers (most compatible)"

MMIO: "32KB cache + 32KB IRAM (balanced)"

Non-32-Bit Access: "Use pgm_read macros for IRAM/PROGMEM"

Port: "esp8266-d59b42 at 192.168.1.135"

Kart Bilgisi Al

Programlayıcı

Önyükleyiciyi Yazdır

Ag portları

esp8266-d59b42 at 192.168.1.135

d) Arduino IDE and PORT screen (OTA port)

Figure 5. *OTA installation*

Application of OTA, Node-RED and ThingSpeak

Over-The-Air (OTA) is a framework that provides over-the-air software installation. It becomes useful especially when it is difficult to connect the ESP module to the computer all the time or when a modification is required in the designed system. It is essential that the ESP module and the computer are connected to the same network. Initially, OTA codes containing OTA definitions were loaded into the card via USB connection. The new codes should have the necessary sections for OTA again, because then we will be able to remotely upload to the card again. OTA (Over the Air) update is achieved through the upload of firmware to an ESP module over a Wi-Fi connection instead of using a serial port. There are different ways (Arduino IDE, Web Browser, HTTP Server) for OTA programming with the ESP boards. In our study, OTA programming was performed on Arduino IDE.

In the present work, Node-RED programming tool was used (nodered.org, 2022). Node-RED debug and Node-RED Dashboard outputs are shown in Figure 6. Three different flow diagrams are shown in Figure 6. In Figure 6a, the data received from the COM4 port are shown on NODE-RED debug. In Figure 6b, the data received from the COM4 port are shown on NODE-RED debug and Node-RED Dashboard. In Figure 6c, the data received from ThingSpeak in the Node-RED flow diagram are shown on NODE-RED debug and Node-RED Dashboard.

Figure 7 shows the data streams stored in the channel received from MQ-135 sensor by using ThingSpeak that is IoT analytics platform service (ThingSpeak for IOT, 2022).

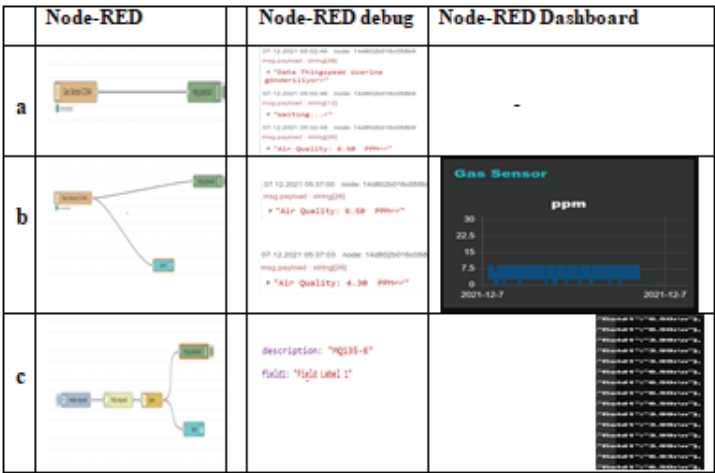


Figure 6. Node-RED output

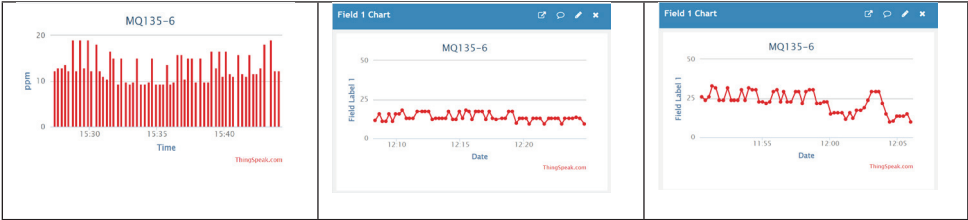


Figure 7. Screenshots related to ThingSpeak output

Conclusion

In the current study, brief information on Node-RED, ThingSpeak, MQ-135 sensor and their use in IoT is explained, and then the results of a study on remote control and monitoring of the data from an MQ-135 sensor, using Node-RED and ThingSpeak are introduced. As shown by the performed application, the use of Node-RED and ThingSpeak can be extended to numerous other applications in IoT environments.

Acknowledgements

This work is performed within the scope of Bartın University’s Specialization Field: “*Smart Logistics and Integrated Region Applications*” as per Turkey’s Council of Higher Education’s (YÖK) “Regional Development-Oriented Mission Differentiation and Specialization Project”.

References

- Bangemann, T., Karnouskos, S., Camp, R. & Carlsson, O. (2014). State of the Art in Industrial Automation in book: *Industrial Cloud-based Cyber-Physical Systems: The IMC-AESOP Approach*. Springer.
- Degreef, P., Merode, D. V. & Tabunshchik, G. (2019). Low-Cost, Open-Source Automation System for Education, with Node-RED and Raspberry Pi, *Smart Industry & Smart Education*. 458–465. Doi: 10.1007/978-3-319-95678-7_51.
- Ferencz, Katalin & Domokos, Jozsef. (2020). Using Node-RED platform in an industrial environment. *Conference: XXXV. Jubileumi Kándó KonferenciaAt: Budapest, Magyarország*.
- GSMA (2019). | *IoT Connections Forecast: The Rise of Enterprise*. Retrieved September 2, 2022, from <https://www.gsma.com/iot/resources/iot-connections-forecast-the-rise-of-enterprise/>
- Jammes, F. & Smit, H. (2005). Service-oriented paradigms in industrial automation | IEEE Explore Retrieved September 2, 2022, from <https://ieeexplore.ieee.org/document/1411764>.
- Lu, C.Y., Chen, F.H., Hsu, W.C., Yang, Y.Q. & Su, T.J. (2020). Constructing Home Monitoring System with Node-RED. *Sensors and Materials*. 32(5), 1701-1710. Doi: /10.18494/SAM.2020.2686
- MQ-135 datasheet | MQ-135 Gas Sensor. Retrieved September 2, 2022, from https://components101.com/sites/default/files/component_datasheet/MQ135%20Datasheet.pdf
- Nodered.org. Retrieved September 2, 2022, from <https://nodered.org/about/>.
- Rajalakshmi, A. & Shahnasser, H., “Internet of Things using Node-Red and alexa,” (2017). *17th International Symposium on Communications and Information Technologies (ISCIT)*, pp. 1-4, doi:10.1109/ISCIT.2017.8261194.
- Sicari, S., Rizzardi, A. & Coen-Porisini, A. (2018). Smart transport and logistics: A Node-RED implementation. *Internet Technology Letters*. <https://doi.org/10.1002/itl2.88>.
- Simpkin, C., Taylor, I., Harborne, D., Bent, G., Preece, A., Ganti, R. K. (2020). Efficient orchestration of Node-RED IoT workflows using a Vector Symbolic Architecture. *Future Generation Computer Systems*. 111, 117-131. Doi: 10.1016/j.future.2020.04.005.
- ThingSpeak for IoT. Retrieved September 2, 2022, from https://thingspeak.com/pages/commercial_learn_more
- Thuluva, A. S., Anicic D., Rudolph S., Adikari M. (2020). Semantic Node-RED for Rapid Development of Interoperable Industrial IoT Applications, *Semantic Web, IOS Press*, 11(6):949-975..

Torres, D., Dias, J. Restivo, P., A. and H. S. Ferreira. (2020). Real-time Feedback in Node-RED for IoT Development: An Empirical Study, *2020 IEEE/ACM 24th International Symposium on Distributed Simulation and Real Time Applications (DS-RT)*, 1-8, doi: 10.1109/DS-RT50469.2020.9213544.



CHAPTER 8

GEOLOGICAL SOURCES, CLASSIFICATION AND NEW TECHNICAL APPLICATIONS OF GEMSTONES

Yeşim ÖZEN¹

¹ Dr. , Konya Technical University, Geological Engineering Department, Konya, Türkiye, yozen@ktun.edu.tr, ORCID: 0000-0003-2302-1958

1. Introduction

For more than four and a half billion years, geological forces reshaped the earth's surface, a dynamic laboratory, and formed the minerals within it. Today, it is known that there are more than 3000 different types of minerals, each with its characteristics. However, approximately 70 of them are included in the very special class called gemstones and they have the necessary properties to make them suitable for use as gemstones. Gemstones, which are mostly minerals, are distinguished from all other minerals by their durability, beauty, and rarity (O'Donoghue, 1988). Given that almost all gemstones are minerals, it is important to identify the mineral. The dictionary definition of a mineral is "matter obtained by mining". The scientific definition of a mineral is a homogeneous or uniform substance formed inorganically by the forces of nature in the earth's crust (Read, 2005). Each mineral has a unique chemical formula and a set of physical properties. There is a smaller group of metallic minerals within this precious mineral group (e.g. Keller and Kampf, 1985; Read, 1988; Keller, 1990). Among them, gold, silver, platinum, and precious metals such as rhodium and iridium, which are platinum group metals, share the feature of being a chemical element on their own with diamond, rather than being compounds of elements like all other jewelry materials (Read, 1988).

Gemstone is a mineral, rock, or petrified organic matter that has been used as a symbol of wealth and status since pre-historic times, gained value as a result of its unique physicochemical properties such as beauty, durability, attractiveness, comparative rarity, being suitable for shaping, and can be cut and polished to be used as jewelry or other ornaments (e.g. O'Donoghue, 1988; Hatipoğlu, 2020).

Gemology is a discipline of Geology. Gemology is a scientific and commercial activity that deals with every method and process in the process of the formation of gemstones on earth, the search and discovery of this gemstone in nature, its processing and its presentation to the taste and use of the consumer. It also provides information about synthetic, imitation, and processed stones (e.g. Philipsborn, 1967; Ramdohr and Strunz, 1978; Hatipoğlu, 2020).

Gemstones have been divided into semi-precious and precious gems for many years in the literature. The terms "precious" and "semi-precious" are often used to separate gemstones. Gemstones include high-value stones such as diamonds, rubies, sapphires, and emeralds, while semi-precious stones include amethyst, citrine, tourmaline, zircon, and peridot. Compared to the value of a low-quality ruby with the value of a good peridot, this practice was meaningless and contradictory to some researchers. In both jewelry and gemology, instead of using the terms precious and

semi-precious, it is classified as a gemstone because of its durability, beauty, and rarity (Read, 1988). Precious gemstones are called jewelry stones, and semi-precious gemstones are called ornament (necklaces, earrings, rings, etc.) and decorative object stones (Hatipoğlu, 2020).

In the process of evaluating the gemstones by processing: cutting, shaving, trimming, etching, polishing, drilling, cabochon, faceting, tumbling, carving, mosaic, etc. They are made from a raw form using one or more methods. Gemstones processed with the methods offer an economic value by using them as jewelry or ornament (necklaces, earrings, blanks, rings, etc.) or as decorative objects (trinkets, vases, statues, key chains, seal handles, walking sticks, etc.).

2. Geological Sources and Formation of Gemstones

Gemstones are formed by chemical reactions in environments with high temperatures and pressure, usually with the presence of more than one solution, in any phase directly related to magma (Hatipoğlu, 2020). As the magma cools, atoms crystallize, forming many different minerals. Granitic rocks can form when formation takes place deep within the earth's crust. The various conditions required for a gem-quality mineral to form are rarely met. The conditions required to produce gem-quality crystals occur much less frequently than in gemstones. For gem crystals, cooling should occur slowly, as rapid cooling produces either glasses or very small crystals. Formed in pockets of gas in rocks, these crystals have time to grow slowly to reach large sizes and incorporate the rarer elements that were recently released from the original melt. Relatively large crystals occur in igneous rocks formed by the crystallization of magma at great depths and consolidated in or near the earth's crust at temperatures 950 to 450°C (O'Donoghue, 1988).

While the gemstones can be found primarily in the rocks, they can be observed more abundantly by being differentiated according to the density factor, especially in placer environments (e.g. Read, 1988; O'Donoghue, 1988; Harding, 2006; Hatipoğlu, 2020). Gemstones tend to be sparsely dispersed throughout a large rock mass or to crystallize as small aggregates or in fractures and cracks and small voids. Most gemstones are found in igneous rocks and stream sediments, but sedimentary and metamorphic rocks may also contain gemstones (e.g. Read, 1988; Harding, 2006). Gemstones found in alluvium or stream sediments have been eroded from the original rock in which they were formed and locally moved and concentrated by water from streams.

2.1. Igneous rocks

Igneous rocks are solidified from molten magma underground or on their surface. The rocks that solidify with the slow cooling of magma in

the depths of the earth are called *plutonic (intrusive)* rocks (for example, granite), those formed by the faster cooling of magma on the surface are called *volcanic (extrusive)* rocks (for example, rhyolite). Towards the end of the crystallization of granite, which is the most gemstone-containing rock of the intrusive rocks, liquids, and gases that remain rich in water or gas may remain in the granite and cool to form cavities covered with crystals such as beryl and topaz, or cool to form pegmatites. Pegmatites are very coarse-grained rocks that form as layers or veins both in the intrusive and in the surrounding rocks. They represent a later stage of magma crystallization and may contain huge crystals of extraordinary size. Inside, some gem-quality aquamarine and topaz crystals can weigh many kilograms. Most of the important valuable minerals such as feldspar, quartz, tourmaline, beryl, topaz, and zircon are found in plutonic rocks, with relatively large crystals formed with a slower cooling rate. The molten magma, which initially begins to form at high temperatures, begins to solidify as the temperature drops. Plagioclase minerals are among the first to solidify, and because they have plenty of space, they form large well-shaped crystals. Quartz is one of the last minerals to solidify as magma continues to cool. When magma reaches the surface, it prevents the elements from forming a crystalline structure as a result of rapid cooling in the surface conditions, and therefore obsidian and volcanic glass formations occur. After the formation of magmatic rocks, the elements carried by the hydrothermal heat to the fractures and cracks form many gemstones, especially quartz, opal, and chalcedony.

On the other hand, geodes are another form of magmatic formation in which precious mineral-containing solutions formed by molten or aqueous residues trapped in magma precipitate as crystals in spherical cavities in basic lavas and other igneous rocks (e.g. Read, 1988; Keller, 1990; Read, 2005; O'Donoghue, 2006; Hatipoğlu, 2020).

2.2. Sedimentary rocks

Sedimentary rocks are formed by the erosion of previously formed old rocks by the action of erosion, rain, wind, and streams. Sedimentary rocks form the second-largest cycle in mineral and rock formation. Except for some organic materials such as amber and jet, sedimentary rocks do not contain primary gem minerals. However, if the original weathered rock contains precious minerals, these are often washed and swept away to form secondary or alluvial deposits. These gemstones are classified as sedimentary jewelry materials (e.g. Read, 1988; Keller, 1990; Read, 2005; O'Donoghue, 2006; Hatipoğlu, 2020). Gemstones that can be found in sedimentary rocks are beryl, opal, quartz, turquoise, malachite, azurite, chrysoprase, and chrysocolla.

2.3. Metamorphic rocks

Metamorphic rocks are formed by the change of chemistry and shape of pre-existing igneous or sedimentary rocks underground by exposure to high pressures and temperatures (for example, marble derived from limestone). They are rocks that are formed as a result of changes in the texture or chemical composition of igneous and sedimentary rocks under the influence of metamorphism. For example, shale can turn into slate and with further metamorphism, it can turn into schist. Sometimes schists contain gem minerals such as garnet, emerald, and corundum.

Major metamorphic facies are *regional metamorphism* and *contact metamorphism*. In addition to the two main regimes of metamorphism, rocks can be subjected to increasing temperatures and pressures through *burial metamorphism*, *deformational metamorphism*, *hydrothermal metamorphism*, *shock metamorphism*, and *dynamic metamorphism*. Pressure and temperature in burial metamorphism are not as high as in regional metamorphism. All these types of metamorphism can cause changes in minerals as well as changes in the texture of rocks.

Regional metamorphism consists of temperature and pressure increases affecting the earth's crust. Contact metamorphism is formed by the intrusion of magma into a pre-existing rock mass. Due to the heat and pressure of this magma, metamorphic changes occur in the rock it enters.

During one of these metamorphic processes, liquid magma can cause reactions that produce varieties of gemstones in metamorphic rocks such as emerald, alexandrite, ruby, sapphire, garnet, spinel, corundum, beryl, andalusite, lapis lazuli, serpentine, nephrite, and jadeite (e.g. Read, 1988; O'Donoghue, 1988; Keller, 1990; Read, 2005; O'Donoghue, 2006; Hatipoğlu, 2020).

3. Classification of Gemstones

Gemstones are materials formed by natural processes without human intervention. Natural gemstones can also be divided into 3 different groups: mineral origin, rock origin, and organic origin. While obsidian is a rock-origin gemstone, amber, jet, coral, and mother-of-pearl are examples of organic-origin gemstones. On the other hand, other naturally occurring gemstones are classified as the mineral origin.

Despite having the same chemical composition and crystal structure, gemstones that differ in color or general appearance can be divided into different groups within themselves. For example, different colored variants of the mineral corundum are ruby and sapphire. On the other hand, quartz mineral is divided into different types such as amethyst, milky quartz, smoky quartz, and citrine. The classification of the most well-known gem-

stones found in nature and previously classified by many researchers (e.g. O'Donoghue, 1988; Read, 1988; Keller, 1990; Read, 2005; O'Donoghue, 2006; Ethem, 2006; Selim, 2015; Hatipoğlu, 2020; mta.gov.tr) is summarized in Table 1.

Table 1. *The classification of gemstones*

Gemstone		Chemical composition
Corundum	Ruby	Al_2O_3
	Sapphire	
Quartz	Amethyst	SiO_2
	Citrine	
	Rose quartz	
	Sunset quartz	
	Aventurine quartz	
	Milky quartz	
	Smoky quartz	
	Rock crystal	
Chalcedony (crypto-crystalline quartz)	Agate	SiO_2
	Sardonyx	
	Onyx	
	Carnelian	
	Bloodstone (Heliotrope)	
	Chrysoprase	
	Jasper	
	Tiger's eye	
	Hawk's eye	
Opal	Black opal	$\text{SiO}_2 \cdot n\text{H}_2\text{O}$
	Fire opal	
	Tree opal	
Obsidian		rich in SiO_2
Spinel		MgAl_2O_4
Malachite		$\text{Cu}_2\text{CO}_3(\text{OH})_2$
Azurite		$\text{Cu}_3(\text{CO}_3)_2(\text{OH})_2$
Rhodochrosite		MnCO_3
Apatite		$\text{Ca}_5(\text{F,Cl,OH})(\text{PO}_4)_3$
Brazilianite		$\text{NaAl}_3(\text{PO}_4)_2(\text{OH})_4$
Turquoise		$\text{CuAl}_6(\text{PO}_4)_4(\text{OH})_8 \cdot 4\text{H}_2\text{O}$
Beryl	Emerald	$\text{Be}_3\text{Al}_2\text{Si}_6\text{O}_{18}$
	Aquamarine	
	Morganite	
	Heliodor	
	Goshenite	
Chrysoberyl	Alexandrite	BeAl_2O_4
	Cat's eye	

Cordierite (Iolite)		$(\text{Mg,Fe})_2\text{Al}_4\text{Si}_5\text{O}_{18}$
Feldspar	Moonstone (Adularia)	$(\text{Na,K})\text{AlSi}_3\text{O}_8$
	Andesine	$(\text{Ca,Na})(\text{Al,Si})_4\text{O}_8$
	Amazonite	KAlSi_3O_8
	Labradorite	$(\text{Ca,Na})(\text{Al,Si})_4\text{O}_8$
	Sunstone (Heliolite)	$(\text{Ca,Na})(\text{Al,Si})_2\text{Si}_2\text{O}_8$
Garnet	Almandine	$\text{Fe}^{2+}_3\text{Al}_2\text{Si}_3\text{O}_{12}$
	Andradite	$\text{Ca}_3\text{Fe}_2(\text{SiO}_4)_3$
	Pyrope	$\text{Mg}_3\text{Al}_2(\text{SiO}_4)_3$
	Grossular	$\text{Ca}_3\text{Al}_2(\text{SiO}_4)_3$
	Spessartine	$\text{Mn}^{2+}_3\text{Al}_2(\text{SiO}_4)_3$
	Uvarovite	$\text{Ca}_3\text{Cr}_2\text{Si}_3\text{O}_{12}$
Jade	Jadeite	$\text{NaAlSi}_2\text{O}_6$
	Nephrite	$\text{Ca}_2(\text{Mg,Fe})_5\text{Si}_8\text{O}_{22}(\text{OH})_2$
Sepiolite		$\text{Mg}_4\text{Si}_6\text{O}_{15}(\text{OH})_2 \cdot 6\text{H}_2\text{O}$
Jet		rich in C
Peridot (Chrysolite)		$(\text{Mg,Fe})_2\text{SiO}_4$
Rhodonite		$(\text{Mn,Fe,Mg,Ca})\text{SiO}_3$
Tourmaline	Rubellite	$\text{Na}(\text{Li,Al})_3\text{Al}_6(\text{BO}_3)_3\text{Si}_6\text{O}_{18}(\text{OH})_4$
	Schorl	$\text{NaFe}^{2+}_3\text{Al}_6\text{Si}_6\text{O}_{18}(\text{BO}_3)_3(\text{OH})_3\text{OH}$
Topaz		$\text{Al}_2\text{SiO}_4(\text{OH,F})_2$
Andalusite		Al_2SiO_5
Kyanite		Al_2SiO_5
Sphene (Titanite)		$\text{CaTi}(\text{SiO}_4)(\text{O,OH,F})$
Anatase		TiO_2
Zircon		ZrSiO_4
Marcasite		FeS_2
Sphalerite		Zns
Scheelite		$\text{Ca}(\text{WO}_4)$
Diaspore		$\alpha\text{-AlO}(\text{OH})$
Diamond		C
Fluorite		CaF_2
Epidote	Epidote	$\text{Ca}_2(\text{Al,Fe})\text{Al}_2\text{O}(\text{SiO}_4)(\text{Si}_2\text{O}_7)(\text{OH})$
	Zoisite/Clinzoisite	$\text{Ca}_2\text{Al}_3\text{O}(\text{SiO}_4)(\text{Si}_2\text{O}_7)(\text{OH})$
Diopside		$\text{CaMgSi}_2\text{O}_6$
Amber		$\text{C}_{10-16}\text{H}_2\text{O}$
Coral		CaCO_3
Pearl		CaCO_3

The eight different metallic elements that cause these unique colors of gemstones are vanadium (V), chromium (Cr), iron (Fe), nickel (Ni), manganese (Mn), copper (Cu), and titanium (Ti) (Table 2).

Table 2. *Elements that color gemstones (Fritsch and Rossman, 1988; Read, 1988).*

Element	Gemstone
Vanadium	Blue zoisite, green vanadium-beryl, blue-violet sapphire
Chromium	Ruby, emerald, alexandrite, pyrope, diopside, jadeite, topaz
Iron	Sapphire, peridot, aquamarine, tourmaline, amethyst, almandine
Nickel	Chrysoprase
Manganese	Rhodochrosite, rhodonite, morganite, rose-quartz, spessartine, amethyst, rubellite
Copper	Malachite, turquoise
Cobalt	Spinel
Titanium	Blue-sapphire, rose-quartz

Gemstones are found, mined, and processed in many regions of the world, and they continue to be the subject of research by many scientists in Turkey (e.g. Hatipoğlu et al, 2011; Hatipoğlu et al., 2013; Selim, 2015; Yılmaz Şahin, 2019; Hatipoğlu, 2020, Arık and Özen, 2020; Arık et al., 2022; Arık and Ruşen, 2022; Kınacı and Öztürk, 2022; Özbay Candan et al., 2022; Sözeri et al., 2022; Üner et al., 2022; Çalık, 2022) and in many countries of the world (e.g. Hainschwang et al., 2013; Zhang and Guanghai, 2022). The characteristics of many gemstones known in nature and previously described by many researchers (e.g. O'Donoghue, 1988; Read, 1988; Keller, 1990; Read, 2005; O'Donoghue, 2006; Selim, 2015; Hatipoğlu, 2020; mta.gov.tr) are given below.

Quartz

The chemical formula of quartz, which is one of the most abundant minerals in nature, is SiO_2 . There are many varieties of quartz with different crystal structures. Quartz, which is mostly found in igneous rocks in nature, is often found in the composition of granite and quartz porphyry rocks. Physically pure quartz is usually colorless and transparent. Minerals such as amethyst, pink quartz, smoky quartz, citrine, chalcedony, agate, opal, tiger's eye, and onyx are quartz varieties that are widely used as gemstones. They are used in jewelry, ornaments, and some special designs.

Amethyst is one of the quartz group minerals. Amethyst, which has purple and lilac colors due to its manganese and iron content, is used as a gemstone (Fig. 1).

Smoky quartz is gray, black, brown, dark brown, and beige-colored mineral of the quartz group (Fig. 1).

Rose quartz is a pink-colored mineral of the quartz group.

Milky quartz is a white-colored mineral of the quartz group.

Citrine, which is the yellow-toned type of the quartz group, gets its color from the small amount of iron it contains.

Sunset quartz is a recently discovered yellowish and orange mineral from the quartz group.

Aventurine is a quartz group mineral found in nature in green, blue, and orange colors.

Rock crystal is clear and colorless quartz, a common gemstone.



Figure 1. Macro photograph of amethyst (Selim, 2015) and smoky quartz (mta.gov.tr).

Cryptocrystalline Quartz (Chalcedony)

Chalcedony is a cryptocrystalline quartz (SiO_2). It has colors ranging from dark blue to light blue and has purplish, translucent, and opaque properties. Because the grains of cryptocrystalline quartz are very small, they can only be seen under a microscope.

Agate is a formation commonly seen in volcanics, consisting of chalcedony and quartz. Agates, which are generally seen as void fillings, consist of concentric bands with uniform thicknesses. Its colors are usually seen as white, gray, and red.

Sardonyx is a type of agate with white and reddish-brown bands.

Onyx primarily refers to the parallel banded variation of chalcedony which is a silicate mineral.

Carnelian is a variety of chalcedony colored by iron oxide and similar to sardonyx.

Bloodstone is an iron-rich variety of chalcedony, also known as heliotrope. The color of the bloodstone is dark green with bright red markings on its surface.

Chrysoprase, a type of chalcedony, is a mineral in light and dark bright apple green colors due to its nickel oxide content. It is translucent and opaque. It is a mineral found especially in serpentines and used as a gemstone with the same physical properties as quartz.

Tiger's eye is a kind of quartz with golden yellow, yellowish-brown, brown color and silky shine. It results from the parallel growth of quartz crystals, altered amphibole fibers often converted to limonite.

Hawk's eye is a fibrous quartz variety observed as blue-gray, blue-green opaque.

Jasper is an aggregate of cryptocrystalline chalcedony and has usually red, brown, or yellow, in color. The common red color of the jasper is related to iron (+3) inclusions.

Opal

Opal is a hydrated silica composition amorphous, naturally rounded and kidney-like mineral, generally formed by the decomposition of silicates and young volcanics (Fig. 2). There are many varieties such as black opal, fire opal, and tree opal.

Obsidian

Obsidian is black, brown, and gray colored gemstone formed due to the rapid cooling of lava as a result of acidic volcanism (Fig. 2). Obsidian is a type of volcanic glass, which does not have any crystal structure (amorphous), has a chemical content of mostly SiO_2 , and is a slippery and shiny surface gemstone.

Corundum

Ruby is a corundum mineral in red tones colored by chromium. The highest quality rubies typically form in marble.

Sapphire is one of the corundum minerals which forms in granitic pegmatites or corundum syenites. The best-known sapphire color is blue, but it can occur in gray, black, and colorless.

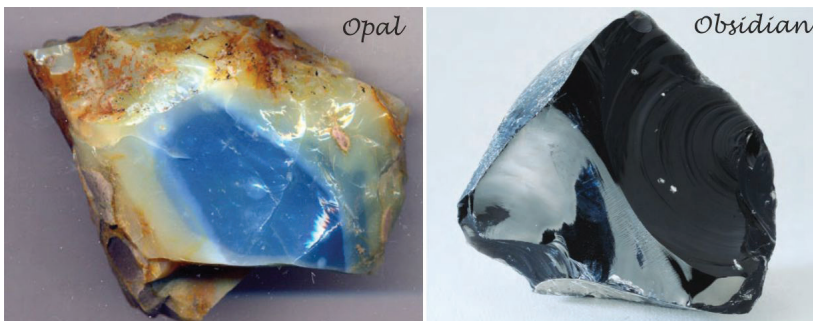


Figure 2. Macro photograph of opal (mta.gov.tr) and obsidian (Selim, 2015)

Diamond

Diamond, one of the hardest known materials, is pure carbon. A modification of the carbon element other than graphite is diamond. Diamond was originally only found in Kimberlites. Diamond is a very valuable mineral with a transparent, glassy luster.

Beryl

One of the most prestigious gemstone families, the beryl family includes some of the most popular and expensive gemstones.

Emerald is the most valuable member of the beryl family, with its green color due to chromium or sometimes vanadium. Emerald can occur in different environments with relatively low-temperature hydrothermal fields or pegmatites.

Aquamarine is a transparent blue and silicate type of beryl family.

Goshenite is the colorless and purest form of beryl. Goshenite is also called the mother of all gemstones, as it can transform into other stones such as emerald ormorganite. Goshenite can be found most commonly in granite and sometimes in metamorphic rocks.

Heliodor known for its range of yellow colors, greenish-yellow, orange-yellow to a deep golden-orange is a mineral of the beryl family. It is usually found in pegmatites.

Morganite also known as rose beryl, pink beryl, and pink emerald is a mineral of the beryl family. It is mostly found in pegmatites.

Chrysoberyl

Chrysoberyl, the main varieties of which are alexandrite and cat's eye, is iridescent, yellowish green, and brownish red, and is a mineral found in pegmatites and granites.

Garnet

Garnet is a common group in metamorphic and igneous rocks.

Almandine is a dark red, brown colored iron alumina garnet (Fig. 3). It is a common mineral, especially in schists and gneisses.

Andradite, a member of the garnet group, occurs as the product of contact metamorphism of carbonate rocks. Andradite is divided into three as black colored *melanite* (titanian andradite), green-colored *demantoid*, and yellow-green-colored *topazolite*.

Grossular is a garnet group mineral found in cinnamon brown, red and yellow colors in contact with metamorphized limestones.

Pyrope which always shows a red color is found in igneous rocks, especially in peridotite, serpentinite, and kimberlite-type rocks.

Spessartine is dark red or bright yellow-orange in color. Spessartine occurs most often in pegmatite and in low-grade metamorphic phyllite.

Uvarovite is a rare member of the garnet group and is green in color. Uvarovite which is associated with chromite, serpentinite, and skarn ore bodies is a chromium-bearing garnet.

Lapis Lazuli

Lapis Lazuli form as a result of the effects of granitic or pegmatitic fluids on marble, schist, and gneiss. It is known for its deep blue color (Fig. 3).



Figure 3. Macro photograph of almandine (Selim, 2015) and lapis lazuli (mta.gov.tr).

Cordierite (Iolite)

The color of iolite changes from sapphire blue to purple, yellowish gray to light smoky or violet blue as the angle of light changes. Iolite is sometimes used as a more economical substitute because of its similarity to sapphire. Cordierite forms by contact or regional metamorphism. Cordierite is also found in gabbro, granite, pegmatite, and norite.

Spinel

Spinel is usually found in contact metamorphic rocks and rarely in igneous rocks. Transparent and smooth crystals are used as gemstones. Spinel with a vitreous or opaque shine is observed as transparent or opaque. It can be seen in various shades of colorless, red, magenta, green, blue, brown, black, or yellow.

Feldspar

Amazonite which is a polymorph of orthoclase is green, bluish-green in color. Amazonite is often found in granites and pegmatites.

Andesine is a member of the plagioclase group and is found in intermediate igneous rocks such as syenite, diorite, and andesite. It also occurs

as clastic grains in sedimentary rocks.

Labradorite is a member of the plagioclase series. Labradorite shows an iridescent effect commonly in blue-green tones. It is usually found in mafic igneous rocks such as anorthosite, basalt, and gabbro.

Moonstone (Adularia) is a member of feldspar. It shows a pearly and iridescent effect in shades of white.

Sunstone, known as “heliolite” or “aventurescent feldspar” is a member of the feldspar group. Sunstone is a mineral that shines when viewed from certain directions. Reflections are seen in orange tones due to the hematite in it.

Tourmaline

Tourmaline is a silicate mineral group in a wide variety of colors. The most common tourmaline varieties are schorl and rubellite. Schorl is black in color because it is rich in iron. Rubellite is pinkish-red tourmaline. Tourmalines are commonly found in pegmatites.

Anatase

Anatase found as small crystals in pegmatite and crystalline schists is a transparent mineral in many beautiful colors such as deep indigo and amber-yellow.

Diopside

Diopside is a pyroxene mineral found in igneous and metamorphic rocks. Diopside is commonly found as a primary mineral in olivine-rich basalts and andesites. It occurs also as a common mineral in kimberlites and peridotites. It is also formed during the contact metamorphism of limestones and dolomites. The color of the diopside commonly changes from light to dark green, brown, blue, white, and colorless.

Diaspore

Diaspore is an aluminum oxide hydroxide mineral. Diaspore, a colorless or grayish-white transparent mineral with a pearlescent luster (Fig. 4), is an alteration product of corundum or emery and is generally found in recrystallized limestone. Along with diaspore, boehmite, and gibbsite, it is an important aluminum mineral in bauxite. Diaspore, also known as Turkizite and zultanite, is mined as a gemstone from Muğla in Turkey, and it is found in veins within a bauxite deposit.

Zircon

Zircon is a natural and transparent gemstone with colorless, yellow, green, and brown types (Fig. 4). It is abundant in the magma of the felsic

character. In addition to the Hafnium isotope, it also contains radioactive uranium and radiogenic lead isotopes. For this reason, zircon is used in radiometric dating methods.

Epidote

The main members of the epidote group are epidote and zoisite/clinozoisite. They are found in metamorphic and pegmatitic rocks. Epidote is commonly found in green, greenish-black, or yellowish-green.



Figure 4. Macro photographs of diaspore (zultanite/Turkizite, Selim, 2015) and zircon (mta.gov.tr).

Marcasite

Marcasite, generally called “white iron pyrite,” is physically and crystallographically different from pyrite. Marcasite is more brittle and lighter than pyrite. On fresh surfaces, it is pale yellow or whitish in color and has a glossy metallic luster. Thin, flat crystals are called “cock’s comb”. When considered a gemstone, pyrite is also called marcasite.

Sphalerite

Sphalerite, which has transparent and translucent properties, is mostly seen as yellow, brown, black, green, red, gray, and sometimes colorless. Sphalerite occurs in contact-metamorphic deposits, as veins in igneous rocks, and mostly in hydrothermal ore deposits.

Scheelite

Scheelite is the most important ore of tungsten metal. Smooth crystalline scheelite is worked as a gemstone. Scheelite is usually found in skarns formed by contact metamorphism and in high-temperature hydrothermal veins. It is observed in various colors from golden yellow, brownish-green to dark brown, orange, and pinkish-gray to reddish-gray. Transparent and crystal surfaces are quite shiny.

Coral

Red corals form and grow as a result of low sedimentation in dark environments on the seafloor.

Amber

Amber is the fossilized resin of a pine tree. Amber is a translucent and easily breakable gemstone that can be seen in various colors from light yellow to red.

Jade

It is known that jade (yeşim), one of the oldest known gemstones, was discovered in the 1800s as two very different minerals: jadeite and nephrite. Nephrite has a lower translucency than jadeite, while jadeite has a glassier appearance.

Jadeite is a pyroxene mineral that can occur in a wide variety of colors but is mostly found in shades of *green*. Jadeite can only form under conditions of metamorphism at high pressure and relatively low temperature. Jadeite is a mineral of jade, especially located in China. However, purple jade named “*Turkish purple jade/Türkiyenite*” (Fig. 5) since the 1980s, which is located in a metamorphic zone on the border between the Late Mesozoic regular blueschist metamorphic belt and the Early Cenozoic intrusive granodiorite was found only in the Harmancık-Bursa region in Turkey in the 1970s (Okay, 1997; Okay, 2002; Hatipoğlu, 2010; Başevirgen et al., 2013).

Nephrite is an amphibole mineral with a medium green, dark green, gray-green, or white color.

Fluorite

Fluorite occurs in hydrothermal veins, fills, and metasomatic deposits in igneous, metamorphic, and sedimentary rocks. As gangue mineral in thin veins of igneous, metamorphic, and sedimentary rocks, in the form of layers in carbonate rocks and by displacement along acid magmatic interferences, in fracture zones and depositional zones, in marginal zones of carbonatite and alkaline rocks, in residual concentrations formed by atmospheric weathering in the main bed, in base metal deposits. It is found in brecciated deposits, pegmatites, and lake sediments. Fluorite is commonly found in green and purple colors (Fig. 5).



Figure 5. Macro photographs of Turkish purple jade/Türkiyenite (Başevirgen, 2012) and fluorite (Selim, 2015).

Topaz

Topaz is a mineral that can occur in various shades of yellow, red, pink, blue, or brown with the property of a gemstone. Pure topaz is colorless and diamond-like. Topaz can lose its color in sunlight. Topaz is found in granites and pegmatites.

Andalusite

Andalusite occurs in metamorphic rocks in pink, reddish brown, rose red, grayish, greenish, purple, and yellowish colors.

Kyanite

Kyanite is a mineral formed by the metamorphism of aluminum-rich rocks under high pressure and has a pale blue color.

Malachite

Malachite is a copper carbonate hydroxide mineral. An opaque, banded mineral in shades of green, malachite is usually formed from the oxidation of primary copper sulfide minerals and is often found in association with azurite.

Rhodochrosite

Rhodochrosite is found in hydrothermal veins in ore deposits formed at low-temperature. Rhodochrosite can be pink, rose, red, rose-red, cherry-red, yellow, yellowish-gray, cinnamon-brown, white, or banded.

Rhodonite

Rhodonite is transparent or translucent vitreous luster in pink, rose-red, and brownish-red colors. Rhodonite usually occurs in hydrothermal deposits and manganese deposits.

Brazilianite

Brazilianite, named after Brazil, is a yellow-green phosphate mineral. Brazilianite commonly occurs in phosphate-rich pegmatites.

Apatite

Apatite is yellow, green, brown, pink, violet, purple, blue, and colorless in color, and it ranges from transparent to translucent. Apatite is rarely used as a gemstone. Coarse crystalline apatite usually occurs in pegmatites, carbonate minerals, and skarns. Apatite can also occur in clastic sedimentary rocks as grains eroded from the source rock.

Pearl

Pearl is a hard, shiny body composed of calcium carbonate produced in the tissues of living shelled mollusks. An ideal pearl is observed as

white, round, and smooth. Natural pearls are gemstones that have been used as gemstones and objects of beauty throughout history.

Sepiolite

Sepiolite (Lületaş), a soft, opaque, and white, gray, cream-colored conchoidal clay mineral, is generally used in the manufacture of pipes and ornaments (Fig. 6). The majority of sepiolites in Turkey are located in Eskişehir. Sepiolite is a secondary mineral formed in association with serpentine and magnesite.

Jet

Jet (Oltu taşı) is a black-colored gemstone formed by the fossilization of the trunk of a tree species (Fig. 6). It is located in the Oltu district of Erzurum in Turkey. Jet is mostly used in the production of ornaments and rosaries.



Figure 6. Macro photographs of jet (*oltu taşı*) and sepiolite (*lületaş*) (*mta.gov.tr*).

Peridot (Chrysolite)

Peridot is a dark yellow-green transparent olivine variety mostly seen in mafic and ultramafic rocks. Gem-quality peridot, which forms deep in the mantle, is rarely seen on the Earth's surface due to its sensitivity to surface conditions.

Sphene (Titanite)

Sphene (Titanite) is rich in titanium and is the only member of the titanite mineral group used as a gemstone. Sphene is especially yellow, light orange, and green, and frequently shows color zoning.

Turquoise

Turquoise, named after Turkey, is an opaque, blue-green mineral that is a hydrated phosphate of copper and aluminum.

4. New Technical Applications of Gemstones

While traditional analytical methods such as a microscope, refractive indices, polariscope, and dichroscope have been used for many years for the analysis of gemstones, in the early 2000s, more powerful analytical instruments and methods were needed to solve gemstone identification problems (e.g. Breeding et al., 2010; Wang et al., 2016; Khan et al., 2022). Among these methods used in the analysis of gemstones in the last decades, “Ultraviolet-visible-near infrared (UV-Vis-NIR) spectroscopy”, “Raman spectroscopic analysis”, “Fourier Transform Infrared (FT-IR) Spectrometry”, “Energy-dispersive X-ray Fluorescence (ED-XRF)”, “Laser Ablation Inductively Coupled Plasma Mass Spectrometry (LA-ICP-MS)”, “Laser Induced Breakdown Spectroscopy (LIBS)”, “Surface analysis by Scanning Electron Microscopy (SEM)”, and “Photoluminescence (PL)” are included, “LA-ICP-Time of-Flight Mass Spectrometry (GemTOF)” was added to these techniques in recent years. While older technologies such as wavelength scanning spectrometers and spectrofluorometers cannot record time-dependent spectra, charge-coupled device (CCD) spectrometers developed in the last decade were able to collect data simultaneously and in a short time across the entire wavelength range. Advancing innovations in laser mapping and computer modeling of the diamond gemstone appearance have changed the way gemstones are cut and graded by jewelry labs.

The techniques and methods frequently used for the analysis of gemstones in recent years (see e.g. Read, 2005, Breeding et al., 2010; Hainschwang et al., 2013; Wang et al., 2016; Milisenda, 2018; Khan et al., 2022) are summarized below.

Laser Ablation Inductively Coupled Plasma Mass Spectrometer (LA-ICP-MS) enables the gemstone or mineral to be cut with a direct pulsed laser beam and its constituents analyzed.

Laser Induced Breakdown Spectroscopy (LIBS) is a short laser pulse focused on the surface of the gemstone that detects certain elements, identifying a gemstone’s potential source.

Fourier transform infrared (FT-IR) spectroscopy provides the absorption and measurement of some of the IR (infrared) radiation passing through the gemstone sample by sample. FT-IR generates spectra for each sample analyzed and these spectra are then compared to known spectra in the reference library.

Raman spectroscopy identifies gemstones, inclusions, and fillers. Raman is a form of vibrational spectroscopy that can be used to analyze very small samples. This is also a nondestructive testing technique and is

very reliable in identifying a mineral's spectra by comparing it to known spectra in a reference library. Since each gemstone has its distinctive spectral pattern, the Raman effect is used as an identification tool. Raman provides different information than FT-IR because the physical way a gemstone analyzes its spectrum is different. Since Raman spectroscopy samples are not destructive, they can be preferred in cases where LIBS and LA-ICP-MS are harmful.

EDXRF (Energy Dissipative X-Ray Fluorescence) Spectrometer is used to analyze the chemical elements in the gemstone.

UV-Vis-NIR (Ultraviolet-Visible-Near Infrared Range) Spectroscopy is a type of electronic spectroscopy that can potentially be used for the quantitative analysis of samples. UV-Vis-NIR analyzes spectra in the Ultraviolet-Visible-Near Infrared range of the spectrum and produces much more accuracy, giving much more detail in graphs. It is also used to determine which element the colors in the mineral depend on.

Photoluminescence (PL)

Laser and ultraviolet-excited luminescence spectroscopy and imaging, which are important techniques for gemstone analysis, are one of the most sensitive spectroscopic methods (Hainschwang et al., 2013). It is an analytical method for detecting optically active crystallographic defects. Photoluminescence (PL) analysis is used in the separation of natural and synthetic gemstones and in the detection of processes. For example, it is possible to distinguish green-colored stones such as ruby and jadeite from their artificially colored counterparts (Milisenda, 2018). PL spectroscopy can also determine the color specificity of certain coral and pearl species (Milisenda, 2018).

LA-ICP-Time of-Flight Mass Spectrometry (LA-ICP-TOF-MS/ GemTOF)

In the last decades, advanced scientific techniques have been used for detailed chemical and structural analysis as well as the analysis of physical properties in gemstone analysis. In contrast to the LA-ICP-Quadrupole-MS (LA-ICP-Q-MS) technique currently used for gemological analysis, a new basic analytical system, the LA-ICP-Time of-Flight Mass Spectrometer (LA-ICP-TOF-MS), has been launched recently. LA-ICP-TOF-MS can simultaneously detect almost all elements in the periodic table, at ultra-high speeds and low detection limits. This groundbreaking technique, therefore, opens up new research possibilities in source identification, age determination, inclusion analysis, and chemical zoning in colored gemstones, diamonds, and pearls (Wang et al., 2016).

5. Conclusion

There are many semi-precious stones such as jade, garnet, diaspore, tourmaline, and turquoise in addition to many precious stones such as diamond, emerald, sapphire, and ruby in the world. This definition of precious and semi-precious from the past has left its place to call it a gemstone for every rare stone with beauty and durability. In recent studies, all rare precious minerals such as diamond, emerald, jade, and garnet are defined as gemstones.

Scientific studies are carried out for the exploration and exploitation of gemstones, which have been formed naturally by geological processes and have been symbols of beauty, wealth, and status since prehistoric times. Interest in gemstones has continued to increase from past to present and it is a known fact that this interest will continue in the future. The increasing demand for gemstones is also leading to improvements in the techniques applied for identifying and analyzing gemstones. It is considered very important to carry out detailed research on the gemstones, for which more information is needed, to define, classify, and determine different usage areas, and to continue the studies on the prospecting for new gemstones.

References

- Arık, F. & Özen, Y. (2020). Tokat Yöresi Jasper Oluşumlarının Mineralojik-Petrografik, Jeokimyasal Özellikleri ve Süstaşı Olarak Kullanılabilirliği. Ömer Halisdemir Üniversitesi Mühendislik Bilimleri Dergisi, 9(1), 451-460 (in Turkish).
- Arık, F., Turhal, E. & Özen, Y. (2022). Almus (Tokat) Yöresindeki Akiklerin Jeokimyasal Özelliklerinin Değerlendirilmesi. Türkiye Jeoloji Bülteni, 65 (3), 233-254 (in Turkish).
- Başevirgen, Y. (2012). Gemmological and Mineralogical Investigations and Genesis of The Massive Purple Jade from The Harmancık-Bursa Region, M.Sc. Thesis, Dokuz Eylül University Graduate School of Natural and Applied Sciences, İzmir (In English).
- Başevirgen, Y., Hatipoğlu, M. & Kibici, Y. (2013). Türkiyenitin (Türk Mor Jade-si) Gemolojik ve Mineralojik İncelemesi ve Oluşum Kökeninin Belirlenmesi, Dumlupınar Üniversitesi Fen Bilimleri Enstitüsü Dergisi, 32, 57 – 78 (in Turkish).
- Breeding, C.M., Shen, A.H., Eaton-Magaña, S., Rossman, G.R., Shigley, J.E. & Gilbertson, A. (2010). Developments in Gemstone Analysis Techniques and Instrumentation During the 2000s, Gems and Gemology, 46, 3.
- Çalık, A. (2022). Yenisoğça Opal Oluşumlarının Jeolojisi ve Mineralojik Özellikleri-Eskişehir, KB Türkiye. Türkiye Jeoloji Bülteni, 65 (3), 297-308 (in Turkish).
- Ethem, M.Y., 2006. A'dan Z'ye Kıymetli ve Yarı Kıymetli Süs Taşları. 2. Baskı, TMMOB, Maden Mühendisleri Odası, 272 p. (in Turkish).
- Fritsch, E. & Rossman, G.R., (1988). An Update on Color in Gems. Part 2: Colors Involving Multiple Atoms and Color Centers. Gems Gemol., 24, 3–15.
- Hainschwang, T., Karampelas, S., Fritsch, E. & Notari, F. (2013). Luminescence spectroscopy and microscopy applied to study gem materials: a case study of C center containing diamonds. Mineralogy and Petrology: Luminescence special issue, 107, 3, 393 - 413.
- Harding, R. (2006). The Geological Sources of Gems, In “Gems, Their Sources, Description, and Identification” edited by O'Donoghue, M., 6th ed., Butterworth-Heinemann.
- Hatipoğlu, M. (2010). Response to jadeite from Turkey, Rocks & Minerals, 85, 301.
- Hatipoğlu, M., Ören, U., Kibici, Y., 2011. Micro-Raman spectroscopy of gem-quality chrysoprase from the Biga-Çanakale region of Turkey, Journal of African Earth Sciences, 61, 4, 273-285.
- Hatipoğlu, M., Chamberlain, S.C., Kibici, Y. (2013). Characterization of the Sündikendağı deposit of moganite-rich, blue chalcedony nodules, Mayıslar-Sarıcakaya (Eskişehir), Turkey, Ore Geology Reviews, 54, 127-

137.

Hatipoğlu, M. (2020). Süstaşları Mineralojisi, Türk Eğitim Yayınları. 237 p., Türkiye (in Turkish).

<https://www.mta.gov.tr> (Date of access: 02.12.2022).

Keller, P.C. and Kampf, A.R. (1985). Gemstones and their origins, Terra, 23, 5.

Keller, P.C. (1990). Gemstones and their origins, Van Nostrand Reinhold, New York.

Khan, R.A., Anwar-ul-Haq, M., Qasim, M., Afgan, M.S, Haq, S.U. & Hussain, S.Z. (2022). Spectroscopic and crystallographic analysis of nephrite jade gemstone using laser induced breakdown spectroscopy, Raman spectroscopy, and X-ray diffraction, Heliyon, 8, 11, e11493.

Kınacı, E.H. & Öztürk, A. (2022). Menderes Masifi'nin Güneybatı Kanadındaki (Bafa Gölü - Milas) Diaspor Oluşumlarının Jeolojik, Jeokimyasal ve Gemolojik Özelliklerinin Araştırılması. Türkiye Jeoloji Bülteni, 65 (3), 309-330 (in Turkish).

Milisenda, C.C. (2018). Gemstones and Photoluminescence, GIA International Gemological Symposium, The Quarterly Journal of the Gemological Institute of America, October 7–9, 2018 | Carlsbad, CA, 54, 3, 258.

O'Donoghue, M. (1988). Formation and occurrence of gemstones. In: Gemstones. Springer, Dordrecht.

O'Donoghue, M. (2006). Gems: Their sources, descriptions and identification (6th edition), Elsevier, Butterworth-Heinemann, 874 p.

Okay, A.I. (1997). Jadeite-K-feldspar rocks and jadeites from northwest Turkey, Mineralogical Magazine, 61, 835-843.

Okay, A.I. (2002). Jadeite–chloritoid–glaucofan–lawsonite blueschists in northwest Turkey: unusually high P/T ratios in continental crust", Journal of Metamorphic Geology, 20, 757-768.

Özbay Candan, E., Kaydu Akbudak, İ., Başbüyük, Z. & Ekincioglu, G. (2022). Tokat Nebiköy Kalsedonlarının Mineralojik-Petrografik ve Gemolojik İncelemesi. Türkiye Jeoloji Bülteni, 65 (3), 287-296 (in Turkish).

Philipsborn, H. von (1967). Tables for determining the minerals according to external characteristics, 2nd edition, Schweitzerbart, Stuttgart (in German).

Ramdohr, P. & Strunz, H. (1978). Klockmann's textbook of mineralogy, Ferdinand Enke Verlag, Stuttgart, 876 p. (in German).

Read, P.G. (1988). Beginner's Guide to Gemmology, 2nd Edition, Heinemann Professional Publishing, London.

Read, P.G. (2005). Gemmology. 3rd edition, Elsevier, 324 p.

Selim, H. (2015). Türkiye'nin değerli ve yarı değerli mücevher taşları. İstanbul Ticaret Odası Yayınları, Yayın no: 2014-4, İstanbul, 102s. (in Turkish).

- Sözeri, K., Günel, H. & Duran, E. (2022). Tokat-Artova Bölgesinde Bulunan Kalsedon Oluşumlarının Mineralojik-Petrografik ve Gemolojik Özellikleri. *Türkiye Jeoloji Bülteni*, 65 (3), 273-286 (in Turkish).
- Üner, B., Yılmaz Şahin, S. & Akkemik, Ü. (2022). Batı Anadolu'da Silisleşmiş Ağaç Türlerinin Bazı Mineralojik ve Gemolojik Özellikleri. *Türkiye Jeoloji Bülteni*, 65 (3), 217-232 (in Turkish).
- Wang, H.A.O., Krzemnicki M.S., Chalain J-P, Lefèvre P., Zhou W. & Cartier L.E. (2016). Simultaneous High Sensitivity Trace-Element and Isotopic Analysis of Gemstones Using Laser Ablation Inductively Coupled Plasma Time-of-Flight Mass Spectrometry. *Journal of Gemmology*, 35(3), 212-223.
- Yılmaz Şahin, S. (2019). Türkiye'nin Değerli ve Yarı Değerli Taşları. *Yurt Madencilik Geliştirme Vakfı Sektörmaden Dergisi*, 72, 26-32 (in Turkish).
- Zhang, Y., and Guanghai S. (2022). Origin of Blue-Water Jadeite Jades from Myanmar and Guatemala: Differentiation by Non-Destructive Spectroscopic Techniques, *Crystals* 12, 10, 1448.



CHAPTER 9

CONVERGENT-DIVERGENT NOZZLE CFD ANALYSIS WITH DIFFERENT DIVERGENT ANGLE AND NPR

N.Filiz TUMEN OZDIL¹, Mehmet Emin TASKİN²

¹ Assoc. Prof. Dr. Adana Alparslan Turkes Science and Technology University, 0000-0003-0083-7524 fozdil@atu.edu.tr

² Adana Alparslan Turkes Science and Technology University, 0000-0002-1825-539X

1. Introduction

Nozzle is the mechanical device that control the flow of the fluid. There are many types of nozzles that is using in the industry. Nozzle is used in steam and gas turbine, jet engine, rocket motor etc. Subsonic or supersonic flows can occur according to Mach number and shape of the nozzle. The inlet section decreases through the throat and then increases through to exit section in the convergent divergent nozzle. With the changing pressure, density and velocity changes.

Numerical analyze of the compressible flow in convergent-divergent nozzle was investigated by Sher Afghan K. et al [1]. The Mach number was selected higher than one that is 2 to obtain shock. Nozzle Pressure Ratio (NPR) was equal to 7.82 for investigated Mach number. In this study, different MPR values were used as variable. To simulate compressible flow for convergent-divergent nozzle was performed via using ANSYS software. As a conclusion, shock train for Mach number 2 was obtained. Pressure, temperature, density and velocity of the flow is related to isolator's length.

Numerical analyze for the convergent-divergent nozzle with variable of different divergent angle was investigated by Madhu. B. P. and G. Mahendramani [2]. The fluent module of ANSYS software was used to generate numerical analyze. Divergent angles were selected as 10-12-16 degrees. As a result of this study, the shock distance increasing with the divergent angle increasing was obtained.

The comparison of the experimental and numerical data was investigated by Srivinas G. and Bhupal R. [3]. In the research, the literature result was used to compare. Convergent nozzle was analyzed. Two experimental and numerical convergent nozzle approaches were used to compare. Results were suitable and consistent the exit Mach number. As a result of the numerical analyze the relationship were acquired.

Method of characteristics to design supersonic nozzles were examined by M. A. Khan et al [4]. According to the Mach number at the exit of the nozzle, to obtain minimum length of divergent section of the convergent-divergent nozzle was generated via using MATLAB software. Obtained design was compared with other design nozzles. As a result, the requires features to obtain consistent design and flow was examined.

In tunnels, longitudinal ventilation with jet blower fan is used to ventilate tunnels. In this study, a convergent divergent nozzle was designed and analyzed to use in tunnels by Nallode C. et al [5]. The geometry of the convergent-divergent nozzle was designed in Catia V5 and numerical nozzle was carried out by using ANSYS software. Pressure, temperature, density, humidity, etc. were used to compare conventional model with results.

Reduced pressure and accelerated air were observed for convergent-divergent nozzle according to conventional cylindrical model.

With numerical method, supersonic flow through rocket nozzle was simulated and investigated by Madhu B.P. et al [6]. By using ANSYS Fluent software. Different divergent angles were used in this study. As a result of the analyze, increasing was observed in velocity from inlet to outlet.

Different type of cross-section for the convergent-divergent nozzle which were rectangular, square, cylinder was investigated by G. Satyanarayana et al [7]. The supersonic nozzle was performed to compare the cross-sectional areas. To generate geometry and numerical analyze, Catia and ANSYS were used respectively. As a result of simulation and comparison, rectangular convergent-divergent nozzle had high velocity and low pressure according to square and circular.

Using computational fluid dynamic (CFD) software ANSYS, convergent-divergent nozzle was analyzed with the parameters that were Mach number, pressure, and velocity by Muhammad Waqas K. and Muhammad A. [8]. $k-\epsilon$ turbulence model was used to generate flow. As a result, with 240 kPa inlet pressure, the shock was observed as overexpanded however, with 300 kPa, the shock was not observed as under expanded.

With two different divergent angle which were 5 and 10 degrees, 2-D convergent-divergent nozzles were analyzed with using ANSYS by A.V.R. Rao, I. Akhil [9]. With the important fluid properties like pressure, temperature, and velocity. The increasing in velocity and decreasing in static temperature and density from inlet to outlet was observed.

With Nozzle equations and the CFD results of the convergent-divergent nozzle via using ANSYS software was carried out by Ramesh K.R. and Yuvarajan D. [10]. The increasing nozzle speed and decreasing static pressure were observed with increasing divergent angle.

In this study, NPR and divergent angle effect on the nozzle characteristic has been investigated numerically. The obtained data from ANSYS fluent module have been compared. NPR (nozzle pressure ratio) and divergent angle have been used as variables. According to these variables, pressure, Mach number distributions have been investigated. The geometry of the convergent divergent nozzle has been designed according to Mach number with 1.75. 2-D CFD (Computational Fluid Dynamic) model has been used to analyze the system via using ANSYS software. The 2-D geometry of nozzle has been designed in Design Modeler software. The duct section has been added the exit of the nozzle. Ratio of the duct length to exit diameter was estimated as 6.

2. Materials and Methods

In this study, nozzle divergent angle and NPR have been investigated in convergent divergent nozzle. NPR value for the correct expansion has been calculated as 5.32. However, 4.32, 5.32, and 6.32 have been carried out with 2 different divergent angle which were 8 and 10 degrees. Dimensions of the system can be shown as in table 1.

Table 1. Nozzle geometry properties

Part Name	Value
Inlet diameter	25 mm
Outlet diameter	10 mm
Throat diameter	8.49 mm
Convergent angle	20°
Divergent Angle	5° and 7°

The duct after convergent divergent nozzle has used with a ratio of outlet diameter to duct length. Ratio has been estimated as 6 according to literature [1]. In Figure 1, the duct geometry after nozzle has been shown.

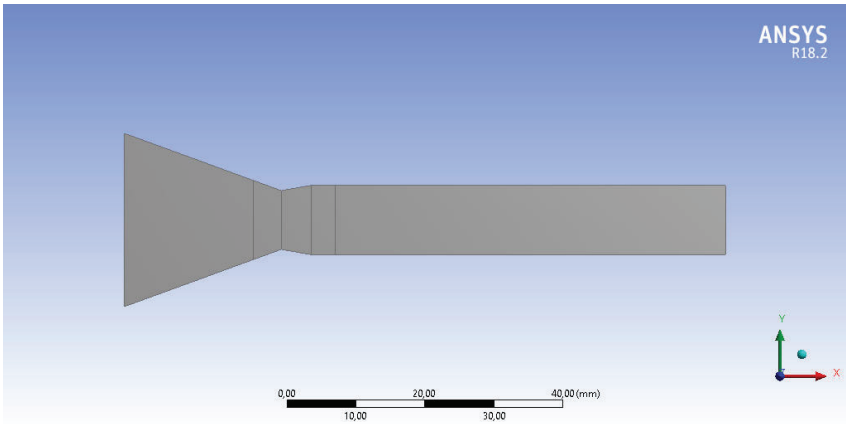


Figure 1. Geometry of duct section

Edge sizing with number of division property has been used to obtain mesh distribution. The mesh distribution in the throat section and the exit section of the nozzle have been divided high divisions. The mesh properties for geometry and throat and exit section of nozzle were illustrated in Figure X-Y respectively.

The analyze has been carried out via using ANSYS software. Nozzle geometry with boundary condition and mesh distribution in all geometry and detailed and specified section have been illustrated in Figure 2,3, and 4 respectively. System has 3 type of boundary which is pressure inlet, pressure outlet and wall. Fluent module has been set up with k-e viscous model and energy equation. The fluid properties have been shown in Table 2 according to literature [1]. Inlet pressure, inlet temperature, outlet pressure and outlet temperature has been used as boundary conditions as 437724 Pa, 300 K, 0 Pa and 300 K respectively. According to inlet section, system has been initialized with standard initializing method.

Table 2. Properties of air

Property of air	
Density (kg/m3)	Ideal gas
Specific heat (J/kg.K)	1006.43 (constant)
Viscosity	Sutherland
Molecular weight (kg/kmol)	28.966 (constant)

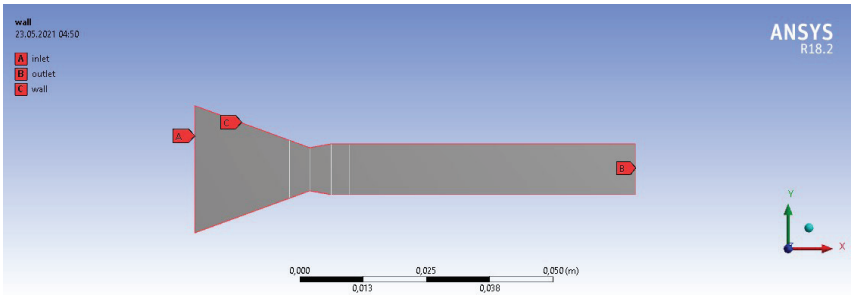


Figure 2. Boundary conditions

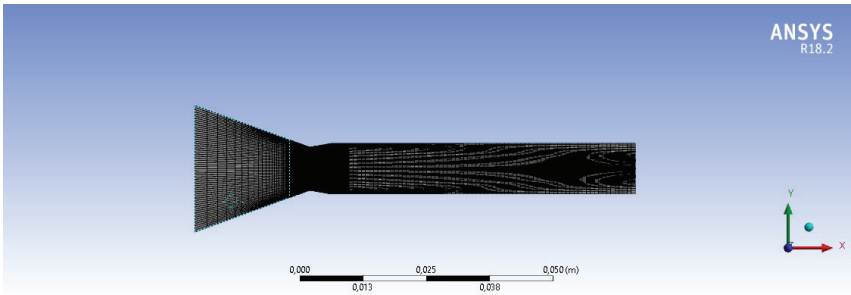


Figure 3. Mesh distribution

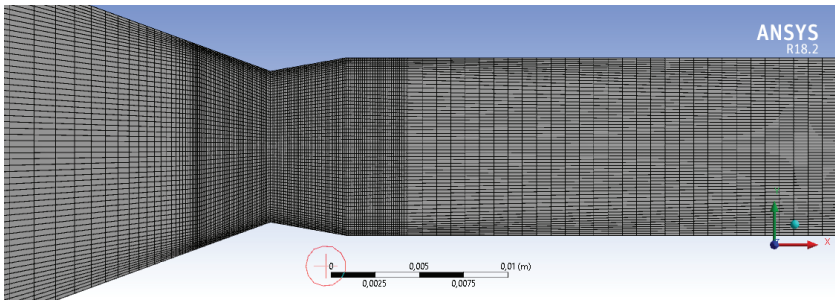


Figure 4. Detailed and specified mesh distribution

3. Results and Discussion

3.1. Pressure Distributions

Convergent-divergent nozzle has been designed according to Mach Number. For this study Mach number has been selected as 1.75 and boundary conditions has been calculated according to that. To obtain correct expansion, NPR has been calculated as 5.32, however, 4.32 and 6.32 has been investigated to compare distributions. NPR effects the inlet pressure directly. So, the system's distribution changes with respect to NPR. Divergent angle has been selected as 8 and 10 degrees to compare the effect of the angle on pressure, temperature, density and velocity distributions.

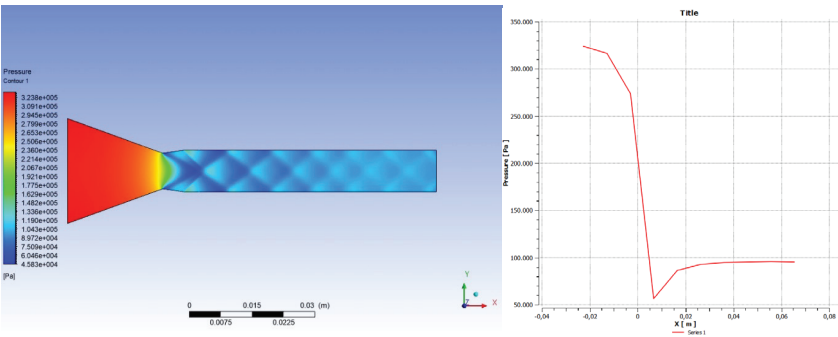


Figure 5 (a). Pressure contour for NPR 4.32 and 8 degree (b) Pressure chart for NPR 4.32 8 degree

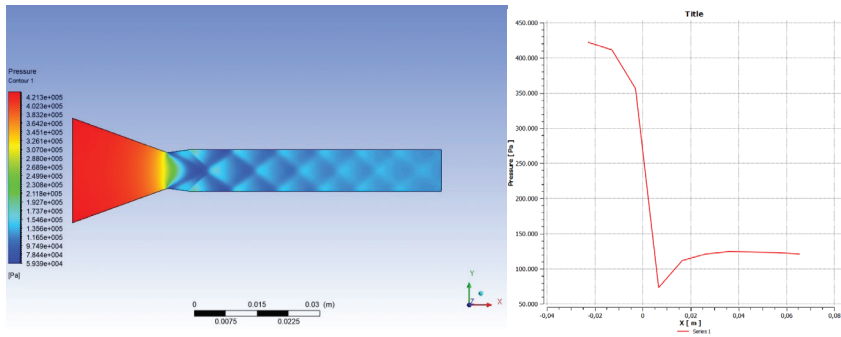


Figure 6 (a). Pressure contour for NPR 5.32 and 8 degree (b) Pressure chart for NPR 5.32 and 8 degree

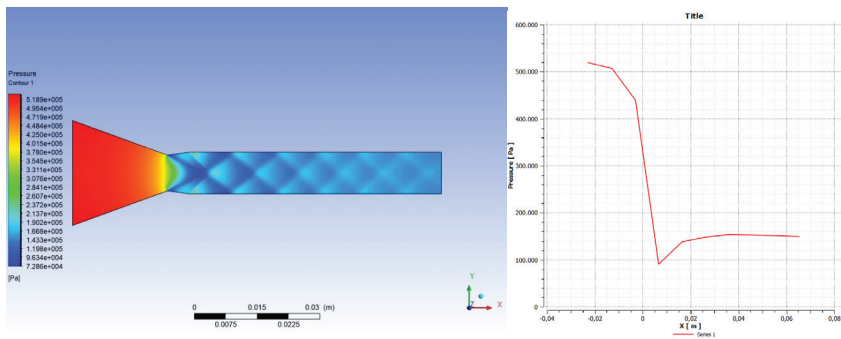


Figure 7 (a). Pressure contour for NPR 6.32 and 8 degree (b) Pressure chart for NPR 6.32 and 8 degree

In figure 5,6 and 7, at (a) section, we can see the pressure distributions and at (b) section we can see the chart for pressure and x position. After nozzle, duct section can be seen. In figure 5,6 and 7, inlet pressure is 3.25×10^5 , 4.25×10^5 , and 5.2×10^5 Pa respectively. Also exit pressures are, 0.9×10^5 , 1.4×10^5 and 1.5×10^5 Pa respectively. The highest pressure has been observed at the inlet section and lowest pressure has been observed at the exit section of convergent divergent nozzle which is the starting section of the nozzle. Inlet pressure is related with NPR, so in figure 8,9, and 10, inlet pressures is 3.25×10^5 , 4.25×10^5 , and 5.2×10^5 Pa respectively. At the exit pressure, 0.95×10^5 , 1.45×10^5 , and 1.55×10^5 respectively. With the increasing divergent angle, there are no change in the inlet section because of the same NPR, however, at the exit section, the pressure is higher at 8-degree divergent angle than 10-degree divergent angle.

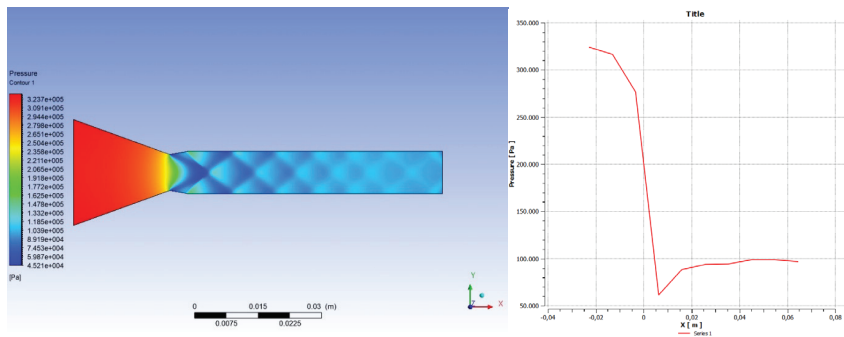


Figure 8 (a). Pressure contour for NPR 4.32 and 10 degree (b) Pressure chart for NPR 4.32 and 10 degree

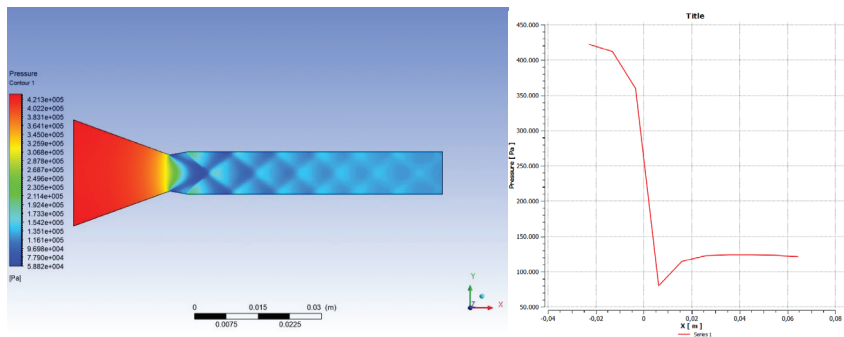


Figure 9 (a). Pressure contour for NPR 5.32 and 10 degree (b) Pressure chart for NPR 5.32 and 10 degree

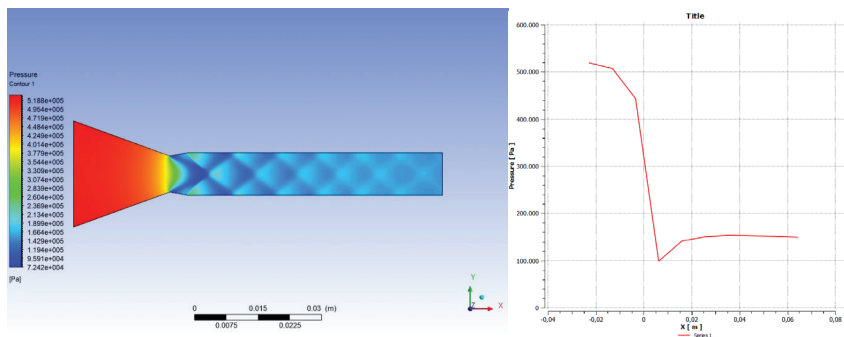


Figure 10(a). Pressure contour for NPR 6.32 and 10 degree (b) Pressure chart for NPR 6.32 and 10 degree

3.2. Density

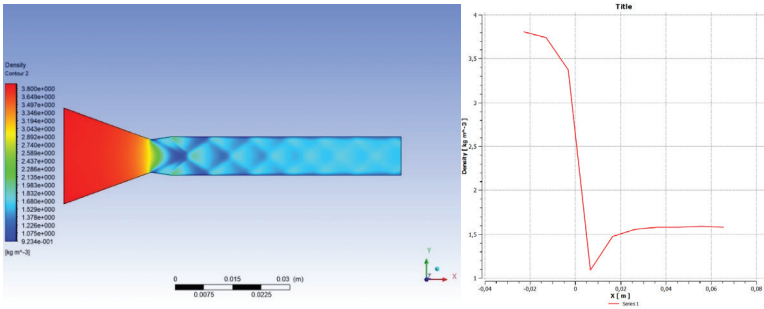


Figure 11 (a). Density contour for NPR 4.32 and 8 degree (b) Density chart for NPR 4.32 and 8 degree

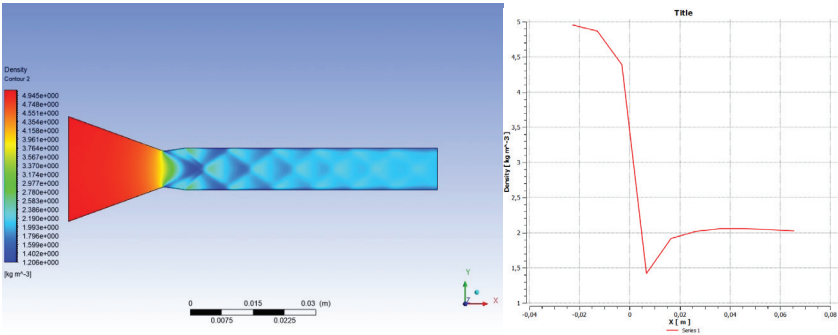


Figure 12 (a). Density contour for NPR 5.32 and 8 degree (b) Density chart for NPR 5.32 and 8 degree

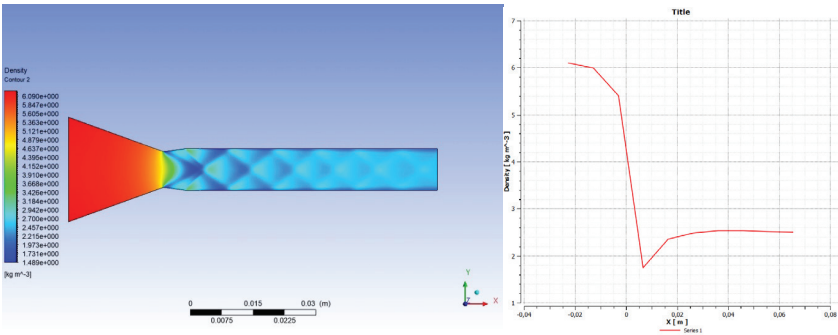


Figure 13 (a). Density contour for NPR 6.32 and 8 degree (b) Density chart for NPR 6.32 and 8 degree

In figure 11,12,13,14,15, and 16, we can see the density distribution on the geometry of the convergent divergent nozzle with duct at (a) section and chart of the density and the x at the (b) section. In figure 11,12, and 13

we can see the density for 8 degree divergent angle, and at the inlet section, density values are 3.8, 4.9, and 6.1 kg/m³ respectively. At the exit of the duct 1.6, 2, and 2.5 kg/m³ respectively. In figure 14,15, and 16 we can see the density for 10 degree divergent angle, and at the inlet section, density values are 3.8, 4.9, and 6.1 kg/m³ respectively. At the exit of the duct 1.6, 2, and 2.5 kg/m³ respectively. The highest value for the density for all cases at inlet section and the lowest value at the convergent divergent nozzle outlet section which is inlet section of the duct.

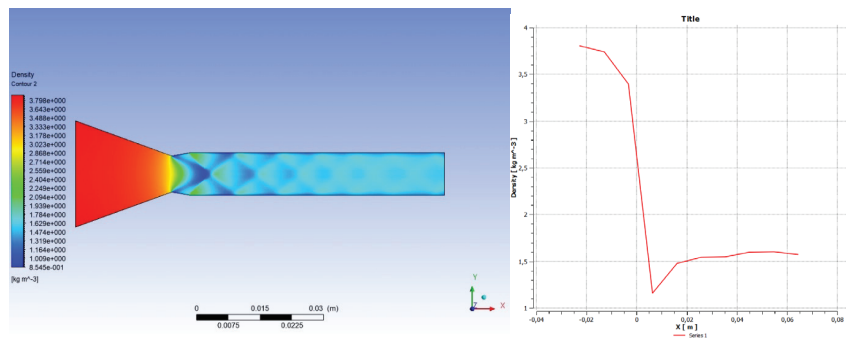


Figure 14 (a). Density contour for NPR 4.32 and 10 degree (b) Density chart for NPR 4.32 and 10 degree

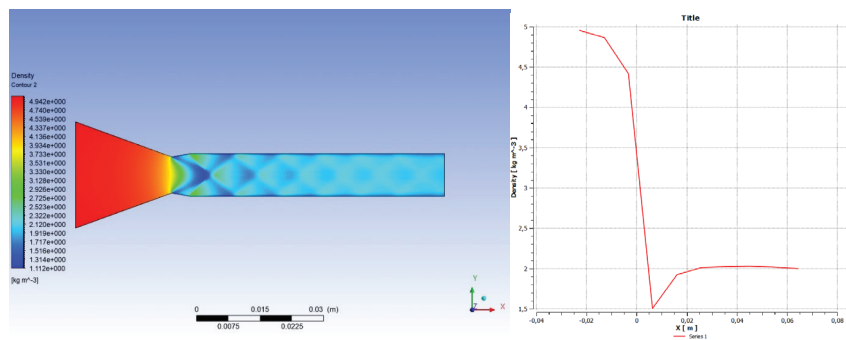


Figure 15 (a). Density contour for NPR 5.32 and 10 degree (b) Density chart for NPR 5.32 and 10 degree

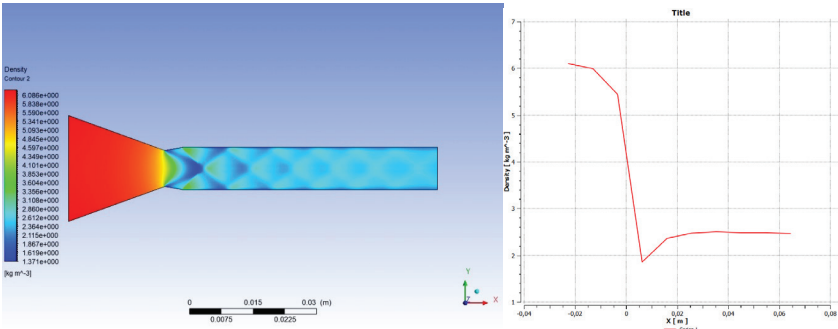


Figure 16 (a). Density contour for NPR 6.32 and 10 degree (b) Density chart for NPR 6.32 and 10 degree

3.3. Temperature

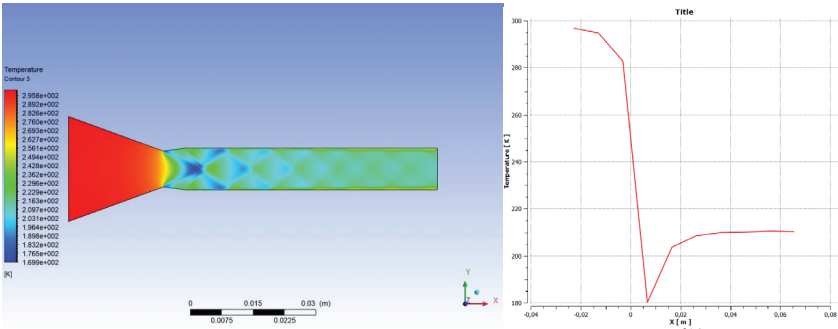


Figure 17 (a). Temperature contour for NPR 4.32 and 8 degree (b) Temperature chart for NPR 4.32 and 8 degree

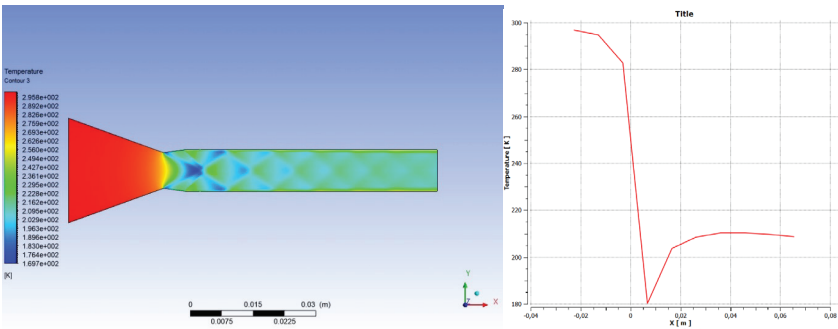


Figure 18 (a). Temperature contour for NPR 5.32 and 8 degree (b) Temperature chart for NPR 5.32 and 8 degree

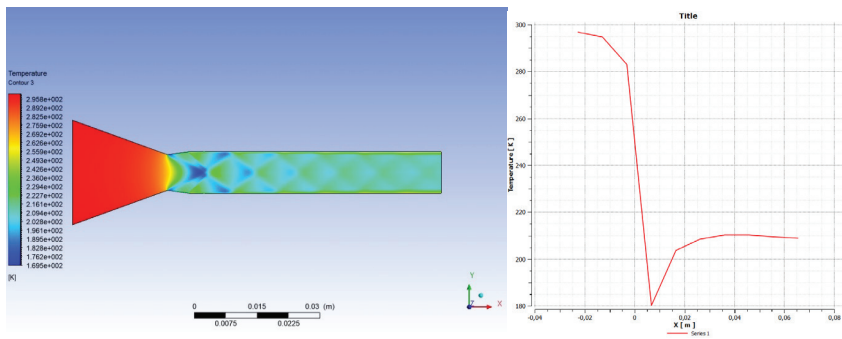


Figure 19 (a). Temperature contour for NPR 6.32 and 8 degree (b) Temperature chart for NPR 6.32 and 8 degree

In figure 17,18,19,20,21, and 22, we can see the temperature contour in geometry at (a) section and temperature chart which has temperature at y axis and x position at x axis at (b) section. In figure 17,18, and 19 we can see the temperature values for 8 degree divergent angle, and at the inlet section, temperature values are 297 K. At the exit section 209 K respectively. In figure 20,21, and 22 we can see the temperature values for 8 degree divergent angle, and at the inlet section, temperature values are 297 K. At the exit section 212 K respectively. The highest value for the density for all cases at inlet section and the lowest value at the convergent divergent nozzle outlet section which is inlet section of the duct. The exit section temperature value is higher at 8 degree divergent angle than 10 degree divergent angle.

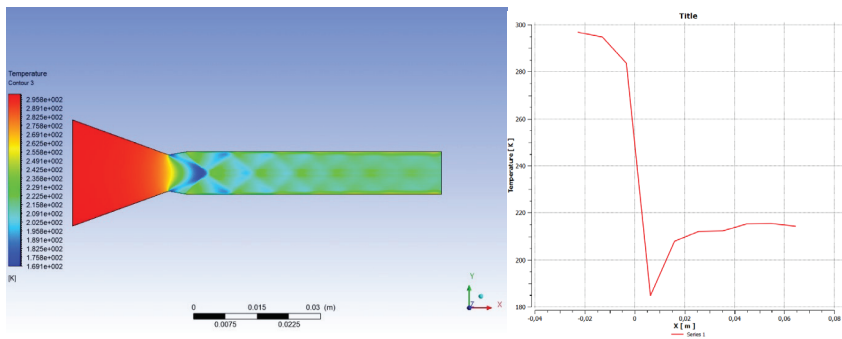


Figure 20 (a). Temperature contour for NPR 4.32 and 10 degree (b) Temperature chart for NPR 4.32 and 10 degree

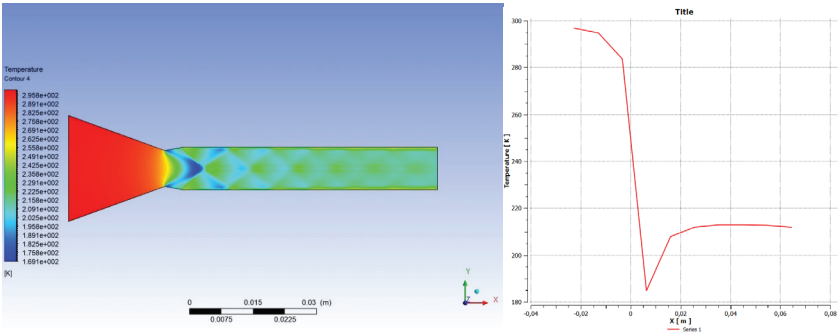


Figure 21 (a). Temperature contour for NPR 5.32 and 10 degree (b) Temperature chart for NPR 5.32 and 10 degree

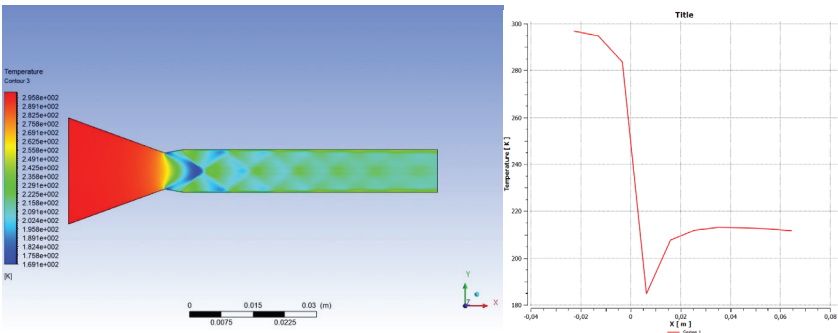


Figure 22 (a). Temperature contour for NPR 6.32 and 10 degree (b) Temperature chart for NPR 6.32 and 10 degree

3.4. Velocity

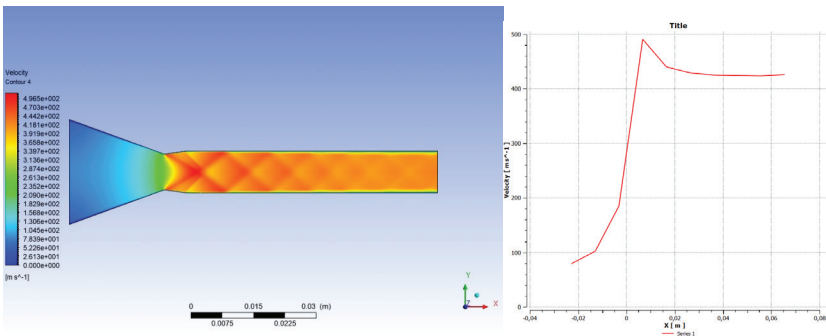


Figure 23 (a). Velocity contour for NPR 4.32 and 8 degree (b) Velocity chart for NPR 4.32 and 8 degree

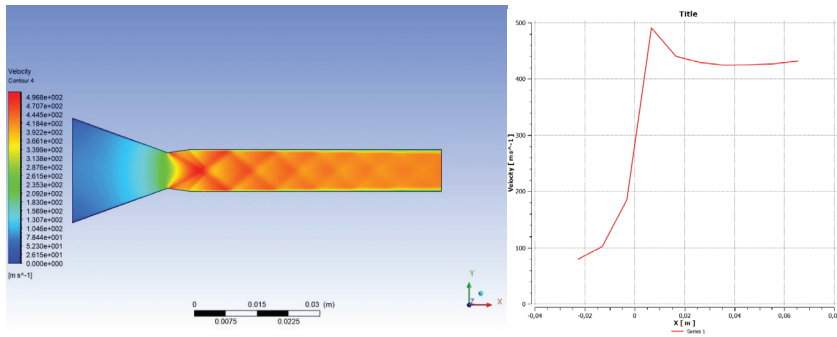


Figure 24 (a). Velocity contour for NPR 5.32 and 8 degree (b) Velocity chart for NPR 5.32 and 8 degree

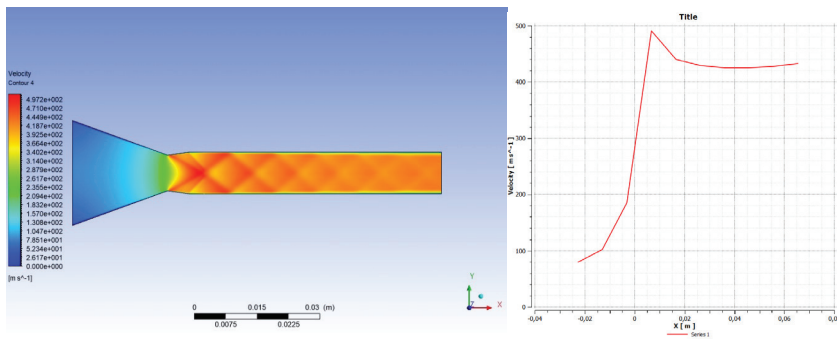


Figure 25 (a). Velocity contour for NPR 6.32 and 8 degree (b) Velocity chart for NPR 6.32 and 8 degree

The velocity at inlet section is low and at the exit section, velocity is high. And also, we can see from the chart, the temperature and pressure are reverse with velocity. This principle comes from Bernoulli equation. In figure 23, 24, 25, 26, 27, and 28, we can see the velocity contour in geometry at (a) section and velocity chart which has velocity at y axis and x position at x axis at (b) section. In figure 23, 24, 25, the inlet velocity is 80 m/s and at the exit section, velocity is 420 m/s. Maximum velocity at the exit of the convergent-divergent nozzle which is the inlet section of duct. After duct, temperature relatively decrease. Because of the no slip condition, through the wall side, the velocity goes to 0 m/s. In figure 26, 27, and 28, inlet velocity and outlet at the duct are 80 and 420 m/s. Also (b) section of the figures, we can see the chart of the velocity.

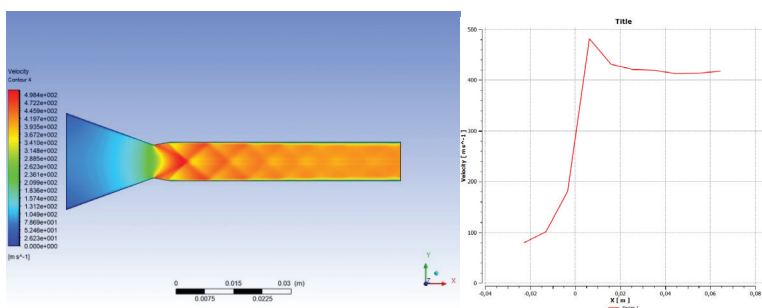


Figure 26 (a). Velocity contour for NPR 4.32 and 10 degree (b) Velocity chart for NPR 4.32 and 10 degree

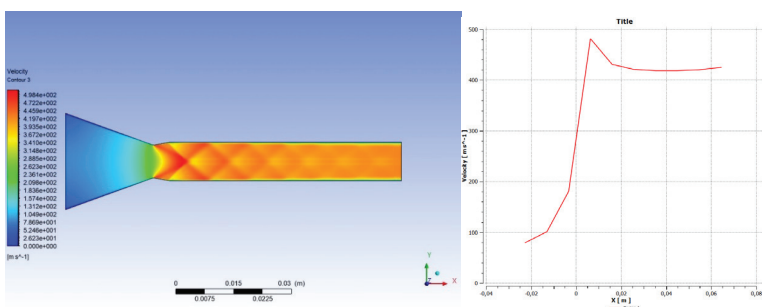


Figure 27 (a). Velocity contour for NPR 5.32 and 10 degree (b) Velocity chart for NPR 5.32 and 10 degree

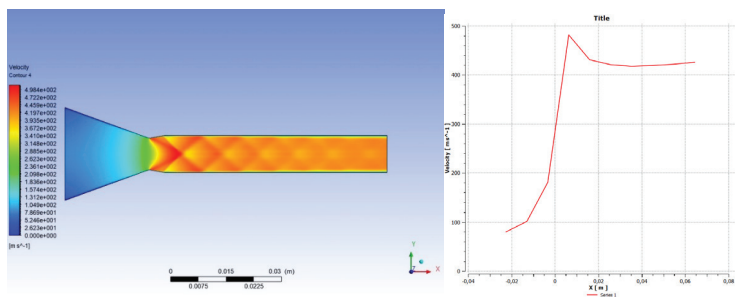


Figure 28 (a). Velocity contour for NPR 6.32 and 10 degree (b) Velocity chart for NPR 6.32 and 10 degree

4. Conclusion

In this study, convergent divergent nozzle has been designed according to Mach number 1.75 which has been analyzed and investigated with CFD methods. NPR has been calculated as 5.32 and 4.32 and 6.32 have also been used to compare. 8 and 10 degrees have been investigated. According to result, the following list can be concluded.

- Fluctuation in the pressure has been observed for Mach number 1.75. This calculation also can be used for the comparison of the other Mach number studies.
- The biggest difference for the divergent angles has been observed for temperature.
- With the decreasing velocity, increasing the temperature has been observed for all section.

References

- [1] Afghan, K.S., Ibrahim, O.M., and Aabid, A., (2021), CFD analysis of compressible flows in a convergent-divergent nozzle. *Materials Today: Proceedings*, vol. 46, pp. 2835-2842.
- [2] Madhu, B.P. and Mahendramani, G., (2020), Numerical simulation of convergent-divergent and contour nozzle for different divergent angle, *International Journal of Mechanical and Production Engineering Research and Development*, vol. 8, pp. 394-401.
- [3] Srinivas, G. and Rakham, B. (2017), Experimental and numerical analysis of convergent nozzle, *IOP Conference Series: Materials Science and Engineering*, vol. 197. No. 1. IOP Publishing.
- [4] Khan, M.A, Sardiwal, S.K., Sharath, M.V.S., Chowdary, D.H., (2013), Design of a supersonic nozzle using method of characteristics, *International Journal of Engineering and Technology* vol. 2, pp. 19-24.
- [5] Nallode, C., Chandrashekar, R., Ahmed, J., Prasad G.M.S. (2017), Design and Performance Analysis of a CD Nozzle for Evacuating Emissions from the Subway Tunnels, *Journal of Applied Mechanical Engineering* vol. 6: 6, pp.1000293
- [6] Madhu, B.P., Sameer, S., Kumar, K.M., Mahendra, M.G., (2017), CFD Analysis of Convergent-Divergent and Contour Nozzle, *International Journal of Mechanical Engineering and Technology* vol. 8.8, pp.670-677.
- [7] Satyanarayana, G., Varun, Ch. and Naidu, S.S., (2013) CFD analysis of convergent-divergent nozzle, *Acta Technica Corviniensis-Bulletin of Engineering* vol. 6.3, pp. 139-144.
- [8] Khalid, M.W. and Ahsan, M., (2020), Computational Fluid Dynamics Analysis of Compressible Flow Through a Converging-Diverging Nozzle using the k- ϵ Turbulence Model, *Engineering, Technology & Applied Science Research* vol.10.1, pp. 5180-5185.
- [9] Ramana Rao, A.V., and Akhil, I., (2016), CFD analysis of a CD nozzle at two divergent angles for prediction of mach number ($M < 1$, $M = 1$, $M > 1$) and flow parameters of newtonian fluid by using ANSYS-FLUENT 14.0. *International Journal of Engineering Science and Research Technology*, vol. 5.5, pp. 413-428.
- [10] Kumar, R., and Devarajan, Y., (2020), CFD simulation analysis of two-dimensional convergent-divergent nozzle. *International Journal of Ambient Energy* vol. 41.13, pp. 1505-1515.



CHAPTER 10

PREDICTION STUDY FOR LONG- TERM WIND SPEED USING MACHINE LEARNING METHODS

Serap AKCAN¹, Metin ÖZŞAHİN²

¹ Associate Professor Dr., Tarsus University, Faculty of Engineering, Department of Industrial Engineering, Mersin, Turkey. serapakcan@tarsus.edu.tr, ORCID: 0000-0003-2621-9142

² Assistant Professor Dr., Osmaniye Korkut Ata University, Faculty of Economics and Administrative Sciences, Department of Management Information Systems, Osmaniye, Turkey. metinozsahin@korkutata.edu.tr, ORCID: 0000-0001-9989-526x

1. INTRODUCTION

Today, with the rapid development of technology, the energy need of the world is increasing. Most of this need is met from fossil fuels. Studies on renewable energy sources gain importance due to the decrease in fossil fuel reserves and increase in environmental pollution. Wind energy is a natural and renewable resource for countries. As wind farms can be installed and removed in a little while, to invest for wind farms is worthwhile for countries. Even though wind energy has several benefits, estimating wind speed is challenging in practice as it is highly variable over time, especially when dealing with long-term forecasts.

Because of the increase in the environmental pollution, renewable energy sources are becoming crucial in the world. Considering renewable energy sources, wind energy is one of the most optimum renewables and one of the cheapest energy sources (Wagner, 2012). Thus, it is predicted that the use of wind energy increases throughout the world. Several research has been investigated to predict wind speed using different algorithms in literature. Lun and Lam (2000) used Weibull distribution parameter for long-term wind records. Ewing et al. (2007) examined time series analysis of wind speed using vector autoregression. Su et al. (2012) investigated correlation analysis for wind speed and failure rate using time series analysis. Assareh et al. (2012) presented artificial neural networks for wind speed prediction. Santamaria- Bonfil et al. (2016) presented a hybrid methodology based on support vector regression for wind speed prediction. Mohandes et al. (2016) used support vector machine method to predict wind speed at hub-height. Ambach and Croonenbroeck (2016) examined a periodic vector autoregressive model with seasonal lags to predict short to medium term wind speed. Doucoure et al. (2016) presented time series prediction with artificial wavelet neural network and multi-resolution analysis for wind speed. Akcan (2017) used time series analysis methods for wind speed forecasting. Daniel et al. (2020) investigated short term wind speed forecasting using statistical and machine learning methods. Their approach included two days ahead wind speed forecasting. Mahdi et al. (2021) presented an application of artificial neural network to predict wind speed in Iraq. Shawon et al. (2021) investigated short term wind speed forecasting methods using one-year historical data. They used ARMA, ARIMA, ANN, SVM methods in their study. Yousuf et al. (2022) analyzed statistical wind speed forecasting models for small sample datasets with four case studies.

Considering long-term-monthly-average wind speed data over the forty years at two meteorological stations throughout Central Anatolia geographical region in Turkey, wind speed prediction using machine learning methods are presented in this study. To evaluate the models' per-

formance, mean absolute error (MAE), mean absolute percentage error (MAPE), mean square error (MSE) and root mean square error (RMSE) statistics were calculated. The paper unfolds as follows: Section 2 presents the methodology. In section 3, case study is given for each of the meteorological stations and finally the conclusion is presented in section 4.

2. METHODOLOGY

2.1. Machine Learning Methods

WEKA is a program of open source of many data mining and machine learning algorithms, including: pre-processing on data, classification, clustering, association rule extraction. WEKA is a machine learning and data mining program coded in Java and produced by the University of Waikato, New Zealand. WEKA uses classification algorithms that yield numerical results as prediction and prediction algorithms (Hall et al., 2009). WEKA software is a widely used data preprocessing tool that contains many algorithms. It is especially designed to be able to analyze datasets containing large data. It is preferred in data mining with its useful and user-friendly interface, data preparation and ability to display statistical diagrams in detail (Witten ve Frank, 2002). WEKA was developed for priority scientific research during the development phase. Later, the usage area has increased by making the interface easy and usable. It can be easily used for different methods such as classification, time series, association analysis, visualization, filtering and data preprocessing (Witten ve Frank, 2002). Using with WEKA version 3.9.5 (figure1), machine learning methods described below were used in this study.



Figure1. WEKA software

2.1.1. Random Forest Algorithm

RandomForest algorithm is a supervised classification algorithm. As the name suggests, it randomly creates a forest. There is a direct relationship between the number of trees in the algorithm and the result it can achieve. The higher the number of trees, the higher the chance of obtaining accurate results (Livingston, 2005).

2.1.2. Random Tree Algorithm

The Random Tree algorithm is randomly selected from the set of possible trees. Each tree in the tree set has an equal chance of being tried as a sample. The distribution of trees shows an even distribution. Random trees can be generated effectively. In addition, models created by many random trees usually have a high accuracy rate (Onan 2015).

2.1.3. Multilayer Perceptron Algorithm

Multilayer Perceptron is used to classify with back propagation method and to learn a multi-layered perceptron, as the name suggests (Desai and Sunil, 2012). This algorithm is included in the literature as another model developed for situations where the artificial neural network class single-layer model is insufficient. In many problems, it is insufficient to apply a linear function alone and this causes the error rate to increase. Multi-layer perceptron (MLP), which were developed after the failure of single-layer perceptron to solve nonlinear problems, consist of an input layer, one or more hidden (intermediate) layers, and an output layer. Multilayer Perceptron structure can be seen in Figure 2.

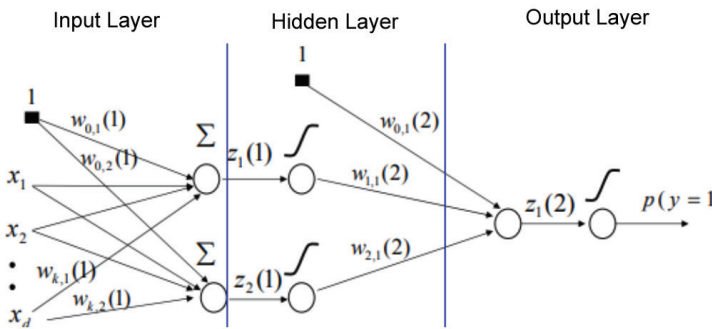


Figure2. Multilayer Perceptron Neural Networks

2.1.4. Linear Regression

The aim of the regression, which is used in the estimation of continuous variables, is to create the model by associating the inputs with the outputs and to make the most accurate estimation. Linear regression tries

to predict the value of one variable using another variable (Yıldırım, 2019).

2.2. Statistical Performance Measures

To decide whether the prediction model is adequate, error values of model should be examined. Therefore, mean absolute error (MAE) (eq.2), mean absolute percentage error (MAPE) (eq.3), mean square error (MSE) (eq.4) and root mean square error (RMSE) (eq.5) are used as statistical performance measures.

$$e_t = A_t - F_t \quad (1)$$

$$MAE = \frac{1}{n} \sum_{t=1}^n |e_t| \quad (2)$$

$$MAPE = \frac{100}{n} \sum_{t=1}^n \left| \frac{e_t}{A_t} \right| \quad (3)$$

$$MSE = \frac{1}{n} \sum_{t=1}^n e_t^2 \quad (4)$$

$$RMSE = \sqrt{\frac{1}{n} \sum_{t=1}^n e_t^2} \quad (5)$$

where, n= number of observations, A_t = actual value at observation t, F_t = prediction value for observation t and e_t = error value at observation t.

3. CASE STUDY

In this study, two meteorological stations throughout Central Anatolia geographical region in Turkey are investigated seen in Table1.

Table 1. Latitude and Longitude of Observed Stations

Geographical region	Station	Latitude	Longitude	Elevation (m)
Central Anatolia	Kayseri	38.6870	35.5000	1094
Central Anatolia	Konya	37.8687	32.4713	1029

WEKA time series algorithms; RandomSupSpace, CVParameter-Selection, MultiScheme, WIHW, InputMappedClassifier, Zeror, RepTree, DecisionStump, LWL, RandomCommitte, Random Forest, M5P, Randomtree, DecisionTable, Bagging, RegressionByDiscretization, M5Rules, SMOreg, Linear regression, IBK, RandomizableFilteredClassifier, AdditiveRegression, MultilayerPerceptron and Kstar were used for prediction long-term wind speed in this study. However, four algorithms that gave

the best prediction results were determined and the results of these four algorithms (RandomForest, RandomTree, Multilayer Perceptron and Linear Regression) were presented in the study. While running these algorithms, the settings in WEKA and used by default are left constant.

The prediction models for each meteorological station are seen in figure3 and figure4. For a good prediction model, performance measure values should be low (Santamaria-Bonfil et al., 2016). The performance measure values (MAE, MAPE, MSE and RMSE) for each station are shown in Table2 and Table3. Based on the data in Table2 and Table3, it can be said that all of the four machine learning algorithms (RandomForest, RandomTree, MultilayerPerceptron and LinearRegression) can be used for prediction long-term wind speed. But, RandomTree algorithm gives the best fit for both stations.

Table 2. Statistical performance measure values for Kayseri Station

Kayseri Station			
Performance Measures	RandomForest	RandomTree	Multilayer Perceptron
MAE	0.112	0.0093	0.0977
MAPE	15.0128	0.9115	9.2146
RMSE	0.1717	0.0146	0.1335
MSE	0.0295	0.0002	0.0178

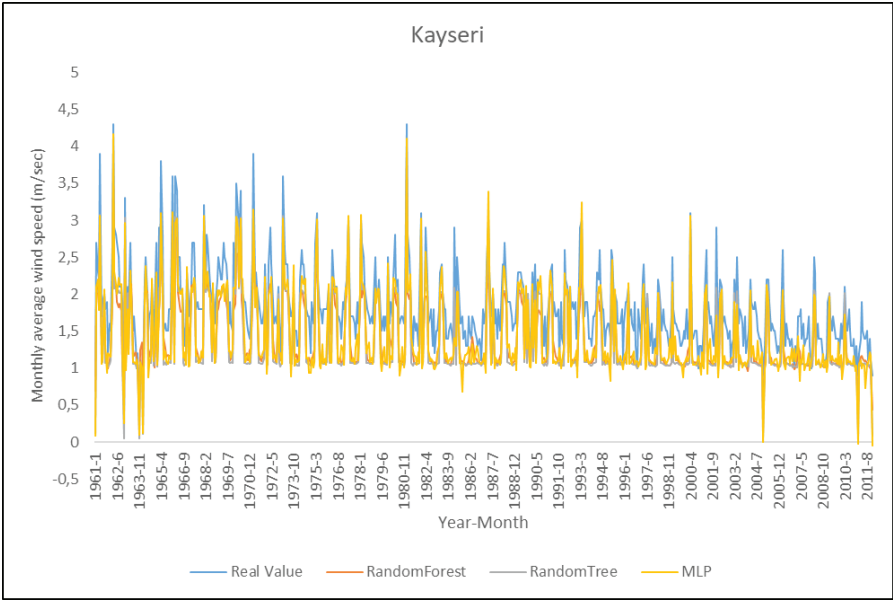


Figure 3. Prediction values for Kayseri Station

When Figure 3 is examined, the errors in the estimation periods of the methods can also be seen. Although RandomTree did not show perfect prediction success at all prediction points, it was successful in terms of overall performance. On the other hand, it is seen that the estimation errors made about the MLP method are generally caused by the fact that it makes an estimation far below the truth. In other words, as can be seen in April 2004, for example, the monthly average wind speed decreased in this period and MLP made an error with an almost zero value estimate here. In other words, as can be seen in April 2004, for example, the monthly average wind speed decreased in this period and MLP made an error with an almost zero value estimate here. The large number of similar examples seems to be the reason why MLP lags behind in all forecasting performances. The monthly average wind speed at Kayseri station has a highly fluctuating structure. This is seen differently even in the same months of each year. For this reason, this makes it difficult for statistical methods to make accurate predictions. On the other hand, the real wind averages at the Kayseri station peak in November 1980. After this date, it is seen that monthly wind speed averages oscillate lower in narrower intervals. For this reason, if the data are separated as before and after this date in future studies, the error rate in the estimations can be further reduced and different methods will perhaps have the potential to be more successful.

Table 3. Statistical performance measure values for Konya Station

Konya Station				
Performance Measures	RandomForest	RandomTree	Multilayer Perceptron	Lineer Regression
MAE	0.1317	0.0088	0.1904	0.3498
MAPE	6.7963	0.9694	10.1792	17.9177
RMSE	0.1819	0.1082	0.2284	0.4727
MSE	0.0331	0.0117	0.0522	0.2235

When Table 3 is examined, we can say that the most suitable method for Konya station estimation is the RandomTree algorithm by looking at the MAE value. Looking at the MAE value, it is seen that the worst method is Linear Regression. This situation is also normal. It can also be seen by looking at the actual wind speeds in Figure 4 that there is no definite trend. When Figure 4 is examined, it can be seen that the graph is divided into 3 parts by looking at the time. It refers to these sections before 1964, between 1964-1987 and after 1987. While higher speeds are detected in the first section, the wind speed in the second section actually shows similar oscillations over a long period and remains almost steady-state. In the last section, there is an uptrend and a wind speed oscillation, which can reach

higher limits and whose movement cannot be clearly defined. It should be noted here that if only the last part is included in the data set, perhaps the performances of the above methods will also change significantly. Here, while recovery occurs in some methods, it may follow a completely opposite course in other methods.

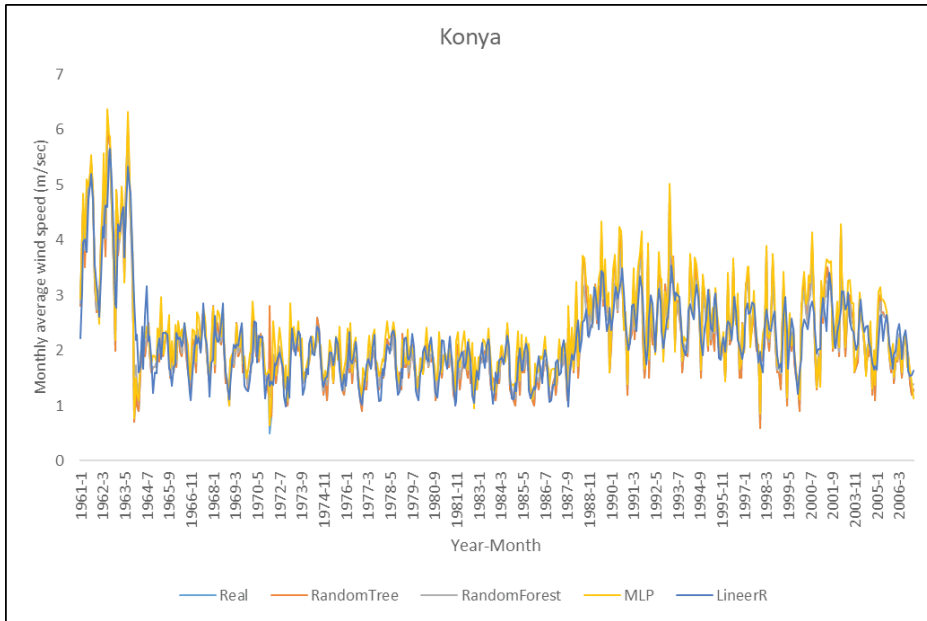


Figure 4. Prediction values for Konya Station

4. CONCLUSION

In this study, data from 2 stations in Turkey, namely Kayseri and Konya station, were used to test the prediction success of machine learning methods. Monthly average wind speed measurements are based on the selected time intervals for these two stations. The data between 1961-2011 for Kayseri station and between 1961-2006 for Konya station were selected. In the tests performed, the RandomTree algorithm showed the best performance in terms of estimation errors. WEKA package program was used to test the success of the algorithms. The prediction values of the algorithms and the actual wind speeds were combined on the same graph and analyzed, and as a result of these examinations, it was seen that there were periodic differences in the data set that affected the forecast performance.

Perhaps, if the last 20 years of data are taken in the data set, the forecast results and forecast success will be even better. For this reason, it will

be necessary to decide on the right range for the data set by focusing on this issue in future studies. However, since these intervals may change from station to station, it would be more accurate to make a decision by looking at more than 40 wind stations in Turkey separately. Another suggestion for future studies would be hybrid methods. It is estimated that the success of prediction will increase with the hybridization of the methods that have been put forward as an alternative to machine learning methods in recent years.

In conclusion, the issue of alternative energy resources is an important issue and making future projections on wind energy will play an important role in deciding the investments to be made in this regard. For this reason, it is necessary to investigate the economic effects of such studies at the same time and to reveal the economic benefit that can be created with different studies. It is useful to remember the effect that such scientific study outputs will guide in future feasibility studies.

REFERENCES

- Akcan S. (2017), Wind speed forecasting using time series analysis methods, Çukurova University Journal of the Faculty of Engineering and Architecture, 32(2), pp. 161-172.
- Ambach D. and Croonenbroeck C. (2016), Space time short to medium term wind speed forecasting, Statistical Methods and Applications, 25 (1): 5- 20.
- Assareh E. et al. (2012), An analysis of wind speed prediction using artificial neural networks: A case study in Manjil Iran, *Energy Sources*, 34: 636- 644.
- Daniel et al. (2020), Short-term wind speed forecasting using statistical and machine learning methods, Algorithms, 13, 132; doi:10.3390/a13060132.
- Desai A. and Sunil R. (2012), Analysis of machine learning algorithms using WEKA. International Journal of Computer Applications, 975- 8887.
- Doucoure B., Agbossou K. and Cardenas A. (2016), Time series prediction using artificial wavelet neural network and multi-resolution analysis: Application to wind speed data, *Renewable Energy*, 92: 202- 211.
- Ewing B.T. et al. (2007), Time series analysis of wind speed using VAR and the generalized impulse response technique, *Journal of Wind Engineering and Industrial Aerodynamics*, 95, 209- 219.
- Hall, M., Frank, E., Holmes, G., Pfahringer, B., Reutemann, P., & Witten, I. H. (2009). The WEKA data mining software: an update. *ACM SIGKDD explorations newsletter*, 11(1), 10-18.
- Livingston, F. (2005), Implementing Breiman's random forest algorithm into Weka. In ECE591Q machine learning journal paper.
- Lun I.Y. and Lam J.C. (2000), A study of Weibull parameters using long-term wind observations, *Renewable Energy*, 20 (2): 154- 153.
- Mahdi B. H., Yousif K. M. and Melhum A. I. (2021), Application of artificial neural network to predict wind speed: case study in Duhok city Iraq, *Journal of Physics: Conference Series*, 1829 (2021) 012002 doi:10.1088/1742-6596/1829/1/012002.
- Mohandes M. et al. (2016), Convertible wind energy based on predicted wind speed at hub-height, *Energy Sources*, 38 (1): 140-148.
- Onan, A. 2015, Sirket iflaslarinin tahmin edilmesinde karar agaci algoritmalarinin karsilastirmali basarim analizi, *Bilisim Teknolojileri Dergisi*, 8(1), 9-19.
- Santamaria-Bonfil G., Reyes-Ballesteros A. and Gershenson C. (2016), Wind speed forecasting for wind farms: A method based on support vector regression, *Renewable Energy*, 85, 790- 809.
- Shawon et al. (2021), Wind speed forecasting by conventional statistical methods and machine learning techniques, 2021 IEEE Electrical Power and Energy Conference, 304-309.

- Su C., Quan J. and Fu Y. (2012), Correlation analysis for wind speed and failure rate of wind turbines using time series approach, *Journal of Renewable and Sustainable Energy*, 4: 032301.
- Wagner H.J., Mathur J. (2012), *Introduction to wind energy systems: basics, technology and operation*, Springer Science & Business Media.
- Witten, I. H., & Frank, E. (2002). Data mining: practical machine learning tools and techniques with Java implementations. *Acm Sigmod Record*, 31(1), 76-77.
- Yıldırım V. (2019), İstatistiksel veri madenciliği teknikleri ile kamu alimleri sektöründe satış tahmini, Yüksek Lisans Tezi, Hacettepe Üniversitesi Fen Bilimleri Enstitüsü, Ankara.
- Yousuf M. U., Al-Bahadly I. and Avcı E. (2022), Statistical wind speed forecasting models for small sample datasets: Problems, improvements, and prospects, *Energy Conversion and Management*, 261: 115658.



CHAPTER 11

CLASSIFICATION AND REGULATIONS OF UNMANNED AERIAL VEHICLES

Faruk GÜNER¹, Hilmi ZENK²

1 Doç.Dr.Faruk Güner, <https://orcid.org/0000-0002-3438-0553>, Department of Mechanical Engineering, Faculty of Engineering, Giresun University, 28200 Giresun, Turkey.

2 Doç.Dr. Hilmi Zenk, <https://orcid.org/0000-0002-1653-8580>, Department of Electrical and Electronics Engineering, Giresun University, 28200 Giresun, Turkey.

Introduction

Unmanned aerial vehicles are used for many purposes today. These systems, which were designed primarily for military intelligence purposes, can now be used for data collection, as well as for attack weapons or useful cargo. Within this wide range of uses, it has become possible to use children's entertainment tools for a number of tasks, including media, first aid and health, energy, agriculture, traffic, cargo, surveillance and supervision, investigation of archaeological sites, mapping of the earth, three-dimensional city or land modeling.

The use of UAVs for military, civil and scientific purposes is increasing all over the world. The width of civil use areas can be shown as the main reason for the widespread use of drones. The cost advantage it brings thanks to the speed it provides in many commercial use areas is another important reason for preference (Kahveci & Can, 2017).

When it is desired to make a definition about drones, it is not very easy to make a precise definition that includes the full scope. It is possible to make different definitions according to the sector in which they are used, the tasks they are assigned and the technologies used. Apart from different definitions, the two definitions made by NATO and the USA are the most accepted ones. For a drone, NATO defines vehicles that are not human, are guided by remote control or have motorized propulsion that autonomously directs itself, can load and unload weapons or useful loads, can land by returning or self-destruct from the target point. According to the US Department of Defense, the UAV is defined as a reinforced aircraft that uses aerodynamic forces as a lifting force, can be autonomously or remotely controlled, can fly, can be developed, can carry a deadly or non-fatal load, and does not include a human operator (Lofù, Tedeschi, Di Noia, & Di Sciascio, 2022).

The most important detail to be considered in the definition of drone is the useful load. If the drone is orbiting in a specific orbit in space and is designed to perform a specific commercial, scientific, and military task during or as a result of that orbit, these are called payload drones. With this approach, systems such as airplanes, UAVs, UAVs, passengers, cameras, military equipment and lighting, apart from the parts that provide flight operation, are also classified as useful loads (Amine Masmoudi, Mancini, Baldacci, & Kuo, 2022). As can be seen in the graph shown in Figure 1 below

First unmanned aerial vehicle I. during World War II with the thought of a flying torpedo. There are researchers who state that these tools go back to the famous mathematician Pythagoras. But in the sense that we know today, the idea that it started to be developed in the years of World War II is more accepted. During World War I, various attempts were made to make the flying, equivalent of the torpedo. The first of these is the Aerial Target

missile, which was developed by Archibald Montgomery Low. Although Aerial Target was not very successful in trials, it was enough to open people's horizons in this field. Another experiment was the Aerial Torpedo, which was developed by the American Navy in the same years. Most of the weight of this wooden plane consisted of explosives, and the way it was directed at the target was quite primitive.

The wind speed, direction and target distance were determined and the number of engine turns required for the missile to reach the target was calculated. When this number was reached during the flight, the doors were opened and the bomb was dropped. After Aerial Torpedo, a lighter version of it was developed. It was used for targets about 100km away. Flying torpedoes have attracted a lot of attention, but few have been successful in flight trials (PG Fahlstrom, 2012). Figure 1 below shows the image of Aerial Torpedo developed by the American Navy.



Figure 1: First Primitive Armed Drone Developed by the American Navy (Demirkıran, 2010)

Falconer target planes, which were developed by a private company after World War II, were produced for a long time and achieved a significant commercial success. In these years, the developments in UAV technology were aimed at revealing flying systems for the diversion of radars. Subsequently, it was tried to increase the range of the target aircraft produced. Another important development in the 1950s is the false target systems used to confuse radars. In the following years, the flight range of the target aircraft was tried to be increased. The 1960s were the years

when target planes began to enter the literature as military spy planes. These target planes carrying cameras were controlled from a station on the ground or from a plane closer to the ground. When the difficulties of their detection were reduced to one side, they caused fewer diplomatic problems because there were no pilots in them. By the 1970s, it was now the cold war years and intelligence activities were becoming more important and critical. This situation was also reflected in UAVs and more complex systems started to be put forward. Designed by Lockheed, Lockheed Aquila is a good example of these complex systems. Aquila was supposed to fly an autopilot, detect enemy troops with sensors on it, transmit a real-time image to the base, and do all this without being captured by Soviet forces. However, the systems that should be on the vehicle were heavy and large systems that attracted excessive power(Demirkiran, 2010).

In the 1980s, Israel participated in the technological race. The Mini Unmanned Aerial Vehicle they have developed, called Scout, is defined as the father of this sector. The scout is designed to have a significant volume that can fly without being caught on radar with a wingspan of 3.96 meters and a fiberglass body. The most important feature that made Scout history is that its camera mounted on a rotating mechanism on it can transfer images in the first real time(Kuzu, 2018). Figure 2 below shows the Scout Unmanned Aerial Vehicle developed by Israel.



Figure 2: Scout Unmanned Aerial Vehicle (Kuzu, 2018)

Satellite communication, which supports the development of GPS, i.e. global positioning systems, has enabled UAVs to move to an upper class. These systems were able to control the flight systems with problematic remote control electronically and satellite communication controls were easily performed with self-repetitive software loops. Thus, longer-distance flights were carried out safely.

Especially thanks to the advancement in battery technology, the useful load capacities carried over a long distance have increased. By the 2000s, UAVs that transmit images on long-range flights and offer assault with weapon systems could be produced.

RECENT INVESTIGATIONS IN UAV SYSTEMS

The minimum requirement for the development of any system is the development of the material. In other words, it is not easy to take major engineering steps without development in material technology. The most well-known example in this regard was the inclusion of materials produced by NASA for space studies in other areas. Today, the fact that nano-structured materials have entered the field of engineering provides important developments in many technology groups (Aktas, Thornton, Binns, & Denby, 2016; Sadeler & Atasoy, 2016; Tan & Savaşkan, 2020). Developments in the field of materials alone are not sufficient, but the development of production methods also provides significant advantages. Since the working environments of UAVs are harsh, it is important to use materials that different production methods have been studied (Sadeler & Atasoy, 2011; Savaşkan, Tan, & Maleki, 2015).

When aviation technology is examined, it will be seen that it is the fastest advancing sector in the world. The first powered airplane to be adopted was made by the Wright brothers in 1903. In the first flight, it was able to stay in the air 40 meters in 11 seconds. Only 66 years later, a passenger plane with twice the speed of sound was produced, and people started to chase bigger dreams (Hilmi Zenk, Şenol, & Güner, 2019).

We see that the most important problem we face today in the creation of new designs is the cost, especially the energy cost. Any system to be designed must have minimum energy consumption. Energy is the most fundamental asset that has caused wars throughout history. Today, energy transportation can still be a cause of war, but it is still insufficient and still a subject that needs to be studied for a long time (Coruhlu, Solgun, Baser, & Terzi, 2022; Güner, Başer, & Zenk, 2021). Unmanned aerial vehicles, especially electric ones, are more preferred. We see that renewable energy sources enter our lives a little more every day. With the positive contribution provided here, it seems inevitable that many systems, from cars to unmanned aerial vehicles, will be electrified. Different approaches should

be taken into account in this regard (Güner & Güney, 2018).

Numerical analysis methods are another instrument in the rapid and low cost of technological progress in engineering studies. Thanks to these methods, rapid results can be obtained in engineering problems where micro-dimensional calculations or experimental investigations, which are very difficult to experimentally examine, will be very costly. Although the results obtained from numerical analyzes are approximate, preparing preliminary information for many studies also provides basic information in the creation of many prototypes. It is due to the nature of the method that numerical methods contain a certain error rate and reveal a certain approximation depending on this error. The most preferred of these methods, which can calculate the approximate error in itself, is the finite element method. Although there are many numerical analysis methods such as finite difference or discrete element method, the finite element method is widely used in Engineering applications with many advantages (Güner, 2020; Güner, Sofuoğlu, & Cora, 2016; H Zenk, Kara, Güney, Güner, & Zenk, 2018). The developments in computer technology have made it widespread and accelerated in the programs of everyone who uses the finite element method. In this way, a prototype that can only be produced experimentally in a few weeks can be subjected to Engineering analyzes that are needed for a few days. Due to including different engineering disciplines like mechanics, electronics, hydrokinetics and energy, the aviation sector increases the experimental study costs even more and it is an area where finite element analyzes are indispensable due to the danger of life (Güner & Zenk, 2019; Güner & Sofuoğlu, 2018; Kara, 2017).

When the studies conducted in the last few years are examined in the literature, it is clearly seen that researchers are trying to spread drones in different areas of use. A 2016 study tried to characterize the networking and communication aspects of UAVs by examining their civilian applications between 2000 and 2015. The authors characterize them on the parameters of data requirements, network duty, and service requirements, especially with quality assessment. In addition, a detailed examination of the adaptability, privacy, security, connectivity and scalability criteria, which are common network requirements, has been made. (Hayat, Yalmaz, & Muzaffar, 2016). Ebeid et al. (2017) evaluated open source flight controllers used in UAVs in their academic research. It tried to explain the basic components required for UAVs as hardware and software, and to compare the existing ones. (Ebeid, Skriver, & Jin, 2017). A study conducted in 2018 that considered each UAV as an independent cell and focused on the communication of these cells attempted to bridge the gap between the 3GPP standardization status and future research. As a result of the study, as a more specific output, the downlink command and control

(C&C) channel for antenna users is discussed. (Geraci, Garcia-Rodriguez, Galati Giordano, Lopez-Perez, & Bjornson, 2018).

A similar study was conducted by another research group in 2019. Researchers have also conducted studies on the development of the integration of UAVs into cellular networks. In addition, in the study, the difficulties of using the interfaces designed for users to control the system and the solutions that facilitate these difficulties were examined. As a result, UAVs also offer suggestions on testbed activities for cellular communication, prototyping and security.(Fotouhi et al., 2019).

Li et al. (2019) published a comprehensive survey on UAV communication towards 5G/B5G wireless networks. They briefly introduced Essentials of the communication system and also discussed related research challenges of the emerging integrated network architecture. In addition to possible future research topics, 5G techniques in current UAV platforms have been categorized in terms of physical layer, network layer and common communication, computing and caching features(Li, Fei, & Zhang, 2019).

In another study in 2019, a detailed evaluation was made of the work done so far in 5G mmWave integration. It is desired to draw attention to 5G mmWave communication for UAV supported wireless networks. Key technical advantages, challenges, and potential applications of this communication method are revealed(Zhang et al., 2019). Ullah et al. (2020) tried to provide detailed information about the regulations and legal regulations applied on UAVs, as well as the potential limitations and challenges expected in the long term. For the standardization of these regulations, they listed sub-titles as: noise reduction, safety, optimum trajectory, channel modeling, energy harvesting techniques, collision avoidance.(Ullah, Al-Turjman, & Mostarda, 2020).

In another study where SDN (Software-Defined Network) and NFV (Network Function Virtualization) technologies were discussed, different classifications of UAVs were made via their use cases. Evaluation, predictions and discussions on the use of SDN/NFV features in UAV systems were made (Sami Oubbati, Atiquzzaman, Ahamed Ahanger, & Ibrahim, 2020). Yueyan et al. conducted a detailed study of multiple UAVs and the communication software and sensors required to control them. (Zhi, Fu, Sun, & Yu, 2019). Similarly, Skorobogatov et al. (20220) presented a study in which the usage areas of UAV systems were evaluated in terms of factors such as communication, airtime and range. As a result of the study, it was stated that it is possible to experience significant developments in the coming years, especially in network communication systems(Skorobogatov, Barrado, & Salami, 2020). In another study, the communication level was taken as one step further and evaluations were made on green UAV

communication systems for 6G. The energy consumption models of existing UAVs and green UAV communication and energy consumption models were compared (Jiang et al., 2022).

In their study, Song et al. created an overview of the general architecture and communication infrastructure of the UAV. In communication architecture, the issue of interference reduction, especially in air-to-ground channel models, is discussed. In addition, the feasibility of UAV-supported air base stations, air relays and data collection/dissemination systems were examined and predictions were made about possible future work areas (Song, Zeng, Xu, & Jin, 2021). In more recent studies, it has been seen that UAVs also try to detect vehicle type from the images obtained in the air by using image processing and deep learning techniques. Image processing and deep learning are of increasing importance in many engineering fields, in academic and industrial research. The sub-topics of the studies are focused on reducing the computational load, increasing the accuracy and optimizing them within themselves. The results of such studies will help researchers in the field of traffic surveillance and artificial intelligence. (Srivastava, Narayan, & Mittal, 2021). Finally, in the article titled “Towards the Unmanned Aerial Vehicles (UAVs): A Comprehensive Review” published by Mohsan et al. in 2022, current uses, development directions and possible futures of UAVs are discussed. As a result, it is foreseen that possible future studies will be on Blockchain and 5G integration (Mohsan, Khan, Noor, Ullah, & Alsharif, 2022).

CLASSIFICATION OF UAVs

As mentioned before, there is no standard approach in UAV classification. However, there are no major differences in the basic definitions and parameters of classification. The criteria used in the classifications are not having an operator, acting remotely or autonomously, and being able to carry a fatal or non-fatal useful load (Yiğit, Yazar, & Karakoç, 2018).

It is possible to divide UAVs into three different classes according to their usage areas, dimensions, types of take-off and landing, wing structures, number of engines, and the foundation is also greased according to these classification weights. UAVs weighing up to 150 kg are classified as Class I, those weighing between 150 kg and 600 kg are classified as Class II and those weighing more than 600 kg are classified as Class III.

Class I UAVs are divided into three subgroups as Micro, Mini and Small. UAVs that are less than 2 kg and fly at an altitude of less than 200 ft and have a duty range of 5 km and are generally used for civilian purposes are counted in the Micro UAV category. Micro UAVs are a definition used for UAVs with wingspan not greater than 150mm. It is used for indoor tasks such as inside the building. It has to fly slowly. It is preferable that it

is suspended in the air and placed somewhere. Figure 3 shows an example of a Micro UAV.



Figure 3 YP brand S86 model Micro UAV (Express, 2022)

Those with a flight altitude of less than 3000 ft and a duty range of 25 km between 2 kg and 20 kg are considered as Mini UAVs. They can serve both military and civilian purposes. Small UAVs are UAVs that fly between 20 kg and 150 kg, at altitudes lower than 5000 ft and within a range of 50 km.

Class II includes UAVs with a weight range of 150-600 kg, which are commonly referred to as Tactical UAVs or TUAVs. They have flight altitudes up to 15,000 ft maximum. Their range can reach up to 200 km. In addition to the STOL short-distance landing and take-off feature, they are also expected to be able to make vertical take-offs and landings. The average flight time is 5 hours. They can go up to 100 kts. They can carry 200 pounds of payload and are usually powered by a diesel engine.

There are three subgroups in Class III. These are evaluated as HALE UAV (High-Altitude Long-Endurance Unmanned Aerial Vehicle), MALE UAV (Medium-Altitude Long-Endurance Unmanned Aerial Vehicle) and AUAV (Attack Unmanned Aerial Vehicle). HALE is a drone built for high altitude, long-term flight. They can fly over 24 hours at an altitude of approximately 4500 m. They can conduct intercontinental reconnaissance and observation with weapons loaded. They are usually controlled from fixed bases. Figure 4 shows the NASA/NOAA Global Hawk HALO tool.



Figure 4 The NASA/NOAA Global Hawk HALO UAS. Image courtesy NASA (Watts, Ambrosia, & Hinkley, 2012)

MALE, on the other hand, are UAVs that can fly for 24 hours at an altitude between 1500 m and 4500 m, which are produced for medium altitude and long-term flight. They are controlled from fixed bases within a distance of 500 km. The AUAV is considered tactical attack combat drones. Their technical capacity is the same as the HALE group and they are considered as a separate group due to their tactical superiority (Chmielewski & Wróblewski, 2017; Sanchez-Aguero et al., 2022; Watts et al., 2012). Figure 5 shows Milano UAV which is categorized as MALE



Figure 5 Milano UAV at Rozas Airport (Sanchez-Aguero et al., 2022)

These classifications can be listed as follows with the abbreviations mentioned in the literature;

MAV (Micro (or Miniature) or NAV (Nano) Air Vehicles): They are so small that soldiers individually can carry one of them in their backpacks. Operation altitude is lower than 330 m. They can fly between 5 and 30 minutes due to their small size batteries.

VTOL (Vertical Take-Off & Landing): If there is no runway for the aerial vehicle and it must be taken off/land vertically VTOL is the best choice. This capability has a great energy demand which decreases the flight durations for VTOLs,

Lase (Low Altitude, Short-Endurance): Also called as sUAS (small Unmanned Aircraft Systems). Deployment/recovery and migration also eliminates the need for runways with its optimized design. They have a weight of 2-5 kg and a wingspan of less than 3 meters, where the option to launch manually or with a miniature catapult, which eliminates the need for a runway, can be applied. low weight concessions cause them to stay in the air for a maximum of 1-2 hours and not be far from the operation center.

Base close: These larger sUAV's those aircraft do require runways due to their larger size, weight and capabilities. 1,500 m altitude for a couple of hours.

TULIP (Low Altitude, Long Endurance): Typically made by the United States Federal Aviation Administration (FAA), this definition refers to sUASs capable of carrying several kilogram payloads for extended periods at an altitude of several thousand meters.

MALE (Medium Altitude, Long Endurance): They are systems that can fly for very long periods at high altitudes such as 9000m. They can carry significant payloads.

HALE (High Altitude, Long Endurance): These are the largest and most complex of the UAV, those may be larger than many general-aviation manned aircraft. Operation altitude is of 20,000 m or more. Flight duration may be over 30 hours with thousands of km in each mission(Watts et al., 2012).

UAVs can be stationary or rotating. While fixed-wing UAVs take off by accelerating on the runway or by throwing them by hand, rotary-wing unmanned aerial vehicles are taken off from anywhere and directed to all kinds of places with the control. There are many types of rotary-winged UAVs, including tricopter, quadcopter, hexacopter and octocopter according to the number of rotors they have, and they are generally called multicopter. Unlike fixed-wing aircraft, multicopters are classified as rotorcraft because they obtain the lifting force from rotating beams. Unlike helicop-

ters, multicopters often use propellers placed symmetrically. The control of the device is achieved by changing the rotational speed of the motors, i.e. by making a difference in the torque load and the thrust/lift characteristics. Figure 6 shows the direction of rotation of the multicopter engines according to the number of engines (Erdoğan, 2016; Vuruşkan, 2014).

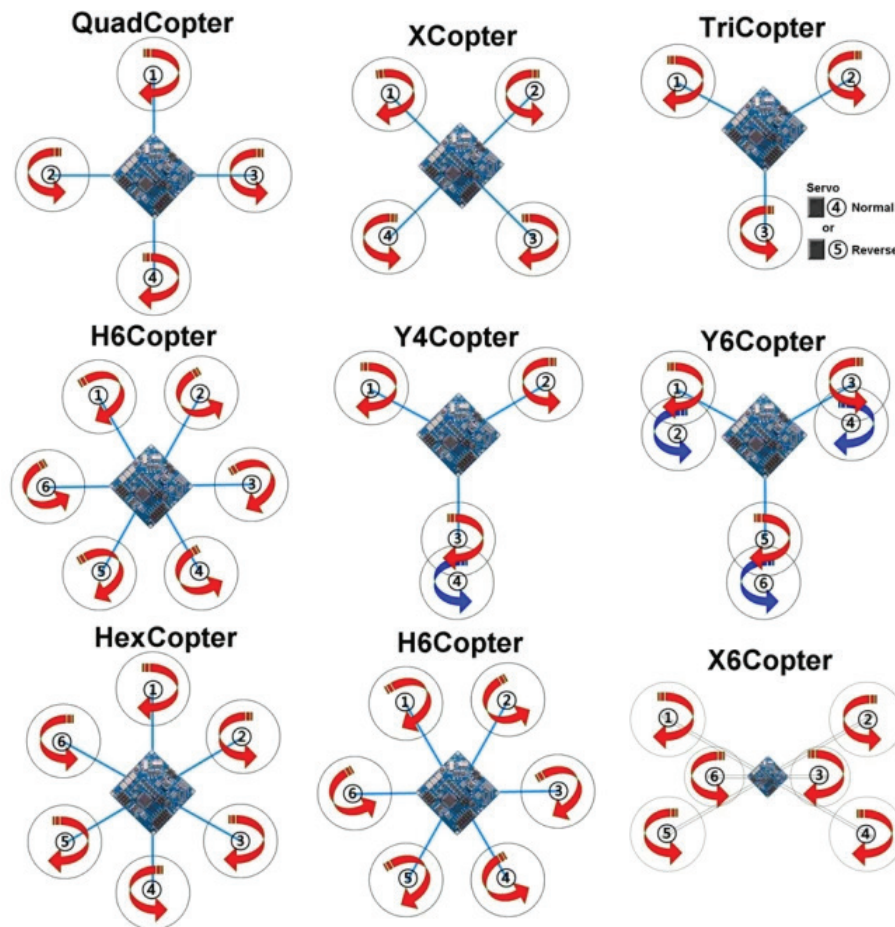


Figure 6: Direction of rotation of multicopter engines according to the number of engines ("Unmanned Engineeria Blog," 2016)

PROGRESSES IN TURKIYE

In our country, UAVs are used more in the military than in the civilian field. UAVs suitable for surveillance, reconnaissance, intelligence and attack situations are produced and used in our country, where there are many factors that endanger human life and extreme attention is required especially in enemy airspace.

It is expected that the size of the world drone systems market will in-

crease in the coming period, and it is predicted that more than half of the market will be created by the USA, followed by European and Asian countries. When examined in particular in Europe, it is observed that France plans to create the largest drone fleet in Europe, which can land/take off vertically, using human-portable, tactical and long-air launch systems.

In our country, Baykar Makine started to develop UAVs with long airborne and medium altitude technology in the 2000s. Bayraktar Mini UAV system, which started to be developed in 2005 with the joint work of Kalekalip-Baykar Makine, entered the tsk inventory as the first domestic UAV in 2007. In the following years, Bayraktar UAV became the first domestic UAV exported in the history of Turkey. Bayraktar TB2 UAV has 25,000 feet flight altitude, 27 hours and 3 minutes of airborne time. It's software can control the system fully automatic so that the UAV can land and departure regardless of ground systems. Also it has navigation features with internal sensor fusion without GPS dependence. Figure 7 shows the TB armed UAV produced by Baykar.



Figure 7: Bayraktar Unmanned Aerial Vehicle("Baykar,")

Various projects are carried out within the scope of micro UAV, mini UAV, tactical UAV projects by Vestel Savunma Sanayi A.Ş. in our country. With the agreement signed between Vestel Defense Industry and SSM, the design of the Karayel, which has 550 kg take-off weight and 150 km data link range, has been completed; flight tests have been carried out and its image is given in Figure 8.



Figure 8: Land Unmanned Aerial Vehicle (Kuzu, 2018)

UAV Related Legal Legislation

Detailed information about the legal legislation applied in the world and Turkey in the design and use of UAV is given below.

Situation in the United States

According to the American Federal Aviation Agency (FAA) Legislation, some important restrictions on the use of UAVs are as follows;

- a) Weight shall not exceed 25 kg,
- b) The pilot using the UAV will be in sight and this limit will not be crossed,
- c) The drone shall not be flown on any person who is not directly involved except those using the device,
- d) To be used only during daytime hours (between official sunrise and sunset hours),
- e) To give road rights to other planes with or without manned or unmanned aircraft,
- f) The maximum speed in the air shall not exceed 160 km/h (87 knots),
- g) The maximum height from the ground shall not exceed 152 meters,
- h) The maximum distance from the ground control station shall not exceed 5 km.

The following criteria are also required for the UAS Operator's Certificate.

- a) Must be at least 17 years old,
- b) The aeronautical test to be performed in an FAA approved test center should be successful and should be renewed every 24 months,
- c) It should be inspected by TSA (Transportation Security Administration),
- d) It should receive a “drone pilot certificate” in accordance with the small drone classification.
- e) In terms of the use of UAVs,
- f) UAV should be less than 25 kg,
- g) Direct vision between the pilot using the UAV and the UAV should always be maintained (VLOS; Visual line of sight),
- h) It should not be flown over people who are not related to the drone,
- i) Only daytime flights should be made,
- j) The maximum air speed should be 160 km/h,
- k) The maximum height from the ground should be 152 m,
- l) The minimum visibility distance from the control point should be 4.8 km,
- m) More than one UAV should not be flown at the same time,
- n) There should be no careless and incorrect use
- o) ATC (Air Traffic Control) permit must be obtained in B, C, D and E class airspaces.

Special rules have been established by the FAA for the use of the US Armed Forces, and according to these rules, military drone pilots are certified according to their military flight experience and by passing the military knowledge exam (Austin, 2010; Kahveci & Can, 2017; Valavanis, 2007).

Situation in the European Union

Legislation and processes in the European Union may differ on a country-by-country basis. In Germany, registration is required for every UAV weighing over 500 grams. There is an obligation to obtain a pilot license in the Netherlands, and in Spain, UAV Flight Schools have been authorized, and in France, “Type Certificate” has been introduced for all UAVs to be flown over the country’s airspace. Many studies have been carried out on this subject and the regulation has been put forward by EUROCONTROL by “UAV Passport (RPAS Passport/Remotely Piloted Aircraft Systems”.

Situation in Turkey

Issues related to UAVs in Turkey were regulated by the General Directorate of Civil Aviation. They were published Unmanned Aerial Vehicle Systems Instruction-(SHT-UAV) on April 22, 2016. However, the exceptional cases that are excluded from the scope of the instructions are given below:

- a) Drones used by Government,
- b) UAVs and systems used only in confined spaces,
- c) Unmanned balloons and similar systems connected to the ground or any platform,
- d) UAVs with a maximum takeoff weight of less than 500 grams.

In article 4 of SHT-UAV, Unmanned Aerial Vehicle System (İHAS) is defined as “UAV and control station, command and control data link, take-off and landing system”. In the same legislation, Unmanned Aerial Vehicle (UAV) is defined as “an aerial vehicle operated as a component of UAV, capable of flying continuously by means of aerodynamic forces, and remotely controlled by the UAV pilot without a pilot on it”. or autonomous operation can be planned or hovered by the UAV pilot”.

When the said Instruction is examined, the UAVs are handled in 4 different groups (UAV0, UAV1, UAV2, UAV3) with reference to the take-off weights. Accordingly, it is accepted that UAV0 (500 gr - 4 kg) and UAV1 (4 – 25 kg) category aircraft are produced for R&D studies and it is obligatory to register them in the internet-based “Registration System” created by the General Directorate. Import eligibility requirements for UAV0 and UAV1 class aircraft are also regulated in Article 6. According to article 8 of the instruction, no certificate or permit to fly certificate is required for aircraft of class UAV0. However, “Safety and Conformity Statement” is accepted, although no certificate is required for aircraft in UAV1 class. For UAV2 (25-150 kg) and UAV3 (150 kg and above) class aircraft, it is mandatory to obtain the documents mentioned above. In Section Three of the SHT-UAV Instruction, Items 16-16 include liability, insurance, registration, registration, flight operation manual and pilot licenses, and some important items are given below(Kahveci & Can, 2017):

- a) Operators/owners of all UAVs and systems are responsible for damages to third parties (Art.10).
- b) For UAVs carrying out commercial activities with UAVs over 25 kg regardless of their weight, insurance is taken out and uninsured flights are not made according to the Regulation on Third Party Financial Liability Insurance of Turkish and Foreign Civil

Aircrafts Flying in Turkish Airspace dated 15/11/2005 and numbered 25994 (Art.10).

- c) The records of the aircraft in the IHA0 and IHA1 categories will be made through the “Registration System” created electronically by the General Directorate (Art.11.)
- d) Registration process is not performed for UAVs in UAV0 and UAV1 class. The drones in the remote controlled UAV2 and UAV3 classes are registered in the aircraft registry by the General Directorate and a registration mark is assigned (Art.12).
- e) No license is issued by the General Directorate for persons who will fly UAV0 and UAV1.
- f) However, these persons are obliged to register by entering the following information and documents into the internet-based Registration System (Art. 14).

Turkish Identity Number, Name-Surname and residence information, Telephone, e-mail, etc. Contact information, Copy of Identity Card, Archive registered criminal record document for those over 18 years old, Letter of undertaking issued and certified by legal representatives stating that they accept future legal and criminal responsibilities for those under 18 years old

- g) UAV0 class pilots must be at least 12 years old and UAV1 class pilots must be at least 15 years old (Art. 14).
- h) Legal and criminal liability for damages caused by UAV pilots under the age of 18 to third parties belongs to the legal representative (Art. 14).
- i) The drone pilot is responsible for the safe conduct of the flight and the fulfillment of the administrative, financial and technical rules related to the flight (Art. 15)
- j) The drone pilot is responsible for the use of useful loads within the legal framework (Art. 15)
- k) In flights to be carried out for sportive and amateur purposes other than commercial activities, provided that the rules specified in the Instruction are complied with, it is not necessary to obtain a flight permit from the General Directorate except for the regions specified in Article 18. For these classes, it is forbidden to fly in places and times prohibited by the largest civil administration supervisor of the site (Art. 17a.
- l) In areas other than residential areas, crowded or very crowded

areas, there is no need to obtain a flight permit in case of commercial flights provided that the requirements specified in Articles 18 and 19 are complied with. 17b.

- m) In case of flying with UAVs in UAV0 and UAV1 class without NOTAM, in areas where flight is not prohibited and in places and times where it is not prohibited by the largest civil administration supervisor of the site (Art. 19
- 1- In cases where meteorological conditions are met only by sight, flights can be carried out between sunrise and sunset hours and at least 2 km of open air,
 - 2- The UAV shall be in the field of view of the pilot in a way that shall not exceed 500 meters horizontally,
 - 3- Do not exceed 400 feet (120 meters) above the ground (AGL),
 - 4- Flight must be carried out at least 50 meters away from people and structures.

REFERENCES

- Aktas, S., Thornton, S. C., Binns, C., & Denby, P. (2016). Gas phase synthesis of core-shell Fe@FeO x magnetic nanoparticles into fluids. *Journal of Nanoparticle Research*, 18(12). doi:10.1007/s11051-016-3659-8
- Amine Masmoudi, M., Mancini, S., Baldacci, R., & Kuo, Y.-H. (2022). Vehicle routing problems with drones equipped with multi-package payload compartments. *Transportation Research Part E: Logistics and Transportation Review*, 164, 102757. doi:10.1016/j.tre.2022.102757
- Austin, R. (2010). *Unmanned Aircraft Systems: UAVS Design, Development and Deployment*: Wiley.
- Baykar. Retrieved from <https://baykartech.com/tr/>
- Chmielewski, P., & Wróblewski, W. (2017). Selected issues of designing and testing of a HALE-class unmanned aircraft. *Journal of Marine Engineering & Technology*, 16(4), 365-376. doi:10.1080/20464177.2017.1376371
- Coruhlu, Y. E., Solgun, N., Baser, V., & Terzi, F. (2022). Revealing the solar energy potential by integration of GIS and AHP in order to compare decisions of the land use on the environmental plans. *Land Use Policy*, 113. doi:10.1016/j.landusepol.2021.105899
- Demirkıran, Z. (2010). Uçan Torpidodan Günümüze İnsansız Hava Araçlarının Gelişimi. *Bilim ve Teknik*, December.
- Ebeid, E., Skriver, M., & Jin, J. (2017, 30 Aug.-1 Sept. 2017). *A Survey on Open-Source Flight Control Platforms of Unmanned Aerial Vehicle*. Paper presented at the 2017 Euromicro Conference on Digital System Design (DSD).
- Erdoğan, A. (2016). *Strip Maps Production with Unmanned Aerial Vehicle*. Selçuk University,
- Express, A. (2022). New Uav Four-sided Obstacle Avoidance Four-axis Folding Aircraft Hd Camera Aerial Remote Control Aircraft Toy.
- Fotouhi, A., Qiang, H., Ding, M., Hassan, M., Giordano, L. G., Garcia-Rodriguez, A., & Yuan, J. (2019). Survey on UAV Cellular Communications: Practical Aspects, Standardization Advancements, Regulation, and Security Challenges. *IEEE Communications Surveys & Tutorials*, 21(4), 3417-3442. doi:10.1109/comst.2019.2906228
- Geraci, G., Garcia-Rodriguez, A., Galati Giordano, L., Lopez-Perez, D., & Bjornson, E. (2018). Understanding UAV Cellular Communications: From Existing Networks to Massive MIMO. *IEEE Access*, 6, 67853-67865. doi:10.1109/access.2018.2876700
- Guner, F., & Zenk, H. (2019). *Hydrokinetic Energy Conversion Systems in Turkey an Experimental Analysis*. Paper presented at the 2nd International Conference on Agriculture, Technology, Engineering and Sciences (ICATES 2019).

- Güner, F. (2020). Numerical Investigation of AISI 4140 Powder High Relative Density Compaction In Terms of Compaction Velocity. *Mechanics*, 26(1), 5-11. doi:10.5755/j01.mech.26.1.22862
- Güner, F., Başer, V., & Zenk, H. (2021). Evaluation of offshore wind power plant sustainability: a case study of Sinop/Gerze, Turkey. *International Journal of Global Warming*, 23(4). doi:10.1504/ijgw.2021.114342
- Güner, F., & Güney, M. Ş. (2018). Situation analyses of hazelnut sector, the necessity and classification of harvesting machines. *Turkish Journal of Agriculture - Food Science and Technology*, 6(9). doi:10.24925/turjaf.v6i9.1141-1147.1926
- Güner, F., & Sofuoğlu, H. (2018). Effects of Process Parameters on Copper Powder Compaction Process Using Multi-Particle Finite Element Method. *IOP Conference Series: Materials Science and Engineering*, 295. doi:10.1088/1757-899x/295/1/012027
- Güner, F., Sofuoğlu, H., & Cora, Ö. N. (2016, 18-20 July 2016). *Numerical investigation of coefficient of friction in copper powder compaction process at micro scale*. Paper presented at the 2016 7th International Conference on Mechanical and Aerospace Engineering (ICMAE).
- Hayat, S., Yanmaz, E., & Muzaffar, R. (2016). Survey on Unmanned Aerial Vehicle Networks for Civil Applications: A Communications Viewpoint. *IEEE Communications Surveys & Tutorials*, 18(4), 2624-2661. doi:10.1109/comst.2016.2560343
- Jiang, X., Sheng, M., Zhao, N., Xing, C., Lu, W., & Wang, X. (2022). Green UAV communications for 6G: A survey. *Chinese Journal of Aeronautics*, 35(9), 19-34. doi:10.1016/j.cja.2021.04.025
- Kahveci, M., & Can, N. (2017). İnsansız Hava Araçları: Tanımı, DÜnyada Ve TÜrkİye Dekİ Yasal Durumu. *Selcuk University Journal of Engineering ,Science and Technology*, 5(4), 511-535. doi:10.15317/Scitech.2017.109
- Kara, A. (2017). Excitation Function Calculations of Neutron-Induced Reactions of Some Zirconium Target Isotopes. *Journal of Fusion Energy*, 36(6), 230-233. doi:10.1007/s10894-017-0143-0
- Kuzu, F. (2018). *APPLICATION OF DIFFERENT CONTROL METHODS TO UNMANNED AERIAL VEHICLE QUADCOPTER*. Firat University,
- Li, B., Fei, Z., & Zhang, Y. (2019). UAV Communications for 5G and Beyond: Recent Advances and Future Trends. *IEEE Internet of Things Journal*, 6(2), 2241-2263. doi:10.1109/jiot.2018.2887086
- Lofü, D., Tedeschi, P., Di Noia, T., & Di Sciascio, E. J. a. p. a. (2022). URANUS: Radio Frequency Tracking, Classification and Identification of Unmanned Aircraft Vehicles.
- Mohsan, S. A. H., Khan, M. A., Noor, F., Ullah, I., & Alsharif, M. H. (2022). To-

- wards the Unmanned Aerial Vehicles (UAVs): A Comprehensive Review. *Drones*, 6(6). doi:10.3390/drones6060147
- PG Fahlstrom, T. G., MH Sadraey. (2012). *Introduction to UAV systems*: John Wiley&Sons.
- Sadeler, R., & Atasoy, S. (2011). Fretting fatigue behaviour of hard anodizing coated 2014-T6 aluminium alloy with dissimilar mating materials under plane bending loading. *Fatigue & Fracture of Engineering Materials & Structures*, 34(6), 383-388. doi:10.1111/j.1460-2695.2010.01527.x
- Sadeler, R., & Atasoy, S. (2016). The effect of contact pad hardness on the fretting fatigue behaviour of AZ61 magnesium alloy. *Fatigue & Fracture of Engineering Materials & Structures*, 39(4), 502-510. doi:10.1111/ffe.12387
- Sami Oubbati, O., Atiquzzaman, M., Ahamed Ahanger, T., & Ibrahim, A. (2020). Softwarization of UAV Networks: A Survey of Applications and Future Trends. *IEEE Access*, 8, 98073-98125. doi:10.1109/access.2020.2994494
- Sanchez-Aguero, V., Valera, F., Vidal, I., Nogales, B., Cabezas, J., & Vidal, C. (2022, 2-5 May 2022). *A virtualization approach to validate services and subsystems of a MALE UAS*. Paper presented at the IEEE INFOCOM 2022 - IEEE Conference on Computer Communications Workshops (INFOCOM WKSHPs).
- Savaşkan, T., Tan, H. O., & Maleki, R. A. (2015). Effects of contact pressure and sliding distance on the lubricated friction and wear properties of Zn-25Al-3Cu alloy: A comparative study with SAE 65 bronze. *International Journal of Materials Research*, 106(10), 1060-1066. doi:10.3139/146.111282
- Skorobogatov, G., Barrado, C., & Salamí, E. (2020). Multiple UAV Systems: A Survey. *Unmanned Systems*, 08(02), 149-169. doi:10.1142/s2301385020500090
- Song, Q., Zeng, Y., Xu, J., & Jin, S. (2021). A survey of prototype and experiment for UAV communications. *Science China Information Sciences*, 64(4). doi:10.1007/s11432-020-3030-2
- Srivastava, S., Narayan, S., & Mittal, S. (2021). A survey of deep learning techniques for vehicle detection from UAV images. *Journal of Systems Architecture*, 117, 102152. doi:10.1016/j.sysarc.2021.102152
- Tan, H. O., & Savaşkan, T. (2020). Determination of Dry Wear Properties of Zn-30Al-Cu Bearing Alloys in Terms of Their Copper Content and Working Conditions Including Pressure and Sliding Velocity. *Journal of Materials Engineering and Performance*, 29(7), 4794-4803. doi:10.1007/s11665-020-04976-7
- Ullah, Z., Al-Turjman, F., & Mostarda, L. (2020). Cognition in UAV-Aided 5G and Beyond Communications: A Survey. *IEEE Transactions on Cognitive Communications and Networking*, 6(3), 872-891. doi:10.1109/tccn.2020.2968311
- Unmanned Engineeria Blog. (2016). Retrieved from <https://unmannedengi->

neerialog.wordpress.com/2016/01/05/tricopter-vs-quadcopter-efficiency-flight-time-and-more/

Valavanis, K. P. (2007). *Advances in Unmanned Aerial Vehicles*: Springer Dordrecht.

Vuruşkan, A. (2014). *The Aerodynamic Desing, Modelling and Analysis of Turac Unmanned Air Vehicle*. Istanbul Technical University,

Watts, A. C., Ambrosia, V. G., & Hinkley, E. A. (2012). Unmanned Aircraft Systems in Remote Sensing and Scientific Research: Classification and Considerations of Use. 4(6), 1671-1692.

Yiğit, E., Yazar, I., & Karakoç, T. H. (2018). İnsansız Hava Araçları (İHA) ‘ Nın Kapsamlı Sınıflandırması Ve Gelecek Perspektifi. *Sürdürülebilir Havacılık Araştırmaları Dergisi*, 3(1), 10-19. doi:10.23890/suhad.2018.0102

Zenk, H., Kara, A., Güney, M., Güner, F., & Zenk, O. (2018). *PMDC Motor Speed Control With Fuzzy Logic Controlled Zeta Converter*. Paper presented at the 4rd International Conference on Engineering and Natural Sciences (ICENS 2018).

Zenk, H., Şenol, H., & Güner, F. (2019). Lunar Excursion Module Landing Control System Design with P, PI and PID Controllers. *Karadeniz Fen Bilimleri Dergisi*, 9(2), 390-405. doi:10.31466/kfbd.647211

Zhang, L., Zhao, H., Hou, S., Zhao, Z., Xu, H., Wu, X., . . . Zhang, R. (2019). A Survey on 5G Millimeter Wave Communications for UAV-Assisted Wireless Networks. *IEEE Access*, 7, 117460-117504. doi:10.1109/access.2019.2929241

Zhi, Y., Fu, Z., Sun, X., & Yu, J. (2019). Security and Privacy Issues of UAV: A Survey. *Mobile Networks and Applications*, 25(1), 95-101. doi:10.1007/s11036-018-1193-x



CHAPTER 12

EVALUATION OF THE EFFECT OF TRAIN-TEST SPLIT RATIO FOR THE PREDICTION OF DAILY PAN EVAPORATION OF ÇORUM PROVINCE

Okan Mert KATİPOĞLU¹

¹ Erzincan Binali Yıldırım University, Faculty of Engineering and Architecture,
Department of Civil Engineering, Erzincan, Türkiye. okatipoglu@erzincan.
edu.tr, orcid.org/0000-0001-6421-6087

1. INTRODUCTION

Accurate estimation of evaporation height in arid regions is critical for water resources management, agricultural productivity, water structure planning and irrigation planning (Al-Mukhtar 2021). Therefore, it is necessary to determine the method that most reliably estimates the evaporation values. Evaporation, one of the most critical parameters of the hydrological cycle, depends on many meteorological parameters such as solar radiation, air vapor pressure, temperature, pressure, and wind. It is, therefore, a complex and challenging task to measure and calculate. Thanks to the developing artificial intelligence (AI) technologies, evaporation data with a nonlinear relationship can be easily calculated. Evaporation data can be predicted effectively through AI models that reveal the relationship between input and output based on the black box principle. In this study, the data of the neighboring Çankırı meteorological station were used to estimate the daily evaporation in Çorum.

With the development of AI technology, the prediction of meteorological variables has become easier and more reliable. The estimation of evaporation data with AI techniques has attracted the attention of many researchers. Shiri et al. (2011) evaluated the ANFIS and ANN methods for estimating daily meteorological parameters and evaporation values. The results showed that the ANFIS model was superior. Allawi and El-Shafie (2016) estimated the daily evaporation using Radial Basis Function Neural Network and ANFIS methods in the Layang reservoir located in the southeastern part of Malaysia. As a result, the RBF-NN technique most successfully predicted the daily evaporation rate. Tezel and Buyukyildiz (2016) used ANN, SVM, and empirical models (Romanenko and Meyer methods) to predict evaporation in the Beysehir meteorology station. It has been determined that ANN is superior to support vector machine (SVM) and empirical methods. Ayşe and Büyükyıldız (2019) evaluated the accuracy of SVM, ANN and ANFIS models for the estimation of monthly evaporation data at the Karaman meteorological station located in Konya closed basin. The analysis results indicated that the SVM algorithm was superior. Al-Mukhtar (2021) used random forest (RF), regression forest (REF), ANN, linear regression (LR), and SVM for predicting evaporation data in Iraq. The training test rate was chosen as 75-25% in the model setup. As a result, it was determined that regression forest models were superior to other models in semi-arid and arid climates. Gümüş et al. (2021) was estimated the monthly pan evaporation measured at Adıyaman and Diyarbakır stations using input combinations of various meteorological parameters and ANN, ANFIS and Expression Programming (GEP) methods. The established model is divided into 70% training and 30% testing. It has been suggested that the GEP method is more useful for practitioners. Ghumman et al. (2021) estimated evaporation values

using Penman and Hamon, ANN and ANFIS methods. It has been determined that the most effective input in evaporation estimation is the average temperature. In addition, ANFIS

simulation results outperformed other techniques. Al Sudani and Salem (2022) applied extreme learning machine (ELM), gradient boosting machine (GBM), quantitative random forest (QRF) and Gaussian process regression (GPR) models to model the monthly evaporation loss at two stations in Iraq. GBM algorithm showed the best performance of monthly evaporation rate. When the studies in the literature are examined, it is seen that studies on the estimation of evaporation values using various meteorological parameters are concentrated. However, it is noteworthy that studies on evaporation estimation with data from neighboring stations and the effect of different training test rates on evaporation estimation are lacking.

This study aims to estimate the evaporation data in the Çorum station. For this purpose, the effect of the training-test ratio on machine learning model performance was evaluated using daily evaporation data from the Çankırı meteorology station. Moreover, Random Forest and GBM algorithms were used to model pan evaporation. The study's second aim is to investigate the training test rate's effect on pan evaporation prediction. For this purpose, the training test rates were used as 90-10%, 80-20%, 70-30%, 60-40%, and 50-50%.

2. MATERIAL AND METHOD

In this study, daily evaporation data of Çankırı numbered 17080 and Çorum meteorological observation stations, numbered 17084, covering the years 1974-2015 were used. Evaporation data were obtained from the State Meteorology General Directorate. Figure 1 shows the geographical coordinates of the stations used in the evaporation estimation shown on the hydrography map.

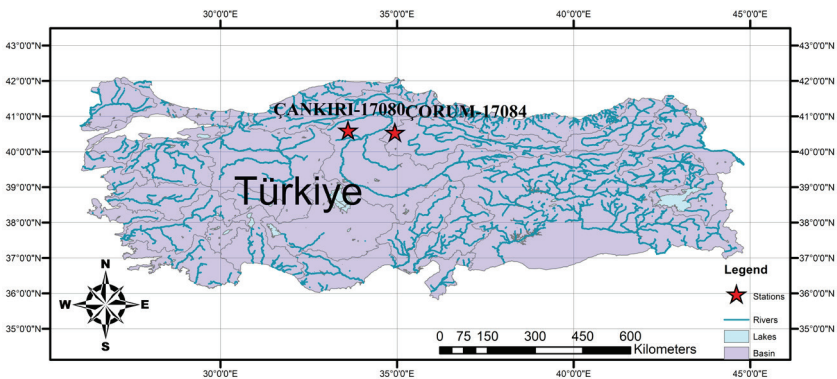


Figure 1. *Geographical locations of the stations used*

Table 1 presents various topographic information on meteorology observation stations from which evaporation data were obtained. Since the locations of the stations are close to each other, they can be used in evaporation estimation.

Table 1. Topographic features of meteorology observation stations

Station No	City	Latitude	Longitude	Altitude
17084	Çorum	40.5461	34.9362	776
17080	Çankırı	40.6082	33.6102	755

The temporal variation graphs of daily pan evaporation data are shown in Figure 2. Accordingly, it is seen that the data overlap with each other. In this respect, it is foreseen that evaporation estimation can be made by establishing the artificial intelligence model.

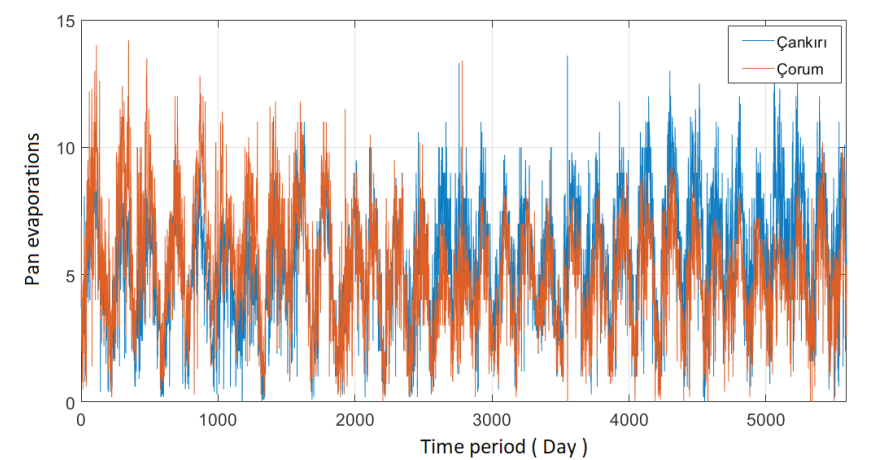


Figure 2. Variation of used daily pan evaporation data with time

In Figure 3, a correlation matrix was created to determine the direction and strength of the relationship between the daily pan evaporation data. Accordingly, there is a positive relationship between meteorology stations at Çankırı and Çorum stations. In addition, in the scattering diagrams of the pan evaporation data, it is seen that the data are distributed around the linear line. Therefore, it can be said that there is a moderate relationship between the data.

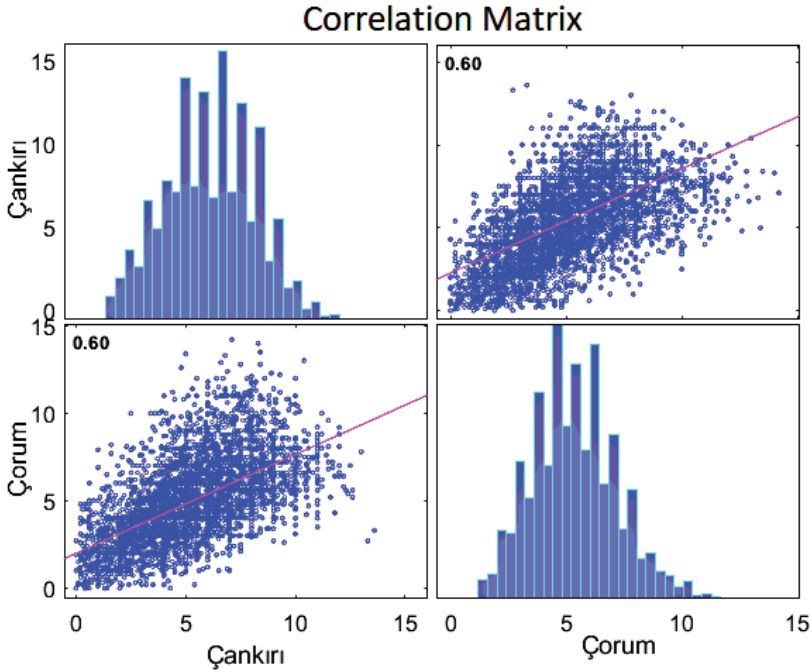


Figure 3. *Correlation matrix of daily pan evaporation data*

2.1. Gradient boosting machine (GBM)

Although decision tree (DT) is a faster technique, GBM is an advanced algorithm that resolves instability in a decision tree. GBM combines the advantages of DT and boosting algorithms. GBM takes advantage of a group of weak learners to develop a strong learner. GBM basically uses the formulation of the gradient descent of the boost technique. In addition, the GBM algorithm can be used to effectively solve classification and regression problems (Al Sudani and Salem 2022; Naganna et al. 2020; Xenochristou et al. 2020).

2.2. Random Forest (RF)

Decision trees (DT) aim to minimize the error of variance. However, there is a possibility of overfitting DTs and local minimum problems occur. RF examines the error due to both variance and bias. RF is the collection of decision trees that limit overfitting to avoid the bias-induced error. RF reduces variance-based error as it trains by dividing random data into subsets. Each data subset creates a separate tree (Agrawal et al. 2022). RF refers to the number of trees used and at the node of a tree by defining the total features used as a basis. This study used the RF technique to estimate the daily evaporation data from neighboring stations.

2.3. Model performance

2.3.1. Statistical criteria

Mean square error (RMSE), coefficient of determination (R^2) and mean absolute error (MAE) statistical indicators were used to evaluate the performance of the applied soft computing techniques. The analyzes were interpreted as optimum RMSE and MAE values of 0 and R^2 values of 1. The formulas for the calculated indicators are given below:

$$RMSE = \sqrt{\frac{\sum_{i=1}^N (A_i - P_i)^2}{N}} \quad (1)$$

$$R^2 = \frac{(\sum_{i=1}^N (A_i - \bar{A})(P_i - \bar{P}))^2}{\sum_{i=1}^N (A_i - \bar{A})^2 \sum_{i=1}^N (P_i - \bar{P})^2} \quad (2)$$

$$MAE = \frac{1}{n} \sum_{i=1}^n |A_i - P_i| \quad (3)$$

where, A_i is the observed i^{th} value, P_i is the predicted i^{th} value, \bar{A} is the average observed value, \bar{P} is the average predicted value and N is the number of the data sample.

2.3.2. Rank Analysis

Rank Analysis is a technique used to reveal the performances of various artificial intelligence techniques used effectively. First, sequencing analysis is applied separately for two training and test datasets. Then, in this analysis, each statistical indicator is numbered according to its suitability. This numbering is based on the number of models used. Finally, the total order values of the numbered models are determined, and the best model is decided (Zhang et al. 2020).

3. Results

In this study, artificial intelligence algorithms such as Random Forest and GBM were used to predict daily evaporation data at the Çorum meteorological observation station numbered 17084. In the study, it was investigated how the success of evaporation estimation would change when various training-test ratios were used. While the daily evaporation data of the Çankırı station was used as input in the setup of the model, the evaporation data from the Çorum station was used as the output. In this direction, the models' performances were tested according to statistical criteria by using ratios of 90-10%, 80-20%, 70-30%, 60-40%, 50-50%. Furthermore, 5-fold

cross-validation was used to eliminate the overfitting problem in artificial intelligence models. For the setup of the model, the daily evaporation data of Çankırı, which is adjacent to the Çorum meteorological station and shows a very high correlation, was used. In addition, gaussian distribution, 5000 trees, shrinkage ratio = 0.01, interaction.depth = 1 in training the GBM model. In the Random Forest model setup, the mtry values were tested as 2,3,4,5,10 and the most suitable RF was determined.

Table 2 shows the data rates used in the training and testing of artificial intelligence (AI) models. The performance of the AI models was evaluated by dividing the evaporation time series at various rates.

Table 2. Training test rates used in the study

	Train ratio (data number)	Test ratio (data number)
Model 1	90% (5029)	10% (559)
Model 2	80% (4470)	20% (1118)
Model 3	70% (3911)	30% (1677)
Model 4	60% (3353)	40% (2235)
Model 5	50% (2794)	50% (2794)

Figure 4 shows the variation of squared error loss values and the number of iterations. According to these values, the optimum iterations of the network were determined.

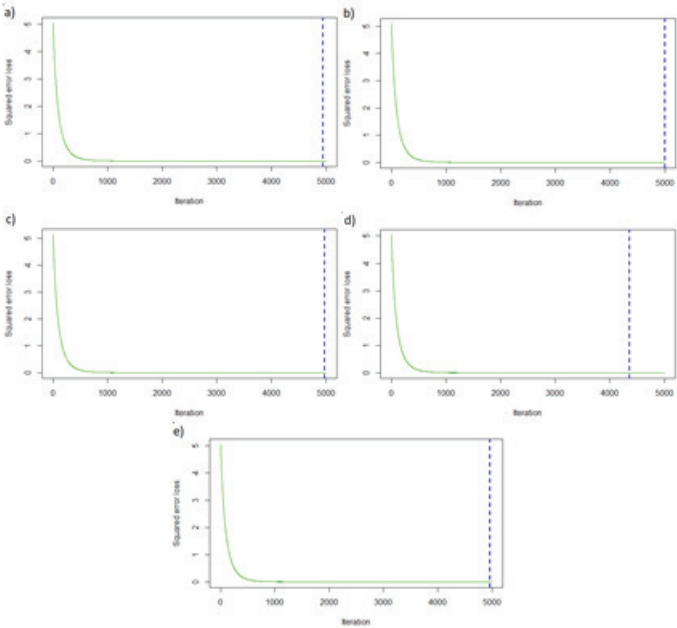


Figure 4. Training error variation of the GMB models: a) Model 1, b) Model 2, c) Model 3, d) Model 4, e) Model 5

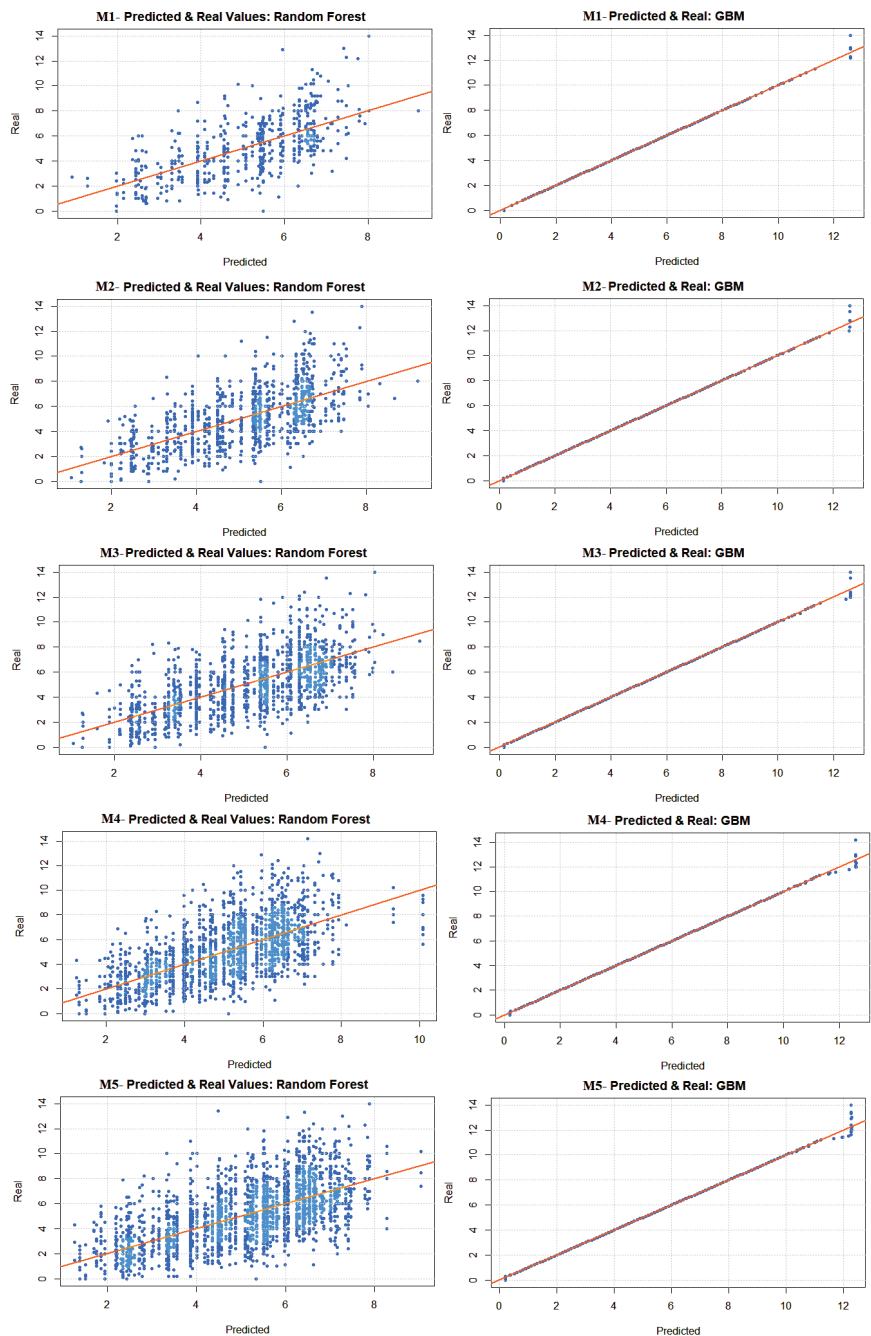


Figure 5. Scatter diagrams of test results of RF and GBM models

The scatter plots of the RF and GBM models are shown in Figure 5. These graphs show the relationship between predicted and actual data.

Scatter diagrams interpret the relationship between actual and target values according to the regression line. The data distribution closest to the regression line shows the most appropriate model. Accordingly, Model 3 (70-30%) was the most suitable data division among RF models, while Model 4 (60-40%) was the best GBM model.

Table 3. Test results of GBM and RF models

	RF			Total Rank
	RMSE	MAE	R ²	
Model 1	1.771	1.408	0.423	11
Rank	3	3	5	
Model 2	1.764	1.406	0.398	11
Rank	4	4	3	
Model 3	1.734	1.371	0.400	14
Rank	5	5	4	
Model 4	1.791	1.411	0.387	6
Rank	2	2	2	
Model 5	1.817	1.422	0.364	3
Rank	1	1	1	
	GBM			Total Rank
	RMSE	MAE	R ²	
Model 1	0.122	0.0437	0.9982	3
Rank	1	1	1	
Model 2	0.105	0.040	0.9986	6
Rank	2	2	2	
Model 3	0.089	0.038	0.9990	12
Rank	4	4	4	
Model 4*	0.085	0.038	0.9992	13
Rank	5	3	5	
Model 5	0.093	0.037	0.9989	11
Rank	3	5	3	

*Indicates the best model.

Model performances according to various data division values of GBM and RF models are shown in Table 4. The performances of the models were evaluated according to various statistical tests. When Table 4 is examined, the highest rank value among the RF models is available in the Model 4 combination. Among the GBM models, the Model 4 structure was determined as the most suitable model. When all models' error rates and R² values were examined, it was determined that the most suitable model was the GBM model, which was established by separating the data as 60% training and 40% testing.

4. Conclusion

This study analyzed the effect of data division on the daily pan evaporation data. RF and GBM algorithms have been established at various training test rates. Model performances were tested according to graphical and statistical indicators. The main results of the study are summarized as follows:

- It is recommended to use 60% training and 40% testing rates to estimate daily evaporation using 5588 data.
- It has been found that the GBM algorithm is ideal for estimating missing evaporation data and extending evaporation time series records.
- The study outputs will help managers, planners and decision-makers in the sustainability management of natural water resources, irrigation, and reservoir planning.
- Optimizing the model parameters with various bio-inspired algorithms is recommended for future studies and evaluating the results by separating the inputs with different signal processing techniques.

In addition, it is necessary to test the algorithms used by making evaporation estimates for different periods and data set lengths.

Acknowledgments The author thanks the general directorate of meteorology for the daily pan evaporation data provided and the Editor for their contributions to the content and development of this paper.

References

- Agrawal, Y., Kumar, M., Ananthakrishnan, S., & Kumarapuram, G. (2022). Evapotranspiration modeling using different tree based ensembled machine learning algorithm. *Water Resources Management*, 36, 1025-1042.
- Al-Mukhtar, M. (2021). Modeling the monthly pan evaporation rates using artificial intelligence methods: a case study in Iraq. *Environmental Earth Sciences*, 80, 1-14.
- Al Sudani, Z. A., Salem, G. S. A. (2022). Evaporation rate prediction using advanced machine learning models: A comparative study. *Advances in Meteorology*, 2022.
- Allawi, M. F., El-Shafie, A. (2016). Utilizing RBF-NN and ANFIS methods for multi-lead ahead prediction model of evaporation from reservoir. *Water Resources Management*, 30, 4773-4788.
- Ayşe, Ö., & Büyükyıldız, M. (2019). Usability of artificial intelligence methods for estimation of monthly evaporation. *Omer Halisdemir University Journal of Engineering Science*, 8, 244-254.
- Ghumman, A.R., Jamaan, M., Ahmad, A., Shafiquzzaman, M., Haider, H., Al Salamah, I. S., & Ghazaw, Y. M. (2021). Simulation of pan-evaporation using Penman and Hamon equations and artificial intelligence techniques. *Water*, 13, 793.
- Gümüş, V., Yeşiltaş, Y., Şimşek, O. (2021). Estimation of monthly pan evaporation of adıyaman and diyarbakır stations with artificial intelligence methods. *Turkish Journal of Nature and Science*. 10, 112-122.
- Naganna, S. R., Beyaztas, B. H., Bokde, N., & Armanuos, A. M. (2020). On the evaluation of the gradient tree boosting model for groundwater level forecasting Knowledge-Based. *Engineering and Sciences*. 1, 48-57.
- Shiri, J., Dierickx, W., Pour-Ali Baba, A., Neamati, S., & Ghorbani, M. (2011). Estimating daily pan evaporation from climatic data of the State of Illinois, USA using adaptive neuro-fuzzy inference system (ANFIS) and artificial neural network (ANN). *Hydrology Research*, 42, 491-502
- Tezel, G., & Buyukyildiz, M. (2016). Monthly evaporation forecasting using artificial neural networks and support vector machines. *Theoretical and applied climatology*, 124, 69-80.
- Xenochristou, M., Hutton, C., Hofman, J., & Kapelan, Z. (2020). Water demand forecasting accuracy and influencing factors at different spatial scales using a gradient boosting machine. *Water Resources Research*, 56:e2019WR026304
- Zhang, H., Zhou, J., Jahed Armaghani, D., Tahir, M., Pham, B., & Huynh, V.

(2020). A combination of feature selection and random forest techniques to solve a problem related to blast-induced ground vibration. *Appl. Sci.*, 10(3), 869.



CHAPTER 13

AN OVERVIEW ON CHARACTERISTICS OF CERAMIC MATERIALS USED IN SEVERAL APPLICATIONS AND RECENT TRENDS

Fatma İrem ŞAHİN¹, Nil ACARALP²

1 Yildiz Technical University, Department of Chemical Engineering,
Davutpasa Campus, 34220, Esenler-Istanbul, Turkey.

2 Yildiz Technical University, Department of Chemical Engineering,
Davutpasa Campus, 34220, Esenler-Istanbul, Turkey. nilbaran@gmail.com

1. INTRODUCTION

Ceramics could be defined as science technology and art for the manufacture of inorganic compounds obtained by shaping, glazing and firing, consisting of clay, kaolin feldspar and quartz type raw materials consisting of one or more metals and non-metals [1]. Ceramics were also known as component of between metallic and non-metallic elements. The materials were mostly oxide, nitride, and carbide. For instance, common ceramic materials were aluminium oxide, silica, silicon nitride, silicon carbide etc. Ceramics were also brittle behaviours and susceptible to fracture. Ceramic materials were more resistant to high temperatures in terms of thermal and electrical conductivity. The ceramic industry generally consisted of clay bricks used in buildings, sewage and water pipes, glazed tiles used in floor and wall cladding, vessels, and refractory materials. The ceramics industry was the cornerstone of many other industries. Therefore, it was important in terms of materials science. This industry used between 70 and 75% of the clay minerals produced worldwide. It was a product that did not harm the environment because it was obtained naturally. It had properties such as resistance to high temperatures, low toughness, and ductility. It showed electrical and thermal insulation. Abundant raw material resources and reducing the need for expensive and strategic metals were among the reasons why it was preferred. Due to the pores in its structure, its tensile strength was low while its compressive strength was high [2-4].

Ceramic was derived from the Latin “keramikos/kermos,” which meant as clay, dirt, or baked goods. Ceramics could be described as inorganic compounds created by the combining and sintering of one or more metals with non-metallic elements in the broadest meaning. Ceramic materials’ characteristics were influenced by the number and distribution of these components in the ceramic structure. An insulating ceramic material could be made conductive by modifying the arrangement of the phases contained in the structure. The first pottery was made in Anatolia approximately 6000 BC according to legend. In Çatalhöyük, the earliest pottery artifacts were discovered. In 6000 BC, the first pottery-type earthenware was discovered in Anatolia. After 3900 BC, the first glazed earthenware was discovered in Egypt. After this date, most civilizations began to use ceramic varieties. The first ceramics factories were built in Germany, and the first porcelain factories were established in Sevr city, France, then Petersburg, Copenhagen, and England in 1770 and 1794, respectively. Ceramics and ceramic variants began to be utilized all over the world. Ceramic raw materials were also abundant in Turkey. Top quality sodium feldspar deposited in Çine, Milas, Bozdoğan. The largest producers were China, India, Brazil, Vietnam, and Spain. UK, Germany, Northern Europe, and The United States developed the usage areas of ceramics. With the rapid

development of the construction industry in the world, usage areas also increased to the same extent. The ceramic industry was rapidly growing especially in developed countries has grown. A significant volume in consumption and production was achieved since the 1960s. After the 1980s, in addition to developed European countries and the United States, developing countries also started their own ceramic industries. While Italy stood out with its design, quality and branding, Spain stood out with its technology-oriented production. Later, traditional ceramics of China and Brazil came to the fore in its products [2], [4-6].

2. CERAMICS

Ceramics was the most comprehensive name of tile, pottery, porcelain, stoneware, glass, brick, tile, sanitary ware, refractory, advanced technology nano technological glass-ceramic formed as solid compounds composed of at least two elements formed under heat and pressure. It was possible to include all non-metallic and organic materials within the scope of ceramics. Especially metal oxide and silicate minerals, which were abundant in nature, artificially produced carbides, nitrides, borides, glasses, glass ceramics and cement-type materials were in the ceramic category [7]. The general classification of ceramic materials was shown in Figure 1.

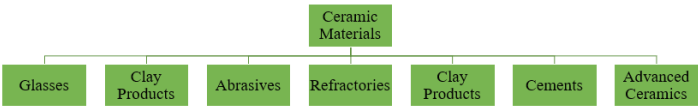


Figure 1. General classification of ceramic materials [8]

Most ceramic materials mixed bond structures in varying proportions between ionic and covalent bonds. Ceramics existed as crystalline and non-crystalline compounds. Glass materials were not crystalline and differ from ceramics in this respect. Elemental materials such as carbon and boron could also be among the ceramics. They were generally found in compound form. The most used and important ceramic materials were given in Table 1 [9].

Table 1. Some significant ceramic materials [9]

Single Oxides	Alumina (Al_2O_3)
	Zirconia (ZrO_2)
	Titania (TiO_2)
	Silica (SiO_2)
	Magnesium Oxide (MgO)
Mixed Oxides	Mullite ($3\text{Al}_2\text{O}_3 \cdot 2\text{SiO}_2$)
	Spinel ($\text{MgO} \cdot \text{Al}_2\text{O}_3$)
Elemental	Carbon (C)
	Boron (B)
Carbides	Silicon Carbide (SiC)
	Boron Carbide (B_4C)
	Titanium Carbide (TiC)
Nitrides	Boron Nitride (BN)
	Silicon Nitride (Si_3N_4)

Ceramics had many specific features. Some of these features were being light, having good mechanical and thermomechanical behaviors, being resistant to corrosion. The general properties of ceramics could be examined under three main headings. These were physical, mechanical, and chemical properties. Most industrial ceramics were composed of metals or semi-metal compounds of carbon, oxygen and nitrogen. Therefore, ceramics had a lower density than most metals. As a result, a light ceramic piece could be as durable as a heavy metal piece. Atomic weight, packing behavior of atoms and pore amount in microstructure were factors affecting density. If the material had a porous structure like ceramic and the crystallographic density calculation was insufficient, it was possible that there was an inverse proportion between pore volume and mass density. The type of bonding as covalent or ionic and the amount of bonds determined the thermal characteristics of ceramics. The resistance of ceramics to temperature changes was even better than many metals, but high and sudden temperature changes could weaken ceramics. Ceramics resisted corrosion more than plastics and metals. They generally did not react with gases, liquids, alkalis, and acids. Many ceramics had very high melting points and some ceramics used at temperatures very close to their melting points. The melting temperature of a ceramic with an increasing covalent bond character and a multivalent ionic bond structure was higher. Ceramic materials as fragile materials underwent non-homogeneous dimensional changes due to thermal shock and tensions. In solid materials, heat was carried by with free electrons, but non-metallic materials such as ceramics were thermal insulators because they did not have enough free electrons. Glass and other amorphous ceramics exhibited greater photon scattering than

crystalline ceramics because their atomic structures were more irregular. As a result, they had lower conductivity. Thermal conductivity declined with temperature in most ceramics, notably in the low temperature zone. Conductivity of electricity ceramics were insulating and dielectric materials in common. They responded in the electric field rather than conducting electricity. A remarkable number of electrons were stored on their surfaces because to the polarization generated by the electric field effect. Capacitors were made from ceramics with excellent dielectric characteristics. Semiconductor properties could be found in some ceramics. The mechanical effect was converted into an electrical response, and the electrical reaction was converted back into a mechanical response with quartz crystal and barium titanate. Mechanical destruction of ceramic materials was usually due to structural defects. Among the main defect sources seen in polycrystalline types; surface treatments surface cracks, voids, residues and during production large grains could be counted. Magnetic ceramics were used in electronic circuits and electric motors. In the electronics industry, ceramics with this piezoelectric property were utilized. As the refractive index grows, ceramic glasses appeared brighter. All the rays inclined to the ceramic glass were not broken, some were reflected. The angle of incidence and reflection were equal. When the porosities contained in the ceramic were destroyed, transparency occurred [3, 9-12]. Some important ceramic materials properties were shown in Figure 2.

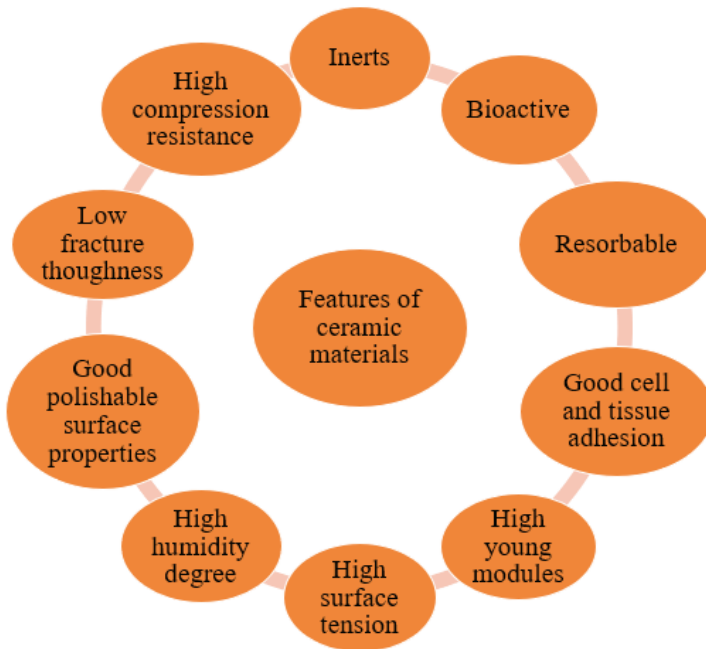


Figure 2. Ceramic Materials Properties [11, 12]

3. TRADITIONAL AND ADVANCED CERAMICS

Traditional ceramics were divided into 3 groups as coarse, fine and technical ceramics according to the purpose of construction. Ceramics whose main mass coloured were called coarse ceramics. For example, construction bricks, tiles, fire bricks, pottery products fell into this group. Products with a white mass were called fine ceramics. For instance, tiles, ceramic tiles, porcelain ware, ceramic sanitary ware, electro-porcelain, and tile making were included in this group. Products developed for use in more techniques, whose mass could be coloured or white, were technical ceramics [13].

Traditional ceramics were obtained by firing the raw materials containing metal oxides at high temperatures after mixing them in certain proportions. It consisted of inorganic materials such as clay, kaolin, feldspar, quartz, calcite, and dolomite. The materials were also mixed and shaped in certain proportions. It had a wide range from household building materials to electrical appliances, from biology, chemical industry to machinery industry [14]. In traditional ceramics, clay and silica were the most popular materials used in traditional pottery. Traditional ceramics had a non-uniform, coarse, and multiphase microstructure. Processing had grown more efficient and cost effective because of increased competition among producers. Machines were commonly utilized and could be linked to computer-assisted process control. Traditional ceramics included brick, tile, porcelain, pottery, tile, refractories, glass, cement, and electrical insulation materials. It was made using all-natural ingredients. [15]. Classification of traditional ceramics was shown in Figure 3.

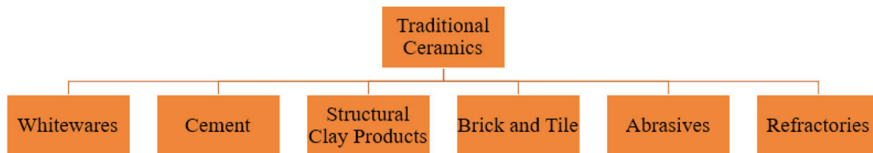


Figure 3. Traditional Ceramics [16]

Advanced ceramics had greater purity values and a more controlled composition. Modern ceramics, engineering ceramics, technical ceramics, and high-tech ceramics were some of the terms used to describe them. Advanced ceramic raw materials were usually created artificially or by purifying natural raw materials. Nitrides, carbides, oxides, sulphides, borides, and silicates were all used in modern ceramics. The difference in the degree of electronegativity of the elements in their composition determined the ratio of their ionic and covalent bonds. Ceramics' flexible modules and hardness were higher than metals due to the ionic and covalent link between the atoms that made up the material. The most essential distinction between engineering ceramics and traditional ceramics was

that engineering ceramics had only one or two phases, whereas traditional ceramics had numerous [3, 12]. Classification of advanced ceramics was shown in Figure 4.

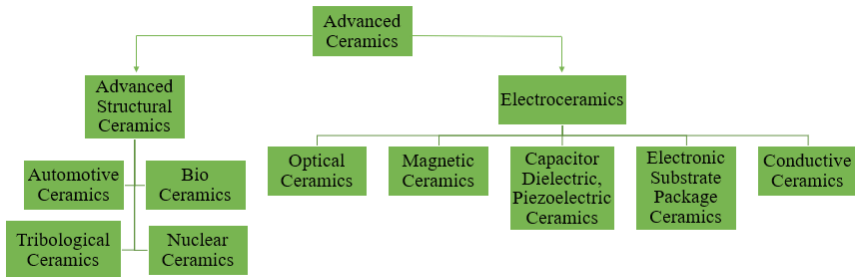


Figure 4. Advanced Ceramics [16]

Advanced ceramic materials had physical and chemical properties that chemical reactions were not easy to carry out. It was more suitable for abrasion and high temperature applications. Besides, it started to be applied in new areas due to its high hardness, high strength, low thermal conductivity and biocompatibility, chemical stability, and abrasion resistance. Ceramic materials became increasingly popular in aerospace and biomedicine [17].

4. FABRICATION OF CERAMICS

The raw materials were divided into three separate groups. Clay, enabled the ceramic material to turn into a permanent structure with its plastic feature. It was used to keep the quartz plastic structure, which had no plasticity, at the desired level. Feldspars played a role in the formation of the crystal structure due to their low melting temperature. The most important of these groups was the clay group. For this reason, areas close to clay reserves were preferred in the establishment of ceramic enterprises. In addition, the raw material properties and supply types to be used differ according to the type of product to be produced, and synthetic raw materials could also be used apart from natural raw materials. Clays were natural, soil-like, fine-grained and water-like clays with a definite crystal structure. Quartz (SiO_2) was a purely material consisting of only silicon and oxygen, but natural quartz was found together with one or more of the aluminium, titanium, lithium, sodium, and magnesium elements that cause impurities. Its non-plastic structure allowed the plasticity from clay to be regulated. It prevented volume reduction during the baking process and reduced the gas generated during the process and helped to move away from the ceramic body. Quartz sand, quartzite, siliceous flint and diatomite types were preferred as quartz in the ceramic industry. Feldspar ($x\text{Al}_2\text{O}_3 \cdot y\text{SiO}_2$) was a material that was the main source of clay group raw materials and the

alkalis in its structure had a low melting temperature. It was a hard material and orthoclase ($K_2O \cdot Al_2O_3 \cdot 6SO_2$) and albite ($Na_2O \cdot Al_2O_3 \cdot 6SiO_2$) were generally used in the ceramic industry [18-20]. Ceramic production techniques could be examined in 5 different categories (Figure 5).

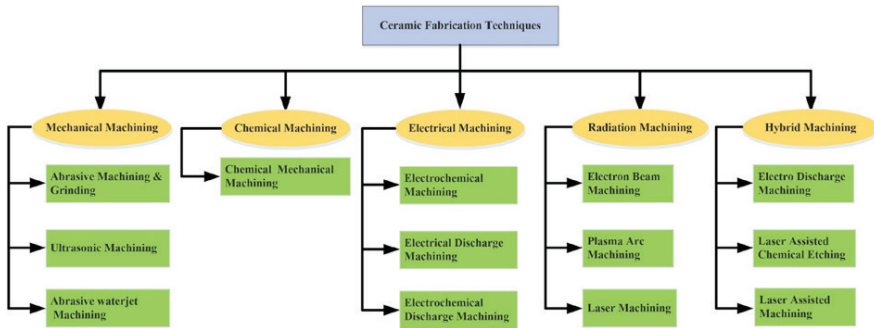


Figure 5. Production techniques of ceramics [17], [20]

The production processes of all ceramic materials were close to each other. Traditional fabrication process consisted of raw material preparation, grinding, granulation, shaping, glazing, drying, and firing stages. Ceramic production began with the preparation of masse raw materials in stock areas and ended at the furnace exit. Although traditionally ceramic production was similar, it differed according to raw material, product, size and working conditions. Crushing and grinding processes had a significant effect on rheology, production behavior, sintering behavior, and improvement of microstructure. Masse was the granule produced by taking various raw materials from the stock area according to the recipe composition and grinding them in ball mills and drying the obtained sludge in a spray dryer. During the masse production, control was made at every stage and the inappropriate semi-finished product was prevented for next stages. Masse raw materials were fed to sludge mills by passing through weighing belts and magnetic separators in factories. Wet grinding systems were widely used in the sludge preparation process. The mud from the mill was sent to the pool. The sieve balance of the sample sludge taken from the pool was checked. The ground material was transferred to sludge pools and fed to the spray dryer from there. Granular mass coming to the presses was pressed into molds of various sizes and patterns. After the glazing process, firing was done as the last step and the process was completed. Ceramic firing was the heating of the shaped and dried semi-finished product in a system and the cooling of the resulting ceramic in a system again [21, 22]. Scheme of the manufacturing process of ceramics was shown in Figure 6.

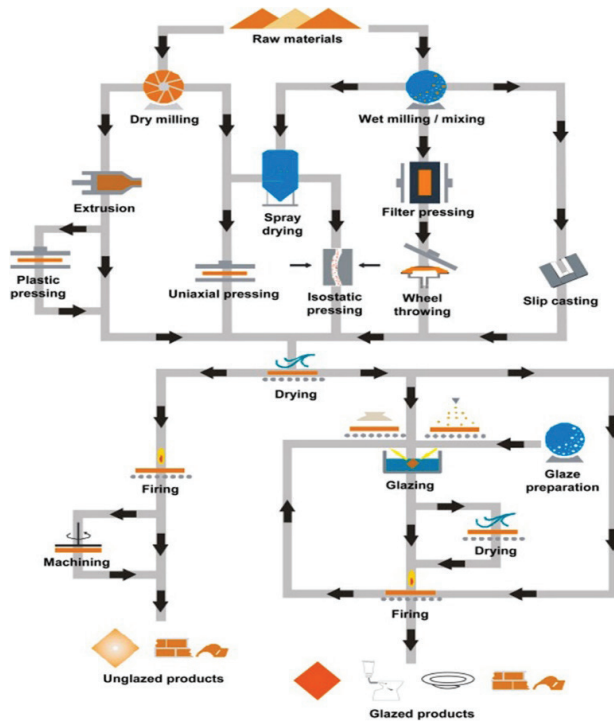


Figure 6. Scheme of the manufacturing process of ceramics [23]

In this process, the raw materials were poured and mixed, extruded, shaped by pressing. During manufacturing process, water was used for thorough mixing and shaping, then evaporated in dryers. The most widely used drying method in the ceramic industry was convection. The heated air was circulated around the ceramics and sometimes the heat could be recovered from the cooling zone of the kiln. The glazing process was applied only to the desired products. Uncooked products were heated from ambient temperature to 800°C . To avoid ceramic pores, bulges and bubbles, outgassing took place. Mixtures of powder base material, binders and stabilizers were subjected to treatment between $800\text{--}2500^{\circ}\text{C}$. The required temperature and baking time changed according to the type of material desired to be produced. Depending on the main reaction when heated up to 1350°C transformations took place. The cooling process started after the heat input processes were completed. Before packaging, the products were quality checked sorted according to their commercial use [23]. A typical example of the ceramic process was given in Figure 7.



Figure 7. Flow chart of ceramic process [24]

5. APPLICATION AREAS OF CERAMICS AND RECENT TRENDS

Ceramic materials were included as functional, religious, ornamental, cultural ceramic, pipe, and wall, earthenware similar as architectural structure, accoutrements, and food-tea-coffee brigades. Tableware kitchenware, detergent cleaning products, electrical-electronics-technological such as machine/equipment parts, human and vehicle, vehicle armor engineering supplies, refractories, and some aerospace technologies equipment in the form of almost quite common were used in various areas [24]. Production value of application areas of the ceramic industry in the Europe was shown in Figure 8.

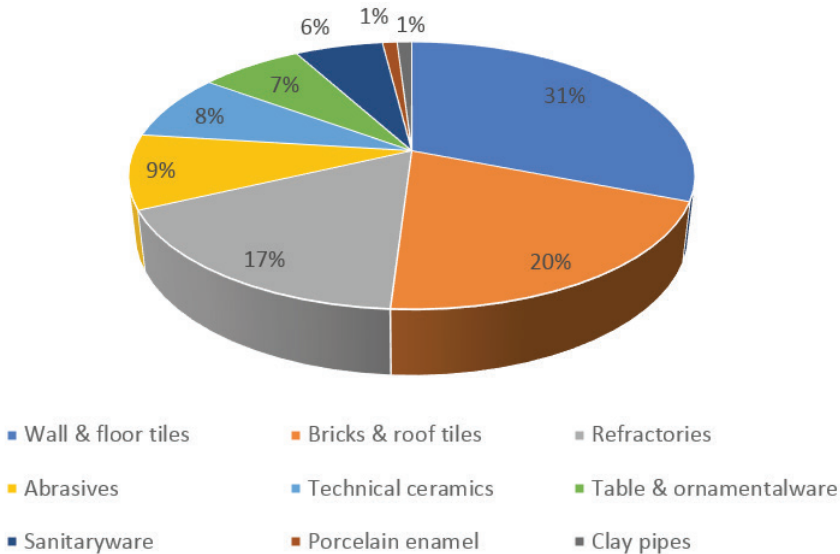


Figure 8. Production value of application areas of the ceramic industry in the Europe [18]

Terracotta figurines which were produced as votive wares since pre-historic times to protect themselves from the anger of the divine powers and to provide their help, carried the religious life of the period. In addition to religious use, these figurines were also produced as items such as toys, decorative items and, rarely, perfume bottles. Structural architecture of ceramic materials coating was used for decoration or surface protection. In addition to other materials, the use of ceramic material in creating a unique line for the space used, was known to be an option for architecture. Ceramics produced with today's technology it offered a wide variety of choices in color, texture, pattern, and form. It provided many advantages with its resistance to climatic changes and ease of application. It was possible to come across ceramics, which were used for another purpose, as a musical instrument in almost every period and in every culture. The

most common ones among ceramic musical instruments were wind and percussion instruments. While the production of ceramics was a handicraft with regional differences until the industrial revolution, it continued in a new field as industrial ceramics after the industrial revolution. With Industrial Age, which started in the 19th century, a new era began for ceramics and entered technology. Coating materials, sanitary ware, refractory fire bricks, ceramic raw materials, kitchen and tableware, were all sub-sectors of the ceramic industry today. Recently, these included thin plates on which electronic circuits for microprocessors were laid. For example, ceramic balls used in roller skates and the ceramic sockets were also very useful. One of the discoveries of modern science and technology was glass ceramics. Glass ceramics that gained machinability were considered as microwave product windows, sample holders of microscopes, seismographic coils, telescope frames. Ceramics also found wide use in the defense industry. Protective vests produced for soldiers and police, armored vehicles and pilot cabins in helicopters were made bulletproof with the help of ceramic materials. Now even fabric could be produced from ceramics. 5000 years ago, the Sumerians engraved the clay tablets for giving the messages. Now, it was being considered to produce smart cards from ferroelectric ceramic, a special high-tech material [25-27].

The usage areas of ceramics in medicine were also very wide. They were used for the restoration and reconstruction of hard tissues in the body. Bio-glass ceramics were very close to the bone structure due to their high apatite content. Bio-glass-ceramic and machinable glass ceramics were also widely used. These materials could be used in bones of the spine, middle ear, larynx, nose, eyes, whole skull, as well as being used as arm, leg, joint, dentistry, maxillofacial surgery, tumor treatment, tooth root and tooth structure. Being biologically compatible and inert was one of its promising features for use in these areas. It continues to be studied in the literature in terms of biological evaluation, cytotoxicity, tissue interface compatibility, and cell adhesion [12], [25], [28].

It had also found application in industrial waste treatment and separation. Its resistance to high temperatures made it preferred in the aviation industry and armor production. Ceramics was also preferred in the production of electronic and optical devices due to its technical characteristics [19]. Various applications for advanced ceramic materials were shown in Figure 9.

In recent years, the use of ceramic materials as composite materials with polymers, glass and metals had become widespread. In last trends, the studies in literature showed that transparent ceramics were prepared by using nano-powders with co-precipitation method. The results confirmed that these ceramic types promised laser materials for lasers. Laser

technology started to be used as a new perspective in ceramic processing. This area was still in the research and development stage. Ceramic production gained important for several applications in the automobile industry, gear and mechanical design, hardware [28, 29].



Figure 9. Various applications for advanced ceramic materials [17]

The increase in the usage areas of ceramics together with the development of the building sector has brought the ceramics industry to a significant volume in consumption and production by growing rapidly, especially in developed countries. In addition to developed European countries and the United States, developing countries have also started to create their own ceramic industries. England, Germany, Northern Europe, and the United States continue to lead in the field of technical ceramics by developing the usage areas of ceramics. The country with the largest share in world production is China, and it is also the largest exporter country. Turkey meets almost all of its domestic market ceramic needs from domestic production. In this respect, the sector is an important sector for the economy [25].

CONCLUSION

Consequently, it was aimed for the reader to get an idea about the features, classification, and production and application areas of ceramics. Ceramics, which were divided into traditional and advanced, have been produced for many years and were produced by developing various properties. Recently, its own features developed and it gained importance in the development of advanced technology tools and devices in different sectors. With the developments in the ceramics industry, ceramic materials were divided into sanitary wares, coating materials, technical materials, refractories, and dining utensils according to their product characteristics.

REFERENCES

- [1] Arcasoy, A. (1983). Ceramic technology, Marmara University. Faculty of Fine Arts, 457(2), İstanbul.
- [2] Büyükkutlu Erdoğan, E. (2019). Treatment of ceramic production process wastewater. M.Sc. Thesis. Erciyes University. Graduate School of Natural and Applied Sciences, Kayseri.
- [3] Callister W.D. & Rethwisch, D. G. (2007). Fundamentals of materials science and engineering: An integrated approach, 3rd Edition, Wiley, USA.
- [4] Eygi, M. S. (2009). Improving the usage of kaolin in ceramic with the aid of polyelectrolyte. PhD Thesis. İstanbul Technical University. Graduate School of Natural and Applied Sciences, İstanbul.
- [5] Camcıoğlu, K. (2020). Occupational health and safety risk assessment in the ceramics sector and an application in state of Uşak. M.Sc. Thesis. Uşak University. Graduate School of Natural and Applied Sciences, Uşak.
- [6] Boch, P. & Nièpce, J. (2007). Ceramic materials: processes, properties, and applications, Wiley, USA.
- [7] Barsoum, M. W. (2003). Fundamentals of ceramics (series in materials science and engineering, 1st Edition, McGraw-Hill, USA.
- [8] Koçak, A. & Karasu, B. (2019). Differences of dry and wet methods in tile production. Al-Jazari Journal of Science and Engineering, 8-23. <https://doi.org/10.31202/ecjse.443880>
- [9] Chawla, K. K. (1993). Ceramic matrix composites, 1st Edition, Springer, USA.
- [10] Petzow, G. & Herrmann, M. (2002). Silicon nitride ceramics. High Performance Non-Oxide Ceramics II, 47–167. https://doi.org/10.1007/3-540-45623-6_2
- [11] Vallet Regí, M. (2001). Ceramics for medical applications. Journal of the Chemical Society, Dalton Transactions, 2, 97–108. <https://doi.org/10.1039/b007852m>
- [12] Kara, S. (2012). A roadmap of biomedical engineers and milestones, Intechopen, Croatia.
- [13] Erdoğan, İ. (2019). Investigation of the usability of thermal power plant fly ashes in ceramic production. M.Sc. Thesis. Sivas Cumhuriyet University. Graduate School of Natural and Applied Sciences, Sivas.
- [14] Liang, Y. & Dutta, S. P. (2001). Application trend in advanced ceramic technologies. Technovation, 21(1), 61–65. <https://doi.org/10.1016/s0166-497200019-5>
- [15] Carter, C. B. & Norton, M. G. (2007). Types of ceramics and their application. Ceramic Material Science and Engineering, Springer, USA.
- [16] Misra, R. & Misra, K. P. (2022). Fundamentals of ceramics: introduction, classification, and applications. Ceramic Science and Engineering, 5–20. <https://doi.org/10.1016/b978-0-323-89956-7.00020-6>
- [17] Ming, W., Jia, H., Zhang, H., Zhang, Z., Liu, K., Du, J., Shen, F. & Zhang, G. (2020). A comprehensive review of electric discharge machining of ad-

- vanced ceramics. *Ceramics International*, 46(14), 21813–21838. <https://doi.org/10.1016/j.ceramint.2020.05.207>
- [18] Kızıler, B. (2017). Treatment of ceramic production process wastewater. M.Sc. Thesis. Bilecik Şeyh Edebali University. Graduate School of Science Engineering and Technology, Bilecik.
- [19] Baklacı, S. (2019). Improvement of surface properties in sanitaryware glazes. Eskişehir Technical University. Graduate School of Science Engineering and Technology, Eskişehir.
- [20] Samant, A. N. & Dahotre, N. B. (2009). Laser machining of structural ceramics - A review. *Journal of the European Ceramic Society*, 29(6), 969–993. <https://10.1016/j.jeurceramsoc.2008.11.010>
- [21] Zeybek, T. Y. (2019). Reuse of vapour condensate in ceramic industry. Dokuz Eylül University. Graduate School of Natural and Applied Sciences, İzmir.
- [22] Çakıcı, R. H. (2014). Investigation of alternative raw materials used in ceramic production and cost reduction studies. M.Sc. Thesis. Istanbul University. Graduate School of Natural and Applied Sciences, İstanbul.
- [23] Furszyfer Del Rio, D. D., Sovacool, B. K., Foley, A. M., Griffiths, S., Bazilian, M., Kim, J. & Rooney, D. (2022). Decarbonizing the ceramics industry: A systematic and critical review of policy options, developments and sociotechnical systems. *Renewable and Sustainable Energy Reviews*, 157, 112081, 1-31. <https://doi.org/10.1016/j.rser.2022.112081>
- [24] Kim, S. H., Kang, E. T., Kim, U. S., Hwang, K. T. & Cho, W. S. (2011). Sintered body characteristics of LAS by addition of CaCO_3 and ZrO_2 using a solid-state reaction. *Journal of the Korean Crystal Growth and Crystal Technology*, 21(5), 218–224. <https://doi.org/10.6111/jkcgct.2011.21.5.218>
- [25] Yıldırım, B. (2021). Usage areas of ceramic material and proposal for establishing a “ceramics university” in our country. *Journal of New Idea*, 13(26), 18-34.
- [26] Çam, A. (2012). Terracotta Figurines. *Journal of Science, Technology and Industry*, 39.
- [27] Okumuş, H. (2017). The fields of usage of ceramics in the past and today. *Journal of Awareness*, 2 (3), 1-14. <https://doi.org/10.26809/Joa.2017.0>
- [28] Xu, M., Girish, Y. R., Rakesh, K. P., Wu, P., Manukumar, H. M., Byrappa, S. M., Udayabhanu, & Byrappa, K. (2021). Recent advances and challenges in silicon carbide (SiC) ceramic nanoarchitectures and their applications. *Materials Today Communications*, 28, 102533, 1-24. <https://doi.org/10.1016/j.mtcomm.2021.102533>
- [29] Li, J., Pan, Y., Zeng, Y., Liu, W., Jiang, B. & Guo, J. (2013). The history, development, and future prospects for laser ceramics: A review. *International Journal of Refractory Metals and Hard Materials*. 39, 44–52. <https://doi.org/10.1016/j.jrmhm.2012.10.010>



CHAPTER 14

PROCEDURES FOR DETERMINING THE VALUE OF TREASURY IMMOVABLES, QUESTIONS AND POSSIBLE SOLUTION SUGGESTIONS

Nuri ERDEM¹

¹ Assoc. Prof. Dr., Department of Geomatics, Faculty of Engineering, Osmaniye Korkut Ata University, Osmaniye, Turkey <https://orcid.org/0000-0002-1850-4616>

1. INTRODUCTION

Immovable properties are very important for all the peoples of the world, economically and socially. Factors such as the gradual increase in the world population, the decrease in agricultural activity areas, the migration from the village to the city and the rapid urbanization due to these increase the value of immovables day by day (Erdem, 2016). Today, the services of determining the real estate values have become an indispensable element of international global economic relations. Valuation activities have a large place in the economic system as a whole and are used for different purposes. The task of determining the real estate values and the ability of these values to be traded in the market as liquidity are the most important elements of a healthy economic structure (HKMO, 2012; IAAO, 1990).

Benefiting from public goods is divided into two parts as “general benefit” and “private benefit”. Unlike general benefit, private use is not free. In order to benefit privately from public goods, it is necessary to have a legally valid relationship with the administration through license, contract or concession. The person who wants to make private use of public goods in a way that prevents others from benefiting has to pay for it. Unlawful occupation (unlawful user) in Turkish Administrative Law to persons who use public goods without any permission or contractual relationship; the fee received from these users is called “*ecrimisil*” (Katipoğlu, 2009).

The problems experienced in determining the value of real estate in a realistic way within the framework of current legal regulations in Turkey both reduce the efficiency and effectiveness of taxes on real estate and have a distorting effect on taxation. Since the real estate market has not developed in a healthy way, there are no regulations regarding objective criteria, especially the Real Estate Tax Law. Therefore, the values that will be subject to real estate tax are based on estimations based on subjective criteria rather than objective criteria (Hacıköylü, 2010; Yomralıoğlu and Nişancı, 2006; Çağdaş, 2007).

In this study, the determination of the value of the treasury immovables and the problems experienced in the application of the compensation will be examined. In the study, first of all, real estate, real estate valuation and *ecrimisil* will be emphasized as a concept, types of *ecrimisil*, problems in determining *ecrimisil* and possible solutions will be presented.

2. ECRIMISIL AND TERMS OF CLAIMS

Cultivating an arable land; to construct buildings or facilities on state-owned land; Actions such as closing a part of the beach without permission, preventing others from entering the sea, are examples of occupation. Since the regulation mentions “occupation, disposition, seizing, holding,

possession or use in any way”, the type of occupation is not important in order to be able to demand compensation. All kinds of exploitation without a legal basis are accepted as occupation (Katipoğlu, 2009).

“Value” in TDK Dictionary; It is defined as “an abstract measure that helps to determine the importance of something, the money of something that can be measured in money, the value of something, the value, the price, the price” (URL_1). The word “value” for real estate in daily use is “market (market) value”, “rent value”, “insurance value”, “use value”, “specific value”, “investment value”, “asset value”, “determined value”. It appears in various forms such as “tax base value”, “recoverable value”, “liquidation or forced sale value”, “special value” and “mortgage-backed loan value”. Many value concepts are used in legislation and literature. In order to make a real estate valuation, the differences in the concept of value should be known (Açlar et al, 2003; Bayram, 2007).

There are many concepts derived from the word value. One of them is “valuation”. Valuation; To appraise is to state the value of something, to put a value on something. According to another definition, valuation; Determining the value of non-monetary economic assets in money, an enterprise’s building, land, machinery-equipment, stock of goods, etc. It is an appraisal and estimation of the value of total assets in the form of (Candaş, 2012; Rissi, 2010).

In general, real estate (real estate) valuation; It can be defined as “the estimation of the probable value of an immovable, immovable project or the rights and benefits attached to the immovable on the valuation day, based on independent, impartial and objective criteria” (Açlar and Çağdaş 2008; CMB). Real estate valuation can be defined as expressing a real estate partially or completely in terms of quality and quantity (Yalpir, 2007).

Ecrimisil receivables and the detection of all kinds of unjustified occupation of public property are carried out by the national real estate services affiliated to the provincial directorates of the Ministry of Environment, Urbanization and Climate Change. These services are in charge of monitoring and detecting occupancy events on public property, and performing evacuation and evacuation procedures. The duties of the Directorate of National Real Estate / Directorate of National Real Estate are determined within the framework of the Provincial National Real Estate Directive. According to this (URL_2);

- To carry out the services related to the management of immovable properties under the private ownership of the Treasury and under the rule and disposal of the State, in cooperation with other public institutions and organizations when necessary,

- Selling, leasing, bartering and establishing limited real rights on the privately owned immovables of the Treasury, renting the places under the rule and disposal of the State and issuing usage permits for these places when deemed necessary,
- Carrying out the processes of appropriating movable and immovable properties and rights to the Treasury, registration of immovable properties and liquidation of movable properties,
- Those that are required to be used for public service from places under the private ownership of the Treasury or under the jurisdiction and disposal of the State; to allocate it to the administrations with general and special budgets and to remove the allocation in case the purpose of allocation disappears or is used out of purpose; To liquidate the structures and facilities belonging to public institutions and organizations other than the Treasury on the immovable properties whose allocation has been canceled, to determine the principles and procedures regarding the liquidation,
- To keep inventory records of immovable properties belonging to the treasury and to determine the principles and procedures for keeping inventory records of immovable properties of other public institutions and organizations,
- To sell the out-of-service movable properties of the flats included in the general budget,
- Programming the construction of the ministry's service buildings, executing the purchases and making repairs,
- To determine the management principles on immovable properties belonging to public institutions and organizations,
- To give an opinion on the draft laws, bylaws and regulations to be prepared by public institutions and organizations regarding the acquisition and management of immovable property,
- Within the scope of the projects, the implementation procedures and principles of which are determined by the Council of Ministers; To develop and evaluate the immovables under the private ownership of the Treasury and under the rule and disposal of the State, to purchase, barter, expropriation and consolidation of the immovables owned by individuals. Surveys, maps, plans, zoning plans, zoning plan amendments and zoning applications of all types and scales regarding all immovables within this scope are made by the Ministry of Environment, Urbanization and Climate Change, upon the request of the Ministry, and are put into effect after approval.

In Article 84 of the Regulation on the Administration of Treasury Real Estates issued based on Article 74 of the State Tender Law and in the General Communiqué on National Real Estate No. 312, it is stated how to determine the places occupied that may be subject to treason. Accordingly, among the immovable properties under the private property of the treasury or under the rule and disposal of the state, those that are not rented, servitude is not established or permission to use are determined by the national real estate services on the spot within a program and their actual status is determined on the spot, and due to the occupation and disposition of the periods before the determination, the compensation is determined, followed and followed up. collection is made (Katipoğlu, 2009). Information that can be used at the discretion of Ecrimisil and other information that is beneficial to know are included. An "Immovable Detection Report" containing all this information is drawn up (Figure 1). In addition, if it is determined that the treasury immovables have been occupied by persons, the administrative fee is determined based on the "Immovable Detection Report" within fifteen days from the date of detection.

05.10/2018

TAŞINMAZ TESPİT TUTANAĞI

İL-İLÇE: Kilis-Merkez-Göten Köyü

TAŞINMAZ NO: [REDACTED]

TABLO I - VARSA FUZULİ SAĞIL VEYA SAĞILLERİN	
Adı, Soyadı veya Ünvanı	[REDACTED]
T.C. Kimlik No/Vergi Kimlik No	[REDACTED]
Adresi	[REDACTED]

TABLO II - TAPU BİLGİLERİ	
1) Bulunduğu köy veya mahallenin adı	Göten Köyü
2) Tapuda kayıtlı olduğu	Pufla, Ada, Parsel
3) Cinsi ve yüzölçümü (m ²) / Bahçesiz Bölüm No	Cilt, Sahifesi, Sıra No / Bahçesiz Bölüm No
4) Hissedilme durumu ve oranı	Tapu Tarihi / Blok No - Kat No
5) Mevki ve sokak	Tarla / 136.700,00 m ²
6) Sınırları	Tamam 4,00 / 4,00

TABLO III - ÜZERİNDE MUHDESAT VARSA	
1) Cinsi ve niteliği	
2) Miktarı	
3) Kime ait olduğu	

TABLO IV - ARAZİ İSE	
1) Arazinin verim gücü	
2) Sulanabilirlik durumu	

TABLO V - BİNA İSE	
1) İnşaatın brüt alanı (m ²)	7
2) İnşaatın sınıfı	
3) İnşaatın türü	
4) Yığılma oranı	
5) Kullanılabilirlik durumu	

TABLO VI - TESBİTE İLİŞKİN BİLGİLER	
1) İlgali veya tasarrufun başlangıç tarihi ve süresi	04.06.2013 - 05.02.2018
2) İlgali veya tasarruf edilen miktar	2.000 m ²
3) İlgali veya tasarrufun amaç ve biçimi	Bağ
4) Kamu hizmetlerine gerekli olup olmadığı	
5) 6811 sayılı Orman Kanunu, 2634 sayılı Tarımsal Yapı Kanunu, 2863 sayılı Kültür ve Tabiat Varlıklarını Koruma Kanunu, 3621 sayılı Kırsal Kanunu kapsamında olup olmadığı	

TABLO VII - TAŞINMAZA AİT TESPİT VE TAHMİN EDİLEN BEDEL

İşgalcinin 15.01.2018 tarihinde elinde bulundurduğu maldan dolayı taşınmazın 2.000 m²'si tarafından kullanıldığı tespit edilmiştir.

TABLO VIII - TAŞINMAZA AİT TESPİT VE TAHMİN EDİLEN BEDEL HESAP TUTANAĞI

1) İlgali veya tasarrufun başlangıcından tespit tarihine kadar yıllar itibarıyla getirilecekleri	
2) Toplam ecrimisil miktarı	
3) Tespitin sona ermesi, trampa, kiraya verme, ön izin ve kullanma izni verilmesi veya irtifak hakkı kurulması gereken hallerde bu işlemler için ilgilinin devralan şahsının yüzölçümü ile trampa, satış ve trampa bedeli ile bir yıllık kira, ön izin, kullanma izni ve irtifak hakkı bedeli	

TESPİT YAPANIN	ADİ SOYADI	UNVANI	İMZA
[REDACTED]	[REDACTED]	Beft Vazir	[REDACTED]
[REDACTED]	[REDACTED]	Tekniker	[REDACTED]

BİLGİLEŞİLERİN	ADİ SOYADI	ADRESİ	İMZA
[REDACTED]	[REDACTED]	(Göten Köyü Muhtarı)	[REDACTED]

İSGALCİLERİN	ADİ SOYADI	ADRESİ	İMZA
[REDACTED]	[REDACTED]	[REDACTED]	[REDACTED]

Figure 1. Immovable Detection Report in Ecrimisil Transactions

3. DETERMINATION OF THE ECRIMISIL AMOUNT, APPRAISAL AND TERMINATION OF THE SHAGIL

Real estate valuation; Public practices such as taxation, expropriation, privatization, land regulations, registration-based transactions, easement rights, and private sector applications such as capital markets, banking, lending and insurance are needed intensely. In order to meet this need and to ensure the transparency of real estate markets (markets based on purchase and sale), countries need to establish and maintain well-functioning valuation systems. As a matter of fact, it is known that legal, institutional and technical studies are carried out in many countries in order to establish or improve valuation systems (Çete, 2008; Köktürk and Köktürk, 2015). In our country, there is a need to establish a system that is compatible with world standards and works well in this area as soon as possible (Anton, 2011; Erdem, 2016).

It is difficult to talk about exact models in determining the real estate value. There may be differences in the methods used by each country in determining the real estate value according to their unique cultures, locational or regional characteristics. Most of the methods are based on peer comparison. Models or methods, on the other hand, try to analyze the market by imitating the thoughts of the users directly (Pagourtzi). and Assimakopoulos, 2003). There are basically three types of valuation methods. These; Peer Comparison Management is Income Capitalization Method and Cost Method.

ecrimisil cost is regulated in Article 75 of the Law No. 2886, Article 85 of the Regulation on the Administration of Treasury Immovables issued based on this law, and Article 5 of the General Communiqué on National Real Estate No. 312. According to the first paragraph of Article 75 of the State Procurement Law numbered 2886, titled “Ecrimisil and Evacuation”, “On the occupation of immovable properties under the private ownership of the State or under its jurisdiction and disposal by real and legal persons, unnecessarily, from places specified in Article 9 of this Law. By being asked, the commission specified in the 13th article is asked to appreciate and determine the reward” (Katipoğlu, 2009). The coordinate list obtained from TKGM is created for the real estate to be determined (Figure 2).



Figure 2. *TKGM screenshot taken for the Immovable to be Determined*

While Ecrimisil is being determined and appreciated, it may affect the value of the Treasury real estate; Land type (wet / dry / barren), Irrigation Projects, Land Cover Data (Meadow-Passage, Forest Boundary Areas), Soil Type Data (Sandy, Loamy, Humus, Lime), Orchard Covering/Mixed, Rocky Condition of the Land, Geometry /Number of Broken Corners, Land Consolidation Projects, Organic Agriculture, Greenhouse, etc. The current value is determined by taking into account all objective measures such as Scope of Activity, Characteristics of the Agricultural Region/Product Segment, Chemical Structure of the Soil, Groundwater Reserves (Figure 3).



T.C.
ELBEYLİ KAYMAKAMLIĞI
Milli Emlak Şefliği

Sayı : [Redacted]

Konu : Rayiç Bedel

DAĞITIM YERLERİNE

İlçemiz Merkez ve köylerinde bulunan, Hazinesin Özel mülkiyetindeki taşınmazlar, Devletin Hüküm ve Tasarrufu altındaki taşınmazlar ile mülkiyeti Suriye uyruklu şahıslara ait taşınmazların, Milli Emlak Şefliğimizce 2021 yılında gerçekleştirilecek olan Ecrimisil ve Kira işlemlerine esas olmak üzere emsal teşkil etmesi açısından aşağıda belirtilen vasıflarına göre almış olduğunuz yıllık bedellerin (m²) bildirilmesi hususunda,

Gereğini arz ederim.

VASFI	ECRİMİSİL BEDELİ BİRİM FİYATI (m ²)	KİRA BEDELİ BİRİM FİYATI (m ²)
KİRA Ç ARAZI		
TABAN ARAZI		
SULAK ARAZI		
ZEYTİN BAĞ		
FİSTİK		
ARSA		
KERPIÇ EV VE AVLUSU		
BETONARME EV		

[Redacted]
Kaymakam

Figure 3. Receipt of Unit Fee from Institutions in Determining the Current Value of the Real Estate

By using the unit price data obtained from the Chamber of Agriculture, an ecrimisil appraisal decision is made by the institution (Figure 4).

ECRİMİSİL KIYMET TAKDİR KARARI

Taşınmaz No / Taksim : [REDACTED]
Karar Tarihi : [REDACTED]
Karar No : [REDACTED]

2886 sayılı Kanuna dayalı olarak çıkartılan yönetmeliğin 18. maddesi gereğince teşekkül eden komisyonumuz toplandı. Aşağıda tapu kaydı ve nitelikleri belirtilen taşınmaz yine aşağıda belirtilen ecrimisil bilgileri uyarınca fuzulen işgal edilmiştir.

TAŞINMAZ VE ECRİMİSİL BİLGİLERİ			
İli	Kilis	Yüzölçümü (m ²)	136.700,00
İlçesi	Merkez	Hazine Yüzölçümü (m ²)	136.700,00
Mahallesi / Köyü	[REDACTED]	Pafila / Çift No	[REDACTED]
Mevkii / Yöre	[REDACTED]	Ada / Sahife No	[REDACTED]
Cinsi	Taahhüt	Parsel / Sıra No	[REDACTED]
Fuzulî Şağilin Adı, Soyadı veya Unvanı	[REDACTED]		
İşgal veya Tasarrufun Başladığı - Bittiği Tarih	04/06/2013 -05/02/2018		
Şahıs İşgali - Haz. Yüzölçümüne İsbet Ed. Alan (m ²)	14.000,00-14.000,00		
İşgal Amacı	BAG		

2886 sayılı Devlet İhale Kanununun 75. maddesi, Hazine taşınmazlarının İdaresi Hakkındaki Yönetmeliğin 85. maddesi ile 336 sıra no.lu MİLE Genel Tebliğinin 5. maddesi hükümlerine göre İdarenin zarara uğrayıp uğramadığına ve işgalcinin kusurlu olup olmadığına bakılmaksızın, taşınmazın işgalci tarafından kullanılmak suretiyle, fiili ve hukuki durumu ile işgalden dolayı varda elde ettiği gelir, aynı yer ve mahalde bulunan emsal nitelikteki taşınmazlar için oluşmuş kira bedelleri veya ecrimisiller, varsa bunlara ilişkin kesinleşmiş yargı kararları, ilgisine göre belediye, ticaret odası, sanayi odası, ziraat odası, borsa gibi kuruluşlardan veya bilirkişilerden soruşturulmak suretiyle edinilecek bilgiler ile taşınmazın değerini etkileyecek tüm unsurlar göz önünde bulundurularak;

Dönemi	İşgal Edilen Alan (m ²)	Birim Bedeli (TL/m ²)	Ecrimisil Bedeli (TL)	Mühdesat Bedeli (TL)
04/06/2013 - 31/12/2013	14.000,00	0,056000	453,22	,00
01/01/2014 - 31/12/2014	14.000,00	0,066000	924,00	,00
01/01/2015 - 31/12/2015	14.000,00	0,075000	1.050,00	,00
01/01/2016 - 31/12/2016	14.000,00	0,080000	1.123,07	,00
01/01/2017 - 31/12/2017	14.000,00	0,083000	1.162,00	,00
01/01/2018 - 05/02/2018	14.000,00	0,090000	124,27	,00
Genel Toplam			4.836,56	,00

olmak üzere, 4.836,56 TL hesaplanan ecrimisil bedeli ile ,00 TL hesaplanan mühdesat bedeli olmak üzere toplam **4.836,56** (DÖRTBİN SEKİZYÜZOTUZALTI TL ELLİALTI KR) ecrimisil bedeli tespit ve takdirine komisyonumuzca oy birliği ile karar verildi.

KOMİSYON BAŞKANI [REDACTED] Müddir Xrd. [Signature]
ÜYE [REDACTED] Şef [Signature]
ÜYE [REDACTED] Defterdar. Yrd. [Signature]

Figure 4. Ecrimisil Appraisal Decision Issued by the Institution

3.1.ECRİMİSİL IN THE ZONED AREA

The works of applying the zoning plans or building projects to the ground are called applications. Today, making applications with the GPS system is both sensitive and easy. If GPS cannot be used in the application to be made and high sensitivity is not desired, corners of buildings and parcels, telegraph, telephone, power transmission line poles and art structures can be used (Figure 5).

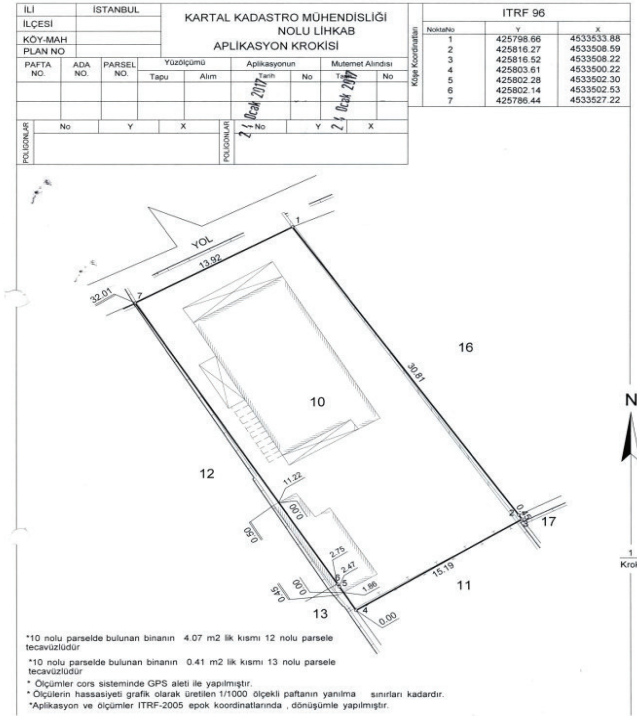


Figure 5. Application Procedures in the Region where Ecrimisil will be taken

It is essential that the immovables are determined at least once a year. However, in mandatory cases, the duration of detection programs can be more than one year. However, detection programs cannot be made for more than five years (Figure 6).

MEOP

Taahhüt İşlemleri

Kira Yönetim

EPİS

Personel

Sms

Rapor

Diğer İşlemler

Tasınmaz Sorgulama

Tespit

Kapat

Tasınmaz No

Kadastro E

Yüzölçümü

602.30

Ana Cinsi

Tarla

İli

Kilis

Ada

Pay

1.00

Cinsi

Tarla

İlçe

Merkez

Parsel

Payda

1.00

Mevkii

Aktaş

Mahalle/Köy

Pafta

038-D-03-

Hazine Yüzölçümü

602.30

Takbii Zemin

Mahalleleri

D-3-D

No

Yazgılar

BOS TAŞINMAZ TESPİT TUTANAĞI

Tespit Sorgulama

İşgalci Kullanıcı

İşgali

İşgal/Tasarıf

Evet

Tespit Durumu

İşgali

Gerçek/Tuzel Kişi

Gerçek Kişi

devam ediyor mu?

İşgal Amaç-Biçimi

Ticari Amaç Kullanım

Tespit Tarihi

12/03/2020

Bul

Temizle

Yeni Kayıt

Bulunan Tespit Sayısı: 5

Düzenle	Tekrarla	Tespit Ekibi	Sıra No	Tespit Durumu	Tespit Tarihi	İşgal Şekli	Ad Soyad / T.C. No	Unvan / Vergi No	İşgal/Tasarıf Başlangıç Tarihi	İşgal/Tasarıf Bitiş Tarihi
			5	İşgali	12/03/2020	Ticari Amaçla Kullanım			12/09/2015	01/09/2018
			4	İşgali	12/03/2020	Ticari Amaçla Kullanım			12/09/2015	12/03/2020
			3	İşgali	12/03/2020	Ticari Amaçla Kullanım			12/09/2015	12/03/2020
			2	İşgali	11/09/2015	Ticari Amaçla Kullanım			10/05/2015	11/09/2015
			1	Bos ve İşgaliz	20/11/2013					

Figure 6. *Example of Ecrimisil in the Commercial Area*

3.2. ECRIMISIL IN AGRICULTURAL AREA

Land; It is defined as “part of the earth, earth, ground, soil” (FIG, 1995). The land within the scope of the study; Unless otherwise stated, it is used as a piece of land that has not undergone a zoning application, whose borders are drawn by hills, mountains, roads, streams, walls, trees or determined by signs, serving to grow agricultural products, except for the meaning of which the boundaries are drawn with this definition. There are approximately 8.57 million hectares of agricultural land not registered in the Farmer Registration System. About 30% of these unregistered lands are used by farmers paying *ecrimisil*. Since there is no contract between the treasury and the people who use these lands, which are used by paying *ecrimisil*, those who use these lands cannot benefit from the supports provided to the agricultural sector. This situation leads to unfair competition and negatively affects agricultural production and yield (Katipoğlu, 2009). The data generally needed in land valuation are given in Table 1.

Table 1. *Data generally needed in agricultural area valuation.*

Fertility of the Soil
The Age of Trees and their annual Economic Return
Migration Rate (%)
national Income Per Capita
Manufacturer Sales Prices
Chemical Fertilizer, Seed and Agrochemical Sales Prices
gross Production Value
Capitalization Rate
Production Expenses (Rent / Labor / Capital)
alternating system
acreage
Not to be Opened for Construction _ to the Soil Protection law
WPI (%)
CPI (%)
PPI (%)
Real Interest Rate (%)
population Density
Unemployment Rate (%)
average monthly household Income (%)
national and regional Economic trends
Labor Charges
the Economics future of the farming Profession
the Cost of Transfer Operations
Frequency of Purchase / Sale Transactions in the Region
the development of the region
population Growth Rate (%)
tax Rates
Gold Prices and Exchange Rate
the Speed of Industrialization
Labor potential in the Surrounding area
Type of terrain (watery / dry / barren)
irrigation Projects
Land Cover Data (Meadow-Pasture, Forest Boundary areas)
Soil Type Data (Sandy, Loamy, Hummus, Calcareous)
orchard Closed /Mixed
the stony State of the Land
Geometry / Number of Broken Corners
Land Consolidation Projects
Organic Farming, Greenhouse Farming, etc. Scope of Activity
Characteristics of the Agricultural Region /Product Segment
Chemical Structure of the Soil
groundwater Reserves

3.3. ECRIMISIL FOR LAND QUALIFIED IMPROVEMENTS

Plot; While it is a piece of land divided by local governments according to the development projections of the city, the land; It is a piece of land that is not used for various purposes such as vineyards, gardens, fields, or is not used in any way. Plot; It is defined as “the place reserved for building on it” in the Turkish Language Association (TDK) Dictionary (URL_1). According to the Zoning Law No. 3194, land (zoning parcel); It is the form of the cadastral parcels within the zoning islands, arranged according to the Zoning Law and zoning regulations. The data generally needed for land valuation are given in Table 2.

Table 2. *Data generally needed in land valuation.*

frontage to the Main Road (Yes / No)
Construction Area
precedent
Verse Zone Plan
Application Zone Plan
Hmax
Front Garden
Side Garden
TAKS
KAKS
building Layout (Separate / Adjacent)
Plan Notes
parcel Type __ Parcel, Cadastral parcel)
the location of the Plot (Corner / Dec)
Infrastructure facilities
Unused Zoning Right
Having a Structure on It
Parcel Size / Geometry
Parcel Depth
The Development Status of the Region
Intensity of Construction

4. FINDINGS AND EVALUATION

Public receivables are revenues included in the budgets of public administrations, arising from financial obligations based on public power and to meet the financing provided for the continuation and stability of public services. There is a difference of opinion in the doctrine as to whether

ecrimisil is a public receivable or not. Some skeptics accept that there is no public receivable, with the mention that the state has receivables arising from unjust enrichment (Katipoğlu, 2009).

In our country, there are many laws, regulations and communiqués related to real estate valuation, especially our Constitution. However, none of them has a regulation that specifies the rules and standards of valuation transactions. There are only some clauses about who will determine the value of the real estate and what methods can be used. Valuation studies should only be carried out by valuation experts who have a valuation license in this field, instead of commissions established within the institutions. The expropriation expertise certificate application used in the valuation area should also be abolished. In order to make these and similar radical changes, first of all, a strong institutional structure should be established in this field. In our country, it is necessary to establish a central valuation administration that regulates, supports and supervises real estate valuation activities. Thus, the audit of private sector valuation firms will be carried out more effectively.

capitalization in valuation is based on the principle that value is determined by the amount and nature of expected income. Income capitalization is one of the three basic methods. The income method is basically a method that can be used in all immovables with or without income generating income (Erdem, 2016). Among the valuation methods, it is a method that is relatively based on mathematical calculations and has little estimation. For this reason, this method is only used on income-generating immovables. Income should be taken as the income of the business and the real estate. Income may be gross or net income currently provided, or it may be possible to calculate a potential (to be obtained in the future) income (Katipoğlu, 2009).

Databases containing information on real estate characteristics and real purchase and sale values in the real estate market should be established in order to access the data needed during the valuation studies and to carry out the studies within the framework of a healthy infrastructure in our country, as in countries with developed systems in the field of real estate valuation. Obtaining information about the real estate from a common database will enable appraisers to access the data they need in a shorter time and easily.

In the TAKBİS system used by TKGM, the classification of immovables should be made healthier, and the immovables sold according to their types and their values should be announced on the official website on a provincial and district basis. For example, it has been seen below that the ecrimisil base price taken from an immovable in a village in the Merkez

District in Kilis Province and the ecrimisil base price received from the immovable in the Neighborhood of the Center at the border of the adjacent area are the same (Figure 7-10). While Ecrimisil is being determined and appreciated, it may affect the value of the Treasury real estate; While it is necessary to consider issues such as zoning status, Surface Area, Quality, Efficiency (in agricultural lands), whether it benefits from infrastructure services, its location, the way the immovable is used, and whether there is income due to occupation, the formation of ecrimisil transactions in this way causes problems.

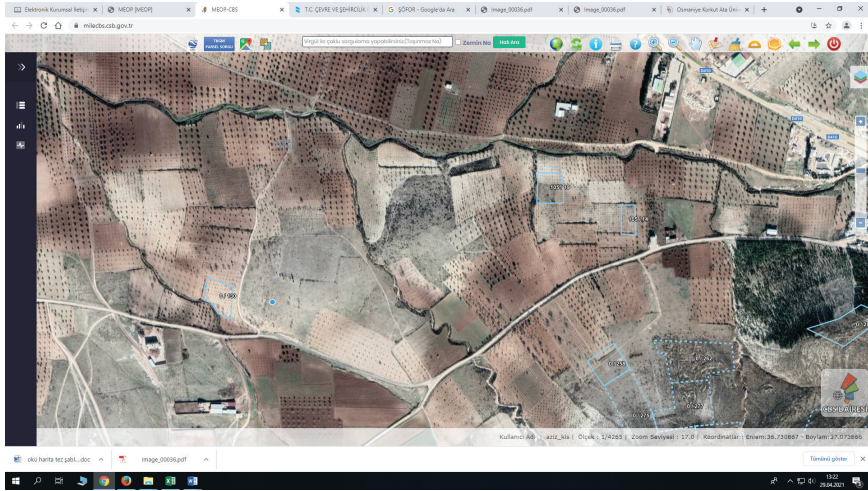


Figure 7. *Satellite Image of the immovable to be purchased Ecrimisil within the borders of the village*

Figure 8. *Base prices received from the MEOP System on the immovable to be purchased Ecrimisil within the boundaries of the village*

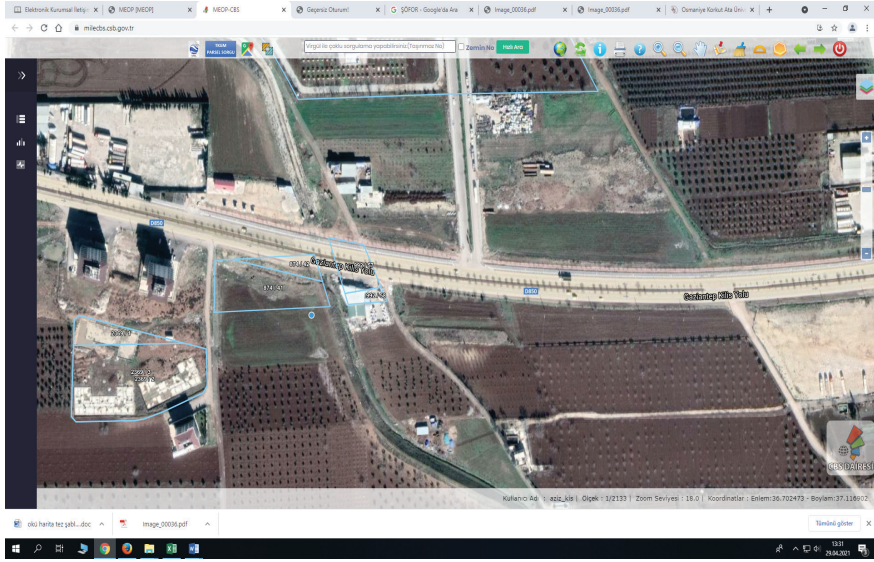


Figure 9. *Satellite Image of the real estate for which Ecrimisil will be purchased within the Contiguous Area Boundaries*

MEOP

Ecrimisil Sorgulama

Yıllık Bedel

Yazışmalar

19/7/2003 tarihinden sonra Hazine tapınmazları üzerinde yapılan yasal olmayan her türlü yapı ve tesisler itaklip-sökülebilir nitelikli olanlar hariç, başka bir işleme gerek kalmaksızın Hazineye intikal edeceğinden bu nitelikteki işgaller için ecrimisil, zeminbirlikte muhdesat da dikkate alınarak tespit ve takdir edilir.

- GİB GÖNDER yapıldığı için değişiklik yapılamaz
- Ecrimisil TEBLİĞ edildiği için değişiklik yapılamaz

Kom. Tak. 16/04/2012 Kom. Tak. No 1 Kom. Tak. 196.86

Tarihi Edilen Bedel

Komisyen Kararı Kaydet

Ecr. Yılı	Başladığı Tarih	Bittiği Tarih	Birim Bedeli	Ecrimisil Bedeli	Bld.Bsk.Bed.	Tic.Od.Bed	Zir.Od.Bed.	G.Tarım H.İl.Md.	Bilirkişi	Emlak Vergi Değeri
2010	26/03/2010	31/12/2010	0.027000	69.76						
2011	01/01/2011	31/12/2011	0.028000	94.36						
2012	01/01/2012	27/03/2012	0.031000	32.74						
				196.86						

Birim Bedeller Kaydet

Figure 10. *Base prices received from the MEOP System on the immovable for which Ecrimisil will be purchased in the Contiguous Area*

During the determination of the immovable transactions, the discovery works made by the experts especially coincide with the crop rotation and the ecrimisil costs are taken from the same immovable at different times. For example, as can be seen from the screenshots below, different

ecrimisil costs have been reflected to the citizens as a result of the determination processes carried out in different periods, and this situation causes great difficulties especially for the villagers who earn their income only from the land (Figure 11-12).

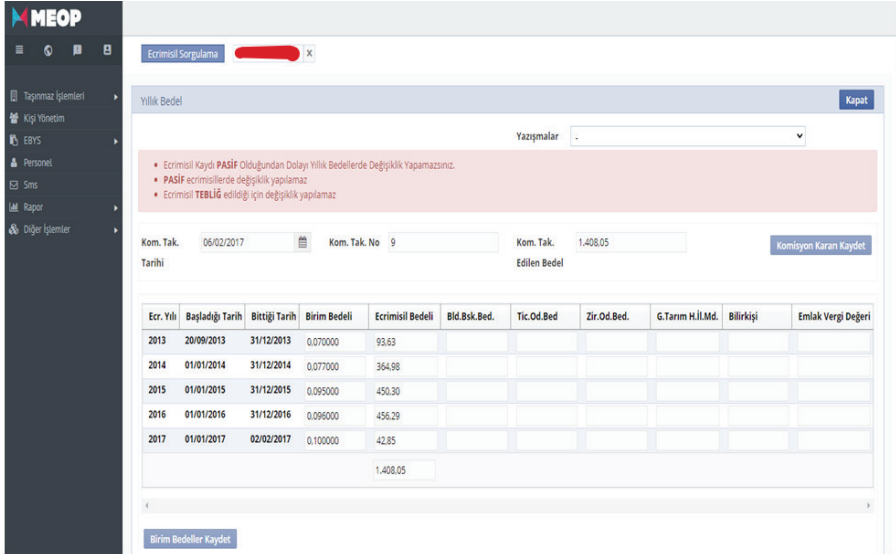


Figure 11. Base prices received in Real Estate Transactions (Grain Type)

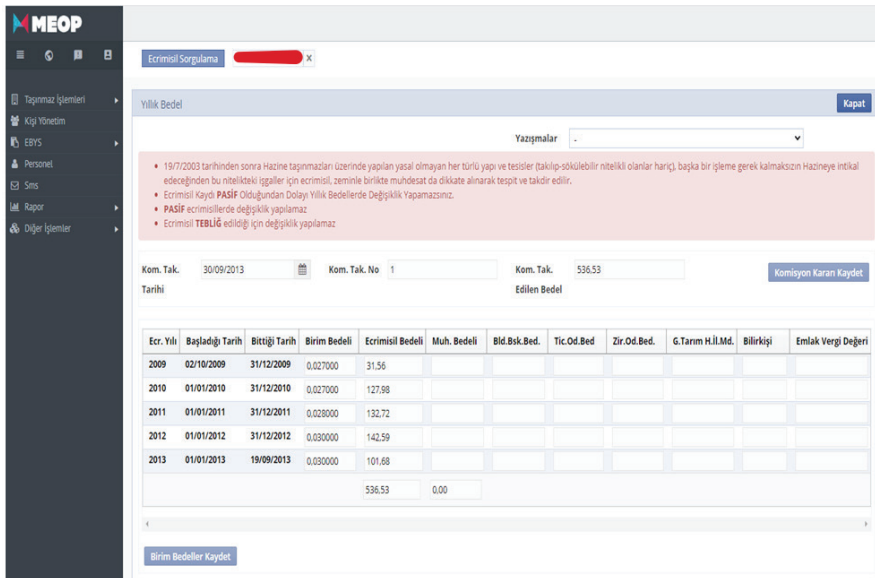


Figure 12. Base fees received in Immovable Transactions (In Garden)

In the field of real estate valuation, which is of great importance for our country in terms of ensuring both economic development and fair taxation, the need to establish a sound and healthy legal, institutional and technical infrastructure has become a necessity. For this, first of all, the policies and standards needed in the field of real estate valuation should be determined and a legislative infrastructure should be established, and then a well-functioning administrative structure and a technical capacity that is open to modern and technological developments should be built (Candaş, 2012).

5. POSSIBLE SOLUTIONS

A large part of the immovable properties under the rule and possession of the state and the private property of the treasury are occupied by persons who do not have valid legal rights. If it is learned that the immovable properties of the private property of the Treasury have been illegally occupied, an immovable should be taken retrospectively from the date of occupation, and the said immovables should be rented to prevent future occupations (Katipoğlu, 2009).

In cooperation between institutions; Ministry of Finance, General Directorate of Land Registry and Cadastre and Municipalities come to the fore. The values that occur in a district every month will be collected by the local finance organization and should be reported to the central unit at the end of the month. This includes expropriation and rent appraisals made by the courts in that district during the relevant month, appraisals for immovables belonging to the Treasury, appraisals based on bank loans, and all appraisals made by municipalities. The local finance organization will separate these values in terms of land, land, building and housing and send them to the center in that way. This information will form the basis for the formation of a GIS compatible value map. The local finance organization will also receive the transactions made in the Land Registry Office in that district on a monthly basis. Storing values as data will guide the practices of many public institutions (Değirmenciler, 2008; Erdem, 2017). Although an application has been made to the Land Registry Directorates with the necessary documents, the requested information cannot be given on the grounds that the submitted documents are invalid, and the “owner of the immovable” is requested to come.

Some privileges should be given to appraisers in terms of access to data within the framework of the law, and if necessary, in return for certain and appropriate fees, they can be provided to access data online by facilitating their access to certain data and minimizing their communication with officers/officers. Especially the creation and storage of data in electronic environment will speed up the processes. For example, data such as cadastral charts, land registry records, and zoning charts can be

presented to appraisers in encrypted form by means of various software in online databases. Necessary infrastructure arrangements can be made for this. Since the transition process to online systems, which should be implemented in official institutions, can be long, applying a single decision in all institutions can be considered as a shorter-term solution. Thus, everyone can receive equal service from every institution (Erdem, 2016).

One of the main problems that institutions encounter when using land registry and cadastre data during their activities for real estate valuation is that some of these data do not reflect the current situation or are far from being a basis for valuation studies. Valuation procedures should be carried out by professional disciplines such as Agricultural Engineering, who have the infrastructure in this field. Survey Engineering, which is a profession that produces and manages spatial information, which is among the most important data of valuation, should assume the role of the leading discipline that organizes and manages valuation studies.

REFERENCES

- Açlar, A., Demir, H., Çağdaş, V., 2003. Real estate valuation expertise and geodesy and photogrammetry (map) engineering, HKMO Journal of Geodesy, Geoinformation and Land Management, Issue: 88, Page: 15-20.
- Anton, C., 2011. Mass Valuation of the Urban Land in Ukraine, Institute of Mining and Geology, Department of Geoinformatics and Geodesy, Specialty Land Surveying and Cadastre, Ukraine.
- Bayram, M., 2007. Expert Training Program in Expropriation Cases, HKMO, Ankara.
- Candaş, E., 2012. Modeling of Legislative Infrastructure for Real Estate Valuation, Istanbul Technical University, Institute of Science and Technology, Master Thesis, Istanbul, 131 p.
- Candaş, E., 2012. Modeling of Legislative Infrastructure for Real Estate Valuation, Istanbul Technical University, Institute of Science and Technology, Master Thesis, Istanbul, 131 p.
- Contemporary, V., 2007. A Real Estate Tax System Design Model Proposal for Turkey, Yıldız Technical University, Institute of Science and Technology, PhD Thesis, Istanbul, 226 p.
- Çete, M., 2008. A Land Management System Approach for Turkey, Karadeniz Technical University, Institute of Science and Technology, PhD Thesis, Trabzon, 243 p.
- Değirmenciler, E., 2008. Real Estate Appraisal Problems and Solution Proposals in Turkey in the Urban Development Process, Kocaeli University, Institute of Social Sciences, Master Thesis, Kocaeli, 103 p.
- Erdem, N., 2016. A Real Estate Appraisal System Approach for Turkey, Erciyes University, Institute of Science and Technology, Department of Surveying Engineering, PhD Thesis.
- Erdem, N., 2017. A Real Estate Valuation System Approach for Turkey. *Geomatics*, 2 (1), 18-39. DOI: 10.29128/geomatik.298417
- FIG, 1995. FIG Statement on Cadastre, Publication, No. 11, Federation internationale des Geomètres.
- Hacıköylü, C., Heper, F., 2010. Problems and solution proposals regarding the determination of tax base in real estate tax, *Journal of Finance*, January-June, Issue 158.
- HKMO, 2012. Symposium Proceedings, Immovable Valuation and Cadastre Symposium in Land Management, ATO International Congress and Exhibition Center, HKMO&TKGM, May 22-23, Ankara, 240 p.
- IAAO, 1990. Property appraisal and Assessment Administration, (Edits: JK Eckert, RJ Gloudemans, R., R., Almy). International Association of Assessing

Officers, Chicago.

Katipoğlu, Y., 2009. Ecrimisil in Public Law, Istanbul Kultur University, Institute of Social Sciences, Master's Thesis, Department of Public Law.

Köktürk, E., Köktürk, E., 2015. Real Estate Valuation, Real Estate Law – Zoning Law – Valuation Methods, Seçkin Publishing, 2nd Edition, Ankara, ISBN 978-975-02-312, 1304 p.

Pagourtzi, E. and Assimakopoulos, V., 2003. Development of real estate evaluation system with the use of GIS technology, In 10th European Real Estate Society Conference, ERES: Conference, Helsinki, Finland.

Rissi, S., B., 2010. Entwicklung Türkischer Immobilienbewertungsverfahren, basierend auf from Erfahrungen der Deutschen Wertermittlungsmethoden, Technische University Munich, Institute for Geodasie, GIS und landmanagement Lehrstuhl for Bodenordnung und.

URL_1: Current Turkish Dictionary, Turkish Language Institution Official Website, <http://www.tdk.gov.tr>, (ET: 2015).

URL_2: <https://osmaniye.csb.gov.tr/mudurlugun-gorevleri-i-88737>

Yalpir, Ş., 2007. Development and Application of Real Estate Valuation Model with Fuzzy Logic Methodology: Konya Example, Selçuk University, Institute of Science, Doctoral Thesis, Konya, 248 p.

Yomralıoğlu, T., Nişancı, R. 2006. The Role and Role of Surveying Engineering in Real Estate Valuation in Turkey, Report 1.0, Karadeniz Technical University, Faculty of Engineering, March, Trabzon.



CHAPTER 15

DATA DRIVEN SURROGATE MODELLING APPROACH FOR ACCURATE MODELLING OF REFLECTARRAY UNIT ELEMENTS

Peyman MAHOUTI¹

¹ Assoc. Prof., Yıldız Technical university, Department of Avionics Orcid ID:
0000-0002-3351-4433

Introduction

Reflectarray antenna (RA) designs had become one of the most acknowledged solutions to achieve antenna designs with high gain and radiation characteristics [1]. This is without any doubt is due to their supreme capability of merging the advantages of parabolic-reflector antennas, phased-array antennas, without a need for a feeding-network for array elements. RA uses a phasing compensation strategy, as it shown in Fig. 1, for each of its element, to manipulate the incoming spherical-wave propagated from the feed antenna (usually a horn antenna) into a plane-wave to focusing the reflected Electromagnetic waves in a shape of pencil beam at the requested direction (θ^0, φ^0) [2]-[4].

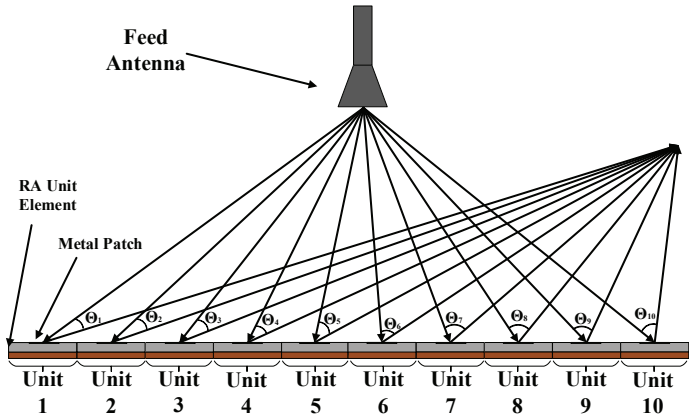


Fig. 1. Schematic of a typical microstrip RA design.

There is a wide list of application for RA designs starting from the space communication (satellite- earth stations), RADAR, or mounted communication systems on vehicles [5-14]. For such interesting topic, many researches had presented many different design approach for proposing a high efficient RA design based on using RA unit elements with multi frequency resonance bands for bandwidth enhancement via implantation of stacked metallic rectangular patches [15-17], parallel dipoles [18-19], concentric ring patches [20], and dual-reflector configurations [21].

The main challenge in RA designs is optimal determination of each and every element in the array. For achieving a RA design with high performance measures, not only designer must struggle against conflicting requirements such as size, operation band etc., that can only be achieved by implementation of unit element designs with complex configuration, but also the designer must carefully determine suitable design value for each element to meet the mentioned requirements. This problem can be considered as a multi-dimension optimization problem. For an example, in a typical

array design with 30x30 elements, there would be 900-unit elements that requires to design to satisfy the required reflection phase with respect to their position and the feed antennas distance. For models without offset or special configurations (multi beam, pattern reconfigurable design etc.) this value can be reduced by taking design symmetrical both in X and Y axis, thus the size would reduce to 15x15. However, even in such case, the design process requires to determine 225 different elements that each of which would have K number of variables $s = [x_1, x_2, \dots, x_K]$ to meet the required reflection phase characteristics that is unique at each array element position. This means that this methodology requires 225 number of Multi objective (Required reflection phase at different operation frequencies for broad band designs)- K dimension optimization process to be run for designing the aimed RA design, of course only if the mentioned symmetrical conditions can be used.

With respect to the given example, such design optimization process or similar ones for larger scale RA design are computationally expensive task which requires a high-end computational setup (High RAM and CPU power) and requires a considerable amount of time even with the usage of state of the art full-wave Electromagnetic (EM) simulation tools [22]. This challenge the designer to make a difficult choice between having a highly accurate modeling approach at the cost of computational cost which might be not even feasible, or have a modeling approach with low accuracy (coarse model) for having computationally feasible design optimization process at the cost of realization errors.

One of the feasible and efficient technique for overcoming this or similar challenging problems is the deployment of an accurate and reliable data driven surrogate regression model representation of unit element. In this approach the data driven surrogate model tries to create a regression strategy to predict the complex relations between the input space (Geometrical design variables, frequency, material setup etc.) with the output space of the given problem [23-26]. For the last decades, many studies had been proposed in field of modelling of microwave stages using Artificial Intelligence (AI) based data driven surrogate models.

Most commonly examples for this field of research can be given as (i) accurate prediction of small/ large signal modelling of active devices or scattering parameter characteristics of microwave transistors based on their DC bias conditions [27-29], (ii) modelling of AC/DC rectifiers for RFID applications [30], (iii) prediction of characteristic impedance for microstrip based transmission lines [31], (iv) and reflection phase of RA designs [32-33]. Commonly in data driven approach for microwave designs either experimental data or 3D EM based simulated data are being

used. Here it must be emphasized that, the main computational cost of data driven surrogate models is the generation of training & validation data sets for surrogate models which requires a considerable effort. However, this is only a single time cost, where after this the obtained model can be used for many different designs optimization process in a computationally efficiency manner.

Ensemble Learning (EL) is the art of carefully binding series of different surrogate models, also known as learners, for solving the aimed regression/classification problem [34]. The principle in EL based surrogate models with learner's models that usually would have low capabilities, are used as building blocks for generating surrogates with higher complexity and capabilities in generating globally accurate responses. Herein, it is aimed to use EL algorithm to create a reliable data driven surrogate model representation for predicting the reflection phase characteristics of a unit RA element for its design variables. Firstly, a RA unit-element design is modelled in a 3D EM simulation tool for creating the training & validation data samples needed for generating data driven surrogate models. Then, in section III, a brief explanation on the theoretical aspects of EL and other state of the art regression algorithms user defined parameters are given alongside of the performance evaluation of algorithms. Finally, brief conclusion section will end the work.

RA Unit Element Design

In this section a square cross like shape presented in Fig. 2 is taken as a novel Reflectarray unit element design which would have a wide range of reflection phase manipulation. As it can be seen from Fig. 3, and Table 1 the design variables allow the element to take shape of many different geometrical design values which would also allow the design to manipulate the reflection characteristic of the incoming EM waves. As it can be seen from Fig. 4, the design variables of unit element model can drastically change the performance reflection phase characteristics. Thus, with respect to this drastic change ability of design variables, the optimal determination of design variables for each and every element is a crucial step for having an accurate design optimization modelling approach. In the next section Ensemble learning technique had been used for creating a data driven surrogate model representation of the proposed RA unit element in Fig. 2, with respect to the design variables defined in range of Table 1.

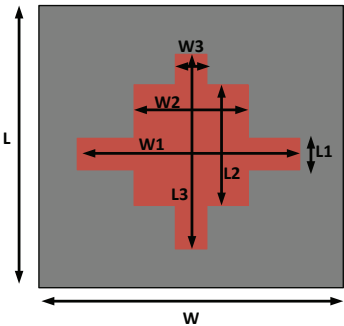


Fig. 2. Schematic view of the Square Cross RA unit element.

Table 1. Lower & Upper boundary conditions of the RA unit design variables in [mm]. $W=L=15$ [mm].

L1	1-14	W1	1-14
L2	1-14	W2	1-14
L3	1-14	W3	1-14

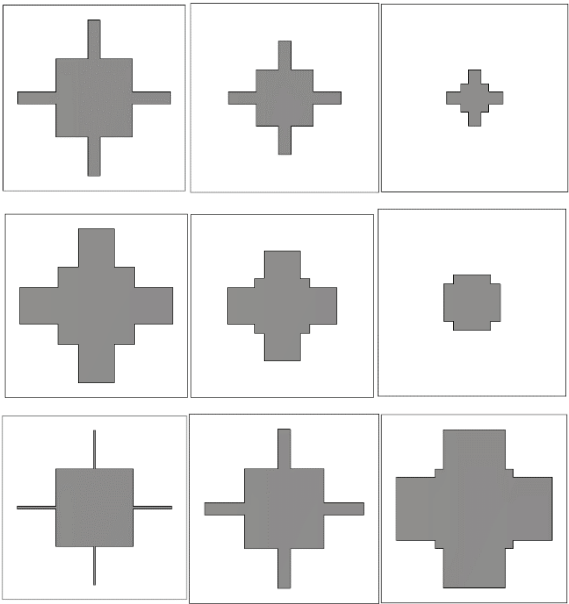


Fig. 3. Different design views for the proposed Square cross unit element for different design values.

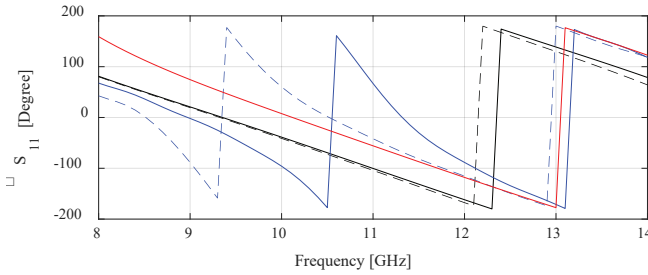


Fig. 4. Reflection phase characteristic of proposed unit element for 5 randomly selected model.

Ensemble Learning Based Modelling of RA Unit Element

One of the recently used state of the art techniques for achieving high performance numerical modelling is Ensemble Learning (EL). In our daily life we also use this strategy for certain decisions or predictions such as in case of a serious illness or a required surgery one would ask the opinion of several doctors before agreeing to a medical procedure, or before purchasing any product with high value one would read user reviewers. In each of these cases, a final decision had been made based on using combination of individual's knowledge. The main principle of EL is similar, the theory of this method is based on using base learners models which usually would have low performance measures as structural blocks for a larger and more involved surrogates to achieve higher performance in their responses. The commonly used techniques for EL can be named as (i) Bagging, a method that is based on deterministic averaging process weak learners, (ii) Boosting, an iterative method which is based on improving the weak learners performance based on the previously obtained performance measures, (iii) Stacking, a method in which N different weak learners are combined using a meta-model to create the output based on the multiple predictions returned by weak learners.

The EL can be divided in three steps (i) Ensemble Generation that is consist of generating sets of learners, (ii) Ensemble Pruning where some of the generated learners are eliminated for better results, (iii) Ensemble Integration where a final surrogate model is achieved by strategically combing the learners [35-36]. This methodology had been an interesting topic for many research in recent years and good results have been reported [37-39]. The advantage of ensembles with respect to single models has been reported in terms of increased robustness and accuracy [40]. Some application of EL are prediction of flood susceptibility [41], PV power generation prediction [42], Groundwater Potential Mapping [43], Regression for Nonlinear and Non-stationary Systems [44], for solar power forecasting [45], and

predication of wind speed [46].

Herein, by using Latin-Hypercube sampling algorithm is used to generates 600 (500 for training and 100 for holdout data sets) samples for based on the given range of design variables in Table 1. In Table II, regression performance of state of the art and commonly used regression algorithms are presented alongside of EL performance measures for cross-fold validation (k=5) and holdout data sets. The hyper-parameters of each model are determined via a grid search protocol based on the k-fold validation. Mean Absolute Error (MAE) is being used for both cross-validation and holdout data sets error metric. Here it is important to achieve a very low MAE performance, for reflection phase. Not only the error of surrogate models can affect the overall performance, but also other effects such as coupling, direction of incident of EM waves would also effect the overall performance large scale RA. Usually in unit element modelling approach of RA designs an average value of ± 10 degrees of MAE is acceptable for modelling approach [48-50]. However, this error cannot be included of model's error, other errors such as manufacturing, placement of elements etc are also included in this criteria. Thus, the performance of the surrogate model must be as low as possible. With respect to this aimed criteria and given results in Table 2, the EL based surrogate model can be defined as an optimal solution for this modelling approach to be used in design optimization of large-scale RA models.

Table 2. Regression performance of series of data driven surrogate models for the proposed RA unit element

Model	Hyper-Parameters	K-fold/Holdout
MLP	Size of Hidden-Layer: three; size of Hidden-Layer Neurons: 10-20-30; Activation function tanh.	6.8/8.1
SVRM	Kernel-function: Radial, Type: Epsilon, Epsilon: 0.25.	5.4/6.8
Gaussian Process Regression	Kernel: ard-matern (5/2); Prediction-technique: Block coordinate; block size: 125	5.9/7.1
EL	Method: Bag; N. Learning Cycle: 250; Learners: Tree.	4.9/5.4

Conclusion

As it mentioned before, without any doubt, Reflectarray antenna (RA) designs had become one of the most acknowledged solutions for high gain antenna designs. However these designs requires a computationally expensive design optimization process due to the complexity of design and large scale of optimization design variables. In this work for achieving a computationally efficient optimization process for large scale RA design, a data driven surrogate modelling approach based on Ensemble Learning

is presented. The proposed methodology is applied on a data set with 500 samples for training and validate on a holdout data set with 100 samples. The performance evaluation of the EL is compared with series of state of the art and commonly used regression algorithm from the literature. Based on the obtained results, the Ensemble learning is a good candidate for creating a data driven surrogate model representation of Reflectarray unit element modelling which can be deployed for design optimization of large scale RA design optimizations. In future works, author aims to extend this research with more detailed analyses including effects such as coupling, direction of incident on unit element modelling stage and have a computational design optimization of a large scale RA design alongside of experimental results.

Acknowledgment

We would like to express our special thanks of gratitude to the Aktif Naser Elektronik and DataRobot, for providing researcher licenses for CST and DataRobot.

REFERENCES

- [1] D. M., Pozar, T. A., Metzler, "Analysis of a reflect array antenna using microstrip patches of variable size. *Electronics Letters*", vol. 27, p. 657–658, 1993.
- [2] J., Huang, J. A., Encinar, "Reflect array Antennas", Wiley-IEEE Press, ISBN: 978-0470-08491-4, 2007.
- [3] F., Güneş, S., Nesil, S., Demirel, "Design and Analysis of Minkowski Reflectarray Antenna Using 3-D CST Microwave Studio-Based Neural Network Model with Particle Swarm Optimization", *International Journal of RF and Microwave Computer-Aided Engineering*, vol.23, no.2, pp.272-284, March 2013, (DOI: 10.1002/mmce.20711).
- [4] F., Güneş, S., Demirel, S., Nesil, "A Novel Design Approach to X-Band Minkowski Reflectarray Antennas using the Full-Wave EM Simulation-based Complete Neural Model with a Hybrid GA-NM Algorithm", *Radioengineering*, Vol. 23, No. 1, April 2014.
- [5] Roederer AG. Reflectarray antennas. In: *IEEE*. ; 2009: 18–22.
- [6] Encinar JA, Zornoza JA. Broadband design of three-layer printed reflectarrays. *IEEE Transactions on Antennas and Propagation* 2003; 51(7): 1662–1664.
- [7] Cadoret D, Laisne A, Gillard R, Le Coq L, Legay H. Design and measurement of new reflectarray antenna using microstrip patches loaded with slot. *Electronics Letters* 2005; 41(11): 623–624.
- [8] Encinar JA, Datashvili LS, Zornoza JA, et al. Dual-polarization dual-coverage reflectarray for space applications. *IEEE Transactions on Antennas and Propagation* 2006; 54(10): 2827–2837.
- [9] Costanzo S, Venneri F, Di Massa G. Bandwidth enhancement of aperture-coupled reflectarrays. *Electronics Letters* 2006; 42(23): 1320–1321.
- [10] WuZH, Zhang WX, Liu ZG, ShenW. A dual-layered wideband microstrip reflectarray antenna with variable polarization. *Microwave and Optical Technology Letters* 2006; 48(7): 1427–1429.
- [11] De Vita P, Freni A, Dassano G, Pirinoli P, Zich R. Broadband element for high-gain single-layer printed reflectarray antenna. *Electronics Letters* 2007; 43(23).
- [12] Pirinoli P, Cong P, Mussetta M, Orefice M. Concentric square ring elements for dual band reflectarray antenna. In: *IEEE*. ; 2009: 1342–1344.
- [13] Moustafa L, Gillard R, Peris F, Loison R, Legay H, Girard E. The phoenix cell: A new reflectarray cell with large bandwidth and rebirth capabilities. *IEEE Antennas and wireless propagation letters* 2011; 10: 71–74.
- [14] Kishor KK, Hum SV. An amplifying reconfigurable reflectarray antenna. *IEEE Transactions on Antennas and Propagation* 2012; 60(1): 197–205.
- [15] Encinar J. Printed circuit technology multilayer planar reflector and method for the design thereof. *European Patent EP* 1999; 1120856: A1.

- [16] Encinar JA. Design of two-layer printed reflectarrays using patches of variable size. *IEEE Transactions on Antennas and Propagation* 2001; 49(10): 1403–1410.
- [17] Misran N, Cahill R, Fusco V. Design optimisation of ring elements for broadband reflectarray antennas. *IEE Proceedings-Microwaves, Antennas and Propagation* 2003; 150(6): 440–444.
- [18] Dieter S, Fischer C, Menzel W. Single-layer unit cells with optimized phase angle behavior. In: *IEEE*. ; 2009: 1149–1153.
- [19] Carrasco E, Barba M, Encinar JA, Arrebola M, Rossi F, Freni A. Design, manufacture and test of a low-cost shaped-beam reflectarray using a single layer of varying-sized printed dipoles. *IEEE Transactions on Antennas and Propagation* 2013; 61(6): 3077–3085.
- [20] Chaharmir M, Shaker J, Cuhaci M, Ittipiboon A. Broadband reflectarray antenna with double cross loops. *Electronics Letters* 2006; 42(2): 65–66.
- [21] Arrebola M, De Haro L, Encinar JA. Analysis of dual-reflector antennas with a reflectarray as subreflector. *IEEE Antennas and Propagation Magazine* 2008; 50(6): 39–51.
- [22] M. Salucci, L. Tenuti, G. Oliveri and A. Massa, “Efficient Prediction of the EM Response of Reflectarray Antenna Elements by an Advanced Statistical Learning Method,” *IEEE Trans. Anten. Prop.*, vol. 66, no. 8, pp. 3995-4007, Aug. 2018.
- [23] Pozar D, Metzler T. Analysis of a reflectarray antenna using microstrip patches of variable size. *Electronics Letters* 1993; 29(8): 657–658.
- [24] Berry D, Malech R, Kennedy W. The reflectarray antenna. *IEEE Transactions on Antennas and Propagation* 1963; 11(6): 645–651.
- [25] Huang J. Microstrip reflectarray antenna for the SCANSCAT radar application. 1990.
- [26] Pozar DM, Targonski SD, Syrigos H. Design of millimeter wave microstrip reflectarrays. *IEEE transactions on antennas and propagation* 1997; 45(2): 287–296.
- [27] Giannini F, Leuzzi G, Orengo G, Albertini M. Small-signal and large-signal modeling of active devices using CAD-optimized neural networks. *International Journal of RF and Microwave Computer-Aided Engineering* 2002; 12(1): 71–78.
- [28] Marinkovic ZD, Markovic VV. Temperature-dependent models of low-noise microwave transistors based on neural networks. *International Journal of RF and Microwave Computer-Aided Engineering* 2005; 15(6): 567–577.
- [29] Gunes F, Mahouti P, Demirel S, Belen MA, Uluslu A. Cost-effective GRNN-based modeling of microwave transistors with a reduced number of measurements. *International Journal of Numerical Modelling: Electronic Networks, Devices and Fields* 2017; 30(3-4): e2089. e2089 JNM-14-0176.R2doi: 10.1002/jnm.2089.
- [30] Ceperic V, Bako N, Baric A. A symbolic regression-based modelling strategy of AC/DC rectifiers for RFID applications. *Expert Systems with Applications* 2014; 41(16): 7061 - 7067. doi: <https://doi.org/10.1016/j.eswa.2014.06.021>

- [31] Mahouti P, Gunes F, Belen MA, Demirel S. *Symbolic Regression for Derivation of an Accurate Analytical Formulation Using Big Data : An Application Example.* ACES JOURNAL 2017; 32(5): 574-591.
- [32] Mahouti P, Gunes F, Caliskan A, Belen A. *A Novel Design of Non-Uniform Reflectarrays with Symbolic Regression and its Realization using 3-D Printer.* ACES JOURNAL 2019; 34(2): 280-285.
- [33] J. Jin, F. Feng, J. Zhang, S. Yan, W. Na, and Q. Zhang, "A novel deep neural network topology for parametric modeling of passive microwave components," in *IEEE Access*, vol. 8, pp. 82273-82285, 2020, doi: 10.1109/ACCESS.2020.2991890.
- [34] Dong, Xibin, Zhiwen Yu, Wenming Cao, Yifan Shi, and Qianli Ma. "A survey on ensemble learning." *Frontiers of Computer Science* 14, no. 2 (2020): 241-258.
- [35] roli, f., giacinto, g., and vernazza, g. *methods for designing multiple classifier systems. in proceedings of the international workshop on multiple classifier systems. lecture notes in computer science*, 2001, vol. 2096. springer, 78–87.
- [36] Mendes-Moreira, J., Soares, C., Jorge, A. M., & Sousa, J. F. D. (2012). *Ensemble approaches for regression: A survey.* *Acm computing surveys (csur)*, 45(1), 1-40.
- [37] liu, y., yao, x., and higuchi, t. 2000. *evolutionary ensembles with negative correlation learning.* *ieee trans. evolut. comput.* 4, 4, 380–387.
- [38] breiman, l. 2001. *random forests.* *mach. learn.* 45, 5–32.
- [39] rodriguez, j. j., kuncheva, l. i., and alonso, c. j. 2006. *rotation forest: a new classifier ensemble.* *ieee trans. pattern anal. mach. intell.* 28, 10, 1619–1630.
- [40] ortiz-boyer, d., hervas-martinez, c., and garcia-pendrajias, n. 2005. *cixl2: a crossover operator for evolutionary algorithms based on population features.* *j. artif. intell. res.* 24, 1–48.
- [41] Choubin, B., Moradi, E., Golshan, M., Adamowski, J., Sajedi-Hosseini, F., & Mosavi, A. (2019). *An ensemble prediction of flood susceptibility using multivariate discriminant analysis, classification and regression trees, and support vector machines.* *Science of the Total Environment*, 651, 2087-2096.
- [42] Ahmad, M. W., Mourshed, M., & Rezgui, Y. (2018). *Tree-based ensemble methods for predicting PV power generation and their comparison with support vector regression.* *Energy*, 164, 465-474.
- [43] Nguyen PT, Ha DH, Avand M, Jaafari A, Nguyen HD, Al-Ansari N, Van Phong T, Sharma R, Kumar R, Le HV, Ho LS, Prakash I, Pham BT. *Soft Computing Ensemble Models Based on Logistic Regression for Groundwater Potential Mapping.* *Applied Sciences*. 2020; 10(7):2469. <https://doi.org/10.3390/app10072469>
- [44] T. Liu, S. Chen, S. Liang and C. J. Harris, "Growing and Pruning Selective Ensemble Regression for Nonlinear and Nonstationary Systems," in *IEEE Access*, vol. 8, pp. 73278-73292, 2020, doi: 10.1109/ACCESS.2020.2987815.
- [45] M. Abuella and B. Chowdhury, "Random forest ensemble of support vector regression models for solar power forecasting," 2017 *IEEE Power & Energy So-*

ciety Innovative Smart Grid Technologies Conference (ISGT), Washington, DC, 2017, pp. 1-5, doi: 10.1109/ISGT.2017.8086027.

- [46] Y. Yang and Y. Yang, "Hybrid Prediction Method for Wind Speed Combining Ensemble Empirical Mode Decomposition and Bayesian Ridge Regression," in *IEEE Access*, vol. 8, pp. 71206-71218, 2020, doi: 10.1109/ACCESS.2020.2984020.
- [47] Cai, J., King, J., Yu, C.; Liu, J.; Sun, L. Support vector regression based behavioral modeling technique for RF power transistors. *IEEE Microwave and Wireless Comp. Lett.*, 2018, Volume 28, pp. 428-430.
- [48] P. Nayeri, F. Yang and A. Z. Elsherbeni, "Broadband Reflectarray Antennas Using Double-Layer Subwavelength Patch Elements," *IEEE Ant. Wirel. Propag. Lett.*, vol. 9, pp. 1139-1142, 2010.
- [49] P. Nayeri, F. Yang, and A. Z. Elsherbeni, "Bandwidth improvement of reflectarray antennas using closely spaced elements," *Prog. Electromagn. Res. C*, 18, 19-29, 2011.
- [50] P. Mahouti, M. A. Belen, N. Çalık and S. Koziel, "Computationally Efficient Surrogate-Assisted Design of Pyramidal-Shaped 3-D Reflectarray Antennas," in *IEEE Transactions on Antennas and Propagation*, vol. 70, no. 11, pp. 10777-10786, Nov. 2022, doi: 10.1109/TAP.2022.3191131.



CHAPTER 16

GEOGRAPHICAL INFORMATION SYSTEMS (GIS) WITH INTELLIGENCE TRANSPORTATION SYSTEM (ITS) IN SOMALIA

*Hatice CananGÜNGÖR¹,
Abdinasir Osman MOHAMED²*

1 Dr.Öğ.Üy. Necmettin Erbakan Üniversitesi Meram MYO Mülkiyet Koruma ve Güvenlik Bölümü, ORCID:0000-0002-5563-9552

2 Yüksek Lisans Öğrencisi Necmettin Erbakan Üniversitesi Fen Bilimleri Enstitüsü ORCID:0000-0002-9537-2688

INTRODUCTION

Transportation systems, their present applications, and the limitations and benefits of geographical information systems. Somalia is one of the countries participating in the process of recovering from the war. It is in the process of developing its economic infrastructure. Several technological advances have been made around ticket cutting as well. The reason for this is that CC cameras can be used to do this from home, so a person has complete knowledge of what happens in their community. Somalia has also made technological progress in airports by making daily flights between the country and abroad with less accidents. This has led to the use of ITS services that they have implemented.

INTRODUCTION TO GIS:

Various authors have defined the geospatial information system in various ways. A set of software, technology, and methods meant to aid in the capture, control, processing, evaluation, mapping, and presentation of geographically referenced information to resolve management and planning issues. (Rhind, 1989).

A computer system that can create, modify, keep, and show geographically related data. (USGS, 1997). A collection of computer-based technologies used to organize geographic data and address geographical challenges. The computer system that allows for the evaluation and display of geographic data. In general, it is a computer-based system that allows for the capture, managing, transformation, evaluation, planning, and visualization of spatial data in order to give management, strategic planning, development, and humanitarian responses. (Omol, 2019).

GIS combines technology, software, and data to store, organize, present, and interpret all forms of geographically related information. Patterns, correlations, and trends will be presented in the shape of GIS-based maps, graphs, and statistics. When your information is placed in a broad setting, it can be easily shared and understood. GIS technology can be utilized to connect any company's current information system. GIS can assist you in obtaining solutions to issues and inquiries. So, if your data is placed in a geographic location, it can be made readily available and accessed. GIS technology is able to connect any enterprise's information system.(ESRI, 2011).

The Geographic Information System (GIS) is among the most significant recent breakthroughs in the study of geography. GIS has had a major impact on spatial assessment and corporate business practice in both the public and private sectors since its inception in the 1970s. A geographic information system (GIS) is, in generally, a system that focuses in the input, administration, assessment, and presentation of geographical (geographically linked) data.(Yadav, 2020).

HISTORY OF GEOGRAPHIC INFORMATION SYSTEM

In his 1968 work, *A Geographic Information System for Metropolitan Management*, Roger Tomlinson invented the term “geographic information system” for the first time. Tomlinson is also known as the “Father of GIS. (Omol, 2019).

When it comes to GIS vocabulary, fundamental GIS texts will provide numerous definitions. This is due to the recognition that there are two basic approaches to GIS. It can be seen from a tool-oriented standpoint, which investigates how software models the world, or from an attitude standpoint, which investigates what GIS enables us to achieve. The instrument approach to GIS explains it in terms of software, such as ArcGIS or Maps. These are typically regarded as sophisticated computer mapping programs. This is a common misconception: GIS software integrates computer mapping with a database management system (DBMS) format such as dbase, Microsoft Access, or Oracle. High-quality graphic output is produced by computer mapping systems such as Adobe InDesign or CorelDraw. Create characteristics, transfer features through one location to another, modify coloring and spacing, and so on. Include geographically referenced database functions.

As a result, the data are presented in two different ways. First, there are rows of organized data, like those found in a typical database. In GIS, this is known as attribute data. Some GIS software programs support the saving of data source in standard database management systems such as those mentioned previously. GIS software is unique in that each row of feature data is also represented by a spatial feature expressed by the coordinate and so network of related. Depending on the data format, this spatial feature could be a point, lines, polygons (technical name for a region or region), or pixels. This is known as spatial data. GIS data combine information about what an object is with information about where it is kept in the database using this mix of an attribute and geographical data. (Gregory, 2005).

Today, there is hardly a sector that has not been influenced by information systems. Today, several applications have been developed to make the best use of information technology. At the same time, it should be noted that maps and geographic information systems are currently very important programs in constructing a location strategy. Geographic information systems are illustrated by the preceding modern software. ArcGIS software, Panorama software, Oasis software, AutoCAD software, and the SAS planetary program are examples of such applications. Cards of various scales are now created in these applications utilizing Global Mapper (and other) software. When it comes to the evolution and development of all these Geographic Information Systems, the concept of Geographic Information System first

appeared in Canada in the mid-1960s under the name Canadian Geographic Information System CGIS. (Kadyrovich-, 2022)

FUNCTIONS OF GEOGRAPHIC INFORMATION SYSTEMS

Seven GIS functions or groupings of functions are used to characterize and identify GIS-T applications:

- Fundamental functions (editing, display, measurements)
- Use an overlay.
- Division that is dynamic.
- The surface modeling is the fourth step.
- Display and analysis of roasters
- Scheduling
- Connects to other applications (for example, transportation modeling packages))(Jain & Kumar, 2016).

Some countries such as Egypt and Somalia had a long history of GIS development and highly competent private sector services in this area. Here, mechanisms such as 'self-contained units' (financially autonomous entities, but subsidized by the state), links with other donor-supported programs, and private-sector commercial operations provide viable options to maintain as well as increase the use of Africaover development and services. For several other countries, cost sharing recovery for services provided by NFPIs to other national users were seen as possible future options. However, clear policies and methods in this regard still seem to be lacking. Therefore, for most of the project countries, the dissemination and continued use of Africaover will depend on government funding and/or donor assistance in the near term.(Lai, 2003).

COMPONENTS OF GIS

Hardware, software, data, people, and methods are the fundamental five components of a GIS.

- GIS software runs on a wide range of hardware types, from central computer servers to desktop PCs, and in standalone or network settings.
- GIS software provides the functionality and resources needed to store, analyze, and show geographic information.
- Data is probably the most crucial component of a GIS. Geographical and related tabular data might be gathered in-house or obtained from a commercial data provider. A GIS integrates spatial data with other data sources and may even use a database management system (DBMS), which is used by most enterprises to organize and keep their data. spatial information

- User/People: GIS technology is useless unless it is controlled and plans to be applied to real-world problems are developed.
- Methods include: A effective GIS uses models and functioning techniques that are unique to each enterprise, in accordance with a well-designed plan and business principles.(Ali, 2020).
- Geographical Information Systems(GIS) have many advantages Since data is linked to a common reference system, GIS may contribute to new ways to think about it and working with old problems; it is simple to use the same data in several applications and to connect previously separate datasets for combined effort.(Ali, 2020).

TRANSPORTATION SYSTEMS ENGINEERING APPLICATIONS OF GIS

Because transportation is geographical in nature, GIS has the potential to generate considerable increases in productivity and efficiency as well as the chance to build new applications for many classic transportation applications. Applications of GIS to transportation, (I) Data retrieval; (II) Data integrator; or (III) Data analysis (Olba, 2006).

INTELLIGENT TRANSPORTATION SYSTEMS

Transportation systems that are intelligent. Urbanization, suburbanization, population expansion and the preference for dispersed communities, as well as the ongoing dependence on the internal combustion as a transportation technology, are all exerting unfavorable consequences on economies and personal life quality in many cities worldwide. Traditional means to addressing these issues boost use of by constructing new roads and extending existing routes. However, we can't construct our way through the bottleneck, as many (but not all) political leaders, decision-makers, and actors recognize. ITS seeks to improve system efficiency using advanced processing, real-time data sensing, and communication technologies, but instead of increasing the physical supply of transportation infrastructure. Decision-makers and stakeholders are becoming aware of the goal. ITS strives to enhance system efficiency with advanced processing, real-time data sensing, and communication technologies, rather than increasing the physical supply of transportation infrastructure. The purpose is to improve the efficiency, safety, and environmental friendliness of transportation networks.(Miller & Shaw, 2001).

Applying ITS to increase transportation safety and efficiency could be an answer to this problem. This can be accomplished by employing sensor technologies, as well as modern communication, information processing, and control technologies(Nengroo et al., 2022.).

AUS provides services and applications in navigation systems, air transportation systems, water transportation systems, and rail systems in addition to road traffic. The Intelligent Transportation System has been separated into generations due to its rising popularity, as well as the demands and improvements in transportation systems.(Qureshi & Abdullah, 2013).

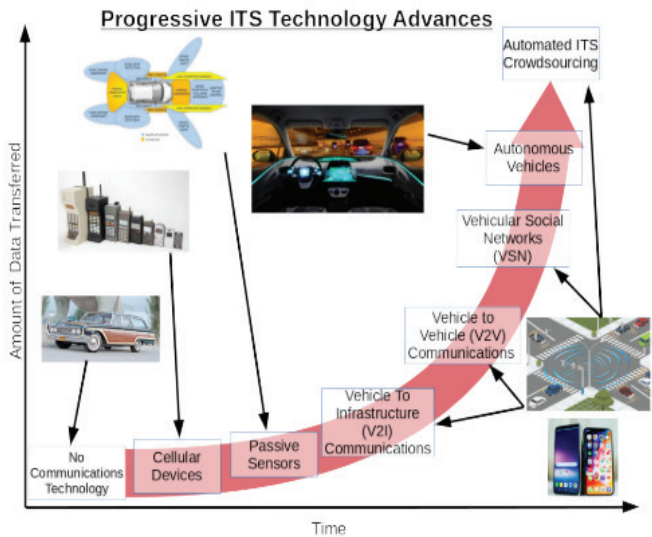


Figure 1. A diagram highlighting the evolution of Intelligent Transportation System (ITS) infrastructure over time, from a minimal/no communication technology baseline to automated. ITS data acquisition systems for the average driver: The developments sit alongside a red exponential growth curve to convey the explosive growth of data generated by these new developments in ITS crowdsourcing technologies, emphasizing the need to design ITS crowdsourcing systems with scalability in mind(Lucic et al., 2020).

SOMALIA’S TRANSPORTATION SYSTEM

Somalia's transportation system covers all types of transportation in the country. The transport infrastructure includes highways, airports, and seaports, as well as a variety of public and private types of vehicles, as well as maritime, aerial, and maritime transportation services.

Roads: Those roads in Somalia are 21,830 km long. Currently, 2,757 km (12%) of the roads are paved, 844 km (3,9%) are gravel, and 18,229 km (83.5%) are unpaved, according to 2010 data. As of May 2015, Puntland had 2,559 km of primary highways, 4,850 km of secondary roads, and

14,421 km of rural or feeder roads. According to the Puntland Ministry of Works and Transport, as of May 2015, there were more than 70,000 registered automobiles in the region. In order to remain competitive on the country's road network, the Puntland Highway Authority (PHA) completed rehabilitation work on the key artery between Garowe and Galkayo in 2012. This artery runs for 750 kilometers through the country's northern regions, including Bosaso, Galkayo, and Garowe. The transportation authority has also undertaken a massive renovation and restoration project on the Garowe-Bosaso Highway since June 2012. Furthermore, in October 2012, the principal arterial connecting Bosaso and Qardho was being renovated. Furthermore, plans are currently being developed for the construction of new roads enabling the littoral communities of the region to have access to the one of the country's major thoroughfares.

Aviation airports: This is a list of airports in Somalia, categorized according to their location and accessibility. It is estimated that Somalia had 62 airports as of 2012. Seven of these airports have asphalt runways, while one has paved runways. Four of the latter have runways that are longer than 3,047 meters, two that are between 2,438 and 3,047 meters, and one that is between 1,524 and 2,437 meters long. There are 55 airports with dirt runways. I believe there are at least three runways that are longer than 3,047 meters; four that are longer than 2,438 meters but less than 3,047 meters; twenty that are between 1,524 meters and 2,437 meters; 24 that are between 914 meters and 1,523 meters; and six that are shorter than 914 meters.

In ports: There are various maritime transport infrastructures in and around the city of Somalia, which is the country's capital and boasts one of the longest coasts on mainland Africa. There are over 15 seaports in all. Mogadishu has several important ports, including Bosaso, Berbera, and Kismayo, all of which are on the coast. Las Kherey and Merca both have two jetty-class ports. Apart from Maydh, Lughaya, A&B, and Eyl, there are also a few minor ports you may be able to find in Aluula, Maydh, Lughaya, Eyl, Qandala, Hafun, Hobyo, Garacad, and El Maan in addition to the major ports.

Railroads: In the beginning, Somalia had only one railway line, which went from Mogadishu to Jowhar. To promote people movement, this railway was known as Villaggio Duca degli Abruzzi at the time. This railway remained in use until the 1960s. A railway of 114 kilometers was built by the colonial authorities of Italian Somaliland in the midst of the 1860's. The rail gauge was 950 mm (3 feet and 38 inches). During the British military control of the territory in the 1940s, it was demolished. There were intentions to rehabilitate the railway in the late 1970s.

RESULTS

Unfortunately, Somalia is one of the underdeveloped countries. When the transportation systems of Somalia are examined, it is seen that it is quite behind in terms of highways. Although In ports; there are various maritime transport infrastructures in and around the city of Somalia, which is the country's capital and boasts one of the longest coasts on mainland Africa. For this GIS and ITS application can be used inports. Especially in the ship transportation in the port, arrangements can be made to save on damages and costs. This is acceptable for GIS and ITS applications as a starting point in Somalia. The results of the implementations by the decision makers can also be applied to other transportation networks within the country. Training courses can be opened for manpower trained in the field of GIS and ITS. Knowledge is power. Using the right information correctly can always bring prosperity to the countries.

Reference

- Ali, E. (2020). *Geographic Information System (GIS): Definition , Development , Applications & Components*. March.
- ESRI. (2011). *GIS for Transportation Infrastructure Management*.
- Gregory, I. N. (2005). A Place in History: A Guide to Using GIS in Historical Research. *Center for Data Digitalisation and Analysis*, 112. <http://www.ccsr.ac.uk/methods/publications/ig-gis.pdf>
- Jain, N., & Kumar, K. (2016). *Map Asia 2003 Transportation Geographical Information System in Transportation Planning*. January.
- Kadyrovich-, K. E. (2022). *HISTORY OF GEOGRAPHICAL INFORMATION SYSTEMS AND ITS IMPORTANCE TODAY* . 98–101.
- Lai, K. C. (2003). *Land Cover Mapping of Eastern Africa Based on Satellite Remote Sensing (Phases I and II) REPORT OF TERMINAL EVALUATION MISSION*. September.
- Lucic, M. C., Wan, X., Ghazzai, H., & Massoud, Y. (2020). Leveraging intelligent transportation systems and smart vehicles using crowdsourcing: An overview. *Smart Cities*, 3(2), 341–360. <https://doi.org/10.3390/smart-cities3020018>
- Miller, B. H. J., & Shaw, S.-L. (2001). Geographic Information Systems for Transportation (GIS-T): Principles and Applications. *Population (English Edition)*, August.
- Nengroo, S. H., Jin, H., Kim, I., & Har, D. (2022). Special Issue on Future Intelligent Transportation System (ITS) for Tomorrow and Beyond. *Applied Sciences (Switzerland)*, 12(12). <https://doi.org/10.3390/app12125994>
- Olba, M. A. A. (2006). GIS Applications in Transportation Analysis and Planning. *CRP 514 Term Paper*, January, 1–51.
- Omol, E. (2019). *Lecture Notes Bit 2307 : Geographical Information Systems*.
- Qureshi, K. N., & Abdullah, A. H. (2013). A survey on intelligent transportation systems. *Middle East Journal of Scientific Research*, 15(5), 629–642. <https://doi.org/10.5829/idosi.mejsr.2013.15.5.11215>
- Yadav, P. (2020). *Applications of Geographical Information System in Transportation Planning (A Case Study of Nagda , Madhya Pradesh)*. November, 159–163.



CHAPTER 17

SUSTAINABLE TECHNIQUES IN COASTAL MANAGEMENT AND PLANNING

Oylum GÖKKURT BAKİ¹

¹ Sinop University, Engineering and Architecture Faculty, Environmental Engineering Department, 57000, Sinop, Turkey, E-mail:ogbaki@sinop.edu.tr (Orchid ID: 0000-0001-7823-0824)

INTRODUCTION

Stating that the coast is unique because it is where land and oceans meet may appear rather obvious, but it is a fact of great significance. The contrast between land and ocean may be dramatic where ocean swells crash against rock cliffs, or more gradual where tides ebb and flow over marshes. It is this interaction between marine and terrestrial environments that makes the coast unique – and uniquely challenging to manage (Kay & Alder, 2002).

Coastal area management aims to increase the environmental quality and to ensure sustainable development in coastal areas within the framework of a sustainable development approach and within the scope of preparation of the environmental management plan. Also, coastal area management is the determination of policy, strategy, program, and land use planning principles and implementation techniques within the framework of environmental management mechanisms in these matters.

The general aim of integrated coastal management in Turkey is to determine the current uses and effects of coastal areas, to provide an integrated policy and sound decision-making process covering all relevant sectors to promote the harmonious and balanced use of the coasts, to carry out protective and precautionary approaches on the coasts, to ensure the development of methods such as national resource and environmental accounting reflecting the value changes that occur as a result of the use of marine areas, and to ensure that relevant individuals, groups and non-governmental organizations have access to reliable data.

Integrated coastal zone management (ICZM) operates in the critical zone where land and sea interact. It is a comprehensive system which both manages development and conserves natural resources. And while so doing, ICZM integrates the concerns of all the stakeholders; i.e. the relevant economic sectors, governmental agencies, and societal interests (Clark, 1997).

The integrated coastal area management studies aim to protect and control the marine environment in front of the coastline (Kapdaşlı, 1992).

To direct the expected developments in the coastal area in harmony with the environment, coastal planning targeting sustainable development is required. For the management of coastal areas to be sustainable, the system must be consistent and have administrative, social, and technical content in a way that will guide the practices. It is also necessary to make a strategy and plan for the legal, regulatory, economic, and public participation tools in administrative, social, and technical content and to put them into practice within the framework of study planning over time.

There are two main oppositions regarding coastal resources. The first is the necessity of using and, hence, consuming coastal resources for human benefit, and the second is the necessity of storing and protecting these resources for long-term uses. In many countries, these two oppositions have reached a critical stage, and coastal areas and resources have been irreparably damaged (World Bank, 1993; Gökkurt Baki, 2011).

Since coastal areas are such important and valuable areas for Turkey, the present study mainly aimed to increase the capacity of local government institutions by improving their knowledge and skills for integrated coastal management, to present the existing legal and institutional regulations, and to reach an appropriate management system, to identify the deficiencies that prevent the effective implementation of the integrated coastal method in the management system, and to reveal the techniques that should be applied in administrative mechanisms and planning to ensure sustainability by revealing the current status in the management of coastal areas.

Coast, Coastal Area, and Management Planning

The coast is an intersection of land and water. A coast should not be regarded only as a demarcation line between the sea and the land. Accepting the coast as a narrow line can bring along various problems in coastal management. Because, a different view of the coast will mean that the policy, strategy, method, and tools to be used for the coast will also vary. The borders of the coast can be determined according to the natural structure of the coastal area, based only on physical criteria, and the areas under the influence of the sea or land environment can be evaluated within the concept by including the economic, social, political, administrative and planning criteria in terms of the area to be managed, as well as the natural characteristics of the coast. (Beatley *et al.*, 1994; Kaypak, 2012). Coasts are the areas where all kinds of water sources such as rivers and lakes meet with the land, not just the sea. Coastal areas are very complex areas where many living and non-living things are located and interact with each other. Coasts can also be used as a shelter, tourism, industry, trade, education, food production, natural, and cultural resources. Coastal areas constitute the intersection of land and sea and have a highly variable natural structure, and are affected by almost all kinds of changes that occur in their vicinity. The fact that coastal areas are used for various purposes including providing living environments for all living things and people, unfortunately in some cases serving as a warehouse where wastes are emptied, shows that the consequences of human activities in these areas are very severe. Therefore, coastal management is much more comprehensive than just coastal protection, or simply the regulation of the coastal environment.

Coastal management can be defined as providing the protection-use balance of the coasts, planning the precautionary and protective measures by considering the possible negative effects and potentials on the coasts in advance, planning the environmental changes in the coastal area, and taking immediate action against them with both technical, managerial and social factors. The main purpose of arranging coastal areas should be to transfer the natural and cultural values of the region and all its beauties to future generations and to rationally use these rich resources (Gökkurt Baki, 2011).

Coastal Management Planning and Technical Specifications

At the onset of the management and planning techniques for coastal areas, the desired objectives, policies and strategies should be planned. Accordingly, it is necessary to plan and arrange some administrative, social and technical titles and to work in an integrated manner with these titles (Figure 1).

At the onset of coastal management, the management approach must be made with an integrated understanding, the responsibilities are shared with a multi-disciplinary working logic, and it is planned in a structure where coordination can be fully realized. Evaluating the dimensions of integration, it is necessary to provide geographical integration, time integration, sectoral integration, and political/institutional integration (Kapdaşlı, 1992). With the integrations expected in these titles, the direction of sustainable techniques and planning is also revealed.

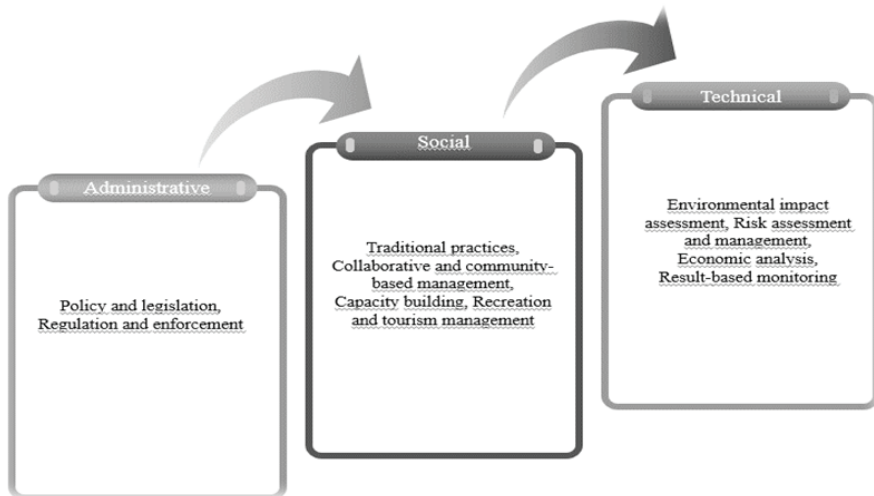


Figure 1. General coastal management and planning techniques (modified from Kay & Alder, 2002)

The management plan puts forward an institutional framework for its implementation and recommendations to decision-makers at the national and local levels for the sustainable use and protection of the coastal ecosystem (Gökkurt Baki, 2011; DHKD-WWF, 1996). Urbanization and economic effects put pressure on coastal areas, leading to new environmental problems emerging or the existing problems changing in terms of quantity and quality. These small areas, where two-thirds of the world's population (Agenda 21, 1993) live, appear as the places where social, economic, and political relations are realized most vividly. When traditional solution methods became inadequate to solve these problems, new solutions emerged on a world scale and integrated coastal management aims to strengthen sustainable management in coastal areas as a dynamic, multi-disciplinary and interactive process. Also, integrated coastal management includes processes such as information collection, ecological-based planning, decision-making, management, and monitoring of implementation and practice. Integrated coastal management describes all uses of coastal areas and the planning process. Integration is realized in different dimensions. Vertical integration can be between public institutions, and local, regional, and national administrative authorities. Horizontal integration takes place across sectors. This is how the integration between public institutions and non-governmental organizations or between social, natural, and engineering sciences, coastal, and marine managers takes place. International integration describes the international coordination that becomes mandatory when the problem areas are located within the borders of two different countries. Regional integration means that the central government takes the lead for solutions to domestic or foreign regional problems (Kaypak, 2012). As seen in the types of integrated coastal zone management, when sustainable management and planning techniques are applied, a management mechanism in accordance with the integrated coastal zone management logic will also be adopted. Thus, the balance of environmental, economic, social, cultural, and recreational goals will be achieved in the long run.

Administrative mechanisms

In the management of coastal areas, it is necessary to deal with the issue from many perspectives. Among these perspectives, it is necessary to examine the policies and legislation, which are included in the administrative mechanisms. Important legal and administrative practices including policy, legislation, directives, zoning plans and status will be discussed under this title.

Ownership in coastal and marine areas is quite complex. Ownership status and responsible management units in the existing coastal and sea areas in these areas where there are many officials and representatives are given in the Table 1.

Table 1. Ownership and responsible management units in coastal and marine areas (Cicin-Sain & Knetch, 1998)

	<i>Offshore land areas</i>	<i>Land areas adjacent to the coast</i>	<i>Sea areas adjacent to the coast</i>	<i>Offshore areas of the sea</i>	<i>Open seas</i>
<i>Ownership</i>	Private	Public/Private	Public in general	Public in general	Public in general
<i>Management level</i>	Local or Regional	A Mixture of National, Regional and Local	A Mixture of National, Regional and Local	National in General	National in General
<i>Working subjects of management units</i>	Multi-purpose institutions	Multi-purpose institutions	Single-purpose institutions	Single-purpose institutions	Single-purpose institutions

Coastal Legislation in Turkey

An important step in the development of coastal legislation was taken with the 1982 Constitution and the coasts were constitutionally guaranteed with Article 43 of the Constitution. The article in the Social and Economic Rights and Duties section; “The coasts are under the rule and disposal of the state. In making use of the shores of seas, lakes, and streams and the coastlines surrounding the shores of seas and lakes, the public interest is primarily considered. The depth of the coasts and coastlines according to their intended use and the possibilities and conditions for people to benefit from these places are regulated by law. (Turkish Constitution, 1982; Yalçinkaya, 2021).

The first legal regulation regarding the planning and construction in the sea, lake, and river coasts in Turkey and the coastlines that are under the influence of these places and are the continuation of these places, was added to the Zoning Law No. 6785 with the Law No. 6785 dated 11.7.1972. Thus, coastal areas have been included in the zoning scheme.

There are provisions related to coasts in many law texts, especially the 1982 Constitution and Coastal Law No. 3621. The primary purpose of the state’s savings on coasts can be expressed as “public interest” within the framework supported by the legislation. However, in the processes carried out for the realization of the purpose of public interest, the existence of immovables owned by the people who own property in the coastal region within the scope of property law is a reality that should be taken into account (Yalçinkaya, 2021).

The Coastal Law No. 3086, which came into force after being published in the Official Gazette dated 01.12.1984 and numbered 18592, is a first in terms of being a law that collects regulations about the coast.

The relevant law states a minimum of 10-meter-wide coastline in the sea, natural and artificial lakes and stream and zoning planned areas, and a minimum of 30-meter-wide coastline in other places (Eke, 1995; Sesli & Akyol, 1999; Yalçınkaya, 2021).

The purpose of the Coastal Law No. 3621 published in the Official Gazette dated 17.4.1990 and numbered 20495 and the Implementation Regulation published in the Official Gazette dated 3.8.1990 and numbered 20594 is to preserve the natural and cultural characteristics of the sea, a natural and artificial lake and river shores and the coastlines that are under the influence of these places and are the continuation of these places, to determine the principles of protection and use for the public benefit, which is open to the benefit of the society, and to cover the regulations on the sea, natural and artificial lakes and river coasts, and the coastlines surrounding the shores of seas and lakes, and the principles of the possibilities and conditions of benefiting from these places for the public benefit. This law is an important step in making a clear and precise definition of coastal areas, specifying the means to protect these areas with methods related to their use, and determining the limits of physical changes that can be made in coastal areas.

Law No. 3830, Implementation Regulation of this law published in the Official Gazette dated 13.10.1992 and numbered 21374, amendments to the said law and regulation published in the Official Gazette dated 30.3.1994 and numbered 21890 and dated 27.7.1996 and numbered 22709. Also, the most important feature of the Regulation on the Implementation of the Coastal Law published in 2004 is to determine the principles of protection and use for the public benefit, open to the benefit of the society, by taking into account the natural and cultural characteristics of the sea, natural-artificial lake and river coasts and the coastlines that are under the influence of these places and are the continuation of these places (Ministry of Public Works and Settlement, 1993).

Different institutions are authorized within the framework of many laws containing regulations on coasts (Table 2). Authorized institutions related to coastal areas in Turkey and the legal basis of these institutions are given in the Table. This is an indication that the authority for the coasts is not gathered on one hand, since different institutions are authorized about the coasts within the framework of the relevant legislation.

Table 2. Authorized institutions related to coastal areas in Turkey and the legal basis of these institutions

Ministry of Internal Affairs (Coast Guard Command Law, Municipality Law)
Ministry of Treasury and Finance (Expropriation Law)
Ministry of Public Works and Settlement (Coastal Law, Zoning Law, Law on Building Inspection)
Ministry of Transport, Maritime Affairs and Communications (Ports Law)
Ministry of Environment, Urbanization and Climate Change (Environmental Law, EIA Regulation, Zoning Law, Coastal Law, Regulation on the Implementation of Coastal Law, National Parks Law, Building Supervision Law, Bosphorus Law)
Ministry of Transport and Infrastructure (Ports Law)
Ministry of Agriculture and Forestry (National Parks Law, Forest Law, Law on the Principles of Emergency Response and Compensation of Damages in Pollution of the Marine Environment with Petroleum and Other Harmful Substances, Fisheries Law)
Ministry of Culture and Tourism (Cultural and Natural Heritage Protection Law, Tourism Promotion Law)
Special Provincial Administrations (Coastal Law, Regulation on the Implementation of Coastal Law)
Metropolitan Municipalities (Metropolitan Municipality Law, Law on Building Inspection)
Municipalities (Municipal Law, Law on Building Inspection)

Coastal areas are within the scope of various legal regulations. In Turkey, there are many legal regulations that directly or indirectly concern coastal areas. This may sometimes also be the reason for the confusion of authority in the coastal area, and accordingly, some problems in the coastal areas are not resolved in the long term.

Zoning status and plans

Development plans in the coastal area are the planning of the economic and social activities carried out in the coastal and marine areas and the ways of benefiting from the coastal areas. These plans should be prepared with a long-term perspective, and be created by considering not only the current use of the coasts but also the future uses. To prepare such a plan, firstly, research is carried out on the coastal environment and utilization forms, usage zoning is conducted, new forms of utilization are envisaged,

and arrangements are made to facilitate the access and use of the coast and sea by the people (Gökkurt Baki, 2011).

One of the most important titles of the administrative mechanisms applied for this purpose is “zoning plans”.

Zoning has also come into common use for allocating publicly owned resources. Zoning serves two main purposes in coastal conservation:

(1) regulatory - for regulatory programs to designate certain areas for particular uses, and

(2) custodial - for nature reserves, to sub-divide them into particular use allocation zones (e.g. diving, nature study, fishing, protection of breeding areas) (Clark, 1997).

In general, zoning plans include the purposes of preserving natural beauties, planning practices for eliminating environmental impacts as a result of urbanization and industrialization, and arranging urbanization according to a modern and sustainable plan and program. Also, it aims to ensure that the structures allowed on the coasts under the legislation are built under a certain plan. Zoning planning in coastal areas is important in terms of determining the current and future use of these areas and creating conditions suitable for the usage requirements of the current legal status of the coasts and coastlines. In this case, to get the expected efficiency from coastal planning, the planning should take all environmental impacts into account as a precautionary measure, be socially acceptable, be compatible with the economic structure, have an architectural and technical aspect, and contain legally appropriate qualifications.

Social Factors

It is known that the management of coastal areas is policies that should be carried out in a sustainable and integrated manner. Another of these policy titles is social requirements and their regulation and harmonization with all environmental, economic, technical, and managerial mechanisms in the management of coastal areas.

In the management of coastal areas, it will be possible to provide sustainable management at a local scale by including all “local” collaborators in an integrated manner and also by creating management plans for social and economic goals. Because each region has its local problems and priorities. Therefore, it is recommended to make plans for local problems rather than general and route planning.

Raising people’s living standards is an important requirement for sustainable coastal areas management that all partners that provide and improve nature, people, and the requirements for life are determined cor-

rectly and take all decisions together.

There are five common principles in the development of community-based management (Drijver and Sajise, 1993; Kay & Alder, 2002) (Table 3).

Table 3. Common principles in developing community-based management

Characteristics	Developing Community-based management
Process approach	Managers and stakeholders agree on overall objectives, and then develop ideas and activities step-by-step towards achieving these objectives.
Participation	All relevant public institutions and organizations authorized with the subject should take joint and sustainable decisions.
Conservation and sustainable use	Sustainable planning needs to be socioeconomically acceptable. For this, it must be developed jointly with all sectors of the society and a consensus must be achieved.
Linkages	Between local management prescriptions, and regional or national level policies and strategies.
Incentive packages	There are an integral part of any community-based management programme. Stakeholders must perceive some benefit from participating in the planning and management of an area.

A community-based management programme has a number of components: community organization, education, civil society organizations involvement, social benefits, government support and institution building (Kay & Alder, 2002).

Capacity Building

Integrated coastal management, in effect, represents a new paradigm of management for the managers, and a new way of thinking and educating for the scientists. The principle of capacity building, one of the key factors for sustainable coastal area management, is one that can overcome implementation problems in long term. This involves raising awareness, participation and increasing capacity (Gökkurt Baki, 2017). “Capacity building” is a central concept in Agenda 21 and in other UNCED agreements. As defined by the UN Development Programme (UNDP) and the UN Division of Law of the Sea (UNDOALOS) in 1994, “Capacity building involves human resource development, the development of organizations and promoting the emergence of an overall policy environment conducive

to the generation of appropriate responses to emerging needs” (Cicin-Sain & Knetch, 1998; UNDP/UNDOALOS, 1994). The components that should be in capacity increase programs are given in the Table 4.

Capacity building efforts thus need to be made in two areas:

1) to re-orient existing managers of ocean and coastal areas toward a more holistic perspective of understanding the interrelationships that exist among multiple human use activities in coastal areas and their ecological impacts and,

2) to train and educate a cadre of coastal professionals in a multi-disciplinary manner emphasizing the inter-relationships among multiple human activities, and natural and physical processes in the coastal zone (Gökkurt Baki & Bat, 2015).

Table 4. Components that should be in capacity building programs (modified from Kay & Alder, 2002; CLBS, 2011; Gökkurt Baki & Bat, 2015)

<i>Capacity building group</i>	<i>Tools</i>	<i>Aim</i>
Human capacity	Education	Addressess the preparation of the required coasytal actors and focus on building an individual’s knowledge.
	Training	
	Professional development	
Institutional capacity	Policy development	Improving institutional arrangements for coastal management.
	Legislative change	
	Restructing	
	Communication	
	Marketing	
	Education	
	Training of professionals (govenrments, business, non-governmental groups,	
	Information dissemination	
Research	Database management	
	Data collection and analysis	
	Database management	
	Results dissemination	

Professional trainers must be employed in the training of professional teams for the sustainable and integrated management of coastal areas. The training of trainers must be carried out by professionals and experts.

Recreation and tourism management

Coastal tourism, together with its sand, sea, and sun features, is considered one of the fastest-growing areas of current tourism. To create a safe, durable, and attractive coastal environment with clean water and healthy coastal habitats, a well-managed sustainable coastal tourism needs to be developed (Figure 2; Figure 3). Integrated coastal zone management is a viable approach to best achieve this goal.



Figure 2. Images of coastal recreational area (original)

Sustainable coastal tourism should include the following statements;

- ❖ Sustainable coastal management practices,
- ❖ Drinking water, air, and healthy coastal ecosystems,



Figure 3. Image of uncontrolled discharged in the coastal area (original; Gök Kurt Baki, 2011)

❖ Ensuring adequate levels of safety for safe swimming and other recreational water uses by managing coastal hazards such as erosion, storms and floods includes beach restoration efforts that emphasize recreational and attractive values, and committed policies to protect wildlife and habitats (Coastlearn, 2009).

Technical aspects

Environmental Impact Assessment

Coastal ecosystems provide numerous services that benefit humans and their communities, including physical protection from natural events, maintenance of species habitat, carbon storage, and recreational opportunities (Comisión Europea, 2009).

“Environmental Impact Assessment (EIA) is a process by which the impacts of a proposal (whether as a policy, management plan or intended development) are identified early on in the decision-making process, so that these considerations are taken into account in the design and approval of the proposal.”(Kay & Alder, 2002).

The goal of taking protective and precautionary approaches on the coasts, included in the logic of environmental impact assessment is of great importance. Under the principle of sustainable development, determining the environmental effects of structuring in coastal areas and analyzing the results to decide on new measures is one of the basic practices of contemporary coastal management (Kapdaşlı *et al.*, 1997). Although there is no coastal-specific environmental impact assessment, the generally applied environmental impact assessments are also valid for coastal areas. However, various tools including land use planning, sectoral development planning, environmental impact assessment, specially protected areas, coastal law, restrictions, and penalties have been used for a long time concerning coastal management, but the desired results cannot be achieved. Accordingly, the efficacy of these tools in practice should be increased (Kaypak, 2012).

Various methods used in environmental impact assessment:

- ❖ - Regarding the effects of various situations, a checklist for a quick assessment.
- ❖ -Key patterns, indicating the effects of proposed activities on various environmental factors.
- ❖ - The creation of models that obtain quantitative values to carry out more detailed studies using a database and to determine the environmental impacts (Rakıcı, 2008).

The primary way to reduce all environmental impacts and human-induced pressures on coastal areas is to adopt ecosystem-based management. Accordingly, some titles and possible implementations are summarized below.

The working framework of ecosystem-based management for coastal zones can be summarized as follows:

(1) Delineation of the management boundary, including both determination of the management area in the coastal zone and identification of the range and types of ecosystems and related stakeholders,

(2) Setting of management goals based on management needs and functions of coastal ecosystems,

(3) Assessment of coastal ecosystems, involving a comprehensive assessment of coastal ecosystems, which should be carried out at a range of temporal and spatial scales,

(4) Formulation of management strategies and actions based on comprehensive assessment and analysis of varying scenarios for coastal ecosystems,

(5) Implementation of coastal zone ecosystem-based management actions through engagement of stakeholders,

(6) Monitoring and assessment of coastal zone ecosystem-based management processes, focussing on the evaluation of the effectiveness of the ecosystem-based management plan,

(7) Promoting adaptive adjustment, including changes that are likely to improve the likelihood of successful management in future (Yuan *et al.*, 2014).

Risk management

Increasing developments in coastal areas are putting the people living here, their property, flora, and fauna at great risk. Especially, a vulnerable situation arises for disasters such as floods, landslides, and tanker accidents. For example, earthquakes are an important coastal risk for the Mediterranean region. On the Black Sea coast, erosion constitutes a coastal risk. Factors that may pose an ecological risk in coastal areas are given in the Table 5.

To reduce the effects and risk of occurrence of natural disasters, these hazards should be evaluated in advance and managed by taking them under control. The standard "environmental risk management" strategy identifies what could go wrong and lists the most serious damage. It examines the probability of these events occurring, how long these disasters can be tolerated if they happen, how these disasters can be prevented, mitigated, or controlled, they can be predicted and planned.

The most appropriate policy option is realized. It evaluates the efficacy of the selected risk mitigation method.

Risk assessment should be a standard part of integrated coastal zone project assessments (Coastlearn, 2009).

Table 5. Factors that may pose an ecological risk in coastal areas (adapted from Yanes *et al.*, 2019)

<i>Factor</i>	<i>High value assessment factor for ecological risk in coastal areas</i>
Uncontrolled pollution effects (solid waste and other environmental problems)	All solid wastes negatively affect the coastal area. Especially inorganic solid wastes (metal, plastic, glass and all hazardous wastes) are the ones that negatively affect the coastal area.
Over-urbanization	It is one of the most important and permanent problems arising from the lack of planning and management in coastal cities.
Land use changes	Changes in land use have significant effects on coastal ecosystem.
Coastal erosion and sedimentation	Antropogenic activities that generate coastal erosion and sedimentation (Yanes <i>et al.</i> , 2019)
Species diversity	Deltas and lagoons are very important in terms of invasive species diversity in the coastal area. In addition, these areas are important in terms of oxygen production and water quality.
Vulnerability	Intense land uses and unplanned urbanization on the coasts and confusion of authority create security vulnerability in coastal areas and ecosystems.

The titles based on UNESCO, 2006 reference the damages and ecological risks that may occur during the use of coastal areas are as follows; (adjusted from UNESCO, 2006; Yanes *et al.*, 2019).

These are; eutrophication, habitat loss or fragmentation, hypoxia, affectation of the water column, bottom disturbance, introduction of exotic species, changes in regimes, implications of endangered species or critical habitats, alterations in turbidity, loss of landscape integrity, productivity affects, affections on more sensitive species, deterioration of environmental quality, impairment of coastal edge integrity, changes in biodiversity, changes in sediments, overfishing—accidental catch—return of fish to the sea, changes in the composition of communities, effects on trophic structure, health effects on populations, habitat degradation.

Economic analysis (Benefit-cost analysis)

Coastal zones are vital economic hubs in terms of settlement, industry, agriculture, trade and tourism, as well as being of great environmental significance (Yuan *et al.*, 2014).

Difficulty in applying economic techniques to evaluate investments with nature values; nature values are difficult to describe in currency.

Also, the features of coastal systems are not always fully understood. The positive or negative effects (benefit and cost) of one activity on another can be neglected. Some economic sectors in coastal cities are given in Table 6.

Table 6. Examples of some economic sectors located in coastal cities (Sorensen & McCreary, 1990; Clark, 1996)

<i>Sectors that generally belong to coastal areas</i>	<i>Sectors that are not in the coastal area but affect the coasts</i>
Navy and other national defense operations	Forestry
Port and harbor development	Fish and wildlife management
Shipping and navigation	Parks and recreation
Recreational boating and harbors	Water pollution control (Deep Sea Discharge)
Commercial and recreational fishing	Energy generation
Mariculture	Transportation
Tourism	
Marine and coastal research	
Shoreline erosion control	
Housing	
Mining	
Industrial development	
Uncontrolled agriculture	

As an example of techniques that can be used in economic evaluation:

❖ **benefit/cost analysis:** In this analysis, discounted earnings and costs are compared. For a development to sustain, the gains must exceed the costs.

❖ **lowest cost analysis:** earnings are not taken into account in this analysis. This method is used when earnings cannot be determined or there are no significant differences between alternative earnings. In this case, considering the discounted costs, the alternative with the lowest possible cost is taken into account (Coastlearn, 2009).

CONCLUSION

The main purpose of coastal management and planning is to make the life of people, as well as all living things, sustainable, and to meet the needs and wishes of all living things. There is a lack of reliable data to meet the need for spatial data for the application of sustainable techniques

in coastal zone management and planning, and this deficiency is still experienced and continues to be a problem for scientists and subject experts. Access to an accessible and reliable data bank is very important for the sustainable management and planning of coastal areas and the healthy implementation of necessary techniques.

In the management of coastal areas, it will be possible to ensure sustainability in the planning of coastal areas by creating plans with approaches that will emphasize administrative, environmental, economic, and social factors. Thus, it will be possible to protect the resources in coastal areas and ensure the continuity of the ecosystem.

While determining the problems and solutions of coastal areas, rote understanding should be avoided and local problems should be determined. All levels of government within a country should be involved in coastal management and planning. Local problems of each area may vary. These differences mean that there will be a need for different solutions. Also, if the coastal area problems are of international and/or regional dimensions, the logic of integration can reach international dimensions and regional dimensions within or outside the country.

Increasing the capacity is very important for the sustainable use of coasts. There are two ways to do this. This is in the form of personal and institutional-based capacity building. In particular, increasing the capacity at the institutional level, in other words, the training of trainers, should be carried out with a professional team.

Traditional management plans and practices should be avoided on the coasts. In the management of coastal areas, comprehensive and ecosystem-based management planning should be adopted immediately and coastal management units should be established for implementation. Because they are both ecologically and economically important areas.

Coastal areas fall under the application area of various legal regulations and there are many legal regulations that directly or indirectly concern coastal areas in Turkey. Since legal regulations are within the jurisdiction of various institutions, confusion may arise among the authorities in coastal areas.

This study will be a guide for managers who are in the decision-making process in the complex and multi-disciplinary management of coastal areas. It is thought that the arrangements to be made in the titles specified in the study will guide the sustainable management of coastal areas.

REFERENCES

- A. Yanes, C. M. Botero, M. Arrizabalaga, J. G. Vásquez, “Methodological proposal for ecological risk assessment of the coastal zone of Antioquia, Colombia”, *Ecological Engineering*, 130, 242–251, 2019.
- Agenda 21, 1993. “Programme of Action for Sustainable Development, Rio Declaration on Environment and Development”, Report of the United Nations Conference on Environment. United Nations, New York.
- B. Cicin-Sain, R.W. Knecht, “Integrated Coastal and Ocean Management: Concepts and Practices”, Island Press, Washington DC, 1998.
- C. Drijver, P. Sajise, “Community-Based Resource Management and Environmental Action Research, in Proceedings of the Experts’ Workshop on Community Based Resource Management: Perspectives, Experiences and Policy Issues, Los Banos: Environmental and Resource Management Project and UPLB”. 1993.
- Coastlearn 2009. “Coastlearn distance learning package CD for integrated coastal zone management”, 2009.
- CLBS, 2011. “CoastLearn-Black Sea Project Meeting Report”, *June 2011, Varna-Bulgaria*
- Comisión Europea, 2009. “Naturaleza y biodiversidad: El papel de la naturaleza en el cambio climático. Oficina de Publicaciones”, Unión Europea.
- DHKD-WWF, 1996. Belek Coastal Management Plan. Natural Life Protection Association, Istanbul.
- F. A. Sesli, N. Akyol, “Türkiye’de Kıyı Alanları Konusunda Geçmişten Günümüze Ulusal Mevzuat”, *TMMOB Harita ve Kadastro Mühendisliği Dergisi*, 86, 101-111, 1999.
- F. Eke, “Kıyı Mevzuatının Gelişimi ve Planlama”. T.C. Bayındırlık ve İskân Bakanlığı Teknik Araştırma ve Uygulama Genel Müdürlüğü, Yayın no:77, Ankara. 1995.
- J.C. Sorensen, S. T. McCreary, “Institutional arrangements for managing coastal resources and environments”, *Coastal Management Publication No. 1 (Rev)*, US National Park Services, Washington D.C. pp. 194, 1990.
- J.R. Clark, “Ocean & Coastal Management”, Vol. 37, No. 2, pp. 191-216, 1997, PI I: S0964-5691 (97)00052-5 0964-5691/97, 1997.
- L. Yuan, Z. Ge, X. Fan, L. Zhang, “Ecosystem-based coastal zone management: A comprehensive assessment of coastal ecosystems in the Yangtze Estuary coastal zone”, *Ocean & Coastal Management*, 95, 2014.
- Ministry of Public Works and Settlement, “Our Coasts, Legislation, Planning and Implementation Seminar”. Ankara. 1993.
- N. M. Yalçinkaya, “Türkiye’de kıyı alanlarında yaşanan sorunlar çerçevesinde hukuki süreçlerin incelenmesi”, *İstanbul Ticaret Üniversitesi Sosyal Bi-*

- limler Dergisi, 20(41), 924-950. doi: 10.46928/iticusbe.980906,2021.
- O. Gökkurt-Baki, "Coastal Management in Sinop City Center", Ondokuz Mayıs University, Institute of Science and Technology, Department of Environmental Engineering, 287 p. 2011.
- O. Gökkurt Baki, L. Bat, "Capacity Building Key Issues on Integrated Coastal Zone Management for Turkey Black Sea Coast", *ICOCEE – CAPPA-DOCIA, 2015, Nevsehir, TURKEY*, May 20-23, 2015.
- O. Gökkurt-Baki, "The coastal zone management in Turkey the principles and basic problems", *Researches on Science and Art in 21st Century Turkey*, Editors: Prof. Dr. Hasan Arapgirlioglu, Assist. Prof. Atilla Atik, Prof. Dr. Robert L. Elliot, Assoc. Prof. Edward Turgeon, Volume 2, Chapter, 243. pp:2163-2168. 2017.
- R. Kay, J. Alder, "Coastal Planning and Management". E & FN Spon. 375 s. 2002.
- S. Kapdaşlı, Kıyı Mühendisliği. İstanbul Teknik Üniversitesi Yayını, İstanbul, 277 s, 1992.
- S. Kapdaşlı, D. Maktav, F. Sunar, "Kıyı Mühendisliğinde Ölçüm Teknikleri ve Uzaktan Algılama Teknolojisi Gereksinimi", 3. Uzaktan Algılama ve Türkiye'deki Uygulamaları Semineri, Bursa, 1997.
- Ş. Kaypak, Kıyı Alanları Yönetiminde Bütünleşik Politikalar, *Integrated Policies in the Management of Coastal Areas Coastal and Marine Areas of Turkey, Türkiye'nin Kıyı ve Deniz Alanları IX. Ulusal Kongresi 14-17 Kasım 2012, Antakya-Hatay*, L. BALAS, A.N. GENÇ (Editörler) Antakya-Hatay, 2012.
- T. Beatley, J. B. David, K. S. Anna, *An Introduction to Coastal Zone Management*, Island Press, Washington, D.C. 331 p. 1994.
- T.C. Rakıcı, *Coastal Area Management and Morphological Evaluation: Terkos Coastal Area Example*, Yıldız Technical University Institute of Science and Technology, Master Thesis, 116 p. 2008.
- Turkish Constitution (1982). "Constitution of the Republic of Turkey", <https://www.mevzuat.gov.tr/MevzuatMetin/1.5.2709.pdf>, (e.t. 25/04/2021)
- UNDP/UNDOALOS 1994. "Report on the Consultative Meeting on Training in Integrated Management of Coastal and Marine Areas for Sustainable Development", Sassari, Sardinia, Italy, 21-23 June, 1993. United Nations Development Programme and, Division for Ocean Affairs, United Nations, New York.
- UNESCO 2006. "A Handbook for Measuring the Progress and Outcomes of Integrated Coastal and Ocean Management". IOC Manuals and Guides, Paris.
- World Bank, 1993. "Guidelines for Integrated Coastal Zone Management". (Ed.: J. C. Post and C. G. Lundin), *Environmentally Sustainable Development Studies and Monographs Series No. 9*, 16 p.



CHAPTER 18

HEAT-MASS TRANSFER ANALOGY OF IMPINGING JETS

*Abdullah BINGOL¹,
Nevin CELIK²
Ihsan DAGTEKIN³*

1 Yk. Muh., Firat University, Department of Mechanical Engineering, 23279, Elazig, Turkey

2 Prof. Dr., Nevin Celik Professor at Firat University, E-mail: nevincelik@firat.edu.tr, ORCID: 0000-0003-2456-5316

3 Prof. Dr., Firat University, Department of Mechanical Engineering, 23279, Elazig, Turkey

1. INTRODUCTION

In heat transfer experiments, it is often very difficult to determine the heat transfer coefficient if the temperature changes rapidly over a small region. Such measurements may contain a high rate of wall-transmission errors. Precise temperature measurement in such complex geometries or flows requires high technology. New methods have been developed in recent years in order to save both money and time during the measurements. One of them is naphthalene sublimation technique based on mass transfer technique.

The impinging jet technique, in which mass transfer measurements are frequently and successfully applied, is very useful in terms of providing a high and controlled local heat/mass transfer coefficient, and many processes such as heating, cooling and drying can be carried out effectively by impinging jets. Applications of this technique are seen in high temperature gas turbine cooling system, cooling of electronic components, drying of wood, textile, paper, film industry, glass processing applications and industrial food processing.

The best known mass transfer method is undoubtedly naphthalene sublimation technique. In this technique, the heat transfer coefficient is determined by utilizing the analogy between mass transfer and heat transfer. With this method, even the most intricate geometries can be measured. For example, thanks to this technique, measurements can be made easily on the inner surface of a pipe, at the edge of a hole, at the end corners of a surface, or in the recesses and protrusions.

This book chapter, which aims to find the heat transfer based on the mass transfer caused by the sublimation of naphthalene, consists of 5 sections. In the second part, which follows the first part of the introduction, literature research, general introduction of naphthalene sublimation technique and its applications, as well as heat-mass transfer analogy are explained. In the third section, the experimental study and the calculation method are introduced. In the fourth section, the experimental results are presented. Finally, the results are evaluated in the fifth section.

2. LITERATURE SURVEY

Impinging air jets have high heat and mass transfer capabilities. Therefore, they are used in many applications such as drying paper, textile and ink, tempering glass, hardening of metals, cooling of electronic devices, cooling of turbine blades. However, constantly developing technology and increasing demands create a desire to increase the already

high heat and mass transfer even higher. However, the increasing value of energy day by day necessitates this increase with the minimum possible cost. Therefore, many experimental and numerical studies have been done and are being done on this topic.

Surface average heat/mass transfer in impinging jet systems is very important especially in cooling, heating and drying processes. For this reason, it is necessary to obtain experimental data on the surface average mass transfer coefficient and to determine whether the jet is used or not. It is important to develop the mass transfer relationship on the surfaces. In this study, the determination of the heat transfer coefficient in impinging jets was carried out by the naphthalene sublimation technique based on the mass transfer method. Since, it is a very broad subject the literature review of impinging jets is limited to studies using mass transfer techniques, especially the well-known naphthalene sublimation technique.

Solak (2017) has been examined the mass transfer that occurs when the jet immersed in a jet cell is impinged on a surface positioned at different angles. The local mass transfer coefficients on the impact surface were determined by using the electrochemical confining diffusion current technique. It was determined that the mass transfer measurements performed on the impact surface reached a maximum value around the jet stagnation point. Sara et al. (2008) described the mass transfer that occurs when a liquid jet is impinged on a rotating surface. The mass transfer coefficients were measured by using the electrochemical confining diffusion current technique. Arzutug's (2003) study covers an analysis on mass transfer between the surface and the rotating jet impinging in a cell. The mass transfer measurements were made with a circular tube jet and it was determined that the mass transfer coefficients gave a maximum around the stopping point. A detailed mass transfer study was also done by Arzutug and Yapici (2009). Local mass transfer coefficients were obtained using the electrochemical limit diffusion current technique. It has been determined that the peak Sherwood values at the impact point increase with the Reynolds number. Feroz and Prasad (2006) presented experimental results regarding the mass transfer coefficient in the impact region of the assembly consisting of multiple jets. The relationship between the nozzle diameter width and the mass transfer coefficient was investigated. Mass transfer increases with nozzle width; The height of the nozzle decreases with increasing surface area and electrode size. Chen et al. (1998) experimentally investigated the mass transfer that would occur with a single impinging air jet. In the study, the air coming out of a circular cross-section jet was again blown onto a circular flat surface. The number of Sherwoods, which increased in proportion to the number of revolutions until a certain period, started to climb after a certain period by disrupting

its linearity. Pekdemir and Davies (1998) experimentally investigated the drying of a rotating cylinder surface with a rectangular jet. Photo-evaporative technique developed by Pekdemir was used in the study. According to this technique, the surface is covered with chromatographic paper and the color change due to wetness is infrared observed under (infrared) light. It is concluded that the optimum jet-to-target surface distance shifts from 4 to 8 as the jet Reynolds number increases. Rhe et al. (2003) conducted an experimental study on heat and mass transfer in multiple jets. At the end of the study, it was reported that for low jet-to-jet values, counter-current effects on heat and mass transfer are dominant, and an increase in local heat and mass transfer coefficients at the impact points occurs at these specified distances. Hong et al. (2009) experimentally investigated the heat and mass transfer to be created by the impinging air jet in the duct. The results obtained from the study are briefly as follows; at $H/D = 6$, for both output configurations, the average Sherwood number obtained when the duct is placed horizontally on the rotating table is significantly reduced relative to that when placed perpendicular to the stationary and rotating table.

The naphthalene sublimation technique has been widely used in various experiments since the 1950s. The experiments aim to find the average and local mass transfer at the surface. Average coefficients are weighed and local coefficients are measured by measuring the depth with special devices. For complex geometries under desired boundary conditions, we can obtain detailed information about mass transfer through local measurements. The geometry of test specimens can be shapes that are easy to cast and measure, such as a flat plate, circular or rectangular cylinder. In the experiments conducted in recent years, local measurements are made in detail in curved shapes such as turbine blades (Chen and Goldstein, 1992) and in difficult geometries such as in-hole surface. The mass transfer of circular discs (Sporrow and Geiger, 1985) and square or rectangular plates at rest at various angles can be studied. Goldstein and Cho (1995) examined the naphthalene sublimation technique in detail. In the study, general information such as the physical properties of naphthalene and its diffusion in the air are given, and then the application of the technique is presented in detail. In the study, information about many naphthalene sublimation applications made in the literature is also given. In addition, limitations in the use of this technique have been stated and recommendations have been made about the places where it will be used. Goldstein et al. (1985) investigated the heat transfer of a protruding cylinder placed perpendicular to the axis on a naphthalene coated flat plate. While simulating heat-mass transfer, they took the naphthalene vapor density in the free stream to zero and created a constant density boundary condition on the surface. This is similar to the constant temperature

boundary condition in heat transfer. Russ and Beer (1997) investigated the heat transfer and flow field on the inner surface of a sinusoidal curved pipe. Since there is mutual symmetry from the axis, half of the pipe is taken. This piece is covered with naphthalene by casting method. A computer-controlled micrometer-level moving table scanned the sinusoidal surface to measure depth. Local Sherwood numbers were determined by using the data obtained. Nusselt number variation could be determined by using the appropriate analogy. Cho et al. (1997) determined the mass/heat transfer occurring around and inside a simple hole drilled on a flat plate using naphthalene sublimation technique. In the study, local and average Sherwood numbers were found for different angles of the hole. Jets form the wide range of uses of naphthalene sublimation technique. In the experimental study conducted by Sparrow and Lovell (1980), mass transfer was measured by striking a circular air jet on a naphthalene surface at right and oblique angles, and the heat transfer rate was passed with an appropriate analogy. The change of the jet tilt angle has displaced the stagnation point. It was observed that the maximum heat and mass transfer rate was not highly sensitive to the jet inclination angle. Sparrow and Wong (1975) investigated the impact of an initially laminar fully developed slit jet onto a water and airtight unbounded plane plate using the naphthalene sublimation technique. Ward and Mahmood (1982), in an experimental study on turbulent rotating and impinging jets, investigated the mass and heat transfer rates of rotating air jets striking a flat plane perpendicularly. Mass transfer data were determined using naphthalene evaporation (sublimation) technique as a thin film. Chilton-Calburn analogy was used to determine the heat transfer rates by using mass transfer. The applicability of this analogy to jet impact systems has been determined by studies. Popiel and Baguslowski (1988) studied the flow patterns of heat/mass transfer formed by the circular jet hitting a flat surface. The mass transfer coefficient formed in the radial direction was measured using the naphthalene sublimation technique. As a result of the study, flow characteristics, radial distribution of mass transfer, mass transfer measurements at stopping point and correlations are given. Chen et al. (1998) used naphthalene sublimation technique in their experimental study to investigate the heat (mass) transfer of the circular jet striking the rotating disk. As a result of the experiments, it was found that; heat (mass) transfer is divided into three regions; impact-dominated region, mixing region, and rotation-dominant region. Kataoka and Mizushima (1974) investigated the effect of free current turbulence on the local heat transfer rate in an impinging circular jet using the electrochemical confining diffusion current technique. As can be seen from the literature review, the naphthalene sublimation technique has proven to be an excellent method for obtaining heat transfer results (Goldstein and Cho, 1995).

Many researchers using the technique have argued that the mass transfer process can be established with cleaner boundary conditions and that it can be studied more easily and more accurately than the related heat transfer process (Sparrow et al., 1985).

3. NAPHTHALENE SUBLIMATION TECHNIQUE

3.1. What is Naphthalene?

Naphthalene is a bright crystalline white compound with its own specific odor. It has an organic structure and belongs to the aromatic compounds class of organic chemistry. The structure of naphthalene is cyclic. Naphthalene is obtained from coal tar by a special method called sublimation. There is plenty of naphthalene in the tar separated from the raw gas while producing gas. Compounds such as *naphthol*, *naphthylamine*, *naphthoquinone* derived from naphthalene serve to obtain dyestuffs.

Naphthalene is insoluble in water, cold alcohol, but soluble in hot alcohol and ether. It has sublimation feature. Picric forms a solid compound with acid. The melting point of this compound is 151°C. By utilizing this reaction, naphthalene is characterized. Since the smell of naphthalene is repellent to moths, it is used to protect woolen goods. Naphthalene has a poisonous effect on the eyes.

3.2. What is Sublimation?

Sublimation is the transformation of a solid into a vapor state without going into a liquid state, or, conversely, the transition of a gaseous material from liquefying to a solid state. This process can be done at normal atmospheric pressure or vacuum. The basis of this process is the equalization of the vapor pressure to the atmospheric pressure before reaching the melting point as a result of heating the solid material. If a compound with a melting point under normal atmospheric pressure is desired to be sublimated, this can be done in a low pressure environment. To do this, first find the vapor pressure of the compound at the moment of its melting point. The substance can then sublime if the working pressure is applied below the vapor pressure at this melting point.

There is no liquid state in sublimation. Dry ice (solid carbon dioxide), naphthalene, iodine, arsenic, and camphor are examples of sublimating substances. Sublimation is a process that takes place by taking heat. The force of attraction between the particles of subliming substances is weak. Therefore, they go directly from the solid state to the gas state. Since the structure of the substance does not change in the sublimation

event, the event is a physical change. Open air pressure is important in sublimation. By reducing the air pressure, the sublimation rate is increased. Sublimation is used to purify some substances in closed containers.

The odor removers we use in the toilets are the naphthalene sublimation substances we use to prevent our clothes from getting mothballs. We feel that naphthalene or deodorizers decrease over time and emit odor, but we do not see the liquid form of these substances. The reason for this is sublimation. Snow and ice sublime, albeit slightly. Laundry hung out to dry in winter is provided to dry even though they are frozen. The direct conversion of gaseous matter to solid is called deposition. Defrosting is the opposite of sublimation. Especially in the winter months, icing occurs on the windows of the cars. The water vapor in the air is directly converted to ice.

One of the most important applications of sublimation is vacuum freeze drying. Some substances that deteriorate when dried with normal techniques are placed in a vacuum chamber and cooled slightly below the triple point temperature of the liquid to be removed by drying. The frozen liquid (usually ice) sublimates and leaves the substance. The resulting steam is either pumped out of the vacuum chamber or refrozen. A common process in stage effects is the production of artificial smoke or fog with solid carbon dioxide (dry ice). Since the triple point pressure is above atmospheric pressure, carbon dioxide evaporates before reaching its melting point and does not liquefy at atmospheric pressure. The vapor that comes out of dry ice by sublimation, because it is very cold, causes the water vapor in the air to condense by giving fog. The most common example of sublimation is the gradual disappearance of falling snow, although the temperature does not drop to 0 °C.

3.3. Properties of Naphthalene

The naphthalene sublimation technique let us to obtain very accurate measurements and is very advantageous in obtaining boundary conditions compared to the heat transfer method. However, the success of this method depends on the correct determination of naphthalene properties. The properties are given in Table 1.

Table 1 Properties of naphthalene (Goldstein ve Cho, 1995)

	Explanation	Unit
Chemical formula	C ₁₀ H ₈	
Molecular mass	128.17	kg/mol
Melting point	80.2	°C
Normal boiling point (P _{air} = 1.01325 bar)	217.993	°C
Freezing point (P _{air} = 1.01325 bar)	80.285	°C
Triple temperature point	80.28	°C
Critic temperature	472.5	°C
Sublimation enthalpy	70.36	kJ/mol
Liquid density (P _{air} = 1.01325 bar, T _{air} = 80.23 °C)	0.978	kg /m ³
“ “ (P _{air} = 1.01325 bar, T _{air} = 120 °C)	0.946	“
“ “ (P _{air} = 1.01325 bar, T _{air} = 130 °C)	0.938	“
Critic pressure	40.51	Bar
Critic volume	413x10 ⁻⁶	M ³ /mol
Solid density (at 20 °C)	1175.0	kg/m ³
Solid thermal conductivity	0.333	W/m-K

Air properties of naphthalene are given in Table 2.

Table 2 Properties of naphthalene vapor in the air (Ambrose vd., 1975)

T (K)	P _v (Pa), (naphth.)	ν x 10 ⁶ (m ² /s)	D _{naphth} x 10 ⁶ (m ² /s)	Sc (naphth.-air)
290	4.918	14.811	6.455	2.290
295	8.206	15.268	6.671	2.284
300	13.434	15.731	6.891	2.278
305	21.604	16.200	7.115	2.272

Schmidt number and the diffusion coefficient of naphthalene in air and are calculated by various researchers. The diffusion coefficient of naphthalene in air was estimated as the average of 0.066 to 0.0702 values at 298.16 K (Goldstein and Cho, 1995). Thus, the diffusion coefficient was found to be 0.0681. As a result, the most generally accepted correlations for diffusion coefficient and Schmidt number are as follows:

$$D_{naphth} = 0.0681 \left(\frac{T}{298.16} \right)^{1.93} \left(\frac{1.013 \times 10^5}{P_{atm}} \right) \text{ cm}^2/\text{s} \quad (1)$$

$$\nu_{air} = 0.1556 \left(\frac{T}{298.16} \right)^{1.7774} \left(\frac{1.013 \times 10^5}{P_{atm}} \right) \text{ cm}^2/\text{s} \quad (2)$$

$$Sc = 2.28 \left(\frac{T}{298.16} \right)^{-0.1526} \quad (3)$$

In all three of the empirical correlations given here, pressures are calculated in Pascal and temperatures in Kelvin.

3.4. Application of Naphthalene Sublimation Technique

The naphthalene surfaces used in the studies where naphthalene sublimation technique is applied are generally seen as naphthalene coated surfaces. Naphthalene coating on test samples includes machining, dipping, spraying, casting, or a combination of these processes. Let's take a brief look at these methods.

Machining: In this method, test samples are obtained from naphthalene blocks obtained by casting or dipping using milling machine or something similar. Our effort is to obtain a large number of products of the same type and to ensure that the samples are smooth. There is a difference between samples from casting and samples that are out of production.

Immersion: This method is perhaps the easiest of all methods. Coating is done by immersing the test piece in a liquid naphthalene furnace. Alternatively, you can dye a test sample with liquid naphthalene. However, with this method we could be reproducible and problems such as uniformity of thickness arise. You can see the immersion especially in thin fin applications.

Spraying: A substrate is formed by spraying molten naphthalene using the spraying method. The coating is a thin layer approximately 0.015-0.115 mm thick. The spray coating process is more suitable for

complex geometries. However, obtaining smooth enough surfaces to make local measurements is difficult in this technique.

Pouring: The pouring method is the most known and most convenient method. This method is simple and can be successfully repeated. The most important point in this method is that the mold surface should be very smooth and polished very well.

3.5. Measurements

There are two ways for measuring the mass transfer rate. These are the weighing method, which is used to measure the average transfer coefficients, and the local measurement method, which is used to measure the local coefficients and requires the use of a special measuring device.

An average coefficient is obtained by weighing the test sample before and after measurement. This method requires a high precision scale. In the weighing method, the natural convection is lower than the local measurements during the measurement. Because the measurement time is as short as 5 seconds.

In order to detect the natural convection losses, an experiment including all process steps should be performed. However, natural convection losses from measurement, installation, assembly and disassembly, re-measurements are included in the losses on the measuring table. Natural convection losses are determined experimentally as the test sample is removed from the measuring table.

3.6. Heat-Mass Transfer Analogy (Analogue)

Mass transfer by convection can be defined as the transfer of mass between a surface and a moving fluid. We know from heat transfer that; If the hot fluid close to the surface is removed and replaced with a colder fluid, the fluid movement significantly affects the heat transfer. Similarly, if the high-concentration fluid near the surface is removed and replaced with a lower-concentration fluid, fluid motion significantly affects mass transfer.

The basis of mass transfer is understood together with the analogy between the heat and mass transfer processes. Dimensional analysis on the equations describing the heat and mass transfer processes shows that equations of the same formula can be obtained for geometrically similar structures and similar boundary conditions. It is concluded that there is a simple relationship between the Sherwood number describing the mass transfer process and the Nusselt number describing the heat transfer

process. The boundary condition for mass transfer experiments corresponds to an isothermal surface for the similar heat transfer problem. Both the non-dimensionalized concentration difference profile and the mass transfer coefficient remain constant in the fully developed region. This is similar to the fact that the friction and heat transfer coefficients remain constant in the fully developed region.

4. EXPERIMENTAL STUDY

4.1. The Experimental Setup

The schematic view of the experimental setup is given in Fig. 1. The experimental setup essentially consists of a round soap-shaped naphthalene placed on a precision balance placed on a simple tripod setup and a heated air jet impinging on it. Solid naphthalene was obtained by the casting method. This process is essentially nothing but filling and solidifying molten naphthalene into a circular cross-section mold.

During the melting process, a sufficient amount of naphthalene powder was kept with an electric heater until it liquefied. The liquefied naphthalene was removed from the heater and after a short wait, that is, when the temperature of the liquid naphthalene was 70 – 80 °C, the molten naphthalene was put into the mold under the condition of room temperature. Casting at high temperature (>80 °C) causes bubbles to form on the naphthalene surface and turns the naphthalene color into a dark color. Low temperature (< 60 °C) causes the formation of traces in the form of waves on the surface during casting.

The mean mass transfer coefficient is obtained by weighing the sample before and after the test. High resolution scales are required for this method. The natural sublimation that occurs during measurement should also be taken into account. High resolution scales currently available have limited weight capacity that they can measure. The weight of the sample may be limited in some cases by the limited weight capacity of the scale. In this study, naphthalene molds with a mass of 20 g were used and mass measurements were carried out with a RADWAG brand WTC 2000 coded balance with 200 gr / 0.01 gr measurement accuracy.

A special hot air fan is prepared to obtain hot air flow. In the heater fan, which was prepared based on the working principle of a hair dryer, the internal apparatus of the hair dryer, which operates with a 2000 W heater, has 3 different power and 3 different speed settings. A heater unit is mounted on one end of a long pipe, which is long enough to provide a fully developed hydrodynamic flow, while a narrow mouth nozzle is attached to the other end to form a flow jet.

The vertical pipe to which the heating unit is connected is connected to the adjustable stand with the help of a clamp. This stand actually consists of a second bar pipe connected to the upper bar of the serum carrier stand used in hospitals at an angle of 90° . At the end of the second pipe connected by welding, the heating unit was connected with a clamp and the verticality of the position was checked with a spirit level (Fig. 2).

The inner diameter of the pipe, through which hot air is passed, is 6 cm long and $32D$, i.e. 192 cm, was chosen to obtain a fully developed hydrodynamic flow. Narrowed orifices of various diameters were used to create a jet stream to the pipe outlet. The constricted half-cone inserted to obtain the jet flow. $D = 3$ cm was chosen as the jet outlet diameter. The narrow mouth nozzle formed is given as dimensionless diameter ratio ($d/D = 0.5$).

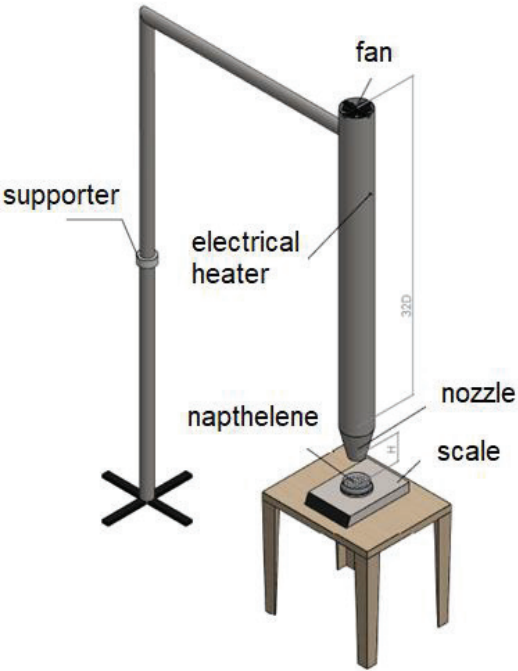


Fig. 1 Setup

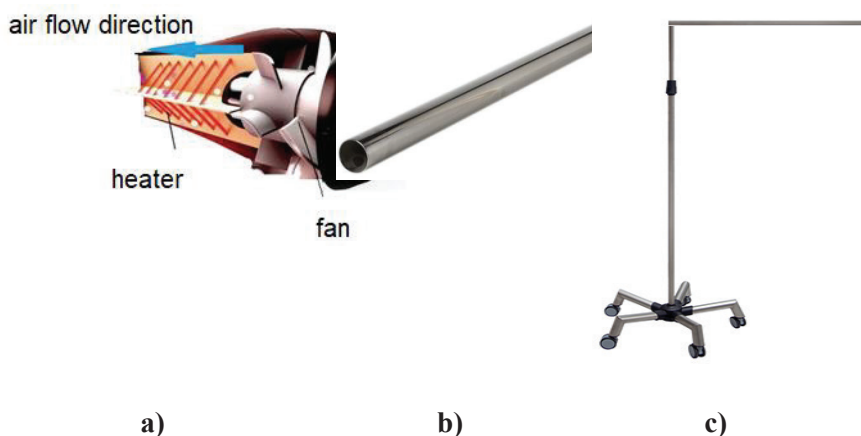


Fig 2. a) Hot jet equipment; **b)** smooth pipe **c)** carrier mechanism

In the experimental setup described in detail above, first of all, the average outlet temperature and velocities of the hot air in the free state were determined at the jet outlet without the naphthalene hitting the surface. Air velocity was measured as average velocity with a brand anemometer. The flow velocity sent by the heated fan unit to the pipe was measured as $U_j = 8 \text{ m/s}$, 15 m/s and 22 m/s , from low to high, in 3 different stages of the hot air jet, respectively. Thus, the Reynolds number could be determined at the jet exit. The same anemometer also gives the average outlet temperature of the current. For verification purposes, temperature measurements were taken at the jet exit with the help of a datalogger and thermocouples installed in the laboratory, and since the results were compatible, the values in the anemometer were taken as basis. Accordingly, the air temperatures in the 3 stages coming out of the hair dryer were recorded as $T_j = 30^\circ\text{C}$, 55°C and 80°C . Ambient temperature and pressure were continuously determined by the pressure and temperature sensors on the datalogger. It was observed that the average ambient temperature was 25°C and the ambient pressure was around 0.98 atm and the values did not change.

4.2. Data Reduction

In the experimental study, the mass of the naphthalene block, which was placed properly in the container on the precision balance, was recorded before the air was blown. Hot air was blown onto the naphthalene surface for a certain period of time by keeping the time with a stopwatch. There was a mass change during the impact, but the exact value was taken as soon as the fan was turned off so that the air weight would not affect it. The difference was calculated as the lost mass, and the mass flux was found by dividing the time. The experiment was repeated in a similar way for each speed, temperature and nozzle diameter change. Measured mass differences, or in other words mass transfer, are due to heat transfer that develops in the system. Therefore, starting from the analogy between heat-mass transfers, the average heat transfer is obtained in terms of Nusselt number with the calculation method given in the following section. The mass transfer data obtained were obtained in terms of heat transfer with the help of heat-mass transfer simulation (analogue). In section 2.9, it was explained that there is a relationship between the Sherwood number, known as the dimensionless number of mass transfer and depends on the Reynolds number and the Schmidt number, and the Nusselt number depends on the Reynolds number and Prandtl number. From this point of view, a functional expression can be formed between the Sherwood number and the Nusselt number. In order to establish this relationship, let's first recall the transport equations of the constant-property stream.

Energy equation:

$$\frac{D\theta}{D\tau} = \frac{1}{RePr} \frac{\partial}{\partial \hat{x}_i} \left[\left[1 + \frac{\alpha}{\nu} \frac{Pr}{Pr_t} \right] \frac{\partial \theta}{\partial \hat{x}_i} \right] \quad (4)$$

The turbulence Prandtl number is a function of the following parameters:

$$Pr_t = f(Re, Pr, \hat{x}_i) \quad (5)$$

In heat convection, velocity and momentum in the thermal boundary layers and the relative humidity magnitudes of heat diffusion are expressed as the dimensionless Prandtl number. The local Nusselt number is functionally written as:

$$Nu = f(Re, Pr, \hat{x}_i) \quad (6)$$

Diffusion equation for two and single phases systems (mass transfer):

$$\frac{Dm}{D\tau} = \frac{1}{ReSc} \frac{\partial}{\partial x_i} \left[\left[1 + \frac{\alpha Sc}{\nu Sc_t} \right] \frac{\partial m}{\partial x_i} \right] \quad (7)$$

The local Sherwood number can be written functionally as:

$$Sh = f(Re, Sc, \hat{x}_i) \quad (8)$$

Here, it would be useful to make a brief explanation about the Sherwood number. As seen in the formula, the Sherwood number is equal to the dimensionless concentration gradient at the surface and is a measure of the mass transfer by convection at the surface. The Sherwood number performs the same function as the Nusselt number in the thermal boundary layer.

As can be seen, the heat and mass transfer equations have similar expressions. Therefore, if the boundary conditions are similar for the given geometry, Nu and Sh have similar solutions as seen in Eq. (6) and Eq. (8) when Pr and Pr_t numbers are equal to Sc and Sc_t numbers, respectively. The heat transfer results obtained from the experiments are also found with empirical equations:

$$Nu = cRe^m Pr^n \quad (9)$$

According to the heat and mass transfer analogy:

$$Sh = cRe^m Sc^n \quad (10)$$

It can also be shown as follows:

$$\frac{Nu}{Sh} = \left(\frac{Pr}{Sc} \right)^n \quad (11)$$

Here, the n exponent was found in the experimental equations in the range of 1/3 to 0.4 (1/3 in flow over a flat plate in laminar flow). If $Pr_t = Sc_t$, the relation is valid for turbulent flow as well as for laminar flow. However, as the flow patterns change, the number of n will also change.

In a naphthalene sublimation test to determine the local and average heat transfer, the calculation technique in its simplest form is as follows: firstly, if local measurement can be made and the sublimation depths on naphthalene surfaces can be precisely measured; These sublimation depths are used to find the mass transfer coefficient. For this, first of all, the heat transfer coefficient should be remembered as follows:

$$h = \frac{q_w}{T_w - T_\infty} \quad (12)$$

hence local mass transfer coefficient is:

$$K_x = \frac{\dot{m}}{\rho_{v,w} - \rho_{v,\infty}} = \frac{\rho_s(\delta_z/\delta_\tau)}{\rho_{v,w}} \text{ (for local)} \quad (13.a)$$

Average (mean) mass transfer coefficient:

$$K_m = \frac{\delta_m/\delta_\tau}{\rho_{v,w}} \text{ (for average)} \quad (13.b)$$

where $\rho_{v,\infty} = 0$ is the vapor density of naphthalene at free flow. Hence:

$$K_m = \frac{\dot{m}}{\rho_{v,w}} \quad (13.c)$$

In the comparison between Eq. (12) and Eq. (13.a), it is seen that; the terms h , q_w and $(T_w - T_\infty)$ in heat transfer mechanism respectively correspond to K , and $(\rho_{v,w} - \rho_{v,\infty})$ in mass transfer mechanism. The vapor density of naphthalene is determined by

$$\rho_{v,w} = P_{v,w}/RT_w \quad (14)$$

Sherwood number depends on the mass transfer coefficient, diffusion coefficient and characteristic length. Since the geometry of the characteristic length impinging jet is circular, the jet exit diameter will be taken as “ d ” here.

$$Sh = \frac{K_m d}{D_{naphth}} \quad (15)$$

Here, the Stanton number, which is the mass transfer coefficient, removes the uncertainty of the diffusion coefficient. For average measurements of the Stanton number with a mass transfer coefficient:

$$St_m = \frac{Sh}{ReSc} = \frac{h_m}{U_\infty} \quad (16)$$

However, here the Schmidt number comes into play in the heat and mass transfer analogy. The Schmidt number is the ratio of the momentum and mass dissipation coefficients, expressed as:

$$Sc = \frac{\nu_{air}}{D_{naphth}} \quad (17)$$

As it will be remembered from the formula expansion, the Schmidt number is similar to the Prandtl.

$$\frac{Sh}{Nu} = \frac{g(Sc)}{g(Pr)} \quad (18)$$

Sherwood number can be shown as a parameter of Schmidt number:

$$Sh = \frac{K_m d}{D_{naphth}} = \frac{K_m d}{v_{air}} \frac{v_{air}}{D_{naphth}} = \frac{K_m d}{v_{air}} Sc \quad (19)$$

Similarly, Nusselt number can be written as:

$$Nu = \frac{h_m d}{k_{air}} \quad (20)$$

If Eq.(19) and Eq.(20) are rearranged, then

$$\frac{\frac{K_m d}{v_{air}} Sc}{\frac{h_m d}{k_{air}}} = \frac{g(Sc)}{g(Pr)} \quad (21)$$

Considering that the exponent of the Prandtl number in the empirical relations predicted for the Nusselt number is also valid for the Schmidt number, let's write the following analogy:

$$g(Sc) = Sc^{0.333}, \quad g(Pr) = Pr^{0.333} \quad (22)$$

$$\frac{K_m k_{air}}{h_m v_{air}} = \left(\frac{Sc}{Pr}\right)^{0.333} \frac{1}{Sc} \quad (23)$$

$$h_m = \frac{K_m k_{air}}{\left(\frac{Sc}{Pr}\right)^{0.333} \frac{1}{Sc} v_{air}} \quad (24)$$

$$Nu = \frac{K_m k_{air}}{\left(\frac{Sc}{Pr}\right)^{0.333} \frac{1}{Sc} v_{air}} \frac{d}{k_{air}} \quad (25)$$

5. EXPERIMENTAL RESULTS

5.1. Sherwood and Nusselt Numbers

The presentation of the test results will be made together with the explanations of the calculated values. Thus, it will be understood more clearly which result is obtained and how. Before starting the experiments, the Reynolds number of the jets should be calculated.

$$Re = \frac{U_j d}{\nu_{air}} \quad (26)$$

Here, jet exit velocities were measured at three different values as $U_j = 8, 15$ and 22 m/s. Jet outlet diameter is $d = 0.03$ m. The viscosity of the air was calculated with the help of the Eq.(2):

$$\nu_{air} = 0.1556 \left(\frac{T}{298.16} \right)^{1.7774} \left(\frac{1.013 \times 10^5}{P_{atm}} \right) \text{ cm}^2/\text{s}$$

All experiments were completed on the same day, without changing the laboratory conditions. During the experiments, the temperature of the ambient air was measured as $T_\infty = 25$ °C. The temperature T_j of the jet stream sprayed into the naphthalene mold was measured as 30 °C, 55 °C and 80 °C as mentioned before. In this case, the temperature that affects the viscosity of naphthalene and even the naphthalene sublimation coefficient is actually the mean temperature ($T_b = (T_\infty + T_j)/2$). The ambient pressure remained constant at $P_{atm} = 0.98$ atm. The pressure and temperature values were replaced in Eq. (2), and the viscosity in cm^2/s was found and then converted to m^2/s .

Table 3 shows the calculation of Reynolds numbers found by taking Eq. (2) into account. As it can be seen from the table, since the temperature of T_b changes, the changing viscosity value has changed the Re number considerably.

Table 3 Reynolds numbers

Jet velocity U_j (m/s)	Jet diameter d (m)	Bulk Temperature T_b (K)	Pressure P_{atm} (Pa)	Viscosity ν_{air} (m^2/s)	Re number
8	0.03	303.16	99298.5	1.61884E-05	14825.3891
15	0.03	303.16	99299.5	1.61883E-05	27797.8844
22	0.03	303.16	99300.5	1.61881E-05	40770.6411
8	0.03	328.16	99298.5	1.86368E-05	12877.7239
15	0.03	328.16	99299.5	1.86366E-05	24145.9755
22	0.03	328.16	99300.5	1.86365E-05	35414.454

8	0.03	353.16	99298.5	2.12347E-05	11302.2569
15	0.03	353.16	99299.5	2.12345E-05	21191.945
22	0.03	353.16	99300.5	2.12343E-05	31081.8324

For mass loss measurement, sublimation was calculated by considering the mass differences of the samples weighed before and after the experiment and the time elapsed during this time. Let's rewrite the Eq. (13.c) clearly:

$$K_m = \left(\frac{\Delta m}{\Delta t \rho_{v,w}} \right)$$

where Δm represents the difference in naphthalene amounts measured before and after the experiment, in other words, the amount of sublimated naphthalene. Δt represents the time elapsed during sublimation, $\rho_{(v,w)}$ represents the density of naphthalene gas on the surface. To calculate $\rho_{(v,w)}$, the ideal gas equation given by Eq. (14) is used or it is obtained from experimental measurements. Say, if the mass flow rate is divided by the volume flow rate, the residual density will be. The volumetric flow rate is equal to the product of the jet velocity and the surface area of the naphthalene mold.

The sequence of operations to calculate the mass transfer coefficient K_m is as follows:

$$\dot{m} = \left(\frac{\Delta m_s}{\Delta t_s} \right) \rightarrow \dot{Q} = U_j A_{naphth} \rightarrow \rho_{v,w} = \left(\frac{\dot{m}}{\dot{Q}} \right) \rightarrow K_m = \left(\frac{\dot{m}}{\rho_{v,w}} \right)$$

The mass transfer coefficient K_m from naphthalene mold was found. The Sherwood number is calculated by substituting the K_m value in Eq. (15).

$$Sh = \left(\frac{K_m d}{D_{naphth}} \right)$$

It should be remembered that the naphthalene diffusion coefficient in the Sh number was found with the help of the empirical equation given in D_{naphth} Eq. (1).

$$D_{naphth} = 0.0681 \left(\frac{T}{298.16} \right)^{1.93} \left(\frac{1.013 \times 10^5}{P_{atm}} \right) \text{ cm}^2/\text{s}$$

In Table 4, the steps to find the Sh number and the obtained values are given for all T_b values. Each measurement time was taken as 120 s. A total of 9 experiments were carried out, each experiment was carried out with a new mothball mold, which was poured beforehand and kept in the refrigerator without sublimation. Thus, sublimation due to natural convection was carried out only in 1 s when the mold is weighed without hitting the jet, 120 s when the jet is dipped, and 1 s when the final temperature is weighed again, i.e. 122 s. According to the information obtained from the literature, 122 s is not a high time period for natural convection and the result is the most more than 0.5%. Therefore, natural convection loss is neglected.

Table 4 Mass Transfer coefficient, diffusion coefficient, and Sherwood numbers

Loss mass m_s (kg)	Time t (s)	Mass Flowrate \dot{m} (kg/s)	Volumetric flowrate \dot{Q} (m ³ /s)	Naphthalene density $\rho_{n,w}$ (kg/m ³)	Mass Transfer coefficient K_m (m/s)	Naphthalene diffusion coefficient D_{naph} (m ² /s)	Sherwood number Sh
0.00130	120	1.017 E-05	0.050868	0.00021313	0.050868	7.105E-06	214.842
0.00376	120	0.00003138	0.0953775	0.00032901	0.0953775	7.108E-06	402.834
0.00545	120	4.543 E-05	0.139887	0.00032496	0.139887	7.101E-06	590.830
0.00314	120	2.621 E-05	0.050868	0.0005153	0.050868	8.282E-06	184.375
0.00567	120	0.0000473	0.0953775	0.00049592	0.0953775	8.276E-06	345.707
0.00712	120	5.935 E-05	0.139887	0.00042429	0.139887	8.275E-06	507.042
0.00488	120	0.00004074	0.050868	0.0008009	0.050868	9.581E-06	160.015
0.00678	120	5.656 E-05	0.0953775	0.00059307	0.0953775	9.531E-06	300.032
0.00904	120	7.538 E-05	0.139887	0.00053887	0.139887	9.536E-06	440.229

Based on the Sherwood number, the Schmidt number, the heat transfer coefficient h_m and then the Nusselt number are found and given in Table 5.

$$Sc = \frac{Sh \nu_{air}}{K_m d} \quad h_m = \frac{K_m k_{air}}{\left(\frac{Sc}{Pr}\right)^{0.333} \frac{1}{Sc} \nu_{air}} \quad Nu = \frac{K_m k_{air}}{\left(\frac{Sc}{Pr}\right)^{0.333} \frac{1}{Sc} \nu_{air}} \frac{d}{k_{air}}$$

Here, the thermal conductivity of k_{air} is found from the tables. The Prandtl number is 0.701 for air.

Table 5 Schmidt numbers, heat transfer coefficients and Nusselt numbers

Sc	h_m (W/m ² K)	Nu
2.24578594	97.60975155	146.4146273
2.24578594	183.0201273	274.5301909
2.24578594	268.4322232	402.6483348
2.07201626	86.04416443	129.0662466
2.07201626	161.334433	242.0016495
2.07201626	236.626218	354.9393271
1.92781752	76.49158699	114.7373805
1.92781752	143.42317	215.1347549
1.92781752	210.356101	315.5341515

5.2. Graphical Presentations

In this section, the mass transfer results and the heat transfer results obtained by analogy will be evaluated graphically. In Figs. 3, 4 and 5, the calculated Nusselt number versus Sherwood numbers are presented for the jet exit temperatures of 30 °C, 55 °C and 80 °C respectively ($H/D = 2$). In Fig. 6, the three mentioned graphs are shown in a single graph. In Fig. 7 Schmidt number versus Sherwood number for $H/D = 2$ is plotted.

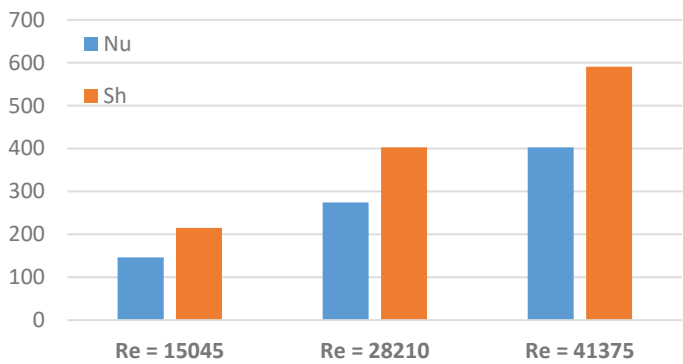


Fig. 3 Nusselt number versus Sherwood number for $T_j = 30\text{ °C}$, $H/D = 2$

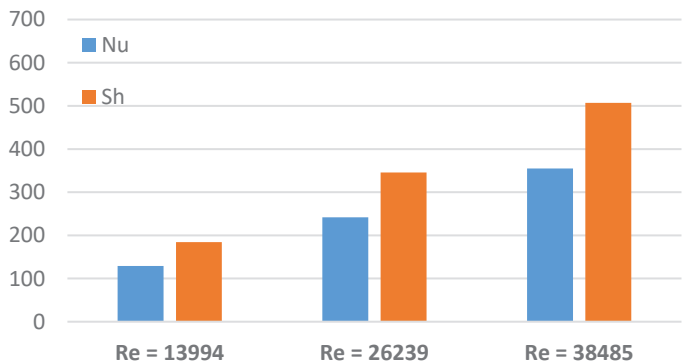


Fig. 4 Nusselt versus Sherwood for $T_j = 55\text{ °}$, $H/D = 2$

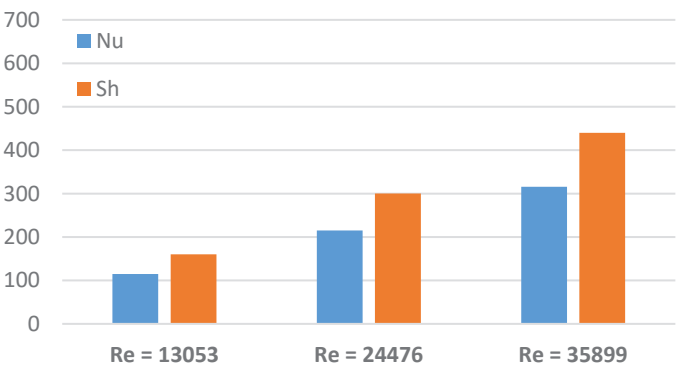


Fig. 5 Nusselt versus Sherwood for $T_j = 80^\circ$, $H/D = 2$

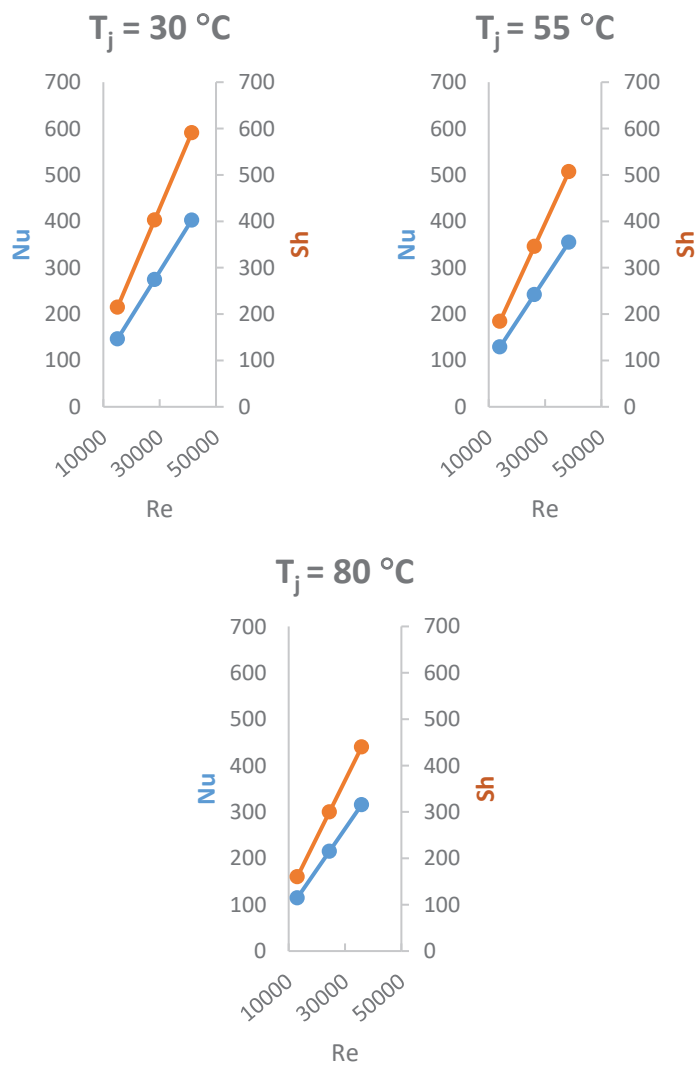


Fig. 6 Nusselt number versus Sherwood number for $H/D= 2$

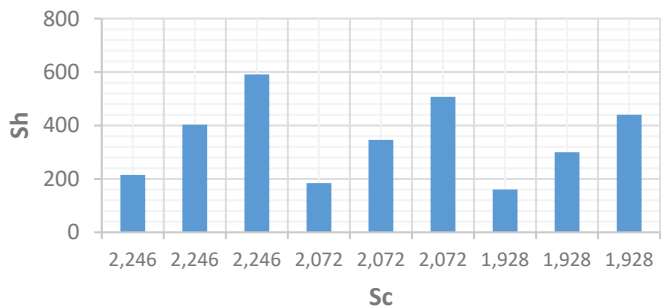


Fig. 7 Schmidt number versus Sherwood number for $H/D= 2$

In Fig. 8, for $H/D = 4$, the Nusselt number and the Sherwood number are shown on two separate vertical axes, and the variation of both depending on the similar Reynolds number is compared. As can be seen, as the change in jet exit temperature increased, mass transfer and heat transfer increased at the same rate. Increasing the Reynolds number, on the other hand, increased both mass transfer and heat transfer. Although the Nusselt number and the Sherwood number have never been exactly the same numerically, the change trends, increase-decrease rates have always progressed similarly. Similar to the Fig. 8, the Nusselt number and the Sherwood number with respect to Reynolds number is presented for $H/D = 6$ and $H/D = 10$ respectively in Fig. 9 and Fig. 10.

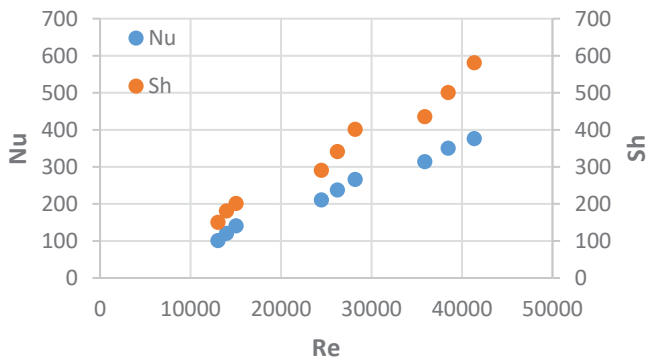


Fig. 8 Nusselt number and Sherwood number versus Reynolds number for $H/D= 4$

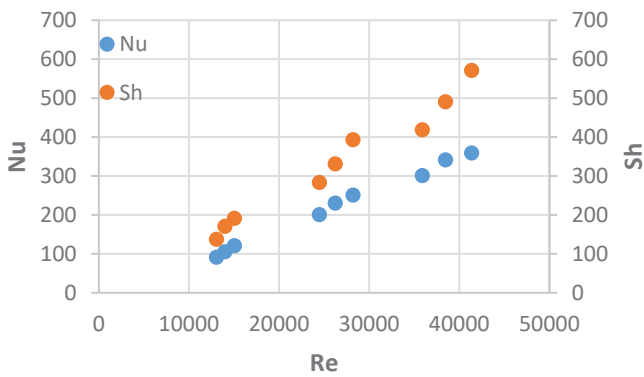


Fig. 9 Nusselt number and Sherwood number versus Reynolds number for $H/D= 6$

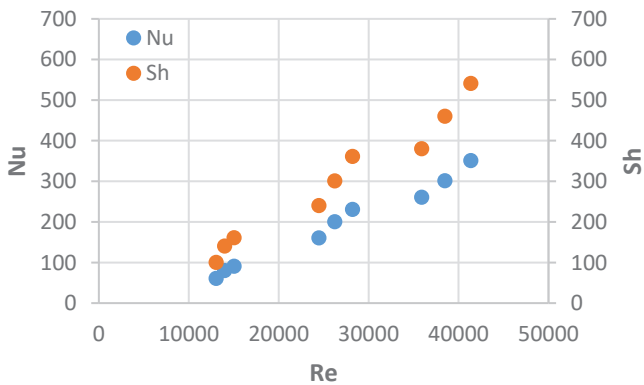


Fig. 10 Nusselt number and Sherwood number versus Reynolds number for $H/D= 10$

REFERENCES

- Ambrose, D., Lawrenson, I.J. and Sparke, C.H.S., (1975). The Vapor Pressure of Naphthalene, *Journal of Chemical Thermodynamics*, 7, 1173-1176.
- Arzutug, M.E. (2003). Mass Transfer in Impinging Swirl Jets, (PhD Thesis), Atatürk University, Erzurum.
- Arzutug, M.E. and Yapici, S. (2009). Electrochemical Mass Transfer in Impinging Swirl Jets, *Ind. Eng. Chem. Res.*, 48, 1593-1602.
- Chen D.W. and Goldstein R. J. (1992). Convective Transport Phenomena on the Suction Surface of a Turbine Blade Including the Influence of Secondary Flows Near the End wall, *Journal of Turbomachinery*, 114(4), 776-787.
- Chen, Y.M., Lee, W.T. and Wu, S.J. (1998). Heat (Mass) Transfer Between an Impinging Jet and a Rotating Disk, *Heat and Mass Transfer*, 34, 195-196.
- Cho, H.H. Jabbari, M.Y. and Goldstein R.J. (1997). Experimental Mass (Heat) Transfer in and near a Circular Hole in a Flat Plate, *International Journal of Heat and Mass Transfer*, 40(10), 2431-2443.
- Feroz S., and Prasad S.R. K. (2006). Mass Transfer Coefficients at the Stagnation Point with Submerged Impinging Multi-Jet Flow of Fluid Electrolyte, *Turkish Journal of Engineering and Environmental Sciences*, 30, 221-229.
- Goldstein, R. J. and Cho, H. H. (1995). A Review of Mass Transfer Measurements Using Naphthalene Sublimation, *Experimental Thermal and Fluid Science*, 10, 416-434.
- Goldstein, R. J., Chyu, M. K., and Hain, R. C. (1985). Measurement of Local Mass Transfer on a Surface in the Region of the Base of a Protruding Cylinder with a Computer-Controlled Data Acquisition System. *International Journal of Heat and Mass Transfer*, 28(5), 977-985.
- Hong, S. K., Lee, D. H., and Cho, H. H. (2009). Effect of Jet Direction on Heat/Mass Transfer of Rotating Impingement Jet. *Applied Thermal Engineering*, 29(14-15), 2914-2920.
- Kataoka, K. and Misusing, T. (1974). Local Enhancement of the Rate of Heat-Transfer in an Impinging Round Jet by Free-Stream Turbulence, *Society of Heat Transfer of Japan*, 2, 305-309.
- Park J.H. and Yoo S.Y. (2004). A Naphthalene Sublimation Study on Heat/Mass Transfer for Flow Over a Flat Plate, *Journal of Mechanical Science and Technology*, 18(7), 1258-1266.

- Pekdemir, T. and Davies, T.W. (1998). Mass Transfer from Stationary Circular Cylinders in A Submerged Slot Jet of Air, *Int. J Heat Mass Transfer*, 41(15), 2361-2370.
- Popiel, C.O., and Boguslawski, L. (1988). Effect of Flow Structure on the Heat or Mass Transfer on a Flat Plate in Impinging Round Jet, Proceedings of 2nd UK national Conference on Heat Transfer, University of Stracthclyde, 1, 663.
- Rhe, D. H., Choi, J. H. and Cho, H.H. (2003). Heat (Mass) Transfer on Effusion Plate in Impingement/Effusion Cooling Systems. *Journal of Thermophysics and Heat Transfer*, 17(1), 95-102.
- Russ, G. and Beer, H., (1997). Heat Transfer and Flow Field in a Pipe with Sinusoidal Wavy Surface -II Experimental Investigation, *Int. J. Heat Mass Transfer*, 40(50), 1071–1081.
- Solak, I. and Laval J. P. (2017). Large-Scale Motions from A Direct Numerical Simulation of A Turbulent Boundary Layer, *Physical Review E.*, 98(3).
- Sparrow, E. M., and Geiger, G. T. (1985). Local and Average Heat Transfer Characteristics for a Disk Situated Perpendicular to a Uniform Flow. *Journal of Heat Transfer*, 107(2), 321-326.
- Sparrow, E. M., and Lovell, B. J. (1980). Heat transfer characteristics of an obliquely impinging circular jet, *Journal of Heat Transfer*, 102(2), 202-209.
- Sparrow, E. M., and Wong, T. C. (1975). Impingement Transfer Coefficients Due to Initially Laminar Slot jets. *International Journal of Heat and Mass Transfer*, 18(5), 597-605.
- Sara O.N., Pekdemir T., Yapici, S. and Yilmaz, M. (2001). Enhancement of Heat Transfer from a Flat Surface in a Channel Flow by Attachment of Rectangular Blocks, *International Journal of Energy Research*, 25, 563-576,
- Ward, J., Mahmood, M., (1982). Heat Transfer from a Turbulent, Swirling Impinging Jet, 7th International Heat Transfer Conference, HTD-3, 401-407.